AREVA

FINAL SAFETY ANALYSIS REPORT FOR THE NUHOMS® HD HORIZONTAL MODULAR STORAGE SYSTEM FOR IRRADIATED NUCLEAR FUEL

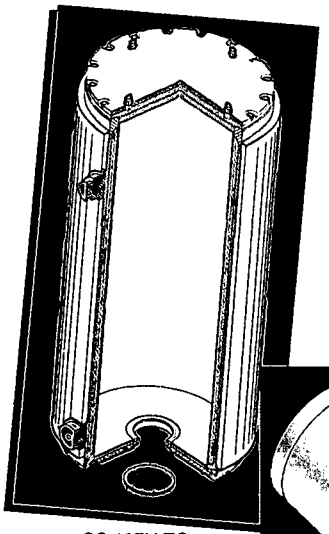

OS 187H TC

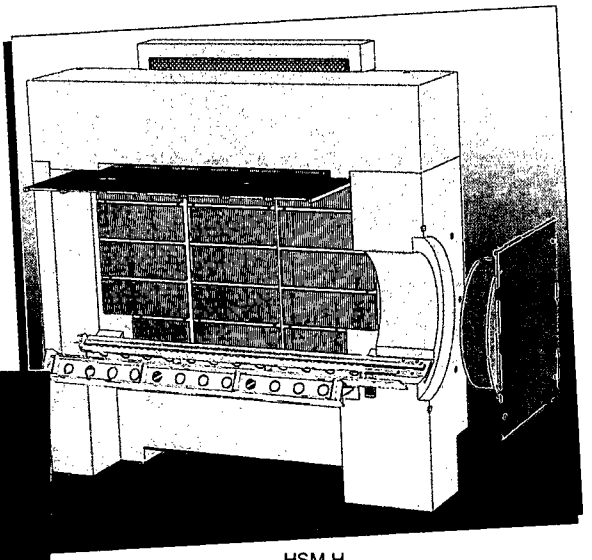

HSM-H

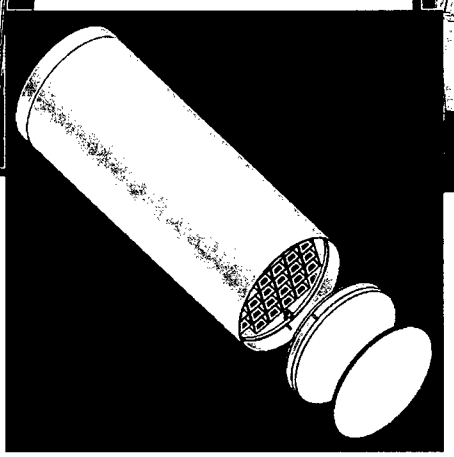

32PTH DSC

NON-PROPRIETARY

VOLUME 3 OF 3

TRANSNUCLEAR INC.

TABLE OF CONTENTS

1. GENERAL INFORMATION 1-1

1.1 Introduction 1-2

1.2 General Description of the NUHOMS® HD System 1-4

1.2.1 NUHOMS® HD System Characteristics 1-4
1.2.2 Operational Features 1-7
1.2.3 32PTH DSC Contents 1-12

1.3 Identification of Agents and Contractors 1-13

1.4 Generic Cask Arrays 1-14

1.5 Supplemental Data 1-15

1.5.1 References 1-15
1.5.2 Drawings 1-15

2. PRINCIPAL DESIGN CRITERIA 2-1

2.1 Spent Fuel to be Stored 2-1

2.1.1 Detailed Payload Description 2-1

2.2 Design Criteria for Environmental Conditions and Natural Phenomena 2-4

2.2.1 Tornado and Wind Loadings 2-4
2.2.2 Water Level (Flood) Design 2-6
2.2.3 Seismic Design 2-7
2.2.4 Snow and Ice Loadings 2-7
2.2.5 Tsunami 2-7
2.2.6 Lightning 2-7
2.2.7 Combined Load Criteria 2-8
2.2.8 Burial under Debris 2-9
2.2.9 Thermal Conditions 2-9

2.3 Safety Protection Systems 2-11

2.3.1 General 2-11
2.3.2 Protection by Multiple Confinement Barriers and Systems 2-11
2.3.3 Protection by Equipment and Instrumentation Selection 2-13
2.3.4 Nuclear Criticality Safety 2-13
2.3.5 Radiological Protection 2-14
2.3.6 Fire and Explosion Protection 2-15
2.3.7 Acceptance Tests and Maintenance 2-16

2.4 Decommissioning Considerations 2-17

2.5 Structures, Systems and Components Important to Safety 2-18

2.5.1 Dry Shielded Canister 2-18
2.5.2 Horizontal Storage Module 2-18
2.5.3 ISFSI Basemat and Approach Slabs 2-19
2.5.4 Transfer Equipment 2-19
2.5.5 Auxiliary Equipment 2-19

2.6 References 2-20

3. STRUCTURAL EVALUATION 3-1

3.1 Structural Design 3-1

3.1.1 Discussion 3-1
3.1.2 Design Criteria 3-10

3.2 Weights 3-13

3.2.1 32PTH DSC Weight 3-14
3.2.2 OS187H Transfer Cask Weight 3-15
3.2.3 HSM-H Weight 3-16

3.3 Mechanical Properties of Materials 3-17

3.3.1 32PTH DSC Material Properties 3-17
3.3.2 HSM-H Material Properties 3-18
3.3.3 OS187H Transfer Cask Material Properties 3-19

3.4 General Standards for 32PTH DSC, HSM-H, and OS187H Transfer Cask. 3-20

3.4.1 Chemical and Galvanic Reactions 3-20
3.4.2 Positive Closure 3-25
3.4.3 Lifting Devices 3-26
3.4.4 Heat 3-26
3.4.5 Cold 3.26

3.5 Fuel Rods General Standards for 32PTH DSC 3-27

3.5.1 Fuel Rod Temperature Limits 3-27
3.5.2 Fuel Assembly Thermal and Irradiation Growth 3-27
3.5.3 Fuel Rod Integrity during Drop Scenario 3-29
3.5.4 Fuel Unloading 3-32

3.6 Normal Conditions of Storage and Transfer 3-33

3.6.1 32PTH DSC Normal Conditions Structural Analysis 3-33
3.6.2 HSM-H Normal Conditions Structural Analysis 3-37
3.6.3 OS187H Transfer Cask Normal Conditions Structural Analysis 3-38

3.7 Off Normal and Hypothetical Accident Conditions 3-41

3.7.1 32PTH DSC Off-Normal and Accident Conditions Structural Analysis 3-41
3.7.2 HSM-H Off-Normal and Accident Conditions Structural Analysis 3-49

3.7.3 OS187H Transfer Cask Off-Normal and Accident Conditions Structural Analysis 3-50

3.8 References 3-54

3.9 Appendices 3-57
3.9.1 32PTH DSC (Canister and Basket) structural Analysis 3.9.1-1
3.9.2 OS187H Transfer Cask Body Structural Analysis 3.9.2-1
3.9.3 OS187H Transfer Cask Top Cover and RAM Access Cover Bolts Analyses 3.9.3-1
3.9.4 OS187H Transfer Cask Lead Slump and Inner Shell Buckling Analyses 3.9.4-1
3.9.5 OS187H Transfer Cask Trunnion Analysis 3.9.5-1
3.9.6 OS187H Transfer Cask Shield Panel Structural Analysis 3.9.6-1
3.9.7 OS187H Transfer Cask Impact Analysis 3.9.7-1
3.9.8 Damaged Fuel Cladding Structural Evaluation 3.9.8-1
3.9.9 HSM-H Structural Analysis 3.9.9-1
3.9.10 OS187H Transfer Cask Dynamic Impact Analysis 3.9.10-1
3.9.11 32PTH DSC Dynamic Impact Analysis 3.9.11-1

3.10 ASME Code Alternatives 3-58

4. THERMAL EVALUATION 4-1

4.1 Discussion 4-1

4.2 Summary of Thermal Properties of Materials 4-3

4.3 Thermal Evaluation for Normal and Off-Normal Conditions 4-9
4.3.1 Thermal Models for Normal and Off-Normal Conditions 4-9
4.3.2 Maximum Temperatures for Normal and Off-Normal Conditions 4-20
4.3.3 Minimum Temperatures for Normal and Off-Normal Conditions 4-20
4.3.4 Maximum Internal Pressures for Normal and Off-Normal Conditions 4-20
4.3.5 Maximum Thermal Stresses for Normal and Off-Normal Conditions 4-20
4.3.6 Evaluation of Thermal Performance for Normal and Off-Normal Conditions 4-20

4.4 Thermal Evaluation for Accident Conditions 4-22
4.4.1 Thermal Models for Accident Conditions 4-22
4.4.2 Maximum Temperatures for Accident Conditions 4-27
4.4.3 Maximum Internal Pressures for Accident Conditions 4-28
4.4.4 Maximum Thermal Stresses for Accident Conditions 4-28
4.4.5 Evaluation of Thermal Performance for Accident Conditions 4-28

4.5 Thermal Evaluation for Loading and Unloading Conditions 4-29
4.5.1 Vacuum Drying 4-29

4.5.2 Reflooding 4-34

4.6 Maximum Internal Pressure 4-36

4.6.1 Average Gas Temperature 4-36
4.6.2 Amount of Initial Helium Backfill 4-37
4.6.3 Free Gas within Fuel Assemblies / BPRA 4-38
4.6.4 Total Amount of Gases within DSC 4-38
4.6.5 Maximum DSC Internal Pressures 4-38
4.6.6 Maximum Pressure in Annulus 4-39

4.7 Axial Decay Heat Profile 4-40

4.8 Effective Fuel Properties 4-43

4.8.1 Discussion 4-43
4.8.2 Summary of Material Properties 4-43
4.8.3 Effective Fuel Conductivity 4-45
4.8.4 Effective Fuel Density and Specific Heat 4-46
4.8.5 Conclusion 4-47

4.9 Effective Conductivity of Fluids in the Transfer Cask 4-48

4.9.1 Effective Conductivity in the Shielding Panel 4-48
4.9.2 Effective Water Conductivity in Annulus between TC and DSC 4-50

4.10 Justification of the Assumed Hot Gap Sizes 4-52

4.10.1 Radial Gap between Basket Rails and DSC shell 4-52
4.10.2 Radial Gap between Lead and the Cask Structural Shell 4-53

4.11 Heat Transfer Coefficients 4-55

4.11.1 Total heat Transfer Coefficient to Ambient 4-55
4.11.2 Free Convection Coefficients 4-55

4.12 Effective Conductivity of Air in Closed Cavity of HSM-H 4-63

4.13 Thermal-Hydraulic Equations for the HSM-H 4-65

4.14 Thermal Evaluation of DSC Containing Damaged Fuel 4-68

4.14.1 Normal / Off-Normal Conditions 4-68
4.14.2 Accident Conditions 4-68
4.14.3 Effective Properties of Damaged Fuel 4-70
4.14.4 Evaluation of DSC Thermal Performance with Damaged Fuel 4-71

4.15 References 4-73

4.16 Appendices 4-75

5. SHIELDING EVALUATION 5-1

5.1. Discussion and Results **5-2**

5.2 Source Specification **5-3**

5.2.1 Gamma Sources 5-5
5.2.2 Neutron Source 5-5

5.3 Model Specification **5-6**

5.3.1 Description of the Radial and Axial Shielding Configurations 5-6
5.3.2 Shield Regional Densities 5-7

5.4 Shielding Evaluation **5-9**

5.4.1 Computer Programs 5-9
5.4.2 Spatial Source Distribution 5-9
5.4.3 Cross-Section Data 5.10
5.4.4 Flux-to-Dose-Rate Conversion 5.10
5.4.5 Model Geometry 5-10
5.4.6 Methodology 5-10
5.4.7. Assumptions 5-11
5.4.8 Normal Condition Models 5-12

5.5 Supplemental Information **5-15**

5.5.1 References 5-15
5.5.2 Sample Input Files 5-17

6. CRITICALITY EVALUATION 6-1

6.1 Discussion and Results **6-2**

6.2 Spent Fuel Loading **6-4**

6.3 Model Specification **6-5**

6.3.1 Description of Criticality Analysis Model 6-5
6.3.2 Package Regional Densities 6-7

6.4 Criticality Calculation **6-8**

6.4.1 Calculational Method 6-8
6.4.2 Fuel Loading Optimization 6-13
6.4.3 Criticality Results 6-22

6.5 Critical Benchmark Experiments **6-23**

6.5.1 Benchmark Experiments and Applicability 6-23
6.5.2 Results of the Benchmark Calculations 6-24

6.6 Supplemental Information **6-25**

6.6.1 References 6-25
6.6.2 KENO Input Files 6-27

7. CONFINEMENT **7-1**

7.1 Confinement Boundary 7-1

7.1.1 Confinement Vessel 7-1
7.1.2 Confinement Penetrations 7-2
7.1.3 Seals and Welds 7-2
7.1.4 Closure 7-2

7.2 Requirements for Normal Conditions of Storage 7-3

7.2.1 Release of Radioactive Material 7-3
7.2.2 Pressurization of Confinement Vessel 7-3

7.3 Confinement Requirements for Hypothetical Accident Conditions 7-4

7.3.1 Fission Gas Products 7-4
7.3.2 Release of Contents 7-4

7.4 Supplemental Data 7-5

7.4.1 Confinement Monitoring Capability 7-5
7.4.2 References 7-5

8. OPERATING PROCEDURES 8-1

8.1 Procedures for Loading the DSC and Transfer to the HSM-H 8-1

8.1.1 Narrative Description 8-1

8.2 Procedures for Unloading the DSC 8-10

8.2.1 DSC Retrieval from the HSM-H 8-10
8.2.2 Removal of Fuel from the DSC 8-11

8.3 Supplemental Information 8-14

8.3.1 Other Operating Systems 8-14
8.3.2 Operation Support System 8-14
8.3.3 Surveillance and Maintenance 8-14

8.4 References 8-15

9. ACCEPTANCE TESTS AND MAINTENANCE PROGRAM 9-1

9.1 Acceptance Criteria 9-1

9.1.1 Visual inspection and Non-Dectructive Examination (NDE) 9-1
9.1.2 Structural and Pressure tests 9-1
9.1.3 Leak Tests 9-1
9.1.4 Components 9-2
9.1.5 Shielding Integrity 9-2
9.1.6 Thermal Acceptance 9-2
9.1.7 Neutron Absorber Tests 9-3

9.2 Maintenance Program 9-5

9.2.1 Inspection 9-5
9.2.2 Tests 9-5
9.2.3 Repair, Replacement and Maintenance 9-6

9.3 Marking 9-6

9.4 Pre-Operational Testing and Training Exercise 9-6

9.5 Specification for Neutron Absorbers 9-7

9.5.1 Specification for Thermal Conductivity Testing of Neutron Absorbers . 9-7
9.5.2 Specification for Acceptance Testing of Neutron Absorbers by Neutron Transmission 9-8
9.5.3 Specification for Qualification testing of Metal Matrix Composites 9-9
9.5.4 Specification for Process Controls for Metal Matrix Composites 9-12

9.6 REFERENCES 9-14

10. RADIATION PROTECTION 10-1

10.1 Ensuring That Occupational Radiation Exposures Are As Low As Reasonably Achievable (ALARA) 10-1

10.1.1 Policy Considerations 10-1
10.1.2 Design Considerations 10-1
10.1.3 Operational Considerations 10-3

10.2 Radiation Protection Design Features 10-4

10.2.1 NUHOMS® System Design Features 10-4
10.2.2 Offsite Dose Calculations 10-4

10.3 Estimated Onsite Collective Dose Assessment 10-8

10.3.1 DSC Loading, Transfer and Storage Operations 10-8
10.3.2 DSC Retrieval Operations 10-8
10.3.3 Fuel Unloading Operations 10-9
10.3.4 Maintenance Operations 10-9
10.3.5 Doses During ISFSI Array Expansion 10-9

10.4 References 10-10

11. Accident Analysis 11-1

11.1 Introduction 11-1

11.2 Off-Normal Operation 11-2

11.2.1 Off-Normal Transfer Load 11-3

11.2.2 Extreme Temperature 11-5
11.2.3 Radiological Impact from Off-Normal Operation 11-6

11.3 Postulated Accident 11-7

11.3.1 Cask Drop 11-8
11.3.2 Earthquake 11-10
11.3.3 Tornado Wind and Tornado Missiles Effect on HSM-H 11-11
11.3.4 Tornado Wind and Tornado Missiles Effect on Transfer Cask 11-18
11.3.5 Flood 11-25
11.3.6 Blockage of HSM-H Air Inlet and Outlet Opening 11-25
11.3.7 Lightning 11-26
11.3.8 Fire/Explosion 11-27

11.4 References 11-28

12. OPERATING CONTROLS AND LIMITS 12-1

13. QUALITY ASSURANCE 13-1

13.1 Introduction 13-2

13.2 "Important-to-Safety & "Safety Related" NUHOMS® HD System Components 13-3

13.3 Description of TN 10CFR 72, Subpart G QA Program 13-5

13.3.1 Project Organization 13-5
13.3.2 QA Program 13-5
13.3.3 Design Control 13-5
13.3.4 Procurement Document Control 13-6
13.3.5 Procedures, Instructions, and Drawings 13-6
13.3.6 Document Control 13-6
13.3.7 Control of Purchased Items and Services 13-6
13.3.8 Identification and Control of Materials, Parts, and Components 13-7
13.3.9 Control of Special Processes 13-7
13.3.10 Inspection 13-7
13.3.11 Test Control 13-7
13.3.12 Control of Measuring and Test Equipment 13-7
13.3.13 Handling, Storage and Shipping 13-7
13.3.14 Inspection and Test Status 13-8
13.3.15 Control of Nonconforming Items 13-8
13.3.16 Corrective Action 13-8
13.3.17 Records 13-8
13.3.18 Audits and Surveillances 13-8

13.4 Conditions of Approval Records 13-9

13.5 Supplemental Information 13-10
13.5.1 References 13-10

14. DECOMMISSIONING **14-1**
14.1 Decommissioning Considerations **14-1**

14.2 Supplemental Information **14-4**

14.2.1 References 14-4

CHAPTER 5
SHIELDING EVALUATION

TABLE OF CONTENTS

5. SHIELDING EVALUATION 5-1

5.1 Discussion and Results 5-2
5.2 Source Specification 5-3
5.2.1 Gamma Sources 5-5
5.2.2 Neutron Source 5-5
5.3 Model Specification 5-6
5.3.1 Description of the Radial and Axial Shielding Configurations 5-6
5.3.2 Shield Regional Densities 5-7
5.4 Shielding Evaluation 5-9
5.4.1 Computer Programs 5-9
5.4.2 Spatial Source Distribution 5-9
5.4.3 Cross-Section Data 5-10
5.4.4 Flux-to-Dose-Rate Conversion 5-10
5.4.5 Model Geometry 5-10
5.4.6 Methodology 5-10
5.4.7. Assumptions 5-11
5.4.8 Normal Condition Models 5-12
5.5 Supplemental Information 5-15
5.5.1 References 5-15
5.5.2 Sample Input Files 5-17

LIST OF TABLES

5-1 NUHOMS® HD 32PTH System Shielding Materials

5-2 Summary HSM-H Dose Rates

5-3 Transfer Cask (Loading/Unloading/Transfer Operations) Side Dose Rate Summary

5-4 Transfer Cask (Loading/Unloading/Transfer Operations) Top End Dose Rate Summary

5-5 Cask (Loading/Unloading/Transfer Operations) Bottom End Dose Rate Summary

5-6 Flux Factor By Fuel Assembly Region

5-7 Westinghouse Fuel Assembly Materials and Masses

5-8 NFAH Material and Masses

5-9 Fuel Assembly Material Masses (kg/assembly)

5-10 SAS2H Gamma Sources for 60 GWd/MTU, 7-Year Cooled MK BW 17x17 Fuel Assembly

5-11 SAS2H Gamma Sources for 210 GWd/MTU, 20-Year Cooled TPA

5-12 SAS2H Gamma Sources for 30 GWd/MTU, 4-Day Cooled BPRA

5-13 SAS2H Neutron Sources for 60 GWd/MTU, 7-10 yr Cooled MK BW 17x17 Fuel Assembly

5-14 ANSI Standard-6.1.1-1977 Flux-to-Dose Factors

5-15 Material Densities for Fuel Assembly Regions (dry)

5-16 Material Densities for Fuel Assembly Regions (wet)

5-17 NUHOMS® HD 32PTH DSC and OS-187H Material Composition (% weight)

5-18 NUHOMS® HD 32PTH DSC and OS-187H Material Composition (atm b-cm)

5-19 Composition and Densities for HSM-H Concrete

5-20 Source Axial Profile

5-21 Summary of NUHOMS® HD 32PTH DSC in the HSM-H, Maximum and Average Dose Rates

5-22 Summary of NUHOMS® HD 32PTH DSC in the OS187H TC, Maximum Dose Rates During Decontamination and Welding Operations

5-23 Summary of NUHOMS® HD 32PTH DSC in the OS187H TC, Maximum Dose Rates During Transfer Operations (Configuration C)

LIST OF FIGURES

5-1 NUHOMS® HD 32PTH System Shielding Configuration (HSM-H)

5-2 Dry Shielded Canister Shielding Configuration

5-3 Right Elevation Cross Section View of HSM-H

5-4 Shielding Configuration of the OS187H Transfer Cask

5-5 OS187H DSC and Annulus Flooded

5-6 One Quarter Cross Section DSC/Basket in Transfer Cask

5-7 OS187H Lids Installed (DSC and Annulus Dry)

5-8 HSM-H Side View at DSC Centerline

5-9 HSM-H Head-on View at X=0

5-10 HSM-H Head-on View at DSC Lid End (X=225)

5-11 HSM-H Head-on View at DSC Bottom End (X=-225)

5-12 HSM-H Detector Locations Head-on View

5-13 HSM-H Detector Locations Side View

5-14 Dose Rates Around the Top of the TC/32PTH-DSC (Configuration A)

5-15 Dose Rates Around the Top of the TC/32PTH-DSC (Configuration B)

5-16 Dose Rates Around the TC/32PTH-DSC (Transfer Configuration)

5-17 Dose Rates On the HSM-H Roof

5-18 Dose Rates On the HSM-H Front and Side

5. SHIELDING EVALUATION

The shielding evaluation presented for the NUHOMS® 32PTH System demonstrates adequacy of the shielding design for the payload described in Chapter 2. The geometry of the NUHOMS® System is described in Chapter 1. The heavy concrete walls and roof of the Horizontal Storage Module (HSM-H) provide the bulk of the shielding for the payload in the storage condition. During fuel loading and transfer operations, the combination of thick steel shield plugs at the ends of the 32PTH-DSC and heavy steel/lead/neutron shield material of the OS187H transfer cask provide shielding for personnel loading and transferring the 32PTH-DSC to the HSM-H. Figure 5-1 through Figure 5-4 and Table 5-1provide the general configuration and material thicknesses of the important components of the NUHOMS® 32PTH System.

For this shielding evaluation, source terms are calculated for the bounding Framatome ANP Advanced MK BW 17x17 (MK BW 17x17) fuel assembly. This fuel assembly is bounding because it contains the greatest mass of fuel.

Also included in the source term is the bounding Non-Fuel Assembly Hardware (NFAH) which is the BPRA.

Several burnup/enrichment combinations with minimum 5 year cooling times are addressed for the fuel to provide more flexibility in qualifying fuel for storage. These combinations form the basis for the NUHOMS® 32PTH System fuel specifications in Chapter 12. Bounding operating histories are assumed for the NFAH with a minimum cooling time of 4 days. The methodology, assumptions, and criteria used in this evaluation are summarized in the following subsections.

Section 5.4 provides a three dimensional (3-D) shielding analysis for the NUHOMS® 32PTH System using MCNP [2,6]

5.1 Discussion and Results

The maximum and average dose rates due to 32 design basis PWR fuel assemblies stored with 32 design basis NFAH (BPRAs) in the NUHOMS® 32PTH System are summarized in Table 5-2 through Table 5-5. Table 5-2 provides the dose rates on the surface of the HSM-H while Table 5-3 through Table 5-5 provide the dose rates on and around the Transfer Cask (top, bottom and sides) during fuel loading, and transfer operations.

As previously stated, the NUHOMS® HD System is capable of storing PWR spent fuel, and non-fuel assembly hardware (NFAH) such as the Burnable Poison Rod Assemblies (BPRAs), Thimble Plug Assemblies (TPAs), and Vibration Suppresser Inserts (VSIs). Based on the source term calculations presented in Section 5.2, the design basis fuel source term is the Framatome MK BW 17x17 fuel assembly with 60 GWd/MTU burnup, a minimum initial enrichment of 4.0 weight % U-235 and a cooling time of 7 years. The design basis NFAH source term is a BPRA assembly irradiated to 30 GWD/MTU and a cooled for 4 days.

A discussion of the method used to determine the design basis fuel and NFAH source terms is included in Section 5.2,. The model specification and shielding material densities are given in Section 5.3. The method used to determine the dose rates due to 32 design basis fuel assemblies with 32 design basis NFAH in the NUHOMS® 32PTH System is provided in Section 5.4.

Normal and off-normal conditions are modeled with the NUHOMS® 32PTH System intact, including the filled neutron shield in the transfer cask. The shielding calculations are performed using the MCNP Monte Carlo transport code [2]. Average and peak dose rates on the front, side, top and back of the HSM-H and the OS187H Transfer Cask System are calculated. Occupational doses during loading, transfer to the ISFSI, and maintenance and surveillance operations are provided in Chapter 10. Locations where streaming could occur are discussed in Chapter 10.

For accident conditions (e.g., cask drop, fire), the transfer cask neutron shield water (shown in Figure 5-4 is assumed to be removed and a 1 inch void in the lead due to "lead slump' is also assumed at the top and/or bottom. Site dose and occupational dose analyses are addressed in Chapter 10 (including requirements for site specific 72.104 and 72.106 analyses).

5.2 Source Specification

Source terms are calculated with the SAS2H (ORIGEN-S) module of SCALE 4.4 [1]. The following sub-sections provide a discussion of the fuel assembly and Non-Fuel Assembly Hardware (NFAH) material weights and composition, gamma and neutron source terms and energy spectrum. The SAS2H results are used to develop source terms suitable for use in the shielding calculations.

There are five principal sources of radiation associated with the NUHOMS® 32PTH System that are of concern for radiation protection. These are:

1. Primary gamma radiation from the spent fuel
2. Primary gamma radiation from activation products in the structural materials found in the spent fuel assembly and the NFAH
3. Primary neutron radiation from the spent fuel
4. Neutrons produced from sub-critical multiplication in the fuel
5. Capture gammas from (n,γ) reactions in the NUHOMS® 32PTH System materials

The first three sources of radiation are evaluated using SAS2H. The capture gamma radiation and sub-critical multiplication are handled as part of the shielding analysis which is performed with MCNP.

The neutron flux during reactor operation is peaked in the active fuel (in-core) region of the fuel assembly and drops off rapidly outside the in-core region. Much of the fuel assembly hardware is outside of the in-core region of the fuel assembly. To account for this reduction in neutron flux, each fuel assembly type is divided into four exposure zones. A neutron flux (fluence) correction is applied to each region to account for this reduction in neutron flux outside the in-core region. The correction factors are given in Table 5-6. The four exposure zones, or regions are [4]:

Bottom—location of fuel assembly bottom nozzle and fuel rod end plugs
In-core—location of active fuel
Plenum—location of fuel rod plenum spring and top plug
Top—location of top nozzle

The Framatome MK BW 17x17 assembly is the bounding fuel assembly design for shielding purposes because it has the highest initial heavy metal loading as compared to the 14x14, 15x15, and other 17x17 fuel assemblies which are also authorized contents of the NUHOMS®-32PTH DSC and described in Chapter 2. The SAS2H/ORIGEN-S modules of the SCALE code with the 44 group ENDF/B-V library are used to generate the gamma and neutron source terms. For the bounding MK BW 17x17 fuel assembly, an initial enrichment of 4.0 wt% U-235 is assumed. The fuel assembly is irradiated with a constant specific power of 25 MW/assy to a total burnup of 60 GWD/MTU. A conservative three-cycle operating history is utilized with a 20 day down time between each cycle. The fuel assembly masses for each irradiation region are listed in Table 5-7.

Data for the WE 17x17 assembly is from Reference [7]. Some values for the WE 15x15 were assumed to be the same as the WE 17x17. The design-basis heavy metal weight is 0.476 MTU. These masses are irradiated in the appropriate fuel assembly region in the SAS2H/ORIGEN-S models. The mass of hardware for the MK BW 17x17 assembly is the greatest; however, the source term from the irradiated hardware for the WE 17x17 is bounding.

If reconstituted fuel assemblies (considered as intact fuel in the criticality analyses) with stainless steel rods undergo further irradiation, their gamma source term on a per DSC basis shall be bounded by the total design basis gamma source terms shown (on an assembly basis) in Table 5-10 for the design basis fuel assembly.

TPA

The TPA materials and masses for each irradiation zone are listed in Table 5-8. These materials are irradiated in the appropriate zone for fourteen cycles of operation. The TPA is irradiated to an equivalent assembly life burnup of 210 GWd/MTU over 14 cycles. The model assumes that the TPA is irradiated in an assembly each with an initial enrichment of 3.50 weight % U-235.The fuel assembly, containing the TPA, is burned for three cycles with a burnup of 15 GWd/MTU per cycle. This is equivalent to an assembly life burnup of 45 GWd/MTU over the three cycles. The results for a cooling time of 20 years are increased by the ratio of 14/3 to achieve the equivalent 210 GWD/MTU source.

BPRA

The BPRA materials and masses for each irradiation zone are also listed in Table 5-8. These materials are irradiated in the appropriate zone for three cycles of operation. The model assumes that the BPRA is irradiated in an assembly each with an initial enrichment of 3.50 weight % U-235. The fuel assembly containing the BPRA is burned for three cycles with a burnup of 10 GWd/MTU per cycle. This is equivalent to an assembly life burnup of 30 GWd/MTU over the three cycles. The source term for the BPRA is taken at 4 days cooling time.

VSI

VSIs are very similar in design to burnable poison rod assemblies: the stainless steel baseplate and hold-down spring assembly designs are identical to those used on older Westinghouse BPRAs. Each VSI contains 24 solid Zircalloy-4 damper rods that are attached to the hold-down assembly using a crimp nut top connector. The damper rods are the same diameter and length as BPRA rodlets. The VSIs are assumed to be equivalent in source strength to BPRAs.

Elemental Compositions of Structural Materials

To account for the source terms due to the elemental composition of the fuel assembly and NFAH structural materials the following methodology is used:

1) The material composition for each irradiation region is determined for the assembly and NFAH type.

2) The elemental compositions for each of the structural materials present in each region is determined by multiplying the total weight of each material in a specific irradiation zone (Table 5-7) by the elemental compositions. The fuel assembly and NFAH elemental composition, including impurities, for each material are taken from Reference [7].

3) The results of each material are summed to determine the total elemental composition for each irradiation zone.

4) The elemental composition is multiplied by the appropriate flux factor given in Table 5-6.

5) Finally, the elemental composition is entered in the light element card of the SAS2H input. The elemental composition for the fuel assembly is shown in Table 5-9.

The SAS2H calculation applies the total flux to the light elements; therefore, the total composition must be adjusted by the appropriate flux factor in the input. A SAS2H input is created for each irradiation zone of each fuel assembly and NFAH type. An example input file for the active fuel zone is shown in Section 5.5.2.

5.2.1 Gamma Sources

Source terms for the fuel bounding Framatome MK BW 17x17 fuel assembly and associated burnup/initial enrichment/cooling times and NFAH components are calculated with SAS2H module and the 44 group ENDF/B-V library. The SAS2H calculated contributions from actinides, fission products, and activation products, as applicable, are included for each irradiation region. The 7-year post irradiation cooling time results for the MK BW 17x17 fuel with 60 GWD/MTU burnup, and 4.0 wt % U-235 initial enrichment are shown in Table 5-10. The post irradiation cooling time results for the TPA, and BPRA are shown in Table 5-11, and Table 5-12, respectively.

Based on the results presented in Table 5-11 and Table 5-12 (maximum gamma source term) the design basis NFAH is the BPRA. The spectrum is dominated by Co-60 for all NFAH. These design basis fuel assembly sources with the BPRA source are used in the MCNP calculations to determine the bounding dose rates on and around the NUHOMS® 32PTH System, including the Transfer Cask.

5.2.2 Neutron Source

The total neutron source for the NUHOMS® 32PTH System is also calculated with SAS2H. The total neutron sources for the MK BW 17x17 assembly is summarized in Table 5-13. Again, the design basis source term is for 60 GWd/MTU burnup, 4.00 weight % U-235 initial enrichment and 7-year cooling time. The neutron source term consists primarily of spontaneous fission neutrons (largely from Cm-244) with (α,O-18) sources of lesser importance, both causing secondary fission neutrons. The overall spectrum is well represented by the Cm-244 fission spectrum.

5.3 Model Specification

The neutron and gamma dose rates on the surface of the HSM-H, and on the surface, and at 1.5 and 3 feet from the surface of the OS187H Transfer Cask are evaluated with the Monte Carlo transport code MCNP [2, 6]. The flux-to-dose conversion factors specified by the ANSI/ANS 6.1.1-1977 5, are used and provided in Table 5-14.

5.3.1 Description of the Radial and Axial Shielding Configurations

Figure 5-1 is a sketch of an HSM-H cut away at the mid-vertical plane. Figure 5-3 is also a cut through the vertical mid-plane, the 32PTH-DSC is shown in phantom lines, and the front door is at the left hand side. The rear wall of the HSM-H module has a minimum thickness of 1 foot. A 3-foot shield wall is placed along the rear and sides of the HSM-H, as shown in Figure 5-1.

The MCNP computer models are built to evaluate the dose rate along the front wall surface, the rear shield wall surface, the vent openings, the roof surface, and on the side shield walls.

Figure 5-4 shows the shielding configuration of the OS187H transfer cask.

5.3.1.1 Storage Configuration

A three-dimensional MCNP model was developed for the HSM-H Model. The HSM length was designated as the x axis (North-South direction), the width as the y axis (East-West direction), and the HSM height as the z axis. The HSM door is designated as the S side and the –x direction, with the E wall as the –y direction. The roof is the +z direction. The E wall is designated as a reflective boundary and an end shield wall (3 ft thick) is attached to the W wall. The geometry of nearly all components of the HSM is Cartesian, except for the 32PTH-DSC, which is cylindrical. The MCNP model is a full 3-D representation of a single DSC inside the HSM-H with the reflective boundary, end and side shield walls. A three foot thick concrete shield wall is placed at the rear of the HSM. A NUHOMS®-32PTH-DSC MCNP model was developed for the transfer cask analysis, discussed below. This model was revised slightly and located within the HSM model. The DSC support rails are not included in the model. The heat shields are modeled as flat plates without fins or louvers and horizontal vent "liner" plates (2cm thk) are modeled in the top side vents.

Two liners are used for gamma dose attenuation at the bottom vents. The "top" liner is a 1-inch steel plate, positioned at the roof of the bottom vent. The "front" liner is a 1-inch steel plate, at the side of the inlet vent (near the HSM front). Due to modeling constraints the "front" liner is modeled as part of the vent. This simplification does not impact the overall gamma dose rates.

5.3.1.2 Loading/Unloading Configurations

The dose rates on the surface, and at 1.5 and 3 feet from the surface of the 32PTH-DSC/ Transfer Cask are evaluated with MCNP. Three different key configurations in the loading/unloading of the spent fuel are analyzed. The three different stages modeled are, (1) Decontamination, (2) Dry Welding and (3) Transfer. Calculations are performed assuming no temporary shielding is utilized for in the configurations, which is normally done at the sites.

Definition of Transfer Cask and 32PTH-DSC Loading Stages

1) Decontamination. The water level in the 32PTH-DSC cavity is assumed to be lowered four inches below the bottom of the top shield plug. The Cask/32PTH-DSC annulus is assumed to remain completely filled with water. (No DSC top cover or cask lid)

2) Dry welding. The 32PTH-DSC cavity is assumed to be completely dry, the 32PTH-DSC inner and outer top cover plates have been installed. The Cask/32PTH-DSC annulus is assumed to remain completely filled with water. (no cask lid)

3) Transfer. The 32PTH-DSC and 32PTH-DSC/Cask annulus are dry.

Dose analysis results for the above conditions are provided in Table 5-22 and Table 5-23.

5.3.1.3 Transfer Configuration

For the transfer configuration the Transfer Cask/32PTH-DSC annulus is completely dry. The 32PTH-DSC inner and outer top cover plates are installed. The top end of the Transfer Cask is in place which consists of a 3" thick steel cover plate and a 2" thick solid neutron shield, and a ¼" thick steel plate cover is over the solid neutron shield.

A three-dimensional MCNP model was developed for the OS-187H transfer cask containing the NUHOMS®-32PTH DSC. The cask/canister length was designated as the z axis (axial direction), the radial direction as the x and y axis. The 32PTH-DSC basket compartments and rails were discreetly modeled in MCNP. The basket was simply modeled as the 8.70" sq, 0.187" thk SS compartments, each compartment surrounded by 0.5" of aluminum. Conservatively, neither boron in the aluminum, nor the SS strips were included in the MCNP basket model. Each of the 32 fuel assemblies was modeled in four axial regions; bottom fitting, fuel, plenum, and top fitting. The axial length of each fuel assembly region modeled was; 4.17", 144", 6.95", and 6.17", respectively. The lead thickness (3.60" nom) in the OS-187H is modeled as 3.56" of lead with a 0.04" void and the density of the lead is reduced to 0.985 TD.

The neutron shield support rings provide support for the skin, which contains the water for the neutron shield. The rings are modeled explicitly in the water filled neutron shield. The trunnions penetrate the neutron shield, which locally changes the shielding configuration of the neutron shield. The trunnions which are explicitly modeled are thick steel structures filled with solid resin neutron shielding material. These structures provide more gamma and neutron shielding than the water that they replace, because they protrude well past the neutron shield and are made of materials which provide more gamma shielding and comparable neutron shielding as compared to the water that they replace.

5.3.2 Shield Regional Densities

Table 5-7 shows the material masses for the four fuel assembly regions. Based on these material masses, and the material compositions [7], material densities for the fuel assembly regions are determined and provided in Tables 5-15 and 5-16 (loading configuration 1 above).

The mass of materials in each fuel assembly region is homogenized over the volume of the region (x-section = 71 in^2). Tables 5-17 and 5-18 provide the shield regional densities for the 32PTH-DSC and OS187H TC.

The concrete for the HSM-H is chosen to be "plain" concrete with a density of 148 lbs/ft^3 with the rebar conservatively neglected. Table 5-19 provides the concrete densities.

The actual fuel layout in the 32PTH-DSC is a cartesian array of fuel assemblies inside stainless steel compartments surrounded by sheets of aluminum material. These regions are modeled discretely as are the rails on the periphery of the basket. A source is modeled for each of the four homogenized fuel assembly regions for all 32 fuel assemblies. The source regions are cuboid in shape with the same 8.426" x 8.426" (17 times the Pitch) x-section and the appropriate axial length.

When the transfer cask/32PTH-DSC annulus and 32PTH-DSC are filled with water, the wet axial densities are used for the homogenized regions.

5.4 Shielding Evaluation

5.4.1 Computer Programs

MCNP [2, 6] is a general-purpose Monte Carlo N-Particle code that can be used for neutron, photon, electron, or coupled neutron/photon/electron transport. The code treats an arbitrary three-dimensional configuration of materials in geometric cells bounded by first- and second-degree surfaces and some special fourth-degree surfaces. Pointwise (continuous energy) cross-section data are used. For neutrons, all reactions given in a particular cross-section evaluation are accounted for in the cross section set. For photons, the code takes account of incoherent and coherent scattering, the possibility of fluorescent emission after photoelectric absorption, absorption in pair production with local emission of annihilation radiation, and bremsstrahlung. Important standard features that make MCNP very versatile and easy to use include a powerful general source; an extensive collection of cross-section data; and an extensive collection of variance reduction techniques that can be employed to track particles through very complex deep penetration problems.

5.4.2 Spatial Source Distribution

The source components are:

- A neutron source due to the active fuel regions of the 32 fuel assemblies,
- A gamma source due to the active fuel regions of the 32 fuel assemblies,
- A gamma source due to the plenum regions of the 32 fuel assemblies,
- A gamma source due to the top nozzle regions of the 32 fuel assemblies,
- A gamma source due to the bottom nozzle region of the 32 fuel assemblies,
- A gamma source due to the 32 BPRAs in the top nozzle, plenum and fuel regions of the 32 fuel assemblies

Axial burnup peaking factors for PWR fuel are taken from Reference [4]. These peaking factors are assumed to match the gamma axial source distribution because the gamma source is proportional to burnup. The neutron source is approximately proportional to the fourth power of the burnup. Therefore, the axial neutron source distribution may be determined as the fourth power of the axial burnup profile.

Axial peaking changes with increasing burnup. The axial peaking factors used are provided in Table 5-20. The OS187H TC and HSM-H calculations use peaking factors for a burnup >46 GWd/MTU because the design basis source occurs at a burnup of 60 GWd/MTU. The neutron and gamma peaking factors are shown as a function of the core height in Table 5-20. These factors are directly applied to each MCNP interval in the fuel region.

The average values of the axial peaking distributions are also provided in Table 5-20. For the gamma distribution, the average value is 1.00. However, for the neutron distribution, the average value of the distribution is greater than 1.00. The average value of the axial neutron distribution may be interpreted as the ratio of the true total neutron source in an assembly to the neutron source calculated by SAS2H/ORIGEN-S for an average assembly burnup.

Therefore, to properly correct the magnitude of the neutron source, the neutron source per assembly as reported in Table 5-13 is multiplied by the average value of the neutron source distribution as reported in Table 5-20.

5.4.3 Cross-Section Data

The cross-section data used is the continuous energy ENDF/B provided with the MCNP code. The cross-section data allows coupled neutron/gamma-ray dose rate evaluation to be made to account for secondary gamma radiation (n,γ), if desired. All of the transfer cask dose rate calculations account for the dose rate due to secondary gamma radiation. For the HSM-H dose rate calculation, the dose rate contribution from the secondary gamma radiation is ignored because it is insignificant.

5.4.4 Flux-to-Dose-Rate Conversion

The flux distribution calculated by the MCNP code is converted to dose rates using flux-to-dose rate conversion factors from ANSI/ANS-6.1.1-1977 [5] given in Table 5-14.

5.4.5 Model Geometry

Figure 5-5 through Figure 5-7 are the MCNP models for the Transfer Cask (TC) containing the 32PTH-DSC. Figures 5-8 through Figure 5-11 are the MCNP models of the HSM-H with the DSC . The figures show dimensions in cm with MCNP surface numbers in brackets. Figures 5-12 and 5-13 show the location of the detectors cells on the HSM surfaces.

5.4.6 Methodology

The methodology used in the shielding analysis of the 32PTH system utilizes the 3-D MCNP code. MCNP allows for explicit 3-D modeling of any shielding configuration and reduces the number of approximations needed. The methodology used herein is summarized below.

1. Sources are developed for all fuel regions using the source term data developed in Section 5.2. Source regions include the active fuel region, bottom end fitting (including all materials below the active fuel region), plenum, and top end fitting (including all materials above the active fuel region). Sources for NFAH are added group-by-group to the fuel sources.
2. Suitable shielding material densities are calculated for all regions modeled.
3. The 3-D Monte Carlo transport code MCNP is used to calculate dose rates on and around the HSM-H and theOS187H TC. The MCNP4 code is selected because of its ability to handle thick, multi-layered shields and account for streaming through both the HSM-H air vents and cask/DSC annulus using 3-D geometry. MCNP4C2 results are used to calculate offsite exposures (see Chapter 10).
4. For the TC, weight windows are utilized for variance reduction. Segmented surface (ring) detectors are used to tally surfaces for dose rate determinations.

For the HSM-H, importance biasing is utilized for variance reduction and tally cells and segmented tally cells are used to determine average and maximum dose rates around the HSM-H.

5. MCNP models are also generated to determine the effects of accident scenarios, such as loss of cask neutron shield, for the OS187H TC.

5.4.7 Assumptions

The following general assumptions are used in the analyses.

5.4.7.1 Source Term Assumptions

1. The primary neutron source in LWR spent fuel is the spontaneous fission of ^{244}Cm. For the ranges of exposures, enrichments, and cooling times in the fuel qualification tables, ^{244}Cm represents more than 85% of the total neutron source. The neutron spectrum is, therefore, relatively constant for the fuel parameters addressed herein and is assumed to follow the ^{244}Cm fission spectrum.

2. Surface gamma dose rates are calculated for the HSM and cask surfaces using the actual photon spectrum applicable for each case.

3. The PWR heavy metal weight is assumed to be 0.476 MTU per assembly to bound existing PWR fuel designs.

4. The source term associated with the BPRAs are bounding for all NFAH (TPAs and VSIs).

5.4.7.2 HSM-H Dose Rate Analysis Assumptions

1. Planes of reflection are used to simulate adjacent HSM-Hs.

2. Embedments and rebar in the HSM-H concrete are conservatively neglected.

3. The borated neutron absorber sheets in the 32PTH-DSC are modeled as aluminum.

4. Axial source distribution assumed as shown in Table 5-20.

5. Fuel is homogenized within the fuel compartment and source region, although the 32PTH-DSC basket is modeled explicitly.

5.4.7.3 OS187H TC Dose Rate Analysis Assumptions

1. The 32PTH-DSC is modeled within the OS187H TC.
2. The OS187H is modeled for the welding operation. No supplemental neutron shielding is assumed to be placed on top of the 32PTH-DSC cover plates during welding.
3. During the accident case, the cask neutron shield (water) is assumed to be lost and a lead slump of 1" is assumed in the cask end.
4. The borated neutron absorber sheets in the 32PTH- DSC are modeled as aluminum.
5. The stainless steel strip plates are conservatively modeled as aluminum.
6. Axial source distribution assumed as shown in Table 5-20.
7. Fuel is homogenized within the fuel compartments and the source regions, although the 32PTH-DSC baskets are modeled explicitly.
8. In the OS187H TC model, the lead shield is assumed at the minimum thickness and with reduced density.

5.4.8 Normal Condition Models

Two basic MCNP models are developed: (1) 32PTH- DSC in the HSM-H and (2) 32PTH-DSC in the OS187H TC. These models are described in subsequent sections.

5.4.8.1 32PTH DSC in HSM-H

Two, three-dimensional MCNP4C2 models are developed for the 32PTH-DSC within a HSM-H, one model for neutrons and the other for gammas. These models are presented in Figures 5-8 through Figure 5-11. The HSM-H length is designated as the x axis, the width as the y axis, and the height as the z axis. The HSM-H door is designated as the south side and the –x direction, with the east wall as the –y direction. The roof is the +z direction. The east wall is designated as a reflective boundary and an end shield wall (3 ft thick) is attached to the west wall.

The bottom (bottom of bottom fitting) of the fuel assembly is assigned to an x plane at -213.84 cm. The center of the HSM-H is at y=0 and z=0. The 32PTH-DSC lid is located 5" from the HSM-H rear wall (x=254.84 cm) which places the bottom of the DSC at x=-215.69 cm, about 20 inches from the door interior. The 32PTH-DSC support rails are not included in the model. The heat shields are modeled as flat plates without fins or louvers, and horizontal vent "liner" plates (2 cm thick) are modeled in the top side vents.

Dose rates are calculated on thin cells surrounding the HSM-H and are segmented into 30 cm increments to capture the peak dose rates. Dose rates are also calculated at the inlet and outlet vents. Dose rates for this scenario are provided in Table 5-21. Dose rates for the front, roof, and side shield wall surface at DSC centerline of the HSM-H are also plotted as a function of distance in Figures 5-17 and 5-18 respectively.

A sample MCNP4C2 model input file of HSM-H with 32PTH-DSC is included in Section 5.5.2.

5.4.8.2 32PTH- DSC in OS187H TC

Two three-dimensional MCNP4B models are employed for shielding analyses of the 32PTH-DSC within an OS187H TC, one model for neutrons and the other for gammas. These models are presented in Figure 5-5 through Figure 5-7. The DSC/TC length was designated as the z-axis in the MCNP models. Select features within the cask and on its surface are neglected because they produce only localized effects and have minimal impact on operational dose rates. Examples of neglected features include relief valves, clevises, and eyebolts.

These items are local features that increase the shielding in a small area without replacing any of the shielding material which is included in the model. The additional shielding material that these features provide is not smeared into the bulk shielding, nor is any credit taken for it in the occupational exposure calculation. The neutron shield support rings provide support for the neutron shield skin, which contains the water for the neutron shield. The fifteen rings are modeled explicitly within the neutron shield.

The trunnions penetrate the neutron shield, which locally changes the shielding configuration of the neutron shield. The trunnions are thick steel structures filled with solid neutron shielding material. These structures protrude well past the neutron shield and are made of materials which provide more gamma shielding and comparable neutron shielding as compared to the 0.96 g/cm^3 water that these replace. The trunnions are also modeled explicitly in MCNP.

Design features relevant to the shielding analysis of the OS187H TC and 32PTH-DSC are modeled in MCNP4B. The overall length of the OS187H TC is 193.32". The outer diameter of the OS187H TC is 92.20" (neutron shield included). The outer diameter excluding the neutron shield is 82.70". The bottom of the OS187H TC is designed to mate with a 32PTH-DSC. The overall length of the 32PTH-DSC is 185.75" (excluding the grapple) and its outer diameter is 69.75". The bottom end of the 32PTH-DSC is in contact with the structural shell assembly of the transfer cask.

In section 5.3.1.2 and 5.3.1.3, the three transfer cask scenarios are described. The basic MCNP models for the OS187H TC described above are modified as described below to represent the loading/transfer configurations.

A. Cask Decontamination

The 32PTH-DSC and the OS187H TC are assumed to be filled with water, including the region between 32PTH-DSC and cask, which is referred to as the "cask/32PTH-DSC annulus." The water in the DSC is assumed to be approximately 4" below the shield plug. The 32PTH-DSC shield plug is assumed to be in place and the temporary shielding has not yet been installed. The DSC top cover and cask lid are not installed. Results for this case are provided in Table5-22.

B. Welding and DSC Draining

Before the start of welding operation, water in the DSC cavity is removed to reduce the potential due to hydrogen generation. A dry DSC cavity is assumed in all welding models to be conservative. Temporary shielding is not installed. In addition, the cask lid is not installed. The cask/32PTH-DSC annulus is assumed to remain completely filled with water. Results for this case are provided in Table 5-22.

C. Transfer

In preparation for transfer to the HSM, the DSC is drained, dried, the tops welded on, the annulus drained, and the cask lid installed. Results for this case are provided in Table 5-23 along with accident dose rates (loss of water in neutron shield tank and 1" lead slump).

Dose rates at the sides, top, and bottom of this cask are presented graphically in Figure 5-14 through Figure 5-16.

A sample MCNP4B model input file for OS187H TC with 32PTH-DSC is included in Section 5.2.2.

5.5 Supplemental Information

5.5.1 References

1. Oak Ridge National Laboratory, RSIC Computer Code Collection, "SCALE: A Modular Code System for Performing Standardized Computer Analysis for Licensing Evaluations for Workstations and Personal Computers," NUREG/CR-0200, Revision 6, ORNL/NUREG/CSD-2/V2/R6.

2. MCNP4B2, "Monte Carlo N-Particle Transport Code System," Los Alamos National Laboratory, CCC-660, RSIC, January 1998.

3. Radiation Shielding, J. Kenneth Shultis and Richard E. Faw, Pretence Hall, 1996.

4. "Recommendations for Addressing Axial Burnup in PWR Burnup Credit Analyses," NUREG/CR-6801, March 2003.

5. "American National Standard Neutron and Gamma-Ray Flux-to-Dose Rate Factors". ANSI/ANS-6.1.1-1977, American Nuclear Society, La Grange Park, Illinois. March 1977.

6. MCNP4C2, "Monte Carlo N-Particle Transport Code System," Los Alamos National Laboratory, CCC-701, RSIC, June 2001.

7. Ludwig, S.B., and J.P. Renier, "Standard- and Extended-Burnup PWR and BWR Reactor Models for the ORIGEN2 Computer Code," ORNL/TM-11018, Oak Ridge National Laboratory, December 1989.

THIS PAGE IS INTENTIONALLY LEFT BLANK

5.1.1 Sample Input Files

(PROPRIETARY INFORMATION)

Figure Withheld Under 10 CFR 2.390

Table 5-1
NUHOMS® HD 32PTH System Shielding Materials

HSM-H

Components	Thickness/Material Modeled
Side Walls	1' concrete
Side Shield Wall	3' concrete
Roof	4' concrete
Rear Wall	Minimum thickness 1' concrete
Rear Shield Wall	3' concrete
Front Door/Front Wall	2.5'/3.5' thick concrete

32PTH-DSC

Components	Thickness/Material Modeled
Bottom Shield Plugs/Cover Plates	8.75" Steel
Top Shield Plugs/Cover Plates	12.00" Steel
Cylindrical shell	0.50" Steel
Basket (main components)	32 Stainless Steel Fuel compartments, 3/16" thick each, and aluminum/ borated aluminum plates total ½" thk

OS187H Transfer Cask

Components	Thickness/Material Modeled
Top Cover Plate	2" resin and 3.25" Steel
Bottom Cover Plate	2.25" resin and 2.75" Steel
Radial walls	
Inner Shell	0.5" Steel
Lead Gamma Shield	3.56" Lead
Structural Shell	1.5"/2.00" Steel
Neutron Shield	4.56" Water
Skin	0.19" Steel

Table 5-2
Summary HSM-H Dose Rates

Surface	Dose Rate Component	Average Surface Dose Rate(2), mrem/hr
Rear(1)	Gamma	0.5
	Neutron	<0.1
Front	Gamma	5.5
	Neutron	0.5
Roof	Gamma	13.9
	Neutron	1.9
Side(1)	Gamma	0.4
	Neutron	0.2

(1) Rear and side does rates are on the outer surfaces of the shield walls.

(2) These dose rates are bounding for 1 meter occupational exposures during transfer operations.

Table 5-3
Transfer Cask (Loading/Unloading/Transfer Operations) Side Dose Rate Summary

Stage of TC/32PTH-DSC Processing	Dose Rate mrem/hr	On Outside Surface		1.5' from Surface		3' from Surface	
		Gamma	Neutron	Gamma	Neutron	Gamma	Neutron
Decontamination	Maximum	241	158	153	95.7	107	65.4
	Minimum	7.8	0.4	26.0	4.0	29.4	8.8
	Average(1) Surface	162	93.9	105	61.2	75.0	43.6
Welding	Maximum	310	95.8	198	59.0	139	40.9
	Minimum	12.3	10.9	27.4	4.2	37.3	10.7
	Average(1) Surface	206	59.3	136	37.3	97.5	26.9
Transfer	Maximum	384	125	238	77.0	165	54.7
	Minimum	15.1	22.2	31.8	7.5	44.2	13.0
	Average(1) Surface	254	81.4	163	50.0	116	35.5

Notes:
(1) Surface weighted average of ring detectors used as tally surfaces

Table 5-4
Transfer Cask (Loading/Unloading/Transfer Operations) Top End Dose Rate Summary

Stage of TC/32PTH-DSC Processing	Dose Rate mrem/hr	On Outside Surface		1.5' from Surface		3' from Surface	
		Gamma	Neutron	Gamma	Neutron	Gamma	Neutron
Decontamination	Maximum	933	118	688	52.0	513	27.5
	Minimum	314	31.7	337	15.1	281	12.2
	Average(1) Surface	646	66.8	430	26.5	361	17.0
Welding	Maximum	95.5	328	77.6	192	52.5	102
	Minimum	39.4	63.1	41.0	66.9	32.0	53.1
	Average(1) Surface	58.9	145	52.7	106	43.3	69.7
Transfer-Storage	Maximum	8.8	24.5	5.2	14.1	3.5	8.7
	Minimum	5.0	11.5	3.9	5.5	2.8	4.5
	Average(1) Surface	6.1	14.1	4.2	8.1	3.0	5.7

Notes:
(1) Surface weighted average of ring detectors used as tally surfaces

Table 5-5
Cask (Loading/Unloading/Transfer Operations) Bottom End Dose Rate Summary

Stage of TC/32PTH-DSC Processing	Dose Rate mrem/hr	On Outside Surface		One Foot from Surface		Three Feet from Surface	
		Gamma	Neutron	Gamma	Neutron	Gamma	Neutron
Transfer	Maximum	475	1350	118	305	53.1	117
	Minimum	9.5	43.3	13.6	40.4	14.0	39.5
	Average(1) Surface	36.5	134	29.7	86.9	23.3	58.9

Notes:
(1) Surface weighted average of ring detectors used as tally surfaces

Table 5-6
Flux Factor By Fuel Assembly Region

Fuel Assembly Region	Flux Factor
Bottom	0.20
In-Core	1.00
Plenum	0.20
Top	0.10

Table 5-7
Westinghouse Fuel Assembly Materials and Masses

Region	Material	Mass (kg/assembly) WE 15x15	WE 17x17	MK BW 17x17
Top Fitting				
Upper Tie Plate	SS 304	6.8	6.8	7.0
Hold Down Springs	Inconel 718	1.1	1.37	1.1
Plenum				
Cladding & Guide Tubes	Zr-4	6.1	5.5	6.3
Plenum Spring	SS 302	1.5	1.9	4.7
Fuel Zone				
Cladding & Guide Tubes	Zr-4	99.2	102.9	109.9*
Grids	Zr-4			8.2
	Inconel-718	5.9	5.9	0.8
Grid Brazing Material				
	Nicrobraze 50	1.2	1.2	-
Miscellaneous				
	SS 304	4.6	4.6	0.1*
Bottom Fitting				
Bottom Tie Plate	SS 304	5.7	5.7	4.3
Total		132.1	135.6	142.4

* Clad is M5™ which is treated as Zr-4

Table 5-8
NFAH Materials and Masses

Component	Region	Material	Mass (kg)
TPA	Top Fitting		
	Baseplate, yoke, holddown bar, etc.	Type 304 SS	2.5
	spring	Inconel 718	0.36
	Plenum		
	Thimble plugs	Type 304 SS	3.3
BPRA/ VSI	Top Fitting		
	Baseplate, yoke, holddown bar, etc	Type 304 SS	2.5
	spring	Inconel 718	0.36
	Plenum		
	Cladding & liner	Type 304 SS	0.80
	Fuel Zone		
	Cladding & liner	Type 304 SS	15.0

Table 5-9
Fuel Assembly Material Masses (kg/assembly)

Scaling Factors	0.1	0.2	1	0.2	
	Top Fitting	Plenum	Active Fuel	Bottom Fitting	Total
15x15					
Chromium	0.1501	0.0555	2.2972	0.2166	2.7194
Manganese	0.0138	0.0060	0.1059	0.0228	0.1485
Iron	0.4879	0.2121	4.4512	0.7848	5.9360
Cobalt	0.0011	0.0003	0.0328	0.0009	0.0350
Nickel	0.1178	0.0268	4.3714	0.1017	4.6177
Zirconium	0.0000	1.1945	97.128	0.0000	98.322
Aluminum	0.0007	0.0000	0.0380	0.0000	0.0387
Silicon	0.0070	0.0030	0.0124	0.0000	0.0224
Titanium	0.0009	0.0000	0.0473	0.0000	0.0481
Niobium	0.0061	0.0000	0.3272	0.0000	0.3333
Molybdenum	0.0033	0.0000	0.1768	0.0000	0.1801
Tin	0.0000	0.0195	1.6608	0.0182	1.6986
17x17					
Chromium	0.1551	0.0698	2.3018	0.2166	2.7433
Manganese	0.0139	0.0076	0.1060	0.0228	0.1503
Iron	0.4927	0.2676	4.4595	0.7848	6.0047
Cobalt	0.0012	0.0003	0.0329	0.0009	0.0353
Nickel	0.1317	0.0339	4.3715	0.1017	4.6388
Zirconium	0.0000	1.0770	100.75	0.0000	101.83
Aluminum	0.0008	0.0000	0.0381	0.0000	0.0389
Silicon	0.0071	0.0038	0.0124	0.0182	0.0415
Titanium	0.0011	0.0000	0.0473	0.0000	0.0484
Niobium	0.0076	0.0000	0.3272	0.0000	0.3348
Molybdenum	0.0041	0.0000	0.1768	0.0000	0.1809
Tin	0.0000	0.0176	1.7200	0.0182	1.7558

Table 5-10
SAS2H Gamma Sources for 60 GWd/MTU, 7-Year Cooled
MK BW 17x17 Fuel Assembly

(γ/s/assembly)

Energy Interval (meV)			Fuel	Bottom	Plenum	Top
1.000E-02	to	5.000E-02	1.532E+15	1.298E+11	1.499E+11	1.096E+11
5.000E-02	to	1.000E-01	4.151E+14	1.643E+10	2.080E+10	2.136E+10
1.000E-01	to	2.000E-01	3.240E+14	8.873E+09	9.762E+09	5.155E+09
2.000E-01	to	3.000E-01	9.290E+13	4.910E+08	5.335E+08	2.563E+08
3.000E-01	to	4.000E-01	6.066E+13	1.432E+09	1.462E+09	3.356E+08
4.000E-01	to	6.000E-01	7.102E+14	2.627E+10	2.539E+10	2.121E+07
6.000E-01	to	8.000E-01	3.087E+15	1.360E+10	1.314E+10	9.567E+08
8.000E-01	to	1.000E+00	3.374E+14	1.819E+10	6.393E+09	1.248E+10
1.000E+00	to	1.330E+00	2.748E+14	4.704E+12	5.982E+12	6.234E+12
1.330E+00	to	1.660E+00	7.314E+13	1.328E+12	1.689E+12	1.760E+12
1.660E+00	to	2.000E+00	5.506E+11	3.493E-01	4.747E+01	4.592E-01
2.000E+00	to	2.500E+00	7.537E+11	3.152E+07	4.009E+07	4.178E+07
2.500E+00	to	3.000E+00	3.712E+10	4.888E+04	6.217E+04	6.478E+04
3.000E+00	to	4.000E+00	4.718E+09	1.175E-14	3.835E-15	1.289E-09
4.000E+00	to	5.000E+00	3.768E+07			
5.000E+00	to	6.500E+00	1.512E+07			
6.500E+00	to	8.000E+00	2.966E+06			
8.000E+00	to	1.000E+01	6.298E+05			
		Total:	6.908E+15	6.247E+12	7.899E+12	8.144E+12

Table 5-11
SAS2H Gamma Sources for 210 GWd/MTU, 20-Year Cooled TPA

light elements - TPA - plenum zone						
				3 cycles		**14 cycles**
	energy interval			γ/second	Fraction	5.5.1.1.1.1
36	1.33E+00	to	1.660E+00	1.03E+11	2.202E-01	4.814E+11
37	1.00E+00	to	1.330E+00	3.65E+11	7.798E-01	1.705E+12
	Total:			4.685E+11		2.186E+12
light elements - TPA - Top Fitting Zone						
	energy interval			γ/second		γ/second
36	1.33E+00	to	1.660E+00	8.19E+10	2.202E-01	3.823E+11
37	1.00E+00	to	1.330E+00	2.90E+11	7.798E-01	1.354E+12
	Total:			3.720E+11		1.736E+12

Table 5-12
SAS2H Gamma Sources for 30 GWd/MTU, 4-day Cooled BPRA

BPRA Source (γ/s/BPRA)

E_{min}, MeV		E_{max}, MeV	Top Region	Plenum Region	In-core Region
0.00E+00	to	5.00E-02	1.170E+11	3.328E+10	3.14E+12
5.00E-02	to	1.00E-01	3.261E+10	9.260E+09	8.73E+11
1.00E-01	to	2.00E-01	1.736E+10	4.906E+09	4.63E+11
2.00E-01	to	3.00E-01	4.695E+09	1.316E+09	1.24E+11
3.00E-01	to	4.00E-01	1.128E+12	5.018E+11	4.74E+13
4.00E-01	to	6.00E-01	5.321E+11	1.474E+11	1.39E+13
6.00E-01	to	8.00E-01	5.487E+08	1.521E+08	1.44E+10
8.00E-01	to	1.00E+00	2.224E+12	7.587E+11	7.16E+13
1.00E+00	to	1.33E+00	2.702E+12	6.848E+11	6.44E+13
1.33E+00	to	1.66E+00	7.630E+11	1.934E+11	1.82E+13
1.66E+00	to	2.00E+00	8.185E+09	2.267E+09	2.14E+11
2.00E+00	to	2.50E+00	1.811E+07	4.590E+06	4.31E+08
2.50E+00	to	3.00E+00	2.808E+04	7.119E+03	6.69E+05
3.00E+00	to	4.00E+00	3.434E-01	1.718E-01	1.63E+01
4.00E+00	to	5.00E+00	0.000E+00	0.000E+00	0.00E+00
5.00E+00	to	6.50E+00	0.000E+00	0.000E+00	0.00E+00
6.50E+00	to	8.00E+00	0.000E+00	0.000E+00	0.00E+00
8.00E+00	to	1.00E+01	0.000E+00	0.000E+00	0.00E+00
		Total:	7.529E+12	2.337E+12	2.20E+14

Table 5-13
SAS2H Neutron Sources for 60 GWD/MTU, 7-10 yr Cooled Fuel
MK BW 17x17 Fuel Assembly

(n/sec/assembly)

Grp	Energy Interval (meV)			7 yr	8 yr	9 yr	10 yr
1	6.43	-	20.0	2.036E+07	1.957E+07	1.882E+07	1.810E+07
2	3.00	-	6.43	2.297E+08	2.209E+08	2.124E+08	2.044E+08
3	1.85	-	3.00	2.519E+08	2.423E+08	2.331E+08	2.244E+08
4	1.40	-	1.85	1.433E+08	1.377E+08	1.325E+08	1.275E+08
5	0.90	-	1.40	1.948E+08	1.872E+08	1.800E+08	1.732E+08
6	0.40	-	0.90	2.129E+08	2.047E+08	1.968E+08	1.893E+08
7	0.10	-	0.40	4.168E+07	4.007E+07	3.853E+07	3.706E+07
			Total:	1.095E+09	1.052E+09	1.012E+09	9.740E+08

Table 5-14
ANSI Standard-6.1.1-1977 Flux-to-Dose Factors

Photon energy (MeV)	Response Function (rem/hr)/(γ/cm^2-s)	Neutron energy (MeV)	Response Function ((rem/hr)/(n/cm^2-s)
0.01	3.96E-06	2.5E-08	3.67E-06
0.03	5.82E-07	1.0E -07	3.67E-06
0.05	2.90E-07	1.0E-06	4.46E-06
0.07	2.58E-07	1.0E-05	4.54E-06
0.10	2.83E-07	1.0E-04	4.18E-06
0.15	3.79E-07	1.0E-03	3.76E-06
0.20	5.01E-07	1.0E-02	3.56E-06
0.25	6.31E-07	1.0E-01	2.17E-05
0.30	7.59E-07	5.0E-01	9.26E-05
0.35	8.78E-07	1.0	1.32E-04
0.40	9.85E-07	2.5	1.25E-04
0.45	1.08E-06	5.0	1.56E-04
0.50	1.17E-06	7.0	1.47E-04
0.55	1.27E-06	10.0	1.47E-04
0.60	1.36E-06	14.0	2.08E-04
0.65	1.44E-06	20.0	2.27E-04
0.70	1.52E-06		
0.80	1.68E-06		
1.0	1.98E-06		
1.4	2.51E-06		
1.8	2.99E-06		
2.2	3.42E-06		
2.6	3.82E-06		
2.8	4.01E-06		
3.25	4.41E-06		
3.75	4.83E-06		
4.25	5.23E-06		
4.75	5.60E-06		
5.0	5.80E-06		
5.25	6.01E-06		
5.75	6.37E-06		
6.25	6.74E-06		
6.75	7.11E-06		
7.5	7.66E-06		
9.0	8.77E-06		
11.0	1.03E-05		
13.0	1.18E-05		
15.0	1.33E-05		

Table 5-15
Material Densities for Fuel Assembly Regions (dry)

Region	In-Core		Plenum		Top		Bottom	
Element	Gram Density g/cm	Atom Density a/bn-cm	Gram Density g/cm	Atom Density a/bn-cm	Gram Density g/cm	Atom Density a/bn-cm	Gram Density g/cm	Atom Density a/bn-cm
O	4.243E-01	1.597E-02	6.462E-04	2.432E-05	0.000E+00	0.000E+00	0.000E+00	0.000E+00
Al	2.264E-04	5.053E-06	1.632E-05	3.644E-07	1.143E-03	2.551E-05	0.000E+00	0.000E+00
Ti	2.944E-04	3.701E-06	1.360E-05	1.710E-07	1.525E-03	1.917E-05	0.000E+00	0.000E+00
Si	3.487E-04	7.476E-06	2.350E-03	5.038E-05	9.855E-03	2.113E-04	1.175E-02	2.519E-04
Cr	1.375E-02	1.592E-04	4.550E-02	5.269E-04	2.162E-01	2.504E-03	2.232E-01	2.585E-03
Fe	2.661E-02	2.885E-04	1.653E-01	1.792E-03	6.861E-01	7.438E-03	8.083E-01	8.763E-03
Ni	2.611E-02	2.678E-04	2.097E-02	2.151E-04	1.837E-01	1.885E-03	1.048E-01	1.075E-03
Mn	6.326E-04	6.934E-06	4.713E-03	5.166E-05	1.933E-02	2.119E-04	2.350E-02	2.576E-04
Zr	6.013E-01	3.970E-03	6.659E-01	4.396E-03	0.000E+00	0.000E+00	0.000E+00	0.000E+00
Mo	1.056E-03	6.631E-06	0.000E+00	0.000E+00	5.725E-03	3.594E-05	0.000E+00	0.000E+00
U-235	1.115E-01	2.857E-04	5.442E-09	1.394E-11	0.000E+00	0.000E+00	0.000E+00	0.000E+00
U-238	2.676E+00	6.771E-03	1.306E-07	3.304E-10	0.000E+00	0.000E+00	0.000E+00	0.000E+00
Total	3.882	2.774E-02	0.905	7.057E-03	1.124	1.233E-02	1.172	1.293E-02

Table 5-16
Material Densities for Fuel Assembly Regions (wet)

Region	In-Core		Plenum		Top(wet)		Bottom	
Element	Gram Density g/cm3	Atom Density a/bn-cm	Gram Density g/cm3	Atom Density a/bn-cm	Gram Density g/cm3	Atom Density a/bn-cm	Gram Density g/cm3	Atom Density a/bn-cm
H	1.717E-02	1.026E-02	6.481E-02	3.872E-02	1.956E-01	1.169E-01	7.856E-02	4.693E-02
O	5.127E-01	1.930E-02	5.191E-01	1.954E-02	1.565E+00	5.889E-02	6.285E-01	2.365E-02
Al	2.264E-04	5.053E-06	1.632E-05	3.644E-07	1.143E-03	2.551E-05	0.000E+00	0.000E+00
Ti	2.944E-04	3.701E-06	1.360E-05	1.710E-07	1.525E-03	1.917E-05	0.000E+00	0.000E+00
Si	3.487E-04	7.476E-06	2.350E-03	5.038E-05	9.855E-03	2.113E-04	1.175E-02	2.519E-04
Cr	1.375E-02	1.592E-04	4.550E-02	5.269E-04	2.162E-01	2.504E-03	2.232E-01	2.585E-03
Fe	2.661E-02	2.885E-04	1.653E-01	1.792E-03	6.861E-01	7.438E-03	8.083E-01	8.763E-03
Ni	2.611E-02	2.678E-04	2.097E-02	2.151E-04	1.837E-01	1.885E-03	1.048E-01	1.075E-03
Mn	6.326E-04	6.934E-06	4.713E-03	5.166E-05	1.933E-02	2.119E-04	2.350E-02	2.576E-04
Zr	6.013E-01	3.970E-03	6.659E-01	4.396E-03	0.000E+00	0.000E+00	0.000E+00	0.000E+00
Mo	1.056E-03	6.631E-06	0.000E+00	0.000E+00	5.725E-03	3.594E-05	0.000E+00	0.000E+00
U-235	1.115E-01	2.857E-04	0.000E+00	0.000E+00	0.000E+00	0.000E+00	0.000E+00	0.000E+00
U-238	2.676E+00	6.771E-03	0.000E+00	0.000E+00	0.000E+00	0.000E+00	0.000E+00	0.000E+00
Total	3.970	4.133E-02	1.424	6.529E-02	2.688	1.881E-01	1.800	8.352E-02

Region	Top (dry)	
Element	Gram Density g/cm3	Atom Density a/bn-cm
H	0.000E+00	0.000E+00
O	0.000E+00	0.000E+00
Al	1.143E-03	2.551E-05
Ti	1.525E-03	1.917E-05
Si	9.855E-03	2.113E-04
Cr	2.162E-01	2.504E-03
Fe	6.861E-01	7.438E-03
Ni	1.837E-01	1.885E-03
Mn	1.933E-02	2.119E-04
Zr	0.000E+00	0.000E+00
Mo	5.725E-03	3.594E-05
U-235	0.000E+00	0.000E+00
U-238	0.000E+00	0.000E+00
Total	1.124	1.233E-02

Table 5-17
NUHOMS®HD 32PTH DSC and OS-187H Material Composition (% weight)

Element	Atomic Weight	Carbon Steel[1]	Stainless Steel 304[1]	Aluminum[1]	Lead[1]	Water[1] (atm fraction)	Air[2]	Polyester Resin[3]
H	1.008					0.666		5.05
B	10.811							1.05
C	12.011	1.00					0.01	35.1
N	14.0067						75.53	
O	15.9994					0.333	23.18	41.7
Al	26.9815			100.00				14.9
Ar	39.948						1.28	
Cr	51.996		19.00					
Mn	54.938		2.00					
Fe	55.847	99.00	68.375					
Ni	58.71		9.50					
Zn	65.37							2.11
Pb	207.19				100.00			
density (g/cc)		7.8212	7.92	2.702	11.17[4]	0.9982	0.0012	1.58

1. Ref [1], 2. Ref [3], 3. Proprietary resin formulation, 4. Use 98.5% of TD (11.344 g/cc)

Table 5-18
NUHOMS®HD 32PTH DSC and OS-187H Material Composition (atm/b-cm)

Element	Carbon Steel	Stainless Steel 304	Aluminum	Lead	Water	Dry Air	Polyester Resin
H					6.673E-02		4.767E-02
B-10							2.098E-04
C	3.921E-03					6.016E-09	3.168E-02
N						3.897E-05	
O					3.337E-02	1.047E-05	2.825E-02
Al			6.031E-02				5.986E-03
Ar						2.315E-07	
Cr		1.743E-02					
Mn		1.736E-03					
Fe	8.349E-02	5.935E-02					
Ni		7.718E-03					
Zn*							3.499E-04
Pb				3.248E-02			

*- Ignored,

Table 5-19
Composition and Densities for HSM-H Concrete

Element	Concrete (atm/b·cm)
H	7.767×10^{-3}
O	4.317×10^{-2}
Na	1.022×10^{-3}
Al	2.343×10^{-3}
Si	1.559×10^{-2}
K	6.776×10^{-4}
Ca	2.855×10^{-3}
Fe	3.019×10^{-4}
total	7.363×10^{-2}

Table 5-20
Source Axial Profile

Zone No.	Zone Center (% of height)	Lower Model Bound (cm)	Upper Model Bound (cm)	Gamma Profile	Neutron Profile	Neutron Normal Factor*	Gamma Normal Factor*
1	2.78	-182.880	-162.544	0.573	0.108	0.00599	0.03186
2	8.33	-162.544	-142.281	0.917	0.707	0.03917	0.05080
3	13.89	-142.281	-121.871	1.066	1.291	0.07205	0.05948
4	19.44	-121.871	-101.681	1.106	1.496	0.08260	0.06105
5	25.00	-101.681	-81.199	1.114	1.540	0.08624	0.06238
6	30.56	-81.199	-61.009	1.111	1.524	0.08410	0.06133
7	36.11	-61.009	-40.599	1.106	1.496	0.08349	0.06171
8	41.69	-40.599	-20.190	1.101	1.469	0.08199	0.06144
9	47.22	-20.190	-0.146	1.097	1.448	0.07936	0.06012
10	52.80	-0.146	20.629	1.093	1.427	0.08106	0.06208
11	58.33	20.629	40.307	1.089	1.406	0.07566	0.05859
12	63.89	40.307	61.301	1.086	1.391	0.07984	0.06234
13	69.44	61.301	80.906	1.081	1.366	0.07319	0.05794
14	75.00	80.906	101.974	1.073	1.326	0.07635	0.06180
15	80.56	101.974	121.579	1.051	1.220	0.06540	0.05633
16	86.11	121.579	142.573	0.993	0.972	0.05581	0.05700
17	91.67	142.573	162.251	0.932	0.755	0.04059	0.05014
18	97.22	162.251	182.880	0.512	0.069	0.00388	0.02888
					average	1.167	1.00

* - Zone weighted profile

Table 5-21
Summary of NUHOMS®HD 32PTH DSC in the HSM-H, Maximum and Average Dose Rates

Dose Rate Location	Maximum Gamma (mrem/hr)	Gamma MCNP 1σ Error	Maximum Neutron (mrem/hr)	Neutron MCNP 1σ Error	Maximum Total(1) (mrem/hr)	Total MCNP 1σ Error
HSM Roof (centerline)	13.2	0.043	1.9	0.021	15.1	0.038
HSM Roof Birdscreen	152.0	0.021	18.5	0.014	170.0	0.019
HSM End (Side) Shield Wall Surface	0.9	0.041	0.5	0.016	1.4	0.022
HSM Door Exterior Surface (centerline)	0.5	0.106	1.0	0.120	1.6	0.162
HSM Front Birdscreen	736.0	0.140	16.1	0.070	752.0	0.137

Dose Rate Location	Average Gamma (mrem/hr)	Gamma MCNP 1σ Error	Average Neutron (mrem/hr)	Neutron MCNP 1σ Error	Average Total (mrem/hr)	Total MCNP 1σ Error
HSM Roof	13.9	0.012	1.9	0.007	15.8	0.010
HSM End (Side) Shield Wall Surface	0.4	0.011	0.2	0.053	0.6	0.019
HSM Front	5.5	0.083	0.5	0.054	6.0	0.076
HSM Back Shield Wall	0.5	0.060	<0.1	0.025	0.5	0.060

Notes:
(1) Gamma and Neutron dose rate peaks do not always occur at same location; therefore, the total dose rate is not always the sum of the maximum gamma plus maximum neutron dose rate.

Table 5-22
Summary of NUHOMS®HD 32PTH DSC in the OS187H TC, Maximum Dose Rates During Decontamination and Welding Operations

Dose Rate Location	Maximum Gamma(3) (mrem/hr)	Gamma MCNP 1σ Error	Maximum Neutron (mrem/hr)	Neutron MCNP 1σ Error	Maximum Total(1) (mrem/hr)	Total MCNP 1σ Error
Decontamination (Configuration A)						
Cask Side Surface (Radial)	241	0.034	158	0.081	399	0.053
Top Axial Surface (@ shield plug)	933	0.183	118	0.405	1050	0.189
Cask Bottom Axial Surface(2)	397	0.129	1430	0.127	1825	0.127
1.5 ft from Cask Side (Radial)	153	0.027	95.7	0.067	249	0.043
1.5 ft from Top Axial Surface	688	0.090	52.0	0.299	739	0.092
1.5 ft from Cask Bottom Axial Surface	95.3	0.173	300	0.120	389	0.129
3 ft from Cask Side (Radial)	107	0.025	65.4	0.063	172	0.039
3 ft from Top Axial Surface	513	0.122	27.5	0.262	539	0.123
Welding (Configuration B)						
Cask Side Surface (Radial)	310	0.027	95.8	0.042	397	0.027
Top Axial Surface	95.5	0.062	328	0.028	421	0.032
Cask Bottom Axial Surface(2)	490	0.125	1240	0.033	1730	0.056
1.5 ft from Cask Side (Radial)	198	0.015	59.0	0.036	256	0.017
1.5 ft from Top Axial Surface	77.6	0.058	192	0.031	269	0.036
1.5 ft from Cask Bottom Axial Surface	136	0.255	279	0.041	415	0.118
3 ft from Cask Side (Radial)	139	0.013	40.9	0.031	179	0.015
3 ft from Top Axial Surface	52.5	0.055	102	0.027	154	0.035

Notes:
(1) Gamma and Neutron dose rate peaks do not always occur at same location; therefore, the total dose rate is not always the sum of the maximum gamma plus maximum neutron dose rate.
(2) The peak bottom surface dose rate is directly below the grapple ring cut out approximately 1" below the bottom of the cask.
(3) Gamma dose rates include secondary gamma.

Table 5-23
Summary of NUHOMS®HD 32PTH DSC in the OS187H TC, Maximum Dose Rates During Transfer Operations (Configuration C)

Dose Rate Location	Maximum Gamma[3] (mrem/hr)	Gamma MCNP 1σ Error	Maximum Neutron (mrem/hr)	Neutron MCNP 1σ Error	Maximum Total[1] (mrem/hr)	Total MCNP 1σ Error
Cask Side Surface (Radial)	384	0.018	125	0.040	508	0.021
Cask Top Axial Surface	8.1	0.029	24.5	0.136	32.1	0.130
Cask Bottom Axial Surface[2]	475	0.112	1350	0.028	1820	0.045
1.5 ft from Cask Side (Radial)	238	0.015	77.0	0.035	315	0.018
1.5 ft from Cask Top Axial Surface	5.2	0.029	14.1	0.158	19.3	0.149
1.5 ft from Cask Bottom Axial Surface	118	0.154	305	0.031	423	0.063
3 ft from Cask Side (Radial)	165	0.013	54.7	0.034	219	0.016
3 ft from Cask Top Axial Surface	3.5	0.054	8.7	0.203	12.1	0.189
3 ft from Cask Bottom Axial Surface	53.1	0.118	117	0.029	170	0.056
Cask 1 m (Radial) Accident Condition	186	0.012	2200	0.003	2390	0.003
Cask 100 m (Radial) Accident Condition	0.1	0.01	1.2	0.004	1.3	0.004

Notes:
(1) Gamma and Neutron dose rate peaks do not always occur at same location therefore the total dose rate is not always the sum of the maximum gamma plus maximum neutron dose rate.
(2) The peak bottom surface dose rate is 1" below the bottom of the cask in the grapple ring area.. The max bottom dose rates, with the RAM access open are 1090 mrem/hr gamma, 1525 mrem/hr neutron.
(3) Gamma dose rates include secondary gamma.

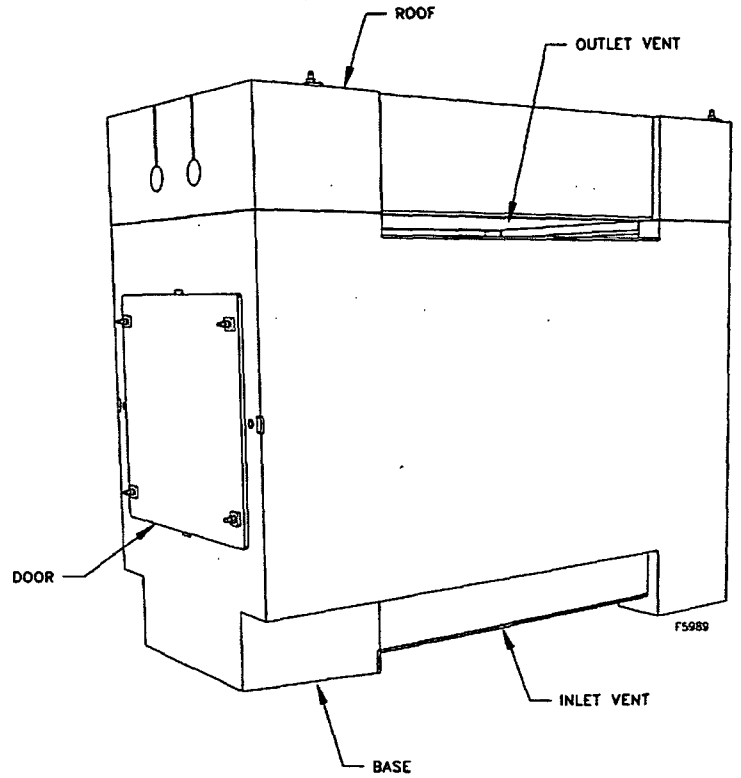

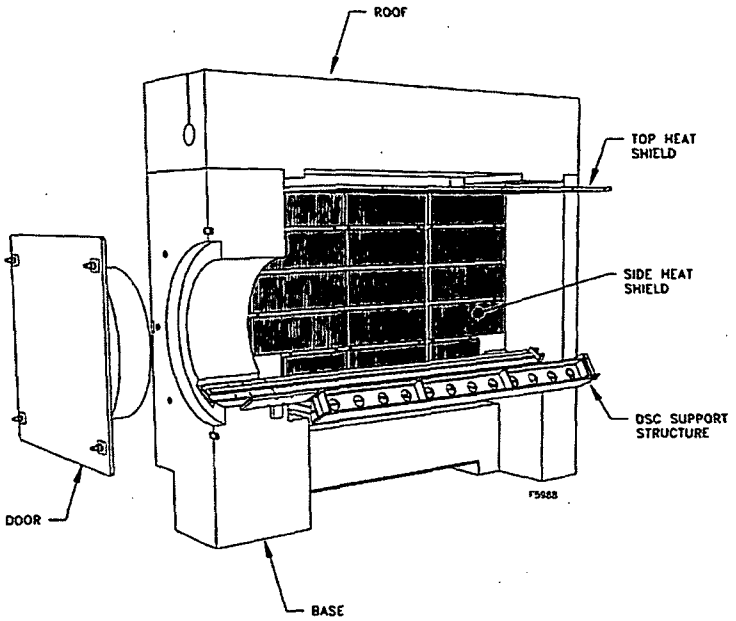

Figure 5-1
NUHOMS® HD 32PTH System Shielding Configuration (HSM-H)

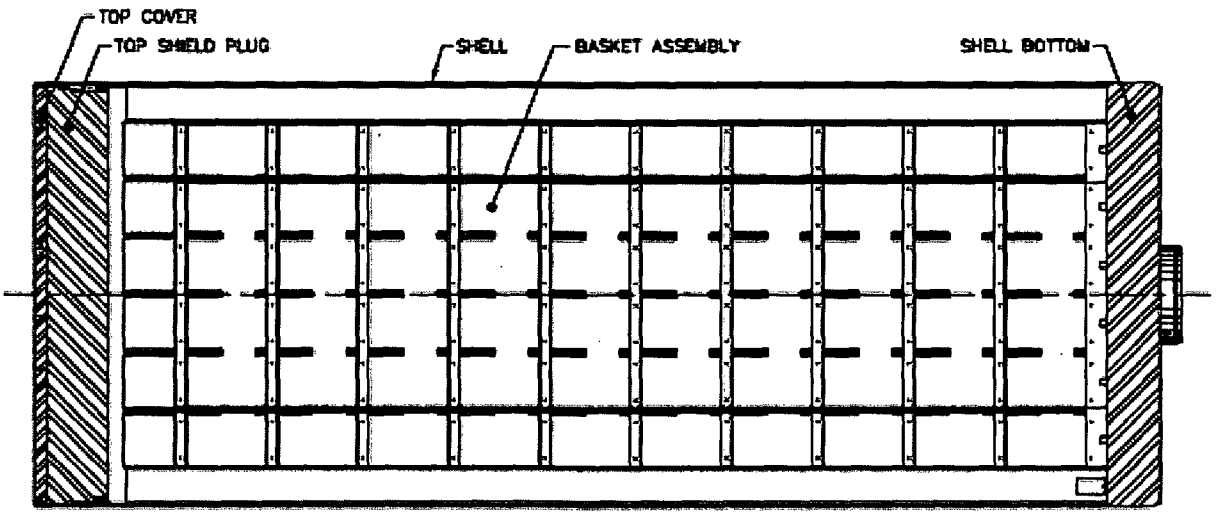

Figure 5-2
Dry Shielded Canister Shielding Configuration

Figure Withheld Under 10 CFR 2.390

Figure 5-3
Right Elevation Cross Section View of HSM-H

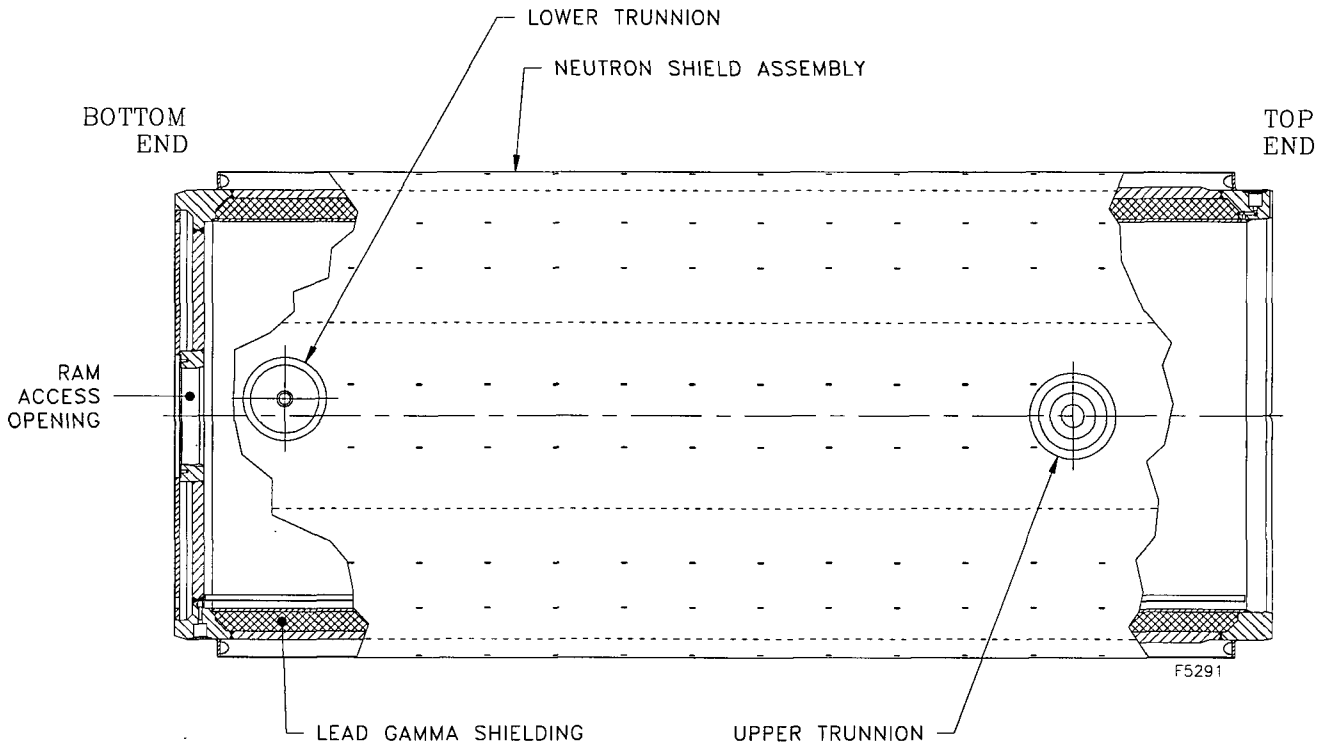

Figure 5-4
Shielding Configuration of the OS187H Transfer Cask

Figure Withheld Under 10 CFR 2.390

Figure 5-5
OS187H DSC and Annulus Flooded

Figure Withheld Under 10 CFR 2.390

Figure 5-6
One Quarter Cross Section DSC/Basket in Transfer Cask

Figure Withheld Under 10 CFR 2.390

Figure 5-7
OS187H Lids Installed (DSC and Annulus Dry)

Figure Withheld Under 10 CFR 2.390

Figure 5-8
HSM-H Side View at DSC Centerline

Figure Withheld Under 10 CFR 2.390

Figure 5-9
HSM-H Head-on View at X=0

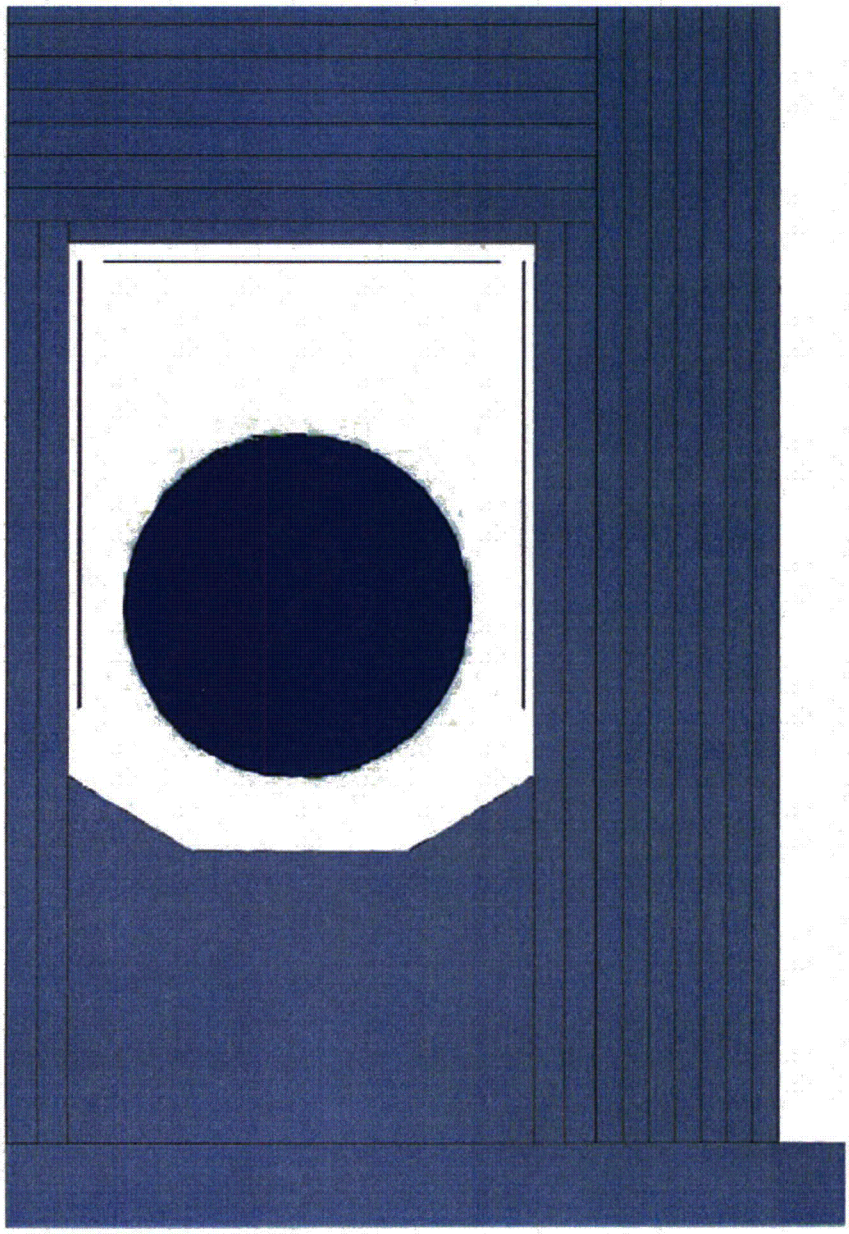

Figure 5-10
HSM-H Head-on View at DSC Lid End (X=225)

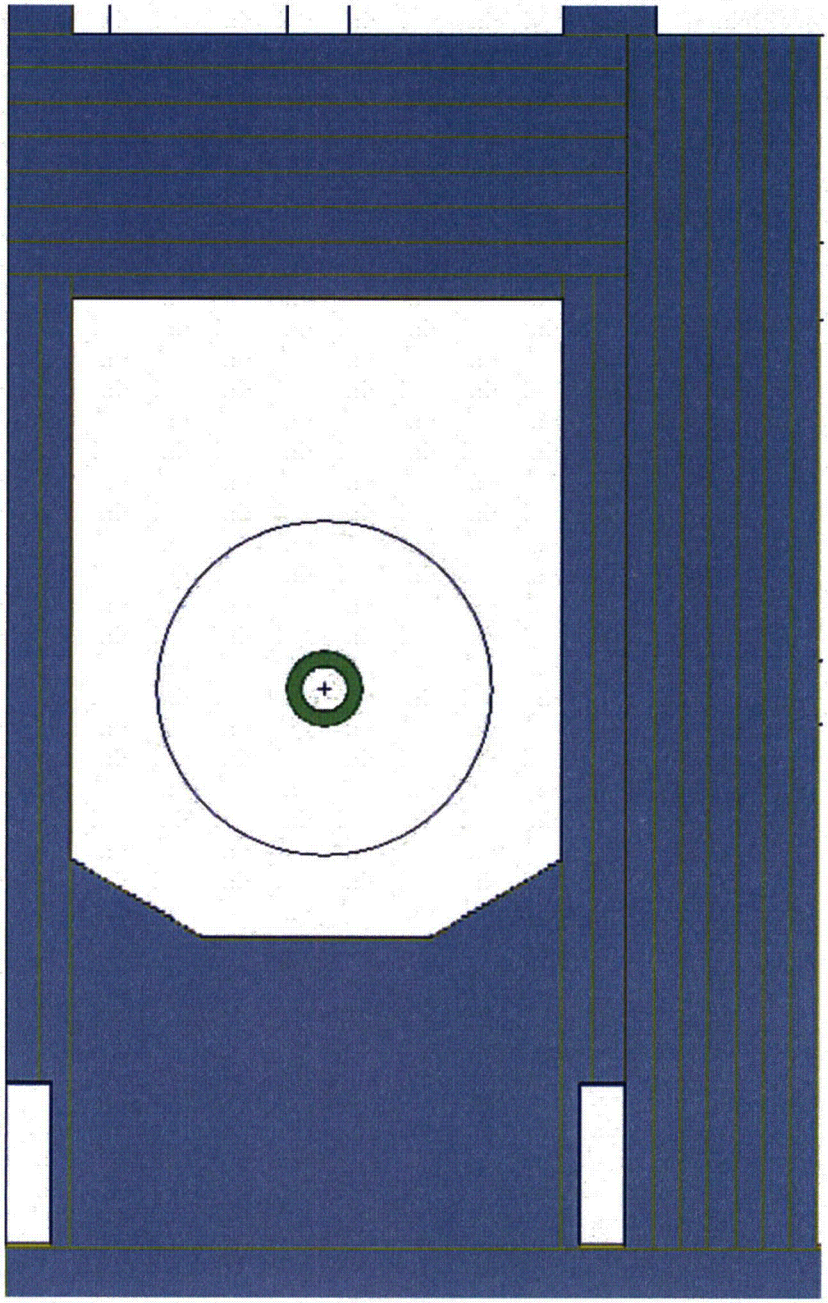

Figure 5-11
HSM-H Head-on View at DSC Bottom End (X=-225)

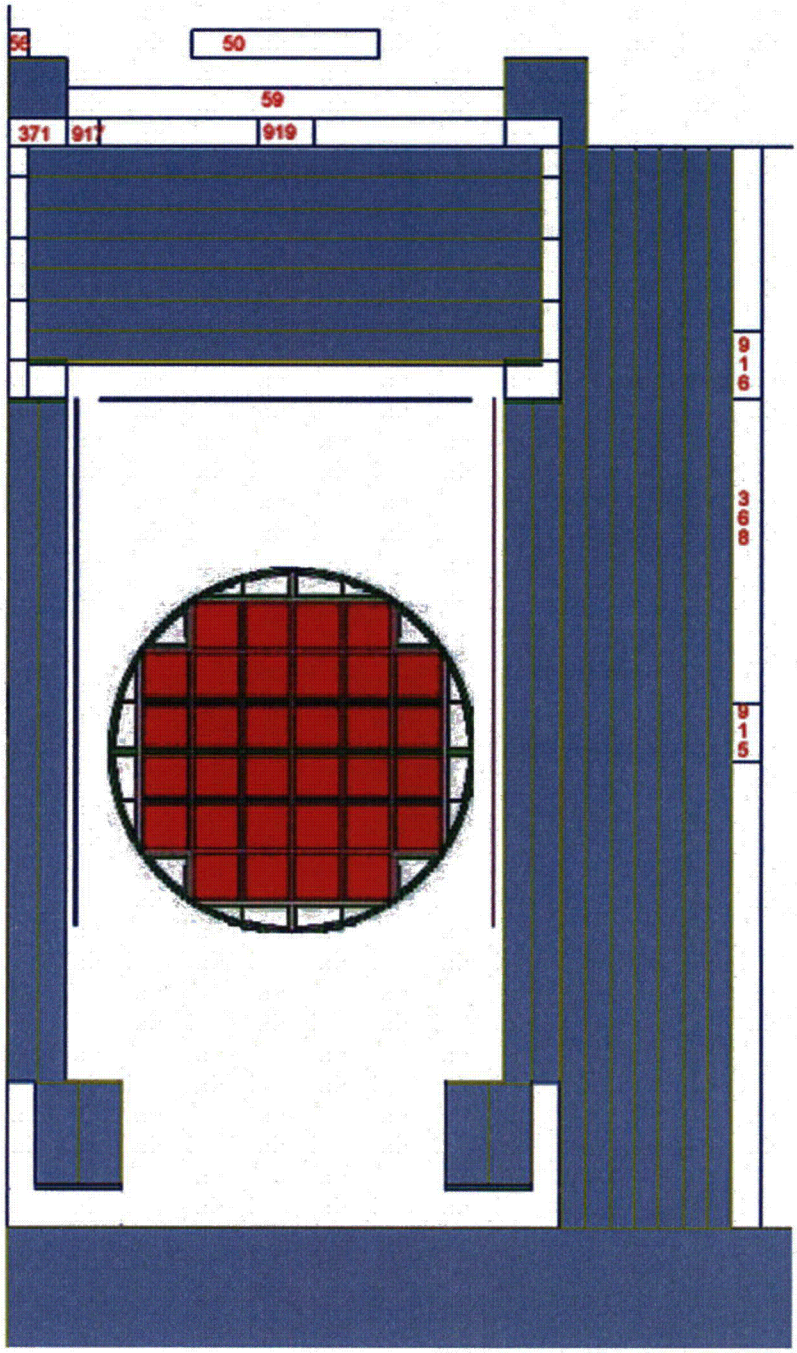

Figure 5-12
HSM-H Detector Locations Head-on View

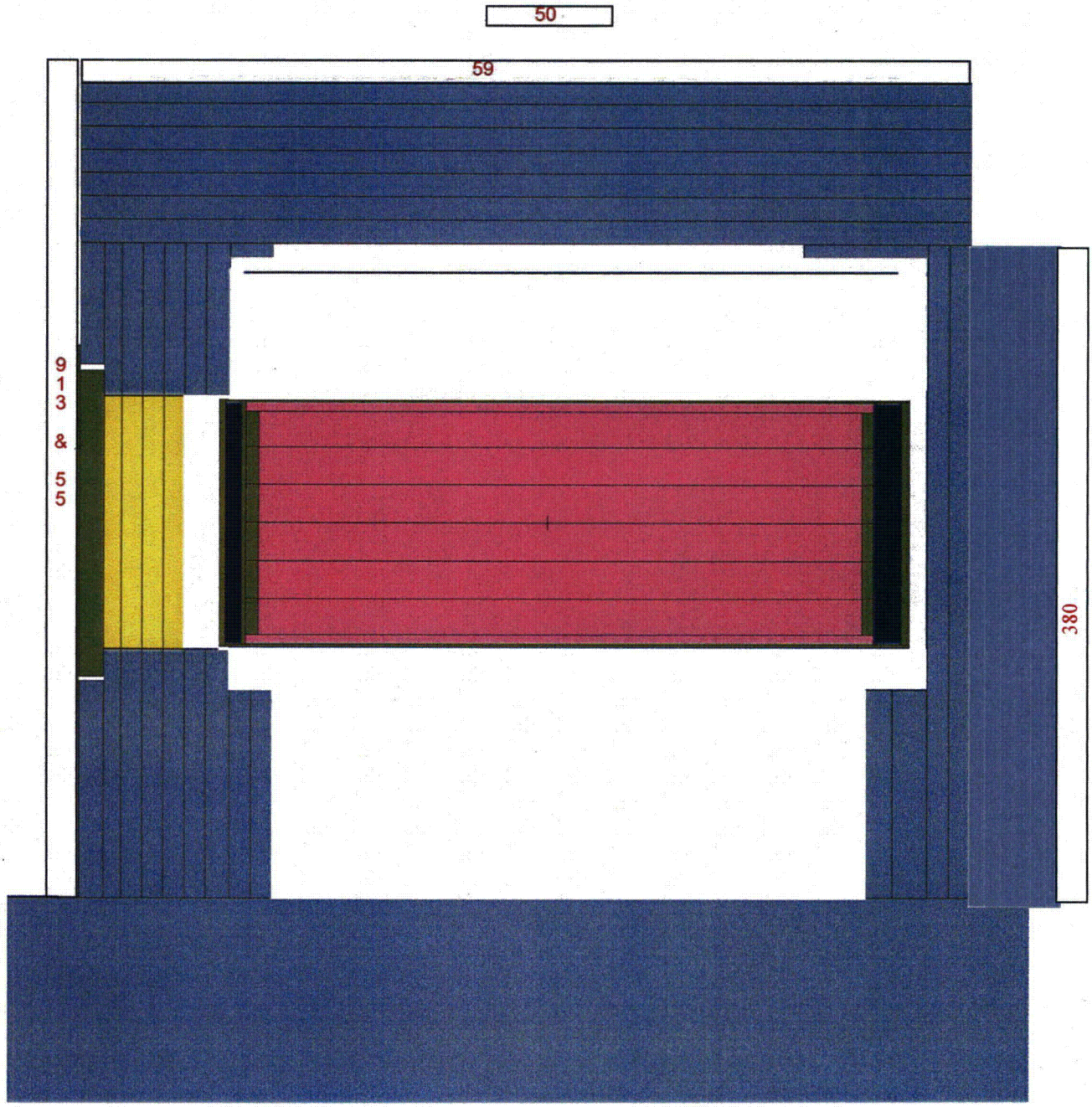

Figure 5-13
HSM-H Detector Locations Side View

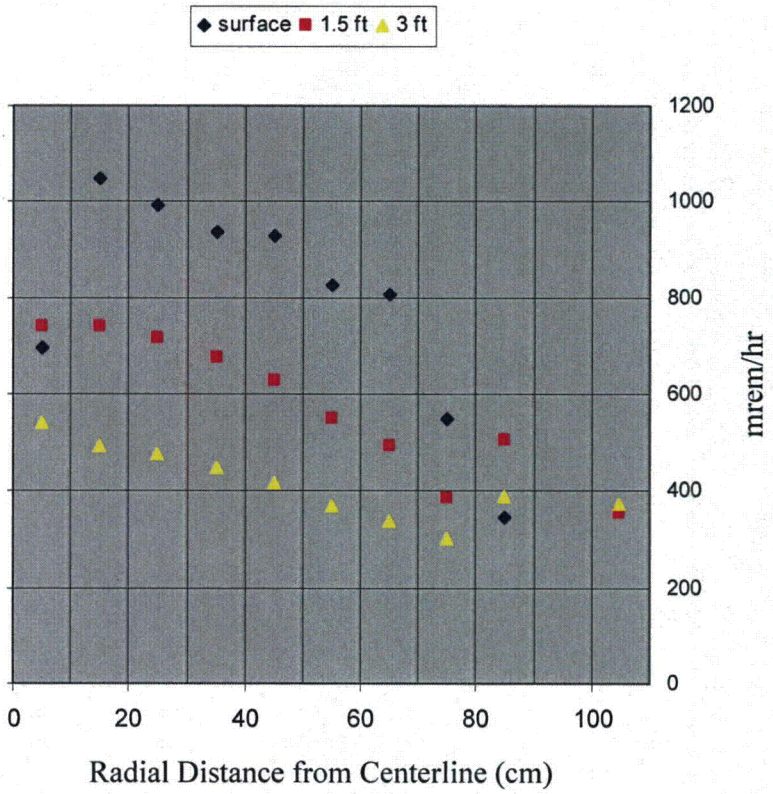

Figure 5-14
Dose Rates Around the Top of the TC/32PTH-DSC
(Configuration A)

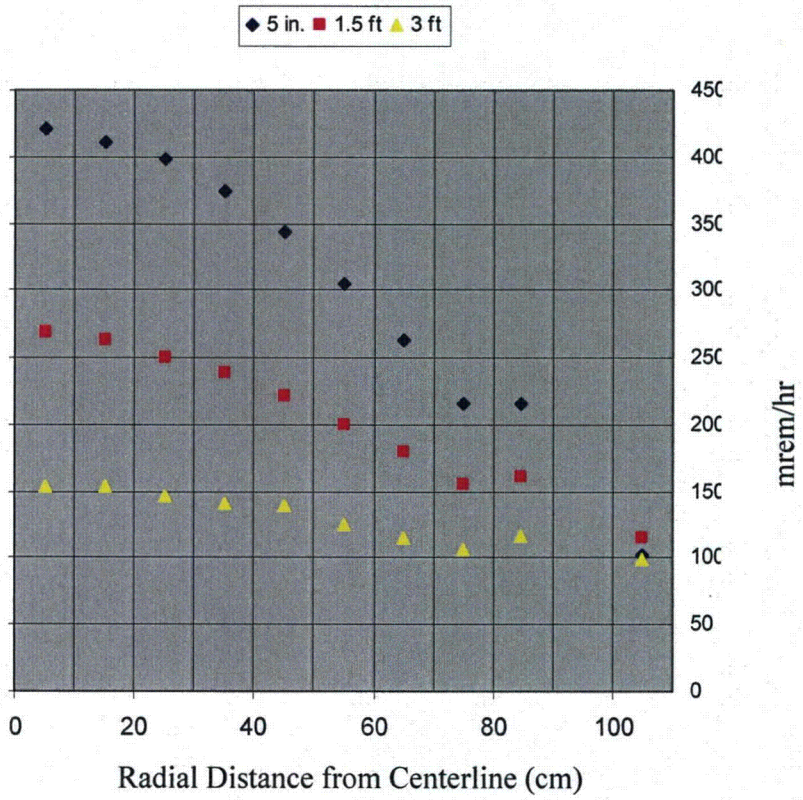

Figure 5-15
Dose Rates Around the Top of the TC/32PTH-DSC
(Configuration B)

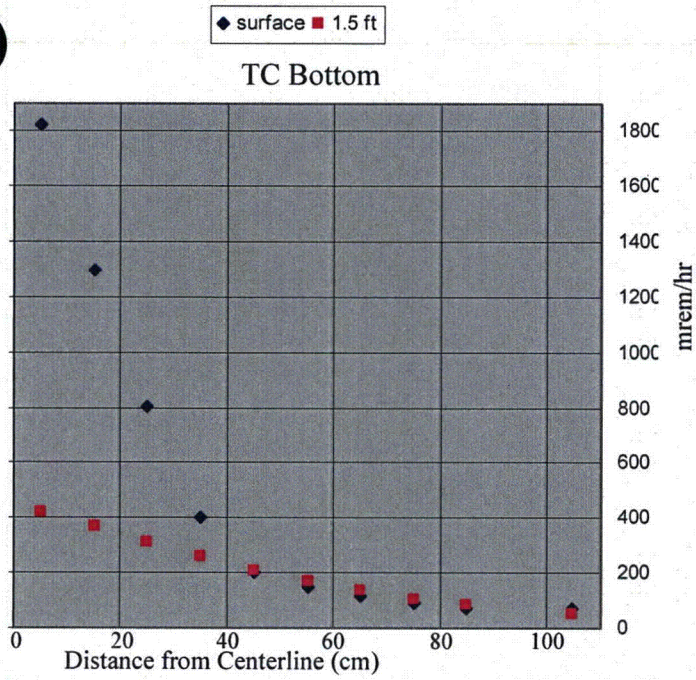

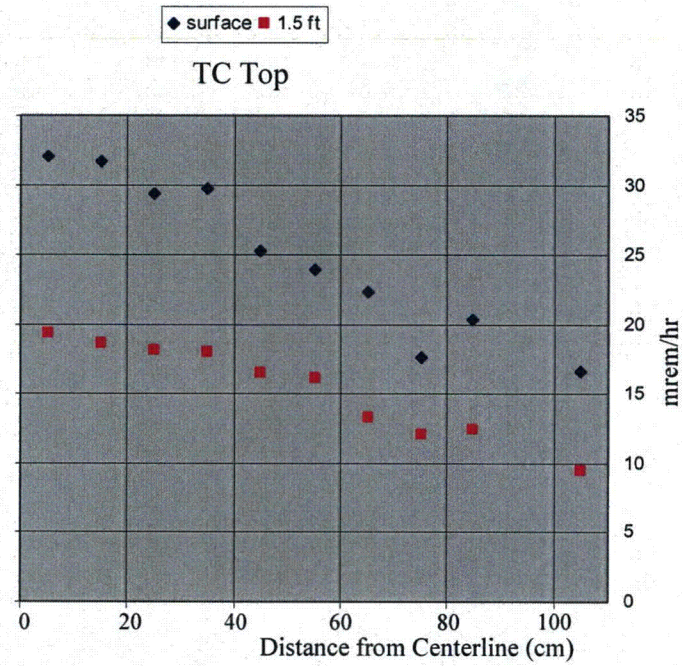

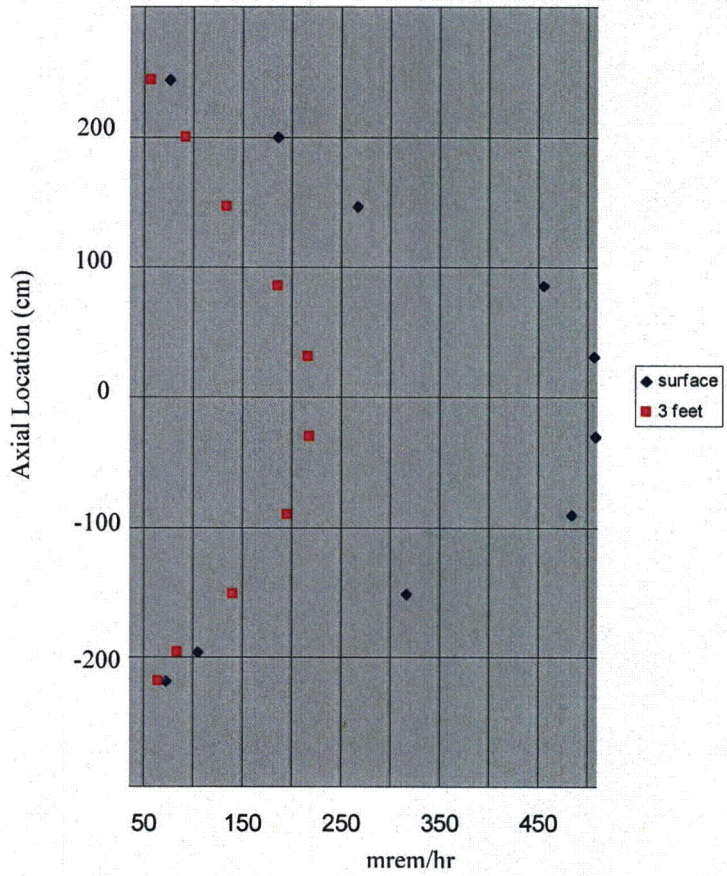

Figure 5-16
Dose Rates Around TC/32PTH-DSC (Transfer Configuration)

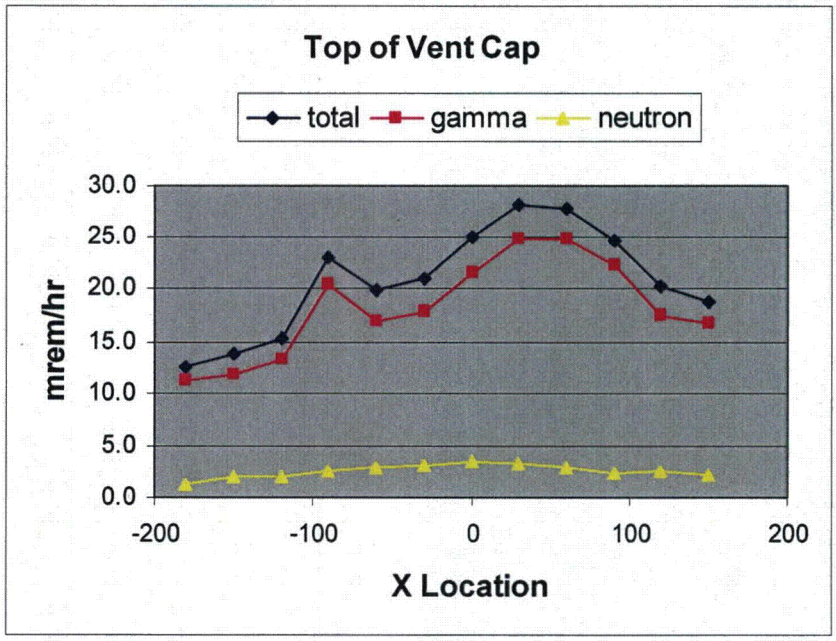

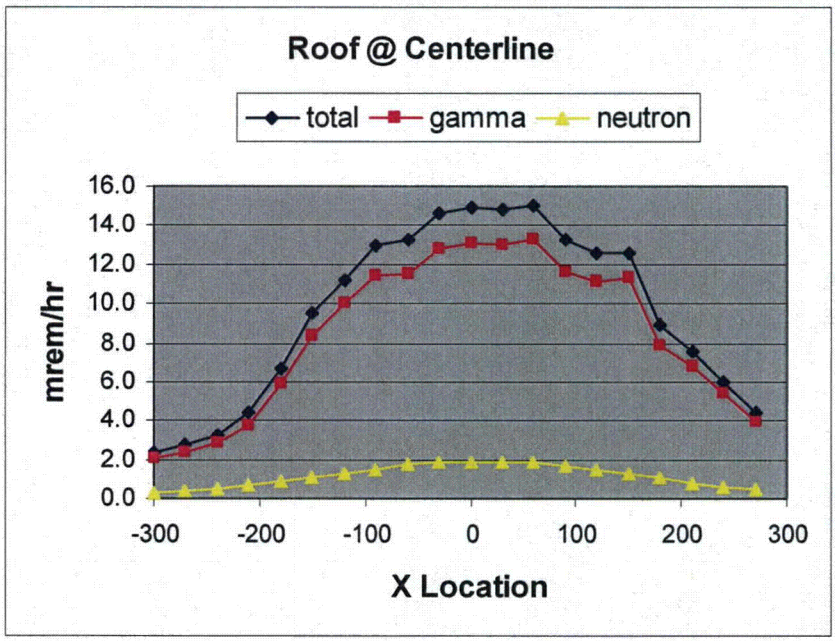

Figure 5-17
Dose Rates On the HSM-H Roof

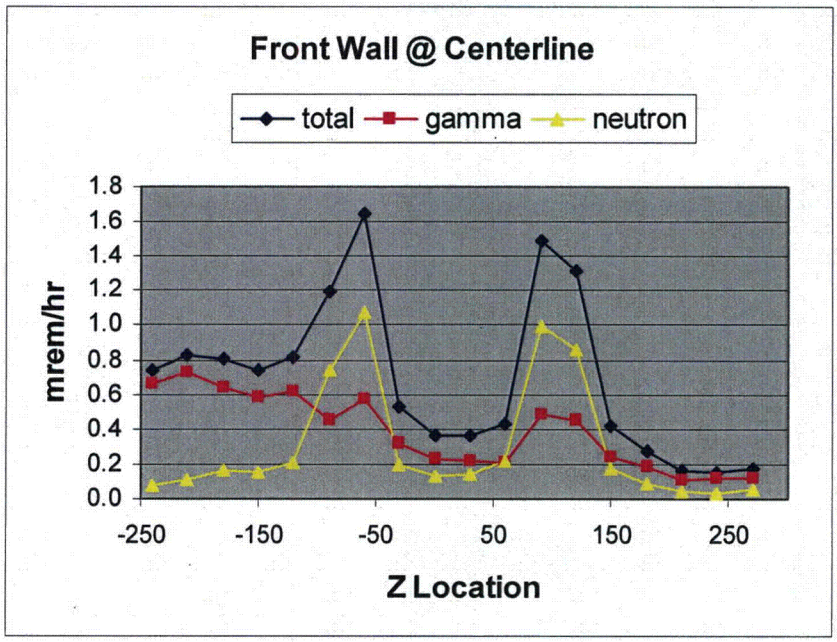

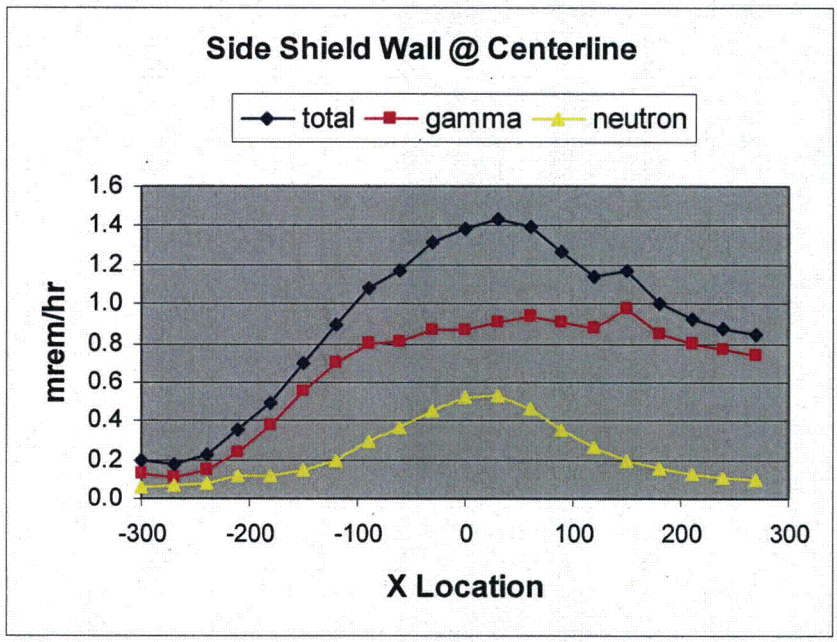

Figure 5-18
Dose Rates On the HSM-H Front and Side

CHAPTER 6
CRITICALITY EVALUATION

TABLE OF CONTENTS

6. CRITICALITY EVALUATION 6-1

6.1 Discussion and Results 6-2

6.2 Spent Fuel Loading 6-4

6.3 Model Specification 6-5

6.3.1 Description of Criticality Analysis Model 6-5

6.3.2 Package Regional Densities 6-7

6.4 Criticality Calculation 6-8

6.4.1 Calculational Method 6-8

6.4.2 Fuel Loading Optimization 6-13

6.4.3 Criticality Results 6-22

6.5 Critical Benchmark Experiments 6-23

6.5.1 Benchmark Experiments and Applicability 6-23

6.5.2 Results of the Benchmark Calculations 6-24

6.6 Supplemental Information 6-25

6.6.1 References 6-25

6.6.2 KENO Input Files 6-27

LIST OF TABLES

Table 6-1 Maximum Initial Enrichment for Each Fuel Design for both Intact and Damaged Fuel Assemblies
Table 6-2 Summary of Limiting Criticality Evaluations for all Fuel Assemblies
Table 6-3 Authorized Contents for NUHOMS®-32PTH DSC
Table 6-4 Fuel Assembly Design Parameters(2) for Criticality Analysis
Table 6-5 NUHOMS®-32PTH - Basket and DSC Dimensions
Table 6-6 NUHOMS® OS187H Transfer Cask Dimensions
Table 6-7 NUHOMS®-32PTH - Fixed Poison Loading Requirements
Table 6-8 Description of the Basic KENO Model Units
Table 6-9 Material Property Data
Table 6-10 Results of the Fuel Assembly Positioning Studies
Table 6-11 Results of the Rail Material Variation Studies
Table 6-12 Results of the Poison Plate Thickness Variation Studies
Table 6-13 Results of the Fuel Compartment Width Variation Studies
Table 6-14 Results of the Fuel Compartment Thickness Variation Studies
Table 6-15 WE 15x15 Class Intact Assemblies Without BPRAs - Final Results
Table 6-16 WE 15x15 Class Intact Assemblies With BPRAs - Final Results
Table 6-17 WE 17x17 Class Intact Assemblies Without BPRAs - Final Results
Table 6-18 WE 17x17 Class Intact Assemblies With BPRAs - Final Results
Table 6-19 Limiting Parameters for Damaged Fuel Calculations
Table 6-20 Results of Optimum Pitch Studies
Table 6-21 Results of the Single Ended Rod Shear Studies
Table 6-22 Results of the Double Ended Rod Shear Studies
Table 6-23 Evaluation of the Shifting of Fuel Rods Beyond the Poison
Table 6-24 Most Reactive Damaged Assembly Configuration
Table 6-25 Double Ended Rod Shear Study with BPRAs
Table 6-26 WE 15x15 Class Damaged Assemblies With BPRAs - Final Results
Table 6-27 WE 17x17 Class Damaged Assemblies With BPRAs - Final Results
Table 6-28 Maximum k_{eff} for Intact Assemblies - Final Results
Table 6-29 Maximum k_{eff} for Damaged Assemblies - Final Results
Table 6-30 Benchmark Results
Table 6-31 USL-1 Results
Table 6-32 USL Determination for Criticality Analysis
Table 6-33 CE 14x14 Class Intact Assemblies - Final Results
Table 6-34 CE 14x14 Class Damaged Assemblies - Final Results

LIST OF FIGURES

Figure 6-1 Basket Views and Dimensions
Figure 6-2 Basket Model Compartment Wall (View G)
Figure 6-3 Basket Model Compartment Wall (View F)
Figure 6-4 Basket Model Compartment Wall With Fuel Assembly (View G)
Figure 6-5 Basket Model Compartment Wall With Fuel Assembly (View F)
Figure 6-6 Basket Compartment With Fuel (Section A)
Figure 6-7 Basket Compartment With Fuel (Section B)
Figure 6-8 Fuel Assembly Positions and Poison Plate Locations in the Basket
Figure 6-9 Fuel Assembly Positions by KENO Unit ID
Figure 6-10 Canister and Transfer Cask Description in the KENO Model
Figure 6-11 Radial Cross Section of the Detailed KENO Model
Figure 6-12 WE 15x15 Fuel Assemblies in the Centered Position
Figure 6-13 WE 15x15 Fuel Assemblies in the Inward Position
Figure 6-14 CE 14x14 Fuel Assembly : Optimum Pitch Study
Figure 6-15 WE 17x17 Fuel Assembly : Single Ended Rod Shear Study
Figure 6-16 WE 15x15 Fuel Assembly : Double Ended Rod Shear Study
Figure 6-17 WE 17x17 Fuel Assembly : 4-inch Shift of Fuel Assembly
Figure 6-18 WE 15x15 Fuel Assembly : 6-inch Shift of Fuel Rods
Figure 6-19 WE 15x15 Fuel Assembly : Double Ended Rod Shear with BPRAs

6. CRITICALITY EVALUATION

The NUHOMS® HD System is designed to meet 10CFR 72.124 1 criticality safety limits during worst case wet loading/unloading operations with the use of fixed neutron absorbing materials (poisons) in the flooded Dry Shielded Canister (32PTH DSC) and credit for soluble boron in the spent fuel pool. The design assures criticality safety under all normal, off-normal and accident conditions associated with fuel handling, 32PTH DSC handling, on-site transfer and 32PTH DSC storage.

The NUHOMS® 32PTH DSC criticality safety is ensured by fixed neutron absorbers, soluble boron in the pool and favorable geometry. Burnup credit is not taken in this criticality evaluation. The basket uses a Borated-Aluminum alloy, Aluminum/B_4C metal matrix composite, or Boral® as its fixed neutron poison material. These materials are ideal for long-term use in the radiation and thermal environments of a DSC. The minimum required boron-10 loading for the metallic plates is 7.0 mg/cm^2 (90% credit taken in the criticality analysis or 6.3 mg/cm^2). Metal Matrix Composites (MMCs) at a minimum areal density of 7.0 mg/cm^2 have been qualified for use as a neutron absorber with 90% credit as justified in Section 9.1.7.2 of this SAR. Similarly, Section 9.1.7.1 provides the justification for the use of 90% credit for borated aluminum. The maximum poison loading for the metallic plates is 50.0 mg B-10/cm^2 (90% credit taken in the analysis or 45.0 mg B-10/cm^2). The minimum required poison loading for Boral® plates is 9.0 mg B-10/cm^2 (75% credit). The maximum poison loading for Boral® plates is 25.0 mg B-10/cm^2 (75% credit). In addition to utilizing five different fixed poison loadings, the soluble boron concentration credited in the analysis is also varied from a minimum of 2000 ppm to a maximum of 2500 ppm.

The results of the detailed analyses demonstrate that the NUHOMS® HD System is criticality safe under normal, off normal and accident conditions including all applicable biases and uncertainties.

6.1 Discussion and Results

The NUHOMS®-32PTH DSC stainless steel basket consists of an egg-crate plate design. The fuel assemblies are housed in 32 stainless steel fuel compartments with the damaged fuel assemblies occupying the positions shown in Chapter 12. The basket structure, including the fuel compartments, is held together with stainless steel insert plates and the poison and aluminum plates that form the egg crate structure. The basket compartment structure is connected to perimeter rail assemblies, portions of it comprising of a solid aluminum interface. The fuel compartment structure is connected to perimeter transition rail assemblies as described shown on the drawings in Section 1.5. The poison/aluminum plates are located between the fuel compartments.

The analysis presented herein is performed for a NUHOMS®-32PTH DSC in the NUHOMS®-OS187H transfer cask (TC) during normal and accident loading conditions. The NUHOMS®-OS187H TC consists of an inner stainless steel shell, lead gamma shield, a stainless steel structural shell and a water neutron shield. This analysis is applicable to any licensed cask of similar construction. The NUHOMS®-32PTH DSC/TC configuration is shown to be subcritical under normal and accident conditions of loading, transfer and storage.

The 32PTH DSC contents are limited to the fuel designs listed in Section 6.2. Computer models of the 32PTH DSC are discussed in Section 0. The criticality evaluation is presented in Section 6.4. The 32PTH DSC was evaluated for the following conditions that bound normal conditions and the off-normal and accident events listed in Chapter 11:

- varied internal moderator density (IMD) within the basket with borated water (water density evaluated includes steam which may be generated during loading and unloading operations),
- variations in material tolerances,
- variations in fuel assembly position in the compartment tubes,
- fresh water in the fuel pellet - cladding annulus,
- postulated change of pin pitch due to fuel grid crushing in a drop accident,
- postulated failures for damaged fuel payloads.

The various effects are evaluated individually, and are combined as required to demonstrate compliance with the requirement of 10CFR 72.124 that "before a criticality accident is possible, at least two unlikely, independent, and concurrent or sequential changes have occurred in the conditions essential to nuclear criticality safety."

The criticality analysis determines the most reactive configuration for the basket and fuel assembly position. Then criticality calculations evaluate a variety of fuel assembly types, initial enrichments and poison loadings (fixed and soluble poison). Finally, the maximum allowed initial enrichment for each fuel assembly type as a function of soluble boron concentration and fixed poison loading is determined and is listed in Table 6-1.

Additionally, calculations are carried out to determine the most reactive damaged fuel assembly (design basis damaged fuel assembly) configuration for each fuel assembly class.

Then criticality calculations evaluate a variety of fuel assembly types, initial enrichments and poison loadings (fixed and soluble poison). Finally, the maximum allowed initial enrichment and the number of damaged assemblies per DSC for each fuel assembly type as a function of soluble boron concentration and fixed poison loading is determined and is also shown in Table 6-1.

These calculations determine k_{eff} with the CSAS25 control module of SCALE-4.4 3 for each assembly type and initial enrichment, including all uncertainties to assure criticality safety under all credible conditions.

The results of these calculations demonstrate that the maximum expected k_{eff}, including statistical uncertainty, will be less than the Upper Subcritical Limit (USL) determined from a statistical analysis of benchmark criticality experiments. The statistical analysis procedure includes a confidence band with an administrative safety margin of 0.05. A series of benchmark calculations were performed with the SCALE 4.4 PC/CSAS25 3 package using the 44-group cross-section library as presented in Section 0. The minimum value of the Upper Subcritical Limit (USL) was determined to be 0.9419.

The results of the limiting criticality analyses are summarized in Table 6-2. The maximum k_{eff} for the normal fuel geometry is 0.9404 ($k_{eff}+2\sigma$) and is based on the Westinghouse 17x17 (WE 17x17) fuel assembly design. The maximum k_{eff} for the damaged fuel geometry is 0.9402 ($k_{eff}+2\sigma$) and is based on the WE 17x17 fuel assembly design.

6.2 Spent Fuel Loading

This section provides a summary of the maximum spent fuel loading and spent fuel parameters for the 32PTH DSC.

The NUHOMS®-32PTH DSC is capable of transferring and storing a maximum 32 intact PWR fuel assemblies. Additionally, a maximum of 16 locations (out of the 32 locations) per DSC can be loaded with damaged PWR fuel assemblies with the remaining locations loaded with intact PWR fuel assemblies. The required placement of the damaged fuel assemblies is defined in Chapter 12. Damaged fuel includes assemblies with known or suspected cladding defects greater than hairline cracks or pinhole leaks. The reactivity of a DSC loaded with less than 32 PWR fuel assemblies is expected to be lower than that calculated in this report since the more absorbing borated water replaces the fuel in the empty locations. Reconstituted fuel assemblies, where the fuel pins are replaced by stainless steel (or Zircaloy) pins that displace the same amount of borated water, are considered intact fuel assemblies. Table 6-3 lists the fuel assemblies considered as authorized contents of the NUHOMS®-32PTH DSC.

Table 6-4 lists the fuel design parameters for the PWR fuel assemblies. Reload fuel from other manufacturers with the same parameters are also considered as authorized contents.

For the fuel assemblies to be loaded in the NUHOMS®-32PTH DSC (except the CE 14x14 class), Burnable Poison Rod Assemblies (BPRAs) are also included as authorized contents. The only change to the package fuel loading is the addition of BPRAs that are modeled as $^{11}B_4C$. Since BPRAs displace borated moderator in the assembly guide tubes, an evaluation is performed to determine the potential impact of BPRA storage on the system reactivity. No credit is taken for BPRA cladding and absorbers; rather the BPRA is modeled as $^{11}B_4C$ in the entire guide tube of the respective design. Thus, the highly borated moderator between the guide tube and the BPRA rodlet is modeled as $^{11}B_4C$. The inclusion of more Boron-11 and carbon enhances neutron scattering causing the neutron population in the fuel assembly to be slightly increased which increases reactivity. The fuel assembly dimensions reported in Table 6-4 remains unchanged for the BPRA cases. The models that include BPRAs only differ in that the region inside the guide tubes and instrument tube are modeled as $^{11}B_4C$ instead of moderator.

Other Non Fuel Assembly Hardware (NFAH) like the Thimble Plug Assemblies (TPAs), and Vibration Suppressor Inserts (VSI) are considered as authorized contents for loading. Integral fuel burnable absorber (IFBA, ZrB_2 coating on fuel pellets) fuel assemblies may also be stored. These components are considered identical to BPRAs for criticality purposes and will be referred to as BPRAs for the rest of the report.

6.3 Model Specification

The following subsections describe the physical models and materials of the NUHOMS®-32PTH DSC as loaded and transferred in the NUHOMS® OS187H TC used for input to the CSAS25 module of SCALE-4.4 3 to perform the criticality evaluation. The reactivity of the DSC under storage conditions is bounded by the TC analysis with zero internal moderator density case. The TC analysis with zero internal moderator density case bounds the storage conditions in the HSM because (1) the DSC internals are always dry (purged and backfilled with He) while in the HSM, and (2) the TC contains materials such as steel and lead which provide close reflection of fast neutrons back into the fueled basket while the HSM materials (concrete) are much further from the sides of the DSC and thereby tend to reflect thermalized neutrons back to the DSC which are absorbed in the DSC materials reducing the system reactivity.

6.3.1 Description of Criticality Analysis Model

The transfer cask and DSC are explicitly modeled using the appropriate geometry options in KENO V.a of the CSAS25 module in SCALE-4.4. Several models are developed to evaluate the fabrication tolerances of the DSC, fuel assembly locations, fuel assembly type, initial enrichments, fixed poison loading, soluble boron concentration and storage of fuel hardware (BPRAs, TPAs, etc.).

The basket design modeled in the calculation is based on the 32PTH basket detailed in Chapter 1 with a section length of 15.03" (13.28" basket section + 1.75" steel plate). The key basket dimensions utilized in the calculation are shown in Table 6-5. The key transfer cask dimensions utilized in the calculation are shown in Table 6-6. The fixed poison modeled in the calculation is based on borated aluminum alloy. A credit of 90% is taken for the fixed poison loading in the analysis. Alternatively, Boral® can be used as a fixed poison. However, the criticality analysis with Boral® assumes crediting only 75% of the fixed poison loading. Therefore, the Boral® loading requirements are appropriately (and conservatively) adjusted and the fixed poison loading requirements are shown in Table 6-7.

The basic calculational KENO model is a 15.03-inch axial section and full-radial cross section of the DSC and cask with periodic boundary conditions at the axial boundaries (top and bottom) and reflective boundary conditions at the radial boundaries (sides). This axial section essentially models one building block of the egg crate basket structure. Periodic boundary conditions ensure that the resulting KENO model is essentially infinite in the axial direction. The model does not explicitly include the water neutron shield; however the infinite array of casks without the neutron shield does contain unborated water between the casks and in the canister - transfer cask gap. This basic building block is shown in Figure 6-1.

The fuel assemblies within the basket are modeled explicitly. The fuel compartment surrounds each fuel assembly which is bounded by the basket plates consisting of 0.50" Aluminum/Borated Aluminum plates (modeled as two 0.25"-thick plates). These plates are arranged to represent an egg-crate design with the 0.075" or 0.187"-Borated Aluminum and the remaining-Aluminum plate. The thermal expansion and egg-crate slot gaps are not modeled (conservative) assuming plate continuity, thus replacing the more absorbing internal moderator with aluminum plate.

KENO model plots in 2D for the various views of the basket compartment are shown in Figure 6-2 through Figure 6-7.

There are a total of 10 poison plates in the NUHOMS®-32PTH basket. They are located at all the faces where six fuel assemblies are lined up. Thus, all the interior 16 fuel assemblies are surrounded by poison plates on all four faces and the outer 16 fuel assemblies do not have poison plates on the radially outward looking face. The fuel assembly and poison plate positions (and the aluminum plate positions) in the KENO model of the basket is shown in Figure 6-8. Even though the poison and aluminum plates have been shown as discrete plates around the fuel compartment, they are all continuous running from one end of the basket to the other.

The basket structure is connected to the DSC shell by perimeter rail assemblies. The rail material is aluminum and SS304 and provide for a heat conduction path from the basket to the DSC shell. These rails are not modeled explicitly in the basic KENO model. They are, however, modeled in KENO as a homogenous (as illustrated in Figure 6-9) mixture of unborated water, Aluminum and SS304. The KENO unit numbers used for the fuel assembly positions are shown in Figure 6-9.

A list of all the geometry units used in the basic KENO model is shown in Table 6-8. Figure 6-10 shows the various radial "cylinders" utilized in the KENO model surrounding the fuel assemblies. Basically, this shows the canister and transfer cask details. For the parametric calculations to determine the most reactive geometry, the fuel assemblies are modeled with an initial enrichment of 4.30 wt. % U-235, a soluble boron concentration of 2500 ppm and a fixed poison loading of 15 mg B-10/cm^2 (Type B basket with a 90% credit for Borated Aluminum poison in the analysis).

In addition, a detailed KENO model with explicit representation of the rail structure, within the limitations of the KENO geometry, is also developed to demonstrate the adequacy and conservatism of the simplified KENO model with "homogenous" rail structure. A radial cross section of the basket with the "detailed" KENO model is shown in Figure 6-11.

The basic KENO model is used to determine the most reactive fuel assembly for a given enrichment, most reactive assembly-to-assembly pitch, and to determine the most reactive DSC configuration accounting for manufacturing tolerances including rail material homogenzation. The second model is of the most reactive configuration identified above. This model is used to determine the maximum allowable initial enrichment for each assembly type as a function of the soluble boron concentration and fixed poison loading, as appropriate.

This basic KENO model is modified to model the various damaged fuel configurations like single shear, double shear, optimum pitch and axial fuel shifting. These models are analyzed to determine the most reactive damaged fuel configuration for each fuel assembly class. The second model is based on the most reactive configuration identified above. This model is used to determine the maximum number of damaged fuel assemblies per DSC and the maximum allowable initial enrichment for each assembly type as a function of the soluble boron concentration and fixed poison loading, as appropriate.

6.3.2 Package Regional Densities

The Oak Ridge National Laboratory (ORNL) SCALE code package 3 contains a standard material data library for common elements, compounds, and mixtures. All the materials used for the TC and canister analysis are available in this data library.

Table 6-9 provides a complete list of all the relevant materials used for the criticality evaluation. The material density for the B-10 in the poison plates includes a 10% reduction.

6.4 Criticality Calculation

This section describes the analysis methodology utilized for the criticality analysis. The analyses are performed with the CSAS25 module of the SCALE system. A series of calculations are performed to determine the relative reactivity of the various fuel assembly designs evaluated and to determine the most reactive configuration without BPRAs. The most reactive intact fuel design, for a given enrichment, as demonstrated by the analyses, is the WE 17x17 standard assembly. The most reactive credible configuration is an infinite array of flooded casks, each containing 32 fuel assemblies, with minimum fuel compartment ID, minimum basket structure thickness and minimum assembly-to-assembly pitch.

A series of calculations are also performed to determine the relative reactivity of the various damaged fuel configurations for each fuel assembly class. The most reactive damaged fuel configuration for the WE17 and WE15 class occurs due to a postulated double-ended shear. The most reactive damaged fuel configuration for the CE14 class occurs when the fuel rods are arranged in an optimum pitch configuration. The most reactive credible configuration analyzed in this calculation is an infinite array of flooded casks, each containing a maximum of 32 damaged fuel assemblies with BPRAs, with minimum fuel compartment ID, minimum basket structure thickness and minimum assembly-to-assembly pitch.

As mentioned in Section 6.1, the NUHOMS®-32PTH DSC is evaluated to determine the maximum initial enrichment of the fuel assemblies (both damaged and intact) per DSC for each assembly class as a function of fixed poison loading and soluble boron concentration levels.

6.4.1 Calculational Method

6.4.1.3 Computer Codes

Criticality analyses were performed using the microcomputer application KENO-Va and the 44 neutron group library based on ENDF-B Version 5 cross-section data that are part of the SCALE 4.4 code package [3]. Validation and benchmarking of these codes is performed in accordance with applicable QA program requirements (see Chapter 13) and is discussed in Section 6.5.

SCALE 4.4 [3] is an extensive computer package which has many applications including cross section processing, criticality studies, and heat transfer analyses among others. The package is comprised of many functional modules, which can be run independently of each other. Control Modules were created to combine certain functional modules in order to make the input requirements less complex. For the purpose of criticality analysis, only four functional modules are used and one control module. These Modules are CSAS25, which includes the three dimensional criticality code KENO-Va and the preprocessing codes BONAMI-S, NITAWL-II and XSDRNPM-S.

KENO-Va, in conjunction with a suitable working library of nuclear cross section data, is used to calculate the multiplication factor, k_{eff}, of systems of fissile material. It can also compute lifetime and generation time, energy dependent leakages, energy and region-dependent absorptions, fissions, fluxes, and fission densities. KENO-Va utilizes a three-dimensional Monte-Carlo computation scheme. KENO-Va is capable of modeling complex geometries including facilities for handling arrays, arrays of arrays, and holes.

SCALE 4.4 is set up so that any number of cross-section libraries may be used with the preprocessing functional and control modules. For the purpose of this analysis, only the 44-group ENDF/B Version 5 library is used.

The preprocessing codes used for this analysis are the functional modules BONAMI-S, NITAWL-II and XSDRNPM-S. They are consolidated into the control module CSAS25. BONAMI-S has the function of performing Bondarenko calculations for resonance self-shielding. The cross sections and Bondarenko factor data are pulled from an AMPX master library. The output is placed into a master library as well. Dancoff approximations allow for different fuel lattice cell geometries. The main function of NITAWL-II is to change the format of the master cross-section libraries to one which the criticality code (KENO-Va) can access. It also provides the Nordheim Integral Treatment for resonance self-shielding. XSDRNPM-S provides cell-weighted cross sections based on the specified unit cell.

The criticality analysis, using the above computer codes, is performed in compliance with the 10CFR 72 [1] requirements. Specifically, all cases are analyzed assuming that the basket in fully flooded with borated water and the neutron shield of the transfer cask is eliminated and the cask is flooded with fresh water. Finally, KENO V.a calculates the k_{eff} of the system that is modeled. A sufficiently large number of neutron histories are run so that the standard deviation is below 0.0010 for all calculations.

6.4.1.3 Physical and Nuclear Data

The physical and nuclear data required for the criticality analysis include the fuel assembly data and cross-section data as described below.

Table 6-4 provides the pertinent data for criticality analysis for each fuel assembly evaluated for the NUHOMS® HD System.

The criticality analysis used the 44-group cross-section library built into the SCALE system. ORNL used ENDF/B-V data to develop this broad-group library specifically for criticality analysis of a wide variety of thermal systems.

6.4.1.3 Bases and Assumptions

The analytical results reported in Section 3.7 demonstrate that the TC containment boundary and canister basket structure do not experience any significant distortion under hypothetical accident conditions. Therefore, for both normal and hypothetical accident conditions the TC geometry is identical except for the neutron shield and skin. As discussed above, the neutron shield and skin are conservatively removed and the interstitial space modeled as water.

The TC is modeled with KENO V.a using the available geometry input. This option allows a model to be constructed that uses regular geometric shapes to define the material boundaries. The following conservative assumptions are also incorporated into the criticality calculations:

(1) No burnable poisons like IFBA, Gadolinia, Erbia or any other absorber, accounted for in the fuel.

(2) The fuel insert hardware like BPRA, TPA, and VSI are conservatively assumed to exhibit neutronic properties similar to $^{11}B_4C$. There is no neutron absorption from any of these hardware and are collectively referred to as BPRAs.

(3) Water density at optimum moderator density.

(4) Unirradiated fuel – no credit taken for fissile depletion due to burnup or fission product poisoning.

(5) The fuel pins are modeled assuming a stack density of 97.5% theoretical density with no allowance for dishing or chamfer. This assumption conservatively increases the total fuel content in the model.

(6) Temperature at 20°C (293K).

(7) The maximum fuel enrichment is modeled as uniform everywhere throughout the assembly. Natural Uranium blankets and axial or radial enrichment zones are modeled as enriched uranium with an average enrichment.

(8) All fuel rods are filled with full density water in the pellet/cladding gap.

(9) Only a 15.03-inch section of the basket with fuel assemblies is explicitly modeled with periodic axial boundary conditions, therefore the model is effectively infinitely long.

(10) It is assumed that for all cases the neutron shield and stainless steel skin of the cask are stripped away and the infinite array of casks are pushed close together with moderator in the interstitial spaces.

(11) The thermal expansion and egg-crate gaps are conservatively replaced with the basket material wherever present. This results in replacing the soluble boron moderator in the gap regions with Aluminum thereby decreasing the neutron absorption around the fuel.

(12) The transition rails between the basket and the canister shell are modeled as a homogenous material consisting of 30% full density water, 35% aluminum and 35% SS304 by volume. This homogenous rail structure assumption will be shown to be adequate and conservative with comparisons using a "detailed" model.

(13) The fixed poison inside the basket is based on either BORAL® or a Borated Aluminum alloy material design. A credit of 90% of the absorber material (B-10) is assumed in the analysis. When BORAL® is used as the fixed poison, a credit of 75% for the absorber material is utilized.

(14) All steel materials are modeled as SS304. The small differences in the composition of the various stainless steels have no effect on results of the calculation.

(15) All zirconium based materials in the fuel are modeled as Zircalloy-4. The small differences in the composition of the various clad / guide tube materials have no effect on the results of the calculation.

(16) No calculations are performed that model the uncovering of poison in the active fuel region of the basket. Even though the size of the cavity in the DSC is larger than the size of the basket, accidents involving a relative shift of the basket and the fuel assemblies at the bottom are not considered credible when the basket (and the DSC) is flooded with borated water and the DSC/TC system is in the vertical position. Therefore, all calculations are carried out with the active fuel region axially surrounded by fixed poison in the basket.

The following are the additional assumptions that are relevant to the damaged fuel assembly calculations:

(1) The cask containment boundary and canister basket structure do not experience any significant distortion under hypothetical accident conditions.

(2) The worst case gross damage resulting from a cask-drop accident is assumed to be either a single-ended or double-ended rod shear with flooding in borated water. A maximum of 4 inches of fuel may be uncovered by the poison plates due to shifting of the sheared rods.

(3) The cases with bare fuel and rubble are not modeled since replacing the clad with borated water results in an increase in absorption. Hence, damaged fuel cases are modeled with the presence of the clad around the fuel pellet.

(4) The bent or bowed fuel rod cases assume that the fuel is intact but that the rod pitch is allowed to vary from its nominal fuel rod pitch.

(5) The single-ended fuel rod shear cases assume that fuel rods that form one assembly face shear in one place and are displaced to new locations. The fuel pellets are assumed to remain in the fuel rods.

(6) The double-ended fuel rod shear cases assume that the fuel rods that form one assembly face shear in two places and the intact fuel rod pieces are separated from the parent fuel rods.

(7) Although only 16 damaged fuel assemblies are authorized contents for the DSC, all 32 fuel assemblies are considered to be damaged in the criticality analyses for damaged fuel.

6.4.1.3 Determination of k_{eff}

The Monte Carlo calculations performed with CSAS25 (KENO V.a) use a flat neutron starting distribution. The total number of histories traced for each calculation is approximately 800,000. This number of histories is sufficient to achieve source convergence and produce standard deviations of less than 0.10% in k_{eff}. The maximum k_{eff} for the calculation is determined with the following formula:

$$k_{eff} = k_{KENO} + 2\sigma_{KENO}.$$

6.4.2 Fuel Loading Optimization

The criticality analysis is performed for the 32PTH DSC loaded with 32 intact or 32 damaged fuel assemblies. The following sub-sections describe the various analyses performed with the intact fuel assemblies.

6.4.2.1 Most Reactive Fuel Assembly and Assembly Position Studies

The first series of analyses determines the most reactive fuel assembly design and the most reactive fuel positioning within the steel tubes. The first KENO run models the fuel assemblies as being centered within the basket compartment tubes. The off-center fuel assembly positioning is modeled by shifting all the fuel assemblies radially inward such that the fuel pins come in contact with the two faces of the compartment tubes. This is "inward" positioning and the fuel assemblies are at the closest approach relative to the center of the basket.

These calculations are repeated for all four fuel assembly designs listed in Table 6-3. These runs are carried out at nominal compartment dimensions with varying internal moderator density assuming a Type B basket and fuel at 4.30 wt% U-235 and a boron concentration of 2500 ppm. All input and output files are included on the attached compact disk. In all other respects, the model is the same as that described in Sections 6.3.1 and 6.3.2. The 2D KENO plots are shown in Figure 6-12 and Figure 6-13 and the results are shown in Table 6-10.

The peripheral rails were not modeled for these calculations. The rail material was assumed to be completely replaced by the internal moderator (borated water at 2500 ppm). This assumption does not affect this parametric study.

The most reactive fuel assembly design is the WE 17x17 standard fuel assembly for the WE17 class, the WE 15x15 standard fuel assembly for the WE15 class and the CE 14x14 Fort Calhoun Fuel assembly for the CE14 class of fuel assemblies. The "inward" positioning of fuel assemblies is most reactive.

6.4.2.2 Determination of the Most Reactive Configuration

The fuel loading configuration of the canister/cask affects the reactivity of the package. Several series of analyses determined the most reactive configuration for the canister/cask.

For this analysis, the most reactive fuel type is used to determine the most reactive configuration. The canister/cask is modeled, with the WE 17x17 standard assembly, over a 15.03-inch axial section with periodic axial boundary conditions and reflective radial boundary conditions. This represents an infinite array in the x-y direction of canister/casks that are infinite in length which is conservative for criticality analysis. The starting model is identical to the model used above. The canister/cask model for this evaluation differs from the actual design in the following ways:

- The boron 10 content in the poison plates is 10% lower than the minimum required,
- The stainless steel and aluminum basket rails, which provide support to the fuel compartment grid, are modeled using a homogenized material and,

- The neutron shield and the skin of the cask are conservatively replaced with water between the casks.

Each evaluation is performed at various internal moderator density (IMD) values to determine the optimum moderator density where the reactivity is maximized. All input and output files are included on the attached compact disk.

The first set of analyses determines the effect of rail material composition variation on the reactivity of the basket. The most reactive configuration from the previous section is utilized as the base case for this evaluation. Four different variations in the rail material compositions are considered in this evaluation. The previous evaluation utilized borated water as the rail material. In this evaluation, the rail materials used are unborated water at 100% density, composition 3 (30% water, 35% aluminum, 35% ss304 by volume), composition 4 (40% water, 30% aluminum, 30% ss304 by volume) and composition 5 (50% water, 25% aluminum, 25% ss304 by volume). The rails are also modeled discretely based on the detailed model, as shown in Figure 6-11, for a comparison of the results.

Based on the actual volume fraction of rail materials, it is expected that the volume of water does not go below 30%. Also, such a variation (composition 3 through 5) adequately accounts for the fabrication tolerances associated with the rail materials. The results of this evaluation are shown in Table 6-11 including the most reactive results from the previous study and the results based on the detailed model. These results indicate that the most reactive rail composition is the one based on composition 3. The results also indicate that the change is k_{eff} due to variation in composition is statistically insignificant. The comparison of k_{eff} results with composition 3 and detailed model indicates that the simplified model (based on homogenous rail) is both adequate and conservative. Therefore, for the rest of the calculation, the rail assemblies will be modeled with a homogenous rail assumption with the material based on composition 3.

The next set of calculations determines the effect of variation in the poison plate thickness in the reactivity of the system. The poison plate thickness is varied from a maximum of 0.187 inches (for the Type D basket) to a minimum of 0.050 inches (for the Type A basket) based on a poison loading of 15.0 mg B-10/cm^2 (Borated Aluminum poison, Type B basket loading). Even though, this large variation in thickness is not expected for a single basket type, these calculations are intended to demonstrate that the effect of variation is statistically insignificant. The variation in the poison plate thickness also results in a compensatory variation in the aluminum plate thickness in order to maintain the total thickness of 0.25 inches. Therefore, the study also indirectly evaluates the effect of variation in the aluminum plate thickness. The results of these calculations are shown in Table 6-12 along with the most reactive results from the previous evaluation.

The results of this evaluation indicate that the effect of variation in the poison plate thickness is statistically insignificant and that the maximum k_{eff} values at all plate thicknesses are about the same. As stated above, the variation in the thickness considered in this evaluation is not expected to represent physical reality; however, the results demonstrate that within the tolerance band for the thicknesses of various basket types, the variation in k_{eff} is statistically insignificant.

These results also indicate that there would be no significant effect on k_{eff} due to the presence of aluminum cladding in case of Boral® poison due to the fact that this study also evaluates the effect of aluminum plate thickness.

The next set of analyses determines the effect of fuel compartment size on the system reactivity. The model starts with the most reactive geometry determined from the previous study. For this evaluation, the compartment size is varied from 8.650 inches to 8.750 inches square. These results are shown in Table 6-13. These results indicate that the most reactive configuration is with the minimum fuel compartment size because the assembly-to-assembly pitch is minimized.

The next set of analyses determines the effect of fuel compartment box thickness on the system reactivity. The model starts with the minimum fuel compartment width from the previous study and the compartment thickness is varied from 0.1775 inches to 0.2325 inches. The results in Table 6-14 show that the most reactive calculated condition occurs with nominal compartment box thickness. The results indicate that the system reactivity is not very sensitive to the box thickness and that the difference in k_{eff} between the nominal and minimum thickness cases is within statistical uncertainty. The balance of this evaluation uses the nominal box thickness because it represents the most reactive configuration from this study.

6.4.2.3 Determination of Maximum Initial Enrichment for Intact Assemblies

The most reactive configuration determined based on parametric studies is with the rail structure represented with Composition 3, poison and aluminum plates at nominal thickness, fuel compartment at minimum width and nominal thickness and the fuel assemblies positioned in the "inward" position. The following analysis uses this configuration to determine the maximum allowable initial enrichment as a function of poison plate loading and soluble boron concentration for the two fuel assembly classes. Only the fuel assembly type, the fixed and soluble poison loading is changed for each model. In addition, the internal moderator density is varied to determine the peak reactivity for the specific configuration.

The canister / cask model for this evaluation differs from the actual design in the following ways:

- the boron-10 content in the borated aluminum poison plates is 10% lower than the minimum required and the boron-10 content in the Boral® poison plates is 25% lower than the minimum required
- the neutron shield and the skin of the cask are conservatively replaced with water between the casks, and
- the worst case geometry and material conditions, as determined in the previous sections, are modeled.

Five different fixed poison loadings are analyzed in the criticality calculations as described in Section 0, corresponding to the five different types of basket based on fixed poison loading (Type A, B, C, D and E). Four different soluble boron concentration levels are analyzed -2000 ppm, 2300 ppm, 2400 ppm and 2500 ppm. The maximum analyzed initial enrichment is 5.0 wt. % U-235.

Calculations are also performed with the presence of BPRAs (bounding for all NFAH) in the guide tubes to determine the maximum allowable enrichment for the WE15 and WE17 fuel assembly classes with NFAH. These calculations are applicable to intact fuel assemblies only. Reconstituted fuel assemblies, where the fuel pins are replaced by non-fuel pins are also considered intact fuel assemblies provided they displace the same amount of moderator.

CE 14x14 Class Assemblies

The most reactive CE 14x14 class assembly is the CE 14x14 Fort Calhoun type fuel assembly with the larger fuel pellet OD. The results for the CE 14x14 class of fuel assemblies are shown in Table 6-33.

WE 15x15 Class Assemblies

The most reactive WE 15x15 class assembly is the WE 15x15 standard fuel assembly. The results for the WE 15x15 class of fuel assemblies without BPRAs are shown in Table 6-15. The results for WE 15x15 class of fuel assemblies with BPRAs are shown in Table 6-16. These results indicate that the presence of BPRAs increases the reactivity of the system and consequently a reduction in the allowable enrichment.

WE 17x17 Class Assemblies

The most reactive WE 17x17 class assembly is the WE 17x17 standard fuel assembly. The results for the WE 17x17 class of fuel assemblies without BPRAs are shown in Table 6-17. The results for WE 17x17 class of fuel assemblies with BPRAs are shown in Table 6-18. These results also indicate that the presence of BPRAs increases the reactivity of the system and consequently a reduction in the allowable enrichment. For calculations with Type C basket, the WE 17x17 assembly results are conservatively applied to WE 15x15 assembly.

6.4.2.4 Determination of the Most Reactive Damaged Fuel Configuration

There are several mechanisms by which a fuel rod may be breached. These mechanisms may occur while the fuel is loaded in the reactor core, in the spent fuel pool, during transport, while in temporary dry storage, and while in permanent dry storage. In addition, the type and extent of fuel rod breach can be broken down into several categories. For this calculation, the method by which the fuel rod is breached is not as important as the extent of the resultant damage. The worst case gross damage resulting from a cask drop accident is assumed to be either a single-ended or double-ended rod shear with moderator intrusion. The bent or bowed fuel rod cases assume that the fuel is intact but not in its nominal fuel rod pitch. It is possible that the fuel rods may be crushed inwards or bowed outwards to a certain degree. Therefore, this will be evaluated by varying the fuel rod pitch from a minimum pitch (based on clad OD) to a maximum based on the fuel compartment size for each fuel assembly class. All pitch variations assume a uniform rod pitch throughout the entire fuel matrix.

The single-ended fuel rod shear cases assume that a fuel rod shears in one place and is displaced to a new location. The fuel pellets are assumed to remain in the fuel rod. This case will be evaluated by displacing one row of rods from the base fuel assembly matrix at small increments towards the side of the fuel compartment. The base fuel assembly matrix will be at nominal

pitch and positioned in the "inward" position within the 32PTH DSC to maximize the separation distance between the fuel array and the sheared row of fuel rods. A smaller rod pitch for the base fuel assembly matrix was not chosen because it has been shown from the pitch cases that decreasing the rod pitch decreases reactivity. Increasing the base fuel assembly rod pitch will increase reactivity, however, the resulting model is similar to and is bounded by the rod pitch varying cases presented above and therefore will not be duplicated here. The single shear cases are analyzed for the two fuel assembly classes.

The double-ended fuel rod shear cases assume that the fuel rod shears in two places and the intact fuel rod piece is separated from the parent fuel rod. Three resulting conditions are exhibited by the occurrence of a double-ended rod shear. These are, the fuel rod piece can remain in place, it can be displaced in the same plane, or it can be displaced to a different plane. The "remain in place" situation results in no deviation from the base fuel assembly matrix, and is therefore considered trivial and will not be evaluated separately. The fuel rod piece displaced in the same plane is equivalent to the single-ended rod shear case discussed above and will not be reevaluated in these cases. The fuel rod piece displaced in a different plane results in two possibilities: an added rod or a removed rod. As in the single-ended shear cases, the base fuel assembly matrix will be positioned in the "inward" position of the 32PTH DSC to allow room for a row of displaced fuel rods. One row of fuel rods of different lengths will be removed from a section of the assembly and added to another to determine if the system exhibits any trends. The nominal rod pitch is used for the base fuel matrix just as in the single-ended shear rod cases. The two fuel assembly classes are analyzed for the double-ended shear configuration.

In order to determine the effect of an axial shift in the fuel assemblies beyond the poison during transfer, bounding calculations that consider a 4" axial shift of fuel assemblies are performed. The nominal rod pitch is used for these cases and both the fuel assembly classes are analyzed for this configuration.

The first step is to determine the most reactive damaged fuel assembly geometry. This was completed using limiting fixed poison loading, soluble boron concentration and assembly enrichment for the various fuel assembly classes. The limiting parameters used for this study are shown in Table 6-19. All 32 assembly locations were filled with damaged fuel assemblies. The intent of these calculations was to determine the most reactive geometry, not to meet the USL. The following is a breakdown of runs made in this analysis:

- Optimum Rod Pitch Study (for fuel assemblies and rod storage baskets).
- Single-ended Shear Study.
- Double-ended Shear Study.
- Shifting of fuel assemblies beyond (4 inches above) the poison sheet height.

With the selection of the most reactive damaged fuel assembly geometry, the next set of analyses determined the maximum k_{eff} for various damaged fuel assembly loading configurations in the NUHOMS® 32PTH DSC. The most reactive damaged fuel assembly geometry for each fuel assembly class determined will be used to determine the maximum enrichment as a function of

fixed poison loading and soluble boron concentration for loading 32 damaged fuel assemblies in the basket. In other words, cases are analyzed for all the configurations described in Table 6-1.

Rod Pitch Study:

The first set of damaged fuel analyses involved a study on the effect of the fuel rod pitch on system reactivity. KENO models with rod pitches ranging from a minimum corresponding to the clad OD to a maximum limited by the fuel compartment size are developed for each fuel assembly class. The results of the rod pitch study are shown in Table 6-20 and a discussion of these results is as follows. For the CE14 fuel assembly class, the optimum pitch was calculated to be 0.620". For the WE15 fuel assembly class, the largest pitch (limited by the fuel compartment size) resulted in the most reactive configuration. For the WE17 fuel assembly class, the second largest pitch resulted in the most reactive configuration.

This study also bounds damaged fuel configurations with missing rods. A separate study to determine the effect on reactivity due to removal of fuel rods at optimum pitch is not necessary due to the presence of soluble boron in the moderator. The removal fuel rods would ensure that the fissile fuel rods are replaced with boron poison and would result in a reduction in k_{eff}. Therefore, the rod pitch study is completed by determining the optimum pitch and the associated maximum k_{eff} at optimum moderator density. The 2D KENO plot for the CE14 fuel assembly is shown in Figure 6-14.

Single Ended Rod Shear Study:

The next set of analyses performed is for the Single-ended rod shear. The Single-ended rod shear study depicts the fuel assembly with its last row of rods separated from the rest of the assembly. The displacement of the sheared row of rods varies radially from fuel assembly up to a maximum that is governed by the fuel assembly width and the fuel compartment size.

To model this in KENO, the base case was slightly modified. First, for a given fuel lattice, the fuel assemblies are modeled as a XX by (XX-1) array where XX corresponds to the fuel assembly class. For example, the WE 15 fuel assembly is modeled as a 15x14 array. Unit 200 is a XX by 1 array comprising of the single sheared row of rods. The units 201, 204, 211 and 214, therefore consist of two arrays, the array describing the truncated fuel assembly and the sheared row of fuel rods. The displaced row of rod array is then shifted (separation distance is "d") away from the fuel assembly. The amount of fuel remains the same, i.e. no new fuel is added to the system. Nominal rod pitch for all of the fuel assembly classes is used for the base XX by (XX-1) fuel assembly. In the cask drop accident scenarios, it is more likely that the fuel assembly will be crushed as a result of the drop and therefore cause local decreases in the rod pitch of the assembly. However, the rod pitch studies outlined above show that a decrease in the fuel rod pitch results in a decrease in system reactivity, therefore for the single-ended rod shear study runs, rod pitch is modeled at nominal value. The study is repeated for all the fuel assembly classes and at varying moderator density for important separation distances. An example plot of a single ended shear configuration with WE 17x17 fuel assembly is shown in Figure 6-15. The results of this evaluation are shown in Table 6-21. The results indicate that there exists an optimum shear row separation distance for each class of fuel assembly where the reactivity is highest.

Double Ended Rod Shear Study:

The three Double-ended Rod Shear cases model a row (XX by 1 array) of dislocated rods severed at different sections axially and then displacing to other sections of the DSC in order to define a conservative bounding condition for fuel rod location subsequent to a double-ended rod shear. To model this in KENO, the base case was accordingly modified. A new KENO unit, UNIT 11 forms one axial section of the basket that models the un-sheared fuel assemblies. The sheared fuel assemblies depleted by one row of fuel rods are modeled as a XX by (XX-1) array where XX corresponds to the fuel assembly class. The corresponding KENO units for the fuel assembly positions are 301, 304, 311, 314, 302, 303, 305 and 312. The unit 12 forms the axial section of the basket that models this depleted array of fuel assemblies. The fuel assemblies that contain the sheared-migrated row of fuel rods are modeled as a XX by (XX+1) array where XX corresponds to the fuel assembly class. The corresponding KENO units for the fuel assembly positions are 401, 404, 411 414, 402, 403, 405 and 412. The unit 13 forms the axial section of the basket that models this depleted array of fuel assemblies. Depending on the fraction of double shear, the array 11 (an axial array of units 11, 12 and 13) is constructed to calculate the reactivity effect. Due to the height of a single axial segment (15.03"), the total axial height of the model for these studies is 150.30" (15.03*10). However, periodic axial boundary conditions are applied making the model essentially infinite. The same rod pitch assumptions made for the Single-ended Shear runs also apply here.

Basically three types of double ended shear studies are evaluated. The first is a half shear where the sheared row breaks into two equal sections resulting in one-half of the fuel assembly being defined by a rod array containing an extra row of fuel rods while the other half is defined by an array depleted by one row of fuel rods. The half shear is represented in this calculation as a $(5/10)^{th}$ shear. The second is a one-third shear where the sheared row breaks into two unequal sections measuring a third of the fuel assembly length and two-third of the fuel assembly length respectively. Therefore, the fuel assembly can be defined by three axially equal sections, one with a regular array of fuel rods, one with an extra row of fuel rods and the other with a depleted row of fuel rods. This is modeled as $(3/10)^{th}$ which is about the same as one-third. The same mechanism can be extended to other shear ratios but the effect on reactivity is expected to reduce with reduction in the shear ratio. The one-fifth shear is also analyzed in this study as $(2/10)^{th}$ shear. The internal moderator density is varied to determine the k_{eff} at optimum density.

Results of the double-ended rod shear study show that the movement of one exterior row of half of the fuel assembly length is the most reactive. The CE14 fuel is only evaluated for the half shear condition since the evaluation results show this is the most reactive. An example plot of a double ended shear configuration with WE 15x15 fuel assembly is shown in Figure 6-16. The results of the evaluation are shown Table 6-22.

Shifting of Fuel Beyond Fixed Poison:

This study analyzes the effect of shifting of loose rods beyond the height of the poison plates. Two types of shifting of fuel rods beyond the poison plates are analyzed in this study. The first calculational model assumes that a four-inch axial section of the entire fuel assembly shifts beyond the poison plates. The height of the axial shift, four-inches, is more than the maximum difference between the basket height and the canister cavity height (about 2.5 inches). The

second calculational model involves a shifting of 8 of the outermost rows of fuel rods (basically two concentric rings of fuel rods) beyond the poison plates by six inches. In KENO, this six-inch section is modeled like a regular fuel assembly with fuel pins defining the 8 outer most rows (and columns) with aluminum occupying the space in the middle. This is done to simulate the sliding of fuel rods around the inlet or outlet nozzle during an accident. These models conservatively bound all the cases associated with the shifting of fuel rods beyond poison like sliding of a single rod, sliding of a row of single sheared rods etc.

To model these in KENO, the base case was modified. First, a new KENO unit, UNIT 11 forms one axial section of the basket that models the fuel assemblies covered with poison. For the shifting of fuel assemblies (first model), a four-inch axial section of the fuel assemblies containing the uncovered fuel assemblies are modeled with the KENO units 301, 304, 311 and 314. The unit 12 forms the axial section of the basket that models this uncovered section of fuel assemblies. Finally, the array 11 (an axial array of units 11 and 12) is constructed to calculate the reactivity effect. Periodic axial boundary conditions are utilized to make this model essentially infinite in length. For the sliding of fuel assemblies (second model), a six-inch axial section of the fuel assemblies containing the eight uncovered rows of fuel rods with aluminum in the middle portion are modeled with the KENO units 301, 304, 311 and 314. The unit 12 forms the axial section of the basket that models this uncovered section of fuel assemblies. Finally, the array 11 (an axial array of units 11 and 12) is constructed to calculate the reactivity effect. Periodic axial boundary conditions are utilized to make this model essentially infinite in length. This study is performed for the two fuel assembly classes with varying moderator density.

The results of these evaluations are shown in Table 6-23. An example plot of a shifting configuration with WE 17x17 fuel assembly is shown in Figure 6-17. An example plot of a sliding configuration with WE 15x15 fuel assembly is shown in Figure 6-18.

6.4.2.5 Determination of the Most Reactive Damaged Configuration

The fuel-loading configuration of the canister/cask affects the reactivity of the package. Several series of analyses performed in the previous sections evaluated the various damaged assembly configurations. A comparison of the maximum k_{eff} due to the various damaged assembly configurations is shown in Table 6-24. The most reactive damaged assembly configuration for the CE14 fuel is the optimum pitch configuration of the rods and for the WE15 and WE17 fuel is the double-ended rod shear with a shear ratio of one-half.

Additionally, the one-half (5/10) double-ended shear configuration is modified to include BPRAs to obtain a bounding damaged assembly configuration. The results of this evaluation, shown in Table 6-25, demonstrate that the configuration with BPRAs is bounding. Therefore, this configuration is the design basis configuration for the WE15 and WE17 fuel assembly classes and will be utilized to determine the k_{eff} of the NUHOMS®-32PTH DSC containing damaged fuel assemblies. An example plot of a double ended shear configuration with WE 15x15 fuel assembly with BPRAs is shown in Figure 6-19.

6.4.2.6 Determination of Maximum Initial Enrichment for Damaged Assemblies

The most reactive damaged assembly configuration for the WE15 and WE17 fuel is based on the double-ended shear model with a shear ratio of one-half with BPRAs while the most reactive damaged assembly configuration for the CE14 fuel is based on an optimum pitch arrangement of rods. The following analysis uses these configurations to determine the maximum allowable initial enrichment as a function of poison plate loading and soluble boron concentration for all the fuel assembly classes. The analysis is carried out with the NUHOMS®-32PTH DSC containing 32 design basis damaged assemblies. Only the fuel assembly type, the fixed and soluble poison loading is changed for each model. In addition, the internal moderator density is varied to determine the peak reactivity for the specific configuration. All calculations for the WE15 and WE17 fuel are performed with the presence of BPRAs (bounding for all NFAH and no NFAH cases) in the guide tubes to determine the maximum allowable enrichment for these two fuel assembly classes with and without NFAH.

The canister / cask model for this evaluation differs from the actual design in the following ways:

- the boron-10 content in the borated aluminum poison plates is 10% lower than the minimum required and the boron-10 content in the boral® poison plates is 25% lower than the minimum required
- the neutron shield and the skin of the cask are conservatively replaced with water between the casks, and
- the worst case geometry and material conditions as determined in Section 6.4.2.2 and the worst case damaged assembly configuration as determined in Section 6.4.2.5, are modeled.

Five different fixed poison loadings are analyzed in the criticality calculations as described in Section 4.2, corresponding to the four different types of basket based on fixed poison loading (Type A, B, C, D and E). Four different soluble boron concentration levels are analyzed - 2000 ppm, 2300 ppm, 2400 ppm and 2500 ppm. The maximum analyzed initial enrichment is 5.0 wt. % U-235.

CE 14x14 Class Assemblies

The results for CE 14x14 class of fuel assemblies are shown in Table 6-34.

WE 15x15 Class Assemblies

The results for WE 15x15 class of fuel assemblies with BPRAs are shown in Table 6-16.

WE 17x17 Class Assemblies

The most reactive WE 17x17 class assembly is the WE 17x17 standard fuel assembly. The results for the WE 17x17 class of fuel assemblies with BPRAs are shown in Table 6-17. For calculations with Type C basket, the WE 17x17 assembly results are conservatively applied to WE 15x15 assembly.

6.4.3 Criticality Results

This section presents the results of the analyses used to demonstrate the acceptability of storing qualified fuel in the 32PTH DSC under normal, off-normal, and accident conditions for fuel loading, handling, and storage.

Table 6-28 lists the bounding results for intact fuel assemblies for all conditions of storage. The highest calculated k_{eff}, including 2σ uncertainty, is for the WE 17x17 Standard fuel assembly with an initial enrichment of 3.80 wt. % U-235, 2300 ppm soluble boron and a poison loading of 7.0 mg B-10/cm^2 (Type A Basket) without BPRAs. The maximum allowable initial enrichment with BPRAs for the WE15 and WE17 (bounding for cases without BPRAs) fuel assembly types and without BPRAs for the CE14 fuel assembly type as a function of fixed poison loading and soluble boron concentration is given in Table 6-1. The input files for the cases with the highest calculated reactivity (with and without BPRAs) are included in the Appendix A.

Table 6-29 lists the bounding results for damaged fuel assemblies for all conditions of storage. The highest calculated k_{eff}, including 2σ uncertainty for the damaged assembly calculations, is 0.9402 and it occurs for the WE 17x17 Standard fuel assembly with an initial enrichment of 4.80 wt. % U-235, 2400 ppm soluble boron and a poison loading of 50.0 mg B-10/cm^2 (Type E Basket). The maximum allowable initial enrichment with BPRAs for the WE15 and WE17 (bounding for cases without BPRAs) fuel assembly types and without BPRAs for the CE14 fuel assembly type as a function of fixed poison loading and soluble boron concentration is given in Table 6-1. The input file for the case with the highest calculated reactivity is included in the Appendix A.

ANS/ANSI-8.1 [5] recommends that calculational methods used in determining criticality safety limits for applications outside reactors be validated by comparison with appropriate critical experiments. An Upper Subcritical Limit (USL) provides a high degree of confidence that a given system is subcritical if a criticality calculation based on the system yields a k_{eff} below the USL.

The criterion for subcriticality is that

$$k_{KENO} + 2\sigma_{KENO} \leq USL,$$

Where USL is the upper subcritical limit established by an analysis of benchmark criticality experiments. In Section 6.5, the minimum USL over the parameter range is determined to be is 0.9419. From Table 6-28 and Table 6-29, for the most reactive case,

$$k_{KENO} + 2\sigma_{KENO} = 0.9390 + 2\ (0.0007) = 0.9404 \leq 0.9419.$$

This indicates that the fuel will remain subcritical. Conclusions regarding specific aspects of the methods used or the analyses presented can be drawn from the quantitative results presented in the associated tables.

6.5 Critical Benchmark Experiments

The criticality safety analysis of the NUHOMS® OS 187H TC containing the NUHOMS® - 32PTH DSC uses the CSAS25 module of the SCALE system of codes. The CSAS25 control module allows simplified data input to the functional modules BONAMI-S, NITAWL-S, and KENO V.a. These modules process the required cross-section data and calculate the k_{eff} of the system. BONAMI-S performs resonance self-shielding calculations for nuclides that have Bondarenko data associated with their cross sections. NITAWL-S applies a Nordheim resonance self-shielding correction to nuclides having resonance parameters. Finally, KENO V.a calculates the effective neutron multiplication (k_{eff}) of a 3-D system.

The analysis presented herein uses the fresh fuel assumption for criticality analysis. The analysis employs the 44-group ENDF/B-V cross-section library because it has a small bias, as determined by 121 benchmark calculations. The Upper Subcritical Limit (USL-1) was determined using the results of these 121 benchmark calculations.

The benchmark problems used in this verification are representative of benchmarks of commercial light water reactor (LWR) fuels with the following characteristics:

A. water moderation

B. boron neutron absorbers

C. unirradiated light water reactor type fuel (no fission products or "burnup credit")

D. close reflection

E. near room temperature (vs. reactor operating temperature)

F. Uranium oxide fuels.

Criticality codes are verified by comparing benchmark calculations to actual critical benchmark experiments. The difference between the calculated reactivity and the experimental reactivity is referred to as 'calculational' bias. This bias may be a function of system parameters such as fuel lattice separation, fuel enrichment, neutron absorber properties, reflector properties, or fuel/moderator volume ratio; or, there may be no specific correlation with system parameters. These experiments are discussed in detail in reference 6.

6.5.1 Benchmark Experiments and Applicability

The benchmark data used for determination of the USL is provided in Table 6.5-1. The set of criticality experiments used as benchmarks are representative of the composition, configuration, and nuclear characteristics of the system modeled. Six parameters were selected in order to demonstrate the applicability of the SCALE 44-group ENDF/B-V cross-section library for the range of conditions spanned by the calculation models. The results of these evaluations are provided in Table 6.5-2. Only those experiments with the parameter in question were used to determine the USL for that parameter. The methodology used to calculate the USL is based on NUREG/CR-6361 6, USL method 1.

USL-1 applies a statistical calculation of the bias and its uncertainty plus an administrative margin (0.05 Δk) to the linear fit of results of the experimental benchmark data developed. The USL from the data set with the best correlation is used as the acceptance criteria for subsequent criticality evaluations. Since there was not a strong correlation for any of the data sets, i.e., the correlation was essentially random and the lowest possible USL-1 result was used as the USL.

The uncertainty due to modeling approximations does not impact the calculated k_{eff}. Worst case tolerances (as specified in the design drawings presented in Chapter 1) are used in the analysis to maximize k_{eff}. Only the tolerances of those dimensions that had a positive effect on k_{eff} were included in the SCALE geometry models.

6.5.2 Results of the Benchmark Calculations

A summary of all of the pertinent parameters for each experiment along with the results of each case is included in Table 6-30. The USL benchmark calculations are shown in reference 9. The best correlation (linear regression correlation for each parameter vs. k_{eff}) is observed for fuel assembly separation distance, with a correlation of 0.656. All other parameters show much lower correlation ratios indicating no real correlation. All parameters were evaluated for trends and to determine the most conservative USL. Since there was no observable correlation, the worst case USL was selected for the identified parameters. Results from the USL evaluation are presented in Table 6-31.

The criticality evaluation presented here used the same cross section library, fuel materials and similar material/geometry options that were used in the 121 benchmark calculations as shown in Table 6-30. The modeling techniques and the applicable parameters for the actual criticality evaluations fall within the range of those addressed by the benchmarks in Table 6-31. The results from the comparisons of physical parameters of each of the fuel assembly types to the applicable USL value are presented in Table 6-32. The minimum value of the USL-1 was determined to be 0.9419 based on comparisons to the most limiting assembly parameters.

6.6 Supplemental Information

6.6.1 References

1. Code of Federal Regulations, Title 10, Part 72, "Licensing Requirements for the Independent Storage of Spent Nuclear Fuel and High-Level Radioactive Waste."

2. Not Used

3. "SCALE, A Modular Code System for Performing Standardized Computer Analyses for Licensing Evaluation", NUREG/CR-0200, Rev. 6 (ORNL/NUREG/CSD-2/R6), Vol. I-III, September 1998.

4. ANSI/ANS 57.2, Design Requirements for Light Water Reactor Spent Fuel Storage Facilities at Nuclear Power Plants, 1983.

5. ANS/ANSI-8.1, American National Standard for Nuclear Criticality Safety in Operations with Fissionable Materials Outside Reactors, 1983.

6. U.S. Nuclear Regulatory Commission, "Criticality Benchmark Guide for Light-Water-Reactor fuel in Transportation and Storage Packages," NUREG/CR-6361, ORNL-TM-13211, March 1997.

7. U.S. Nuclear Regulatory Commission, "Recommendations for Preparing the Criticality Safety Evaluation of Transportation Packages," NUREG/CR-5661, ORNL/TM-11936, April 1997.

8. Transnuclear Specification, "Design Criteria Document for the 10494 NUHOMS®-32PTH System for Transportation and Storage."

9. Transnuclear Calculation 1095-42, rev. 0, "Criticality Benchmarks."

THIS PAGE IS INTENTIONALLY LEFT BLANK

6.6.2 KENO Input Files

(PROPRIETARY INFORMATION)

Proprietary Information Withheld Under 10 CFR 2.390

Table 6-1
Maximum Assembly Average Initial Enrichment for Each Fuel Design for both Intact and Damaged Fuel Assemblies

Assembly Class and Type[(1),(2)]	Maximum Assembly Average Initial enrichment of U-235 as a Function of Soluble Boron Concentration and Fixed Poison Loading (Basket Type)				
	Basket Type	Minimum Soluble Boron Concentration			
		2000 ppm	2300 ppm	2400 ppm	2500 ppm
CE 14x14 Intact Fuel Assembly (without BPRA)	**A**	**4.05**	**4.40**	**4.45**	**4.55**
	B	**4.55**	**4.90**	**5.00**	**-**
	C	**4.70**	**5.00**	**-**	**-**
	D	**5.00**	**-**	**-**	**-**
	E	**-**	**-**	**-**	**-**
WE 15x15, WES 15x15 Intact Fuel Assembly (with and without BPRAs)	**A**	**3.50**	**3.70**	**3.80**	**3.90**
	B	**3.80**	**4.10**	**4.20**	**4.30**
	C	**3.95**	**4.25**	**4.35**	**4.45**
	D	**4.20**	**4.50**	**4.70**	**4.80**
	E	**4.50**	**4.80**	**4.90**	**5.00**
WE 17x17, WEV 17x17 WEO 17x17 MK BW 17x17 Intact Fuel Assembly (with and without BPRAs)	**A**	**3.50**	**3.70**	**3.80**	**3.90**
	B	**3.80**	**4.10**	**4.20**	**4.30**
	C	**3.95**	**4.25**	**4.35**	**4.45**
	D	**4.20**	**4.50**	**4.60**	**4.70**
	E	**4.45**	**4.70**	**4.90**	**5.00**
CE 14x14 Damaged Fuel Assembly (without BPRAs)	**A**	**3.90**	**4.20**	**4.25**	**4.35**
	B	**4.35**	**4.70**	**4.80**	**4.90**
	C	**4.50**	**4.85**	**4.95**	**5.00**
	D	**4.85**	**5.00**	**-**	**-**
	E	**5.00**	**-**	**-**	**-**
WE 15x15, WES 15x15 Damaged Fuel Assembly (with and without BPRAs)	**A**	**3.40**	**3.60**	**3.70**	**3.80**
	B	**3.75**	**4.00**	**4.10**	**4.20**
	C	**3.85**	**4.15**	**4.25**	**4.35**
	D	**4.10**	**4.40**	**4.50**	**4.60**
	E	**4.35**	**4.70**	**4.80**	**4.90**
WE 17x17, WEV 17x17 WEO 17x17 MK BW 17x17 Damaged Fuel Assembly (with and without BPRAs)	**A**	**3.40**	**3.60**	**3.70**	**3.80**
	B	**3.75**	**4.00**	**4.10**	**4.20**
	C	**3.85**	**4.15**	**4.25**	**4.35**
	D	**4.10**	**4.40**	**4.50**	**4.60**
	E	**4.30**	**4.65**	**4.80**	**4.90**

(1) WE 15x15 bounds all 15x15
(2) WE 17x17 bounds all 17x17

Table 6-2
Summary of Limiting Criticality Evaluations for all Fuel Assemblies

Limiting Assembly Position- The fuel assembly is located in the corner of each compartment tube closest to the 32PTH DSC centerline.				
CE 14x14 Fuel Assembly				
Case	**K_{eff}**	**σ**	**K_{eff} + 2σ**	**USL**
Intact Fuel - 70% IMD, Type A Basket (7.0 mg B-10/cm^2), 2300 ppm Boron, 4.4 wt. % U-235	0.9383	0.0007	0.9397	0.9419
Damaged Fuel – Optimum Pitch, 70% IMD Type B Basket (15.0 mg B-10/cm^2), 2400 ppm Boron, 4.8 wt. % U-235	0.9386	0.0007	0.9400	0.9419
WE 15x15 Fuel Assembly				
Case	**K_{eff}**	**σ**	**K_{eff} + 2σ**	**USL**
Intact Fuel - 90% IMD, No BPRA, Type D Basket (32.0 mg B-10/cm^2), 2500 ppm Boron, 4.9 wt. % U-235	0.9383	0.0008	0.9399	0.9419
Intact Fuel - Full IMD, With BPRA, Type D Basket (32.0 mg B-10/cm^2), 2400 ppm Boron, 4.7 wt. % U-235	0.9388	0.0007	0.9402	0.9419
Damaged Fuel - Double Ended Shear Full IMD, With BPRA, Type E Basket (50.0 mg B-10/cm^2), 2300 ppm Boron, 4.7 wt. % U-235	0.9361	0.0007	0.9375	0.9419
WE 17x17 Fuel Assembly				
Case	**K_{eff}**	**σ**	**K_{eff} + 2σ**	**USL**
Intact Fuel - 70% IMD, No BPRA, Type A Basket (7.0 mg B-10/cm^2), 2300 ppm Boron, 3.8 wt. % U-235	0.9390	0.0007	0.9404	0.9419
Intact Fuel - 80% IMD, With BPRA, Type A Basket (7.0 mg B-10/cm^2), 2500 ppm Boron, 3.9 wt. % U-235	0.9381	0.0008	0.9397	0.9419
Damaged Fuel - Double Ended Shear Full IMD, With BPRA, Type E Basket (50.0 mg B-10/cm^2), 2400 ppm Boron, 4.8 wt. % U-235	0.9388	0.0007	0.9402	0.9419

Table 6-3
Authorized Contents for NUHOMS®-32PTH DSC

Assembly Type[1]	Array
Westinghouse 17x17 Standard (WE 17x17) Westinghouse 17x17 Vantage 5H (WEV 17x17)	17x17
Westinghouse 17x17 OFA (WEO 17x17)	17x17
Framatome ANP Advanced MK BW 17x17 (MK BW 17x17)	17x17
Westinghouse 15x15 Standard (WE 15x15) Westinghouse 15x15 Surry Improved (WES 15x15)	15x15
CE 14x14 Standard (CE 14x14)	14x14

(1) Equivalent reload fuel assemblies that are enveloped by the fuel assembly design characteristics listed above are also acceptable.

Table 6-4
Fuel Assembly Design Parameters[2] for Criticality Analysis

Manufacturer[1]	Array	Version	Active Fuel Length (inches)	# Fuel Rods per Assembly	Pitch (inches)	Fuel Pellet OD (inches)
Westinghouse	17x17	Standard Vantage	144	264	0.4960	0.3225
Westinghouse	17x17	OFA	144	264	0.4960	0.3088
Framatome	17x17	MK BW	144	264	0.4960	0.3195
Westinghouse	15x15	Std / Surry	144	204	0.5630	0.3669
CE	14x14	Std	137	176	0.5800	0.3765
CE	14x14	Ft. Calhoun	128	176	0.5800	0.3815
Manufacturer[1]	**Array**	**Version**	**Clad Thickness (inches)**	**Clad OD (inches)**	**Guide Tube OD Inst. Tube OD (inches)**	**Guide Tube ID Inst. Tube ID (inches)**
Westinghouse	17x17	Standard Vantage	0.0225	0.374	24 @ 0.4820 1 @ 0.4740	24 @ 0.4500 1 @ 0.4440
Westinghouse	17x17	OFA	0.0225	0.360	24 @ 0.4820 1 @ 0.4740	24 @ 0.4500 1 @ 0.4440
Framatome	17x17	MK BW	0.0225	0.374	24 @ 0.4820 1 @ 0.4820	24 @ 0.4500 1 @ 0.4500
Westinghouse	15x15	Std / Surry	0.0243	0.422	20 @ 0.5450 1 @ 0.5450	20 @ 0.5100 1 @ 0.5100
CE	14x14	Std	0.0280	0.440	5 @ 1.115	5 @ 1.035
CE	14x14	Ft. Calhoun	0.0280	0.440	5 @ 1.115	5 @ 1.035

(1) Equivalent reload fuel assemblies that are enveloped by the fuel assembly design characteristics listed above are also acceptable.
(2) All Dimensions shown are nominal

Table 6-5
NUHOMS®-32PTH - Basket and DSC Dimensions

Parameter	Actual inches	Model inches (cm)
Compartment Inside (Nominal)	8.700	8.700 (22.0980)
Compartment Inside (Maximum)	8.750	8.750 (22.2250)
Compartment Inside (Minimum)	8.650	8.650 (21.9710)
Compartment wall (Nominal)	0.1875	0.1875 (0.47625)
Compartment wall (Maximum)	0.2325	0.2325 (0.59055)
Compartment wall (Minimum)	0.1775	0.1775 (0.45085)
Stainless steel strip height	1.75	1.75 (4.445)
Stainless steel strip thickness	0.50	0.50 (1.27)
Poison/Al plates height	13.18	13.18 (33.477)
Poison/Al plates thickness	0.50	0.50 (1.27)
horizontal gap	0.07	No Gap (replaced with Aluminum)
vertical slot width / height	1.00 / 5.75	No Slot (replaced with Aluminum)
DSC inside radius	34.375	34.500 (87.630)
DSC wall thickness	0.500	0.500 (1.270)

Table 6-6
NUHOMS® OS187H Transfer Cask Dimensions

Parameter	Actual	Model
DSC Shell Radius (OR)	34.875 inches	35.000 inches
Water Gap Radius	34.875" to 35.25"	35.000" to 35.375"
Inner Shell Radius (0.50" thick)	35.25" to 35.75"	35.375" to 35.875"
Gamma Shield Radius (3.56" thick)	35.75" to 39.31"	35.875" to 39.435"
Structural Shell Radius (1.50" thick)	39.31" to 40.81"	39.435" to 40.935"
Neutron Shield Radius (5.00" thick)	40.81" to 45.81"	Not modeled
Neutron Shield Skin Radius (0.188")	45.81" to 46.00"	Not modeled

Table 6-7
NUHOMS®-32PTH - Fixed Poison Loading Requirements

Basket Type	Borated Aluminum Loading	Boral® Loading
A	7.0 mg B-10/cm^2 Thickness = 0.050"	9.0 mg B-10/cm^2 Thickness = 0.075"
B	15.0 mg B-10/cm^2 Thickness = 0.075"	19.0 mg B-10/cm^2 Thickness = 0.075"
C	20.0 mg B-10/cm^2 Thickness = 0.075"	25.0 mg B-10/cm^2 Thickness = 0.075"
D	32.0 mg B-10/cm^2 Thickness = 0.125"	Not Applicable
E	50.0 mg B-10/cm^2 Thickness = 0.187"	Not Applicable

Note: New neutron absorbers or changes to existing absorbers will be qualified as per information provided in Chapter 9.

Table 6-8
Description of the Basic KENO Model Units

Geometry Units	Description
1	Fuel Pin Cell
2	Guide Tube
3	Instrument Tube
21 - 23	Basket Cells with Poison along the West Face of F/A
31 - 33	Basket Cells without Poison along North Face of F/A
41 - 43	Basket Cells without Poison along the East Face of F/A
51 - 53	Basket Cells with Poison along the South Face of F/A
25,35,45,55	Arrays that define the West, North, East and South Faces of the Basket Cell without fuel
61 - 63	Basket Cells without Poison along the West Face of F/A
71 - 73	Basket Cells without Poison along North Face of F/A
81 - 83	Basket Cells without Poison along the East Face of F/A
91 - 93	Basket Cells without Poison along the South Face of F/A
65,75,85,95	Arrays that define the West, North, East and South Faces of the Basket Cell without fuel and poison
201	Basket Cell with Fuel Assembly Positions 201, 202, 205, 206 representing the South West Interior Positions
204	Basket Cell with Fuel Assembly Positions 203, 204, 207, 208, 235, 236 representing the South East Positions
211	Basket Cell with Fuel Assembly Positions 211, 212, 215, 216, 231, 232 representing the North West Positions
214	Basket Cell with Fuel Assembly Positions 213, 214, 217, 218, 233, 234, 237, 238 representing the North East Positions
202	Basket Cell with Fuel Assembly Positions 225, 226 representing West Facing Corner (South West) Positions
203	Basket Cell with Fuel Assembly Positions 221, 222 representing South Facing Corner (South West) Positions
205	Basket Cell with Fuel Assembly Positions 223, 224 representing the South Facing Corner (South East) Positions
212	Basket Cell with Fuel Assembly Positions 227, 228 representing West Facing Corner (North West) Positions
241 - 245	Array of Basket Cells defining the outer 16 locations
245	Array of Basket Cells defining the inner 16 locations
10	Global Unit

Table 6-9
Material Property Data

Material	ID	Density g/cm^3	Element	Weight %	Atom Density (atoms/b-cm)
UO_2 (Enrichment - 5.0 wt%)	1	10.686	U-235	4.407	1.20673E-03
			U-238	83.743	2.26382E-02
			O	11.850	4.76898E-02
Zircaloy-4	2	6.56	Zr	98.23	4.2541E-02
			Sn	1.45	4.8254E-04
			Fe	0.21	1.4856E-04
			Cr	0.10	7.5978E-05
			Hf	0.01	2.2133E-06
Water (Pellet Clad Gap)	3	0.998	H	11.1	6.6769E-02
			O	88.9	3.3385E-02
Stainless Steel (SS304)	4	7.94	C	0.080	3.1877E-04
			Si	1.000	1.7025E-03
			P	0.045	6.9468E-05
			Cr	19.000	1.7473E-02
			Mn	2.000	1.7407E-03
			Fe	68.375	5.8545E-02
			Ni	9.500	7.7402E-03
Borated Water (2500 ppm Boron)	5	1.000	H	11.165	6.67692E-02
			O	88.586	3.33846E-02
			B-10	4.605E-02	2.77126E-05
			B-11	2.038E-01	1.11547E-04
UO_2 (Extra Fuel) (Enrichment - 5.0 wt%)	6	10.686	U-235	4.407	1.20673E-03
			U-238	83.743	2.26382E-02
			O	11.850	4.76898E-02
$^{11}B_4C$ in BPRA	7	2.555	B-11	78.56	1.0988E-01
			C	21.44	2.7470E-02
Aluminum	8	2.70	Al	100.0	6.0307E-02
Type A Borated Aluminum Poison Plate (6.30 mg B-10/cm^2)	9	2.693	B-10	1.842	2.98348E-03
			B-11	0.205	3.01496E-04
			Al	97.953	5.88756E-02
Water	10	0.998	H	11.1	6.6769E-02
			O	88.9	3.3385E-02
Lead	11	11.34	Pb	100.0	3.2969E-02
Rail Material	12	4.024	Water	7.44	
			SS304	69.04	
			Aluminum	23.50	
Type B Borated Aluminum Poison Plate (13.5 mg B-10/cm^2)	9	2.693	B-10	2.632	4.26218E-03
			B-11	0.292	4.30715E-04
			Al	97.076	5.83483E-02
Type D Borated Aluminum Poison Plate (28.8 mg B-10/cm^2)	9	2.693	B-10	3.368	5.45561E-03
			B-11	0.374	5.51316E-04
			Al	96.258	5.78562E-02

Table 6-10
Results of the Fuel Assembly Positioning Studies

Description	K_{keno}	σ_{keno}	K_{eff}	Filename
Framatome 17x17 MK BW Fuel Assembly				
Centered, 70% IMD	0.9216	0.0008	0.9232	adfr17mkb_c070.out:
Centered, 80% IMD	0.9235	0.0006	0.9247	adfr17mkb_c080.out:
Centered, 90% IMD	0.9219	0.0008	0.9235	adfr17mkb_c090.out:
Centered, 100% IMD	0.9153	0.0008	0.9169	adfr17mkb_c100.out:
Inward, 70% IMD	0.9239	0.0008	0.9255	adfr17mkb_o070.out:
Inward, 80% IMD	**0.9263**	**0.0007**	**0.9277**	**adfr17mkb_o080.out:**
Inward, 90% IMD	0.9250	0.0007	0.9264	adfr17mkb_o090.out:
Inward, 100% IMD	0.9194	0.0007	0.9208	adfr17mkb_o100.out:
Westinghouse 15x15 Standard Fuel Assembly				
Centered, 70% IMD	0.9210	0.0007	0.9224	we15std_c070.out:
Centered, 80% IMD	0.9220	0.0007	0.9234	we15std_c080.out:
Centered, 90% IMD	0.9187	0.0007	0.9201	we15std_c090.out:
Centered, 100% IMD	0.9101	0.0007	0.9115	we15std_c100.out:
Inward, 70% IMD	**0.9242**	**0.0008**	**0.9258**	**we15std_o070.out:**
Inward, 80% IMD	0.9231	0.0008	0.9247	we15std_o080.out:
Inward, 90% IMD	0.9231	0.0008	0.9247	we15std_o090.out:
Inward, 100% IMD	0.9148	0.0008	0.9164	we15std_o100.out:
Westinghouse 17x17 OFA Fuel Assembly				
Centered, 70% IMD	0.9069	0.0007	0.9083	we17ofa_c070.out:
Centered, 80% IMD	0.9057	0.0008	0.9073	we17ofa_c080.out:
Centered, 90% IMD	0.9027	0.0007	0.9041	we17ofa_c090.out:
Centered, 100% IMD	0.8955	0.0007	0.8969	we17ofa_c100.out:
Inward, 70% IMD	0.9106	0.0007	0.9120	we17ofa_o070.out:
Inward, 80% IMD	**0.9108**	**0.0006**	**0.9120**	**we17ofa_o080.out:**
Inward, 90% IMD	0.9050	0.0007	0.9064	we17ofa_o090.out:
Inward, 100% IMD	0.8984	0.0006	0.8996	we17ofa_o100.out:

Table 6-10
Results of the Fuel Assembly Positioning Studies
(Continued)

Description	K_{keno}	σ_{keno}	K_{eff}	Filename
Westinghouse 17x17 Standard Fuel Assembly				
Centered, 70% IMD	0.9212	0.0008	0.9228	we17std_c070.out:
Centered, 80% IMD	0.9264	0.0007	0.9278	we17std_c080.out:
Centered, 90% IMD	0.9233	0.0007	0.9247	we17std_c090.out:
Centered, 100% IMD	0.9194	0.0007	0.9208	we17std_c100.out:
Inward, 70% IMD	0.9245	0.0008	0.9261	we17std_o070.out:
Inward, 80% IMD	**0.9289**	**0.0008**	**0.9305**	**we17std_o080.out:**
Inward, 90% IMD	0.9277	0.0007	0.9291	we17std_o090.out:
Inward, 100% IMD	0.9217	0.0007	0.9231	we17std_o100.out:
CE 14x14 Standard Fuel Assembly				
Centered, 60% IMD	0.8799	0.0007	0.8813	ce14std_c060.out:
Centered, 70% IMD	0.8834	0.0007	0.8848	ce14std_c070.out:
Centered, 80% IMD	0.8807	0.0007	0.8821	ce14std_c080.out:
Centered, 90% IMD	0.8723	0.0007	0.8737	ce14std_c090.out:
Centered, 100% IMD	0.8619	0.0007	0.8633	ce14std_c100.out:
Inward, 60% IMD	0.8826	0.0008	0.8842	ce14std_o060.out:
Inward, 70% IMD	**0.8862**	**0.0007**	**0.8876**	**ce14std_o070.out:**
Inward, 80% IMD	0.8842	0.0007	0.8856	ce14std_o080.out:
Inward, 90% IMD	0.8772	0.0008	0.8788	ce14std_o090.out:
Inward, 100% IMD	0.8676	0.0007	0.8690	ce14std_o100.out:
CE 14x14 Fort Calhoun Fuel Assembly				
Centered, 60% IMD	0.8808	0.0008	0.8824	ce14ftc_c060.out:
Centered, 70% IMD	0.8851	0.0007	0.8865	ce14ftc_c070.out:
Centered, 80% IMD	0.8828	0.0007	0.8842	ce14ftc_c080.out:
Centered, 90% IMD	0.8756	0.0008	0.8772	ce14ftc_c090.out:
Centered, 100% IMD	0.8679	0.0007	0.8693	ce14ftc_c100.out:
Inward, 60% IMD	0.8826	0.0008	0.8842	ce14ftc_o060.out:
Inward, 70% IMD	**0.8883**	**0.0007**	**0.8897**	**ce14ftc_o070.out:**
Inward, 80% IMD	0.8865	0.0008	0.8881	ce14ftc_o080.out:
Inward, 90% IMD	0.8815	0.0008	0.8831	ce14ftc_o090.out
Inward, 100% IMD	0.8717	0.0008	0.8733	ce14ftc_o100.out:

Table 6-11
Results of the Rail Material Variation Studies

Description	K_{keno}	σ_{keno}	K_{eff}	Filename
Detailed Model, 70% IMD	0.9285	0.0008	0.9301	rail_act_070.out:
Detailed Model, 80% IMD	0.9317	0.0007	0.9331	rail_act_080.out:
Detailed Model, 90% IMD	0.9290	0.0007	0.9304	rail_act_090.out:
Detailed Model, 100% IMD	0.9239	0.0007	0.9253	rail_act_100.out:
Water Rail, 70% IMD	0.9271	0.0009	0.9289	rail_h2o_070.out:
Water Rail, 80% IMD	0.9292	0.0008	0.9308	rail_h2o_080.out:
Water Rail, 90% IMD	0.9288	0.0008	0.9304	rail_h2o_090.out:
Water Rail, 100% IMD	0.9230	0.0008	0.9246	rail_h2o_100.out:
Composition 3, 70% IMD	0.9298	0.0008	0.9314	rail_h3o_070.out:
Composition 3, 80% IMD	**0.9324**	**0.0007**	**0.9338**	**rail_h3o_080.out:**
Composition 3, 90% IMD	0.9319	0.0008	0.9335	rail_h3o_090.out:
Composition 3, 100% IMD	0.9244	0.0007	0.9258	rail_h3o_100.out:
Composition 4, 70% IMD	0.9273	0.0007	0.9287	rail_h4o_070.out:
Composition 4, 80% IMD	0.9309	0.0007	0.9323	rail_h4o_080.out:
Composition 4, 90% IMD	0.9298	0.0007	0.9312	rail_h4o_090.out:
Composition 4 100% IMD	0.9232	0.0007	0.9246	rail_h4o_100.out:
Composition 5, 70% IMD	0.9287	0.0008	0.9303	rail_h5o_070.out:
Composition 5, 80% IMD	0.9312	0.0007	0.9326	rail_h5o_080.out:
Composition 5, 90% IMD	0.9279	0.0007	0.9293	rail_h5o_090.out:
Composition 5, 100% IMD	0.9244	0.0007	0.9258	rail_h5o_100.out:
Borated Water, 70% IMD	0.9245	0.0008	0.9261	we17std_o070.out:
Borated Water, 80% IMD	0.9289	0.0008	0.9305	we17std_o080.out:
Borated Water, 90% IMD	0.9277	0.0007	0.9291	we17std_o090.out:
Borated Water, 100% IMD	0.9217	0.0007	0.9231	we17std_o100.out:

Table 6-12
Results of the Poison Plate Thickness Variation Studies

Description	K_{keno}	σ_{keno}	K_{eff}	Filename
0.187", Max Thickness, 70% IMD	0.9299	0.0008	0.9315	poison_max_070.out:
0.187", Max Thickness, 80% IMD	0.9322	0.0008	0.9338	poison_max_080.out:
0.187", Max Thickness, 90% IMD	0.9304	0.0008	0.9320	poison_max_090.out:
0.187", Max Thickness, 100% IMD	0.9237	0.0008	0.9253	poison_max_100.out:
0.050", Min Thickness, 70% IMD	0.9292	0.0007	0.9306	poison_min_070.out:
0.050", Min Thickness, 80% IMD	0.9323	0.0007	0.9337	poison_min_080.out:
0.050", Min Thickness, 90% IMD	0.9294	0.0008	0.9310	poison_min_090.out:
0.050", Min Thickness, 100% IMD	0.9245	0.0007	0.9259	poison_min_100.out:
0.075", Nom Thickness, 70% IMD	0.9298	0.0008	0.9314	rail_h3o_070.out:
0.075", Nom Thickness, 80% IMD	**0.9324**	**0.0007**	**0.9338**	**rail_h3o_080.out:**
0.075", Nom Thickness, 90% IMD	0.9319	0.0008	0.9335	rail_h3o_090.out:
0.075", Nom Thickness, 100% IMD	0.9244	0.0007	0.9258	rail_h3o_100.out:

Table 6-13
Results of the Fuel Compartment Width Variation Studies

Description	K_{keno}	σ_{keno}	K_{eff}	Filename
8.750", Max Width, 70% IMD	0.9270	0.0007	0.9284	boxid_max_070.out:
8.750", Max Width, 80% IMD	0.9301	0.0008	0.9317	boxid_max_080.out:
8.750", Max Width, 90% IMD	0.9283	0.0008	0.9299	boxid_max_090.out:
8.750", Max Width, 100% IMD	0.9203	0.0007	0.9217	boxid_max_100.out:
8.650", Min Width, 70% IMD	0.9327	0.0007	0.9341	boxid_min_070.out:
8.650", Min Width, 80% IMD	**0.9341**	**0.0007**	**0.9355**	**boxid_min_080.out:**
8.650", Min Width, 90% IMD	0.9325	0.0007	0.9339	boxid_min_090.out:
8.650", Min Width, 100% IMD	0.9279	0.0008	0.9295	boxid_min_100.out:
8.700", Nom Width, 70% IMD	0.9298	0.0008	0.9314	rail_h3o_070.out:
8.700", Nom Width, 80% IMD	0.9324	0.0007	0.9338	rail_h3o_080.out:
8.700", Nom Width, 90% IMD	0.9319	0.0008	0.9335	rail_h3o_090.out:
8.700", Nom Width, 100% IMD	0.9244	0.0007	0.9258	rail_h3o_100.out:

Table 6-14
Results of the Fuel Compartment Thickness Variation Studies

Description	K_{keno}	σ_{keno}	K_{eff}	Filename
0.2325", Max Thickness, 70% IMD	0.9308	0.0007	0.9322	boxod_max_070.out:
0.2325", Max Thickness, 80% IMD	0.9334	0.0007	0.9348	boxod_max_080.out:
0.2325", Max Thickness, 90% IMD	0.9318	0.0007	0.9332	boxod_max_090.out:
0.2325", Max Thickness, 100% IMD	0.9258	0.0007	0.9272	boxod_max_100.out:
0.1775", Min Thickness, 70% IMD	0.9321	0.0008	0.9337	boxod_min_070.out:
0.1775", Min Thickness, 80% IMD	0.9333	0.0007	0.9347	boxod_min_080.out:
0.1775", Min Thickness, 90% IMD	0.9318	0.0008	0.9334	boxod_min_090.out:
0.1775", Min Thickness, 100% IMD	0.9272	0.0007	0.9286	boxod_min_100.out:
0.1875", Nom Thickness, 70% IMD	0.9327	0.0007	0.9341	boxid_min_070.out:
0.1875", Nom Thickness, 80% IMD	**0.9341**	**0.0007**	**0.9355**	**boxid_min_080.out:**
0.1875", Nom Thickness, 90% IMD	0.9325	0.0007	0.9339	boxid_min_090.out:
0.1875", Nom Thickness, 100% IMD	0.9279	0.0008	0.9295	boxid_min_100.out:

Table 6-15
WE 15x15 Class Intact Assemblies Without BPRAs - Final Results

Description	K_{keno}	σ_{keno}	K_{eff}	Filename
Type A Basket (7.0 mg B-10/cm^2), 2300 ppm Boron, 3.8 wt. % U-235				
60% IMD	0.9326	0.0007	0.9340	we15b23_p07e38_060.out:
70% IMD	0.9360	0.0006	0.9372	we15b23_p07e38_070.out:
80% IMD	0.9356	0.0007	0.9370	we15b23_p07e38_080.out:
90% IMD	0.9295	0.0008	0.9311	we15b23_p07e38_090.out:
100% IMD	0.9198	0.0007	0.9212	we15b23_p07e38_100.out:
Type B Basket (15.0 mg B-10/cm^2), 2300 ppm Boron, 4.2 wt. % U-235				
60% IMD	0.9234	0.0007	0.9248	we15b23_p15e42_060.out:
70% IMD	0.9340	0.0008	0.9356	we15b23_p15e42_070.out:
80% IMD	0.9367	0.0007	0.9381	we15b23_p15e42_080.out:
90% IMD	0.9361	0.0007	0.9375	we15b23_p15e42_090.out:
100% IMD	0.9294	0.0008	0.9310	we15b23_p15e42_100.out:
Type D Basket (32.0 mg B-10/cm^2), 2300 ppm Boron, 4.6 wt. % U-235				
60% IMD	0.9090	0.0008	0.9106	we15b23_p32e46_060.out:
70% IMD	0.9246	0.0007	0.9260	we15b23_p32e46_070.out:
80% IMD	0.9315	0.0007	0.9329	we15b23_p32e46_080.out:
90% IMD	0.9342	0.0006	0.9354	we15b23_p32e46_090.out:
100% IMD	0.9320	0.0007	0.9334	we15b23_p32e46_100.out:
Type E Basket (50.0 mg B-10/cm^2), 2300 ppm Boron, 4.9 wt. % U-235				
60% IMD	0.9034	0.0007	0.9048	we15b23_p50e49_060.out:
70% IMD	0.9216	0.0007	0.9230	we15b23_p50e49_070.out:
80% IMD	0.9304	0.0007	0.9318	we15b23_p50e49_080.out:
90% IMD	0.9362	0.0007	0.9376	we15b23_p50e49_090.out:
100% IMD	0.9341	0.0007	0.9355	we15b23_p50e49_100.out:
Type A Basket (7.0 mg B-10/cm^2), 2400 ppm Boron, 3.9 wt. % U-235				
60% IMD	0.9333	0.0007	0.9347	we15b24_p07e39_060.out:
70% IMD	0.9373	0.0008	0.9389	we15b24_p07e39_070.out:
80% IMD	0.9355	0.0007	0.9369	we15b24_p07e39_080.out:
90% IMD	0.9299	0.0008	0.9315	we15b24_p07e39_090.out:
100% IMD	0.9203	0.0008	0.9219	we15b24_p07e39_100.out:
Type B Basket (15.0 mg B-10/cm^2), 2400 ppm Boron, 4.3 wt. % U-235				
60% IMD	0.9259	0.0007	0.9273	we15b24_p15e43_060.out:
70% IMD	0.9344	0.0008	0.9360	we15b24_p15e43_070.out:
80% IMD	0.9373	0.0007	0.9387	we15b24_p15e43_080.out:
90% IMD	0.9340	0.0007	0.9354	we15b24_p15e43_090.out:
100% IMD	0.9278	0.0007	0.9292	we15b24_p15e43_100.out:

Table 6-15
WE 15x15 Class Intact Assemblies Without BPRAs - Final Results
(Continued)

Description	K_{keno}	σ_{keno}	K_{eff}	Filename
Type D Basket (32.0 mg B-10/cm^2), 2400 ppm Boron, 4.7 wt. % U-235				
60% IMD	0.9115	0.0007	0.9129	we15b24_p32e47_060.out:
70% IMD	0.9263	0.0008	0.9279	we15b24_p32e47_070.out:
80% IMD	0.9338	0.0007	0.9352	we15b24_p32e47_080.out:
90% IMD	0.9333	0.0007	0.9347	we15b24_p32e47_090.out:
100% IMD	0.9305	0.0008	0.9321	we15b24_p32e47_100.out:
Type E Basket (50.0 mg B-10/cm^2), 2400 ppm Boron, 5.0 wt. % U-235				
60% IMD	0.9050	0.0009	0.9068	we15b24_p50e50_060.out:
70% IMD	0.9219	0.0010	0.9239	we15b24_p50e50_070.out:
80% IMD	0.9299	0.0009	0.9317	we15b24_p50e50_080.out:
90% IMD	0.9340	0.0011	0.9362	we15b24_p50e50_090.out:
100% IMD	0.9319	0.0010	0.9339	we15b24_p50e50_100.out:
Type A Basket (7.0 mg B-10/cm^2), 2500 ppm Boron, 3.9 wt. % U-235				
60% IMD	0.9270	0.0007	0.9284	we15b25_p07e39_060.out:
70% IMD	0.9326	0.0007	0.9340	we15b25_p07e39_070.out:
80% IMD	0.9301	0.0007	0.9315	we15b25_p07e39_080.out:
90% IMD	0.9215	0.0008	0.9231	we15b25_p07e39_090.out:
100% IMD	0.9119	0.0008	0.9135	we15b25_p07e39_100.out:
Type B Basket (15.0 mg B-10/cm^2), 2500 ppm Boron, 4.4 wt. % U-235				
60% IMD	0.9282	0.0008	0.9298	we15b25_p15e44_060.out:
70% IMD	0.9355	0.0007	0.9369	we15b25_p15e44_070.out:
80% IMD	0.9357	0.0008	0.9373	we15b25_p15e44_080.out:
90% IMD	0.9353	0.0006	0.9365	we15b25_p15e44_090.out:
100% IMD	0.9273	0.0008	0.9289	we15b25_p15e44_100.out:
Type D Basket (32.0 mg B-10/cm^2), 2500 ppm Boron, 4.9 wt. % U-235				
60% IMD	0.9171	0.0008	0.9187	we15b25_p32e49_060.out:
70% IMD	0.9316	0.0007	0.9330	we15b25_p32e49_070.out:
80% IMD	0.9364	0.0007	0.9378	we15b25_p32e49_080.out:
90% IMD	**0.9383**	**0.0008**	**0.9399**	**we15b25_p32e49_090.out:**
100% IMD	0.9336	0.0008	0.9352	we15b25_p32e49_100.out:

Table 6-16
WE 15x15 Class Intact Assemblies With BPRAs - Final Results

Description	K_{keno}	σ_{keno}	K_{eff}	Filename
Type A Basket (7.0 mg B-10/cm^2), 2300 ppm Boron, 3.7 wt. % U-235				
60% IMD	0.9187	0.0007	0.9201	we15bp23_p07e37_060.out:
70% IMD	0.9290	0.0008	0.9306	we15bp23_p07e37_070.out:
80% IMD	0.9315	0.0007	0.9329	we15bp23_p07e37_080.out:
90% IMD	0.9302	0.0007	0.9316	we15bp23_p07e37_090.out:
100% IMD	0.9260	0.0007	0.9274	we15bp23_p07e37_100.out:
Type B Basket (15.0 mg B-10/cm^2), 2300 ppm Boron, 4.1 wt. % U-235				
60% IMD	0.9105	0.0007	0.9119	we15bp23_p15e41_060.out:
70% IMD	0.9239	0.0007	0.9253	we15bp23_p15e41_070.out:
80% IMD	0.9324	0.0007	0.9338	we15bp23_p15e41_080.out:
90% IMD	0.9342	0.0007	0.9356	we15bp23_p15e41_090.out:
100% IMD	0.9338	0.0007	0.9352	we15bp23_p15e41_100.out:
Type D Basket (32.0 mg B-10/cm^2), 2300 ppm Boron, 4.5 wt. % U-235				
60% IMD	0.8947	0.0008	0.8963	we15bp23_p32e45_060.out:
70% IMD	0.9124	0.0008	0.9140	we15bp23_p32e45_070.out:
80% IMD	0.9263	0.0008	0.9279	we15bp23_p32e45_080.out:
90% IMD	0.9324	0.0008	0.9340	we15bp23_p32e45_090.out:
100% IMD	0.9335	0.0008	0.9351	we15bp23_p32e45_100.out:
Type E Basket (50.0 mg B-10/cm^2), 2300 ppm Boron, 4.8 wt. % U-235				
60% IMD	0.8869	0.0008	0.8885	we15bp23_p50e48_060.out:
70% IMD	0.9087	0.0008	0.9103	we15bp23_p50e48_070.out:
80% IMD	0.9218	0.0007	0.9232	we15bp23_p50e48_080.out:
90% IMD	0.9296	0.0008	0.9312	we15bp23_p50e48_090.out:
100% IMD	0.9358	0.0008	0.9374	we15bp23_p50e48_100.out:
Type A Basket (7.0 mg B-10/cm^2), 2400 ppm Boron, 3.8 wt. % U-235				
60% IMD	0.9222	0.0008	0.9238	we15bp24_p07e38_060.out:
70% IMD	0.9309	0.0008	0.9325	we15bp24_p07e38_070.out:
80% IMD	0.9344	0.0007	0.9358	we15bp24_p07e38_080.out:
90% IMD	0.9312	0.0006	0.9324	we15bp24_p07e38_090.out:
100% IMD	0.9252	0.0007	0.9266	we15bp24_p07e38_100.out:
Type B Basket (15.0 mg B-10/cm^2), 2400 ppm Boron, 4.2 wt. % U-235				
60% IMD	0.9140	0.0009	0.9158	we15bp24_p15e42_060.out:
70% IMD	0.9266	0.0007	0.9280	we15bp24_p15e42_070.out:
80% IMD	0.9319	0.0007	0.9333	we15bp24_p15e42_080.out:
90% IMD	0.9335	0.0007	0.9349	we15bp24_p15e42_090.out:
100% IMD	0.9322	0.0007	0.9336	we15bp24_p15e42_100.out:

Table 6-16
WE 15x15 Class Intact Assemblies With BPRAs - Final Results
(Continued)

Description	K_{keno}	σ_{keno}	K_{eff}	Filename
Type D Basket (32.0 mg B-10/cm^2), 2400 ppm Boron, 4.7 wt. % U-235				
60% IMD	0.9016	0.0009	0.9034	we15bp24_p32e47_060.out:
70% IMD	0.9200	0.0007	0.9214	we15bp24_p32e47_070.out:
80% IMD	0.9317	0.0007	0.9331	we15bp24_p32e47_080.out:
90% IMD	0.9368	0.0008	0.9384	we15bp24_p32e47_090.out:
100% IMD	**0.9388**	**0.0007**	**0.9402**	**we15bp24_p32e47_100.out:**
Type E Basket (50.0 mg B-10/cm^2), 2400 ppm Boron, 4.9 wt. % U-235				
60% IMD	0.8862	0.0008	0.8878	we15bp24_p50e49_060.out:
70% IMD	0.9083	0.0009	0.9101	we15bp24_p50e49_070.out:
80% IMD	0.9219	0.0010	0.9239	we15bp24_p50e49_080.out:
90% IMD	0.9298	0.0009	0.9316	we15bp24_p50e49_090.out:
100% IMD	0.9351	0.0010	0.9371	we15bp24_p50e49_100.out:
Type A Basket (7.0 mg B-10/cm^2), 2500 ppm Boron, 3.9 wt. % U-235				
60% IMD	0.9251	0.0007	0.9265	we15bp25_p07e39_060.out:
70% IMD	0.9330	0.0008	0.9346	we15bp25_p07e39_070.out:
80% IMD	0.9358	0.0007	0.9372	we15bp25_p07e39_080.out:
90% IMD	0.9342	0.0007	0.9356	we15bp25_p07e39_090.out:
100% IMD	0.9276	0.0007	0.9290	we15bp25_p07e39_100.out:
Type B Basket (15.0 mg B-10/cm^2), 2500 ppm Boron, 4.3 wt. % U-235				
60% IMD	0.9154	0.0008	0.9170	we15bp25_p15e43_060.out:
70% IMD	0.9273	0.0007	0.9287	we15bp25_p15e43_070.out:
80% IMD	0.9339	0.0008	0.9355	we15bp25_p15e43_080.out:
90% IMD	0.9338	0.0007	0.9352	we15bp25_p15e43_090.out:
100% IMD	0.9319	0.0006	0.9331	we15bp25_p15e43_100.out:
Type D Basket (32.0 mg B-10/cm^2), 2500 ppm Boron, 4.8 wt. % U-235				
60% IMD	0.9051	0.0008	0.9067	we15bp25_p32e48_060.out:
70% IMD	0.9221	0.0008	0.9237	we15bp25_p32e48_070.out:
80% IMD	0.9314	0.0007	0.9328	we15bp25_p32e48_080.out:
90% IMD	0.9371	0.0007	0.9385	we15bp25_p32e48_090.out:
100% IMD	0.9371	0.0008	0.9387	we15bp25_p32e48_100.out:
Type E Basket (50.0 mg B-10/cm^2), 2500 ppm Boron, 5.0 wt. % U-235				
60% IMD	0.8903	0.0010	0.8923	we15bp25_p50e50_060.out:
70% IMD	0.9105	0.0009	0.9123	we15bp25_p50e50_070.out:
80% IMD	0.9224	0.0009	0.9242	we15bp25_p50e50_080.out:
90% IMD	0.9306	0.0010	0.9326	we15bp25_p50e50_090.out:
100% IMD	0.9334	0.0009	0.9352	we15bp25_p50e50_100.out:

Table 6-16
WE 15x15 Class Intact Assemblies With BPRAs - Final Results
(Continued)

Description	K_{keno}	σ_{keno}	K_{eff}	Filename
Type A Basket (7.0 mg B-10/cm^2), 2000 ppm Boron, 3.50 wt. % U-235				
60% IMD	0.9200	0.0007	0.9214	we15bp20_p07e35_060.out:
70% IMD	0.9312	0.0008	0.9328	we15bp20_p07e35_070.out:
80% IMD	0.9362	0.0007	0.9376	we15bp20_p07e35_080.out:
90% IMD	0.9370	0.0007	0.9384	we15bp20_p07e35_090.out:
100% IMD	0.9318	0.0007	0.9332	we15bp20_p07e35_100.out:
Type B Basket (15.0 mg B-10/cm^2), 2000 ppm Boron, 3.80 wt. % U-235				
60% IMD	0.9037	0.0008	0.9053	we15bp20_p15e38_060.out:
70% IMD	0.9204	0.0009	0.9222	we15bp20_p15e38_070.out:
80% IMD	0.9290	0.0007	0.9304	we15bp20_p15e38_080.out:
90% IMD	0.9335	0.0008	0.9351	we15bp20_p15e38_090.out:
100% IMD	0.9328	0.0007	0.9342	we15bp20_p15e38_100.out:
Type D Basket (32.0 mg B-10/cm^2), 2000 ppm Boron, 4.20 wt. % U-235				
60% IMD	0.8903	0.0007	0.8917	we15bp20_p32e42_060.out:
70% IMD	0.9105	0.0007	0.9119	we15bp20_p32e42_070.out:
80% IMD	0.9255	0.0007	0.9269	we15bp20_p32e42_080.out:
90% IMD	0.9324	0.0007	0.9338	we15bp20_p32e42_090.out:
100% IMD	0.9354	0.0007	0.9368	we15bp20_p32e42_100.out:
Type E Basket (50.0 mg B-10/cm^2), 2000 ppm Boron, 4.50 wt. % U-235				
60% IMD	0.8827	0.0008	0.8843	we15bp20_p50e45_060.out:
70% IMD	0.9063	0.0008	0.9079	we15bp20_p50e45_070.out:
80% IMD	0.9236	0.0008	0.9252	we15bp20_p50e45_080.out:
90% IMD	0.9320	0.0008	0.9336	we15bp20_p50e45_090.out:
100% IMD	0.9380	0.0008	0.9396	we15bp20_p50e45_100.out:

Table 6-17
WE 17x17 Class Intact Assemblies Without BPRAs - Final Results

Description	K_{keno}	σ_{keno}	K_{eff}	Filename
Type A Basket (7.0 mg B-10/cm^2), 2300 ppm Boron, 3.8 wt. % U-235				
60% IMD	0.9303	0.0007	0.9317	we17b23_p07e38_060.out:
70% IMD	**0.9390**	**0.0007**	**0.9404**	**we17b23_p07e38_070.out:**
80% IMD	0.9376	0.0007	0.9390	we17b23_p07e38_080.out:
90% IMD	0.9355	0.0008	0.9371	we17b23_p07e38_090.out:
100% IMD	0.9279	0.0006	0.9291	we17b23_p07e38_100.out:
Type B Basket (15.0 mg B-10/cm^2), 2300 ppm Boron, 4.1 wt. % U-235				
60% IMD	0.9177	0.0007	0.9191	we17b23_p15e41_060.out:
70% IMD	0.9292	0.0008	0.9308	we17b23_p15e41_070.out:
80% IMD	0.9340	0.0008	0.9356	we17b23_p15e41_080.out:
90% IMD	0.9320	0.0008	0.9336	we17b23_p15e41_090.out:
100% IMD	0.9271	0.0007	0.9285	we17b23_p15e41_100.out:
Type D Basket (32.0 mg B-10/cm^2), 2300 ppm Boron, 4.55 wt. % U-235				
60% IMD	0.9082	0.0008	0.9098	we17b23_p32e46_060.out:
70% IMD	0.9233	0.0008	0.9249	we17b23_p32e46_070.out:
80% IMD	0.9335	0.0008	0.9351	we17b23_p32e46_080.out:
90% IMD	0.9352	0.0007	0.9366	we17b23_p32e46_090.out:
100% IMD	0.9346	0.0007	0.9360	we17b23_p32e46_100.out:
Type E Basket (50.0 mg B-10/cm^2), 2300 ppm Boron, 4.8 wt. % U-235				
60% IMD	0.8977	0.0008	0.8993	we17b23_p50e48_060.out:
70% IMD	0.9163	0.0007	0.9177	we17b23_p50e48_070.out:
80% IMD	0.9283	0.0008	0.9299	we17b23_p50e48_080.out:
90% IMD	0.9330	0.0007	0.9344	we17b23_p50e48_090.out:
100% IMD	0.9350	0.0008	0.9366	we17b23_p50e48_100.out:
Type A Basket (7.0 mg B-10/cm^2), 2400 ppm Boron, 3.8 wt. % U-235				
60% IMD	0.9261	0.0007	0.9275	we17b24_p07e38_060.out:
70% IMD	0.9317	0.0007	0.9331	we17b24_p07e38_070.out:
80% IMD	0.9328	0.0008	0.9344	we17b24_p07e38_080.out:
90% IMD	0.9275	0.0007	0.9289	we17b24_p07e38_090.out:
100% IMD	0.9189	0.0007	0.9203	we17b24_p07e38_100.out:
Type B Basket (15.0 mg B-10/cm^2), 2400 ppm Boron, 4.2 wt. % U-235				
60% IMD	0.9193	0.0006	0.9205	we17b24_p15e42_060.out:
70% IMD	0.9316	0.0007	0.9330	we17b24_p15e42_070.out:
80% IMD	0.9335	0.0008	0.9351	we17b24_p15e42_080.out:
90% IMD	0.9326	0.0007	0.9340	we17b24_p15e42_090.out:
100% IMD	0.9296	0.0008	0.9312	we17b24_p15e42_100.out:

Table 6-17
WE 17x17 Class Intact Assemblies Without BPRAs - Final Results
(Continued)

Description	K_{keno}	σ_{keno}	K_{eff}	Filename
Type D Basket (32.0 mg B-10/cm^2), 2400 ppm Boron, 4.7 wt. % U-235				
60% IMD	0.9122	0.0007	0.9136	we17b24_p32e47_060.out:
70% IMD	0.9271	0.0009	0.9289	we17b24_p32e47_070.out:
80% IMD	0.9360	0.0008	0.9376	we17b24_p32e47_080.out:
90% IMD	0.9383	0.0007	0.9397	we17b24_p32e47_090.out:
100% IMD	0.9373	0.0008	0.9389	we17b24_p32e47_100.out:
Type E Basket (50.0 mg B-10/cm^2), 2400 ppm Boron, 4.9 wt. % U-235				
60% IMD	0.8992	0.0007	0.9006	we17b24_p50e49_060.out:
70% IMD	0.9165	0.0008	0.9181	we17b24_p50e49_070.out:
80% IMD	0.9285	0.0007	0.9299	we17b24_p50e49_080.out:
90% IMD	0.9335	0.0007	0.9349	we17b24_p50e49_090.out:
100% IMD	0.9339	0.0007	0.9353	we17b24_p50e49_100.out:
Type A Basket (7.0 mg B-10/cm^2), 2500 ppm Boron, 3.9 wt. % U-235				
60% IMD	0.9299	0.0006	0.9311	we17b25_p07e39_060.out:
70% IMD	0.9350	0.0008	0.9366	we17b25_p07e39_070.out:
80% IMD	0.9333	0.0008	0.9349	we17b25_p07e39_080.out:
90% IMD	0.9278	0.0007	0.9292	we17b25_p07e39_090.out:
100% IMD	0.9193	0.0007	0.9207	we17b25_p07e39_100.out:
Type B Basket (15.0 mg B-10/cm^2), 2500 ppm Boron, 4.3 wt. % U-235				
60% IMD	0.9224	0.0007	0.9238	we17b25_p15e43_060.out:
70% IMD	0.9327	0.0007	0.9341	we17b25_p15e43_070.out:
80% IMD	0.9341	0.0007	0.9355	we17b25_p15e43_080.out:
90% IMD	0.9325	0.0007	0.9339	we17b25_p15e43_090.out:
100% IMD	0.9279	0.0008	0.9295	we17b25_p15e43_100.out:
Type D Basket (32.0 mg B-10/cm^2), 2500 ppm Boron, 4.8 wt. % U-235				
60% IMD	0.9137	0.0009	0.9155	we17b25_p32e48_060.out:
70% IMD	0.9282	0.0009	0.9300	we17b25_p32e48_070.out:
80% IMD	0.9358	0.0008	0.9374	we17b25_p32e48_080.out:
90% IMD	0.9373	0.0007	0.9387	we17b25_p32e48_090.out:
100% IMD	0.9356	0.0007	0.9370	we17b25_p32e48_100.out:
Type E Basket (50.0 mg B-10/cm^2), 2500 ppm Boron, 5.0 wt. % U-235				
60% IMD	0.8996	0.0007	0.9010	we17b25_p50e50_060.out:
70% IMD	0.9174	0.0008	0.9190	we17b25_p50e50_070.out:
80% IMD	0.9273	0.0009	0.9291	we17b25_p50e50_080.out:
90% IMD	0.9326	0.0008	0.9342	we17b25_p50e50_090.out:
100% IMD	0.9329	0.0008	0.9345	we17b25_p50e50_100.out:

Table 6-18
WE 17x17 Class Intact Assemblies With BPRAs - Final Results

Description	K_{keno}	σ_{keno}	K_{eff}	Filename
Type A Basket (7.0 mg B-10/cm^2), 2000 ppm Boron, 3.50 wt. % U-235				
60% IMD	0.9184	0.0007	0.9198	we17bp20_p07e35_060.out:
70% IMD	0.9302	0.0007	0.9316	we17bp20_p07e35_070.out:
80% IMD	0.9370	0.0008	0.9386	we17bp20_p07e35_080.out:
90% IMD	0.9377	0.0006	0.9389	we17bp20_p07e35_090.out:
100% IMD	0.9355	0.0007	0.9369	we17bp20_p07e35_100.out:
Type B Basket (15.0 mg B-10/cm^2), 2000 ppm Boron, 3.80 wt. % U-235				
60% IMD	0.9045	0.0007	0.9059	we17bp20_p15e38_060.out:
70% IMD	0.9198	0.0007	0.9212	we17bp20_p15e38_070.out:
80% IMD	0.9300	0.0007	0.9314	we17bp20_p15e38_080.out:
90% IMD	0.9339	0.0009	0.9357	we17bp20_p15e38_090.out:
100% IMD	0.9359	0.0007	0.9373	we17bp20_p15e38_100.out:
Type C Basket (20.0 mg B-10/cm^2), 2000 ppm Boron, 3.95 wt. % U-235				
60% IMD	0.8982	0.0007	0.8996	we17bp20_p20e40_060.out:
70% IMD	0.9174	0.0008	0.9190	we17bp20_p20e40_070.out:
80% IMD	0.9295	0.0007	0.9309	we17bp20_p20e40_080.out:
90% IMD	0.9338	0.0008	0.9354	we17bp20_p20e40_090.out:
100% IMD	0.9366	0.0008	0.9382	we17bp20_p20e40_100.out:
Type D Basket (32.0 mg B-10/cm^2), 2000 ppm Boron, 4.20 wt. % U-235				
60% IMD	0.8890	0.0007	0.8904	we17bp20_p32e42_060.out:
70% IMD	0.9110	0.0007	0.9124	we17bp20_p32e42_070.out:
80% IMD	0.9257	0.0009	0.9275	we17bp20_p32e42_080.out:
90% IMD	0.9338	0.0007	0.9352	we17bp20_p32e42_090.out:
100% IMD	0.9375	0.0008	0.9391	we17bp20_p32e42_100.out:
Type E Basket (50.0 mg B-10/cm^2), 2000 ppm Boron, 4.45 wt. % U-235				
60% IMD	0.8771	0.0008	0.8787	we17bp20_p50e45_060.out:
70% IMD	0.9020	0.0007	0.9034	we17bp20_p50e45_070.out:
80% IMD	0.9203	0.0009	0.9221	we17bp20_p50e45_080.out:
90% IMD	0.9324	0.0008	0.9340	we17bp20_p50e45_090.out:
100% IMD	0.9372	0.0007	0.9386	we17bp20_p50e45_100.out:
Type A Basket (7.0 mg B-10/cm^2), 2300 ppm Boron, 3.7 wt. % U-235				
60% IMD	0.9195	0.0007	0.9209	we17bp23_p07e37_060.out:
70% IMD	0.9298	0.0008	0.9314	we17bp23_p07e37_070.out:
80% IMD	0.9328	0.0007	0.9342	we17bp23_p07e37_080.out:
90% IMD	0.9338	0.0007	0.9352	we17bp23_p07e37_090.out:
100% IMD	0.9292	0.0007	0.9306	we17bp23_p07e37_100.out:

Table 6-18
WE 17x17 Class Intact Assemblies With BPRAs - Final Results
(Continued)

Description	K_{keno}	σ_{keno}	K_{eff}	Filename
Type B Basket (15.0 mg B-10/cm^2), 2300 ppm Boron, 4.1 wt. % U-235				
60% IMD	0.9105	0.0008	0.9121	we17bp23_p15e41_060.out:
70% IMD	0.9243	0.0008	0.9259	we17bp23_p15e41_070.out:
80% IMD	0.9332	0.0007	0.9346	we17bp23_p15e41_080.out:
90% IMD	0.9375	0.0007	0.9389	we17bp23_p15e41_090.out:
100% IMD	0.9358	0.0007	0.9372	we17bp23_p15e41_100.out:
Type C Basket (20.0 mg B-10/cm^2), 2300 ppm Boron, 4.25 wt. % U-235				
60% IMD	0.9046	0.0007	0.9060	we17bp23_p20e43_060.out:
70% IMD	0.9219	0.0007	0.9233	we17bp23_p20e43_070.out:
80% IMD	0.9314	0.0007	0.9328	we17bp23_p20e43_080.out:
90% IMD	0.9355	0.0007	0.9369	we17bp23_p20e43_090.out:
100% IMD	0.9369	0.0007	0.9383	we17bp23_p20e43_100.out:
Type D Basket (32.0 mg B-10/cm^2), 2300 ppm Boron, 4.5 wt. % U-235				
60% IMD	0.8936	0.0009	0.8954	we17bp23_p32e45_060.out:
70% IMD	0.9137	0.0009	0.9155	we17bp23_p32e45_070.out:
80% IMD	0.9276	0.0007	0.9290	we17bp23_p32e45_080.out:
90% IMD	0.9340	0.0007	0.9354	we17bp23_p32e45_090.out:
100% IMD	0.9376	0.0008	0.9392	we17bp23_p32e45_100.out:
Type E Basket (50.0 mg B-10/cm^2), 2300 ppm Boron, 4.7 wt. % U-235				
60% IMD	0.8813	0.0007	0.8827	we17bp23_p50e47_060.out:
70% IMD	0.9005	0.0008	0.9021	we17bp23_p50e47_070.out:
80% IMD	0.9181	0.0008	0.9197	we17bp23_p50e47_080.out:
90% IMD	0.9281	0.0008	0.9297	we17bp23_p50e47_090.out:
100% IMD	0.9337	0.0007	0.9351	we17bp23_p50e47_100.out:
Type A Basket (7.0 mg B-10/cm^2), 2400 ppm Boron, 3.8 wt. % U-235				
60% IMD	0.9227	0.0007	0.9241	we17bp24_p07e38_060.out:
70% IMD	0.9308	0.0007	0.9322	we17bp24_p07e38_070.out:
80% IMD	0.9348	0.0007	0.9362	we17bp24_p07e38_080.out:
90% IMD	0.9344	0.0008	0.9360	we17bp24_p07e38_090.out:
100% IMD	0.9319	0.0008	0.9335	we17bp24_p07e38_100.out:
Type B Basket (15.0 mg B-10/cm^2), 2400 ppm Boron, 4.2 wt. % U-235				
60% IMD	0.9119	0.0007	0.9133	we17bp24_p15e42_060.out:
70% IMD	0.9275	0.0007	0.9289	we17bp24_p15e42_070.out:
80% IMD	0.9333	0.0008	0.9349	we17bp24_p15e42_080.out:
90% IMD	0.9361	0.0008	0.9377	we17bp24_p15e42_090.out:
100% IMD	0.9367	0.0007	0.9381	we17bp24_p15e42_100.out:

Table 6-18
WE 17x17 Class Intact Assemblies With BPRAs - Final Results
(Continued)

Description	K_{keno}	σ_{keno}	K_{eff}	Filename
Type C Basket (20.0 mg B-10/cm^2), 2400 ppm Boron, 4.35 wt. % U-235				
60% IMD	0.9074	0.0008	0.9090	we17bp24_p20e44_060.out:
70% IMD	0.9234	0.0008	0.9250	we17bp24_p20e44_070.out:
80% IMD	0.9318	0.0008	0.9334	we17bp24_p20e44_080.out:
90% IMD	0.9364	0.0007	0.9378	we17bp24_p20e44_090.out:
100% IMD	0.9366	0.0007	0.9380	we17bp24_p20e44_100.out:
Type D Basket (32.0 mg B-10/cm^2), 2400 ppm Boron, 4.6 wt. % U-235				
60% IMD	0.8958	0.0008	0.8974	we17bp24_p32e46_060.out:
70% IMD	0.9152	0.0009	0.9170	we17bp24_p32e46_070.out:
80% IMD	0.9266	0.0008	0.9282	we17bp24_p32e46_080.out:
90% IMD	0.9335	0.0008	0.9351	we17bp24_p32e46_090.out:
100% IMD	0.9348	0.0007	0.9362	we17bp24_p32e46_100.out:
Type D Basket (50.0 mg B-10/cm^2), 2400 ppm Boron, 4.9 wt. % U-235				
60% IMD	0.8873	0.0008	0.8889	we17bp24_p50e49_060.out:
70% IMD	0.9093	0.0007	0.9107	we17bp24_p50e49_070.out:
80% IMD	0.9241	0.0008	0.9257	we17bp24_p50e49_080.out:
90% IMD	0.9314	0.0008	0.9330	we17bp24_p50e49_090.out:
100% IMD	0.9381	0.0007	0.9395	we17bp24_p50e49_100.out:
Type A Basket (7.0 mg B-10/cm^2), 2500 ppm Boron, 3.9 wt. % U-235				
60% IMD	0.9243	0.0007	0.9257	we17bp25_p07e39_060.out:
70% IMD	0.9338	0.0008	0.9354	we17bp25_p07e39_070.out:
80% IMD	**0.9381**	**0.0008**	**0.9397**	**we17bp25_p07e39_080.out:**
90% IMD	0.9362	0.0009	0.9380	we17bp25_p07e39_090.out:
100% IMD	0.9295	0.0007	0.9309	we17bp25_p07e39_100.out:
Type B Basket (15.0 mg B-10/cm^2), 2500 ppm Boron, 4.3 wt. % U-235				
60% IMD	0.9141	0.0007	0.9155	we17bp25_p15e43_060.out:
70% IMD	0.9277	0.0007	0.9291	we17bp25_p15e43_070.out:
80% IMD	0.9357	0.0008	0.9373	we17bp25_p15e43_080.out:
90% IMD	0.9374	0.0007	0.9388	we17bp25_p15e43_090.out:
100% IMD	0.9358	0.0007	0.9372	we17bp25_p15e43_100.out:
Type C Basket (20.0 mg B-10/cm^2), 2500 ppm Boron, 4.45 wt. % U-235				
60% IMD	0.9094	0.0006	0.9106	we17bp25_p20e45_060.out:
70% IMD	0.9242	0.0007	0.9256	we17bp25_p20e45_070.out:
80% IMD	0.9335	0.0008	0.9351	we17bp25_p20e45_080.out:
90% IMD	0.9358	0.0007	0.9372	we17bp25_p20e45_090.out:
100% IMD	0.9372	0.0008	0.9388	we17bp25_p20e45_100.out:

Table 6-18
WE 17x17 Class Intact Assemblies with BPRAs – Final Results
(Continued)

Description	K_{keno}	σ_{keno}	K_{eff}	Filename
Type D Basket (32.0 mg B-10/cm^2), 2500 ppm Boron, 4.7 wt. % U-235				
60% IMD	0.8992	0.0007	0.9006	we17bp25_p32e47_060.out:
70% IMD	0.9154	0.0007	0.9168	we17bp25_p32e47_070.out:
80% IMD	0.9272	0.0007	0.9286	we17bp25_p32e47_080.out:
90% IMD	0.9341	0.0007	0.9355	we17bp25_p32e47_090.out:
100% IMD	0.9356	0.0008	0.9372	we17bp25_p32e47_100.out:
Type E Basket (50.0 mg B-10/cm^2), 2500 ppm Boron, 5.0 wt. % U-235				
60% IMD	0.8871	0.0008	0.8887	we17bp25_p50e50_060.out:
70% IMD	0.9102	0.0007	0.9116	we17bp25_p50e50_070.out:
80% IMD	0.9260	0.0007	0.9274	we17bp25_p50e50_080.out:
90% IMD	0.9343	0.0008	0.9359	we17bp25_p50e50_090.out:
100% IMD	0.9379	0.0008	0.9395	we17bp25_p50e50_100.out:

Table 6-19
Limiting Parameters for Damaged Fuel Calculations

Fuel Assembly Type	Enrichment	Boron Concentration	Fixed Poison Loading
CE 14x14	4.90 wt. % U-235	2300 ppm	15 mg B-10/cm^2
Westinghouse 15x15	4.90 wt. % U-235	2500 ppm	32 mg B-10/cm^2
Westinghouse 17x17	4.80 wt. % U-235	2500 ppm	32 mg B-10/cm^2

Table 6-20
Results of Optimum Pitch Studies

Description	K_{keno}	σ_{keno}	K_{eff}	Filename
WE 15x15, 4.9 wt. % U-235, 2500 ppm, 32 mg B-10/cm^2 (Type D Basket)				
Pitch = 0.4220", 90% IMD	0.7062	0.0009	0.7080	we15_pitch4220_090.out:
Pitch = 0.4500", 90% IMD	0.7766	0.0009	0.7784	we15_pitch4500_090.out:
Pitch = 0.4750", 90% IMD	0.8280	0.0007	0.8294	we15_pitch4750_090.out:
Pitch = 0.5000", 90% IMD	0.8741	0.0009	0.8759	we15_pitch5000_090.out:
Pitch = 0.5250", 90% IMD	0.9106	0.0009	0.9124	we15_pitch5250_090.out:
Pitch = 0.5500", 90% IMD	0.9324	0.0007	0.9338	we15_pitch5500_090.out:
Pitch = 0.5630", 60% IMD	0.9208	0.0007	0.9222	we15_pitch5630_060.out:
Pitch = 0.5630", 70% IMD	0.9327	0.0007	0.9341	we15_pitch5630_070.out:
Pitch = 0.5630", 80% IMD	0.9398	0.0007	0.9412	we15_pitch5630_080.out:
Pitch = 0.5630", 90% IMD	0.9381	0.0008	0.9397	we15_pitch5630_090.out:
Pitch = 0.5630", 100% IMD	0.9323	0.0007	0.9337	we15_pitch5630_100.out:
Pitch = 0.5750", 60% IMD	0.9251	0.0007	0.9265	we15_pitch5750_060.out:
Pitch = 0.5750", 70% IMD	0.9359	0.0007	0.9373	we15_pitch5750_070.out:
Pitch = 0.5750", 80% IMD	0.9397	0.0007	0.9411	we15_pitch5750_080.out:
Pitch = 0.5750", 90% IMD	0.9381	0.0007	0.9395	we15_pitch5750_090.out:
Pitch = 0.5750", 100% IMD	0.9327	0.0008	0.9343	we15_pitch5750_100.out:
Pitch = 0.5877", 60% IMD	0.9304	0.0007	0.9318	we15_pitch5877_060.out:
Pitch = 0.5877", 70% IMD	0.9399	0.0008	0.9415	we15_pitch5877_070.out:
Pitch = 0.5877", 80% IMD	**0.9417**	**0.0007**	**0.9431**	**we15_pitch5877_080.out:**
Pitch = 0.5877", 90% IMD	0.9361	0.0007	0.9375	we15_pitch5877_090.out:
Pitch = 0.5877", 100% IMD	0.9291	0.0007	0.9305	we15_pitch5877_100.out:

Table 6-20
Results of Optimum Pitch Studies
(Continued)

Description	K_{keno}	σ_{keno}	K_{eff}	Filename
WE 17x17, 4.8 wt. % U-235, 2500 ppm, 32 mg B-10/cm^2 (Type D Basket)				
Pitch = 0.3740", 90% IMD	0.7028	0.0007	0.7042	we17_pitch3740_090.out:
Pitch = 0.4000", 90% IMD	0.7757	0.0007	0.7771	we17_pitch4000_090.out:
Pitch = 0.4250", 90% IMD	0.8372	0.0008	0.8388	we17_pitch4250_090.out:
Pitch = 0.4500", 90% IMD	0.8859	0.0008	0.8875	we17_pitch4500_090.out:
Pitch = 0.47500", 90% IMD	0.9215	0.0008	0.9231	we17_pitch4750_090.out:
Pitch = 0.4960", 60% IMD	0.9164	0.0008	0.9180	we17_pitch4960_060.out:
Pitch = 0.4960", 70% IMD	0.9308	0.0008	0.9324	we17_pitch4960_070.out:
Pitch = 0.4960", 80% IMD	0.9377	0.0008	0.9393	we17_pitch4960_080.out:
Pitch = 0.4960", 90% IMD	0.9376	0.0008	0.9392	we17_pitch4960_090.out:
Pitch = 0.4960", 100% IMD	0.9355	0.0008	0.9371	we17_pitch4960_100.out:
Pitch = 0.5100", 60% IMD	0.9233	0.0008	0.9249	we17_pitch5100_060.out:
Pitch = 0.5100", 70% IMD	0.9348	0.0009	0.9366	we17_pitch5100_070.out:
Pitch = 0.5100", 80% IMD	0.9404	0.0008	0.9420	we17_pitch5100_080.out:
Pitch = 0.5100", 90% IMD	**0.9405**	**0.0008**	**0.9421**	**we17_pitch5100_090.out:**
Pitch = 0.5100", 100% IMD	0.9351	0.0007	0.9365	we17_pitch5100_100.out:
Pitch = 0.5172", 60% IMD	0.9258	0.0007	0.9272	we17_pitch5172_060.out:
Pitch = 0.5172", 70% IMD	0.9371	0.0007	0.9385	we17_pitch5172_070.out:
Pitch = 0.5172", 80% IMD	0.9402	0.0007	0.9416	we17_pitch5172_080.out:
Pitch = 0.5172", 90% IMD	0.9386	0.0007	0.9400	we17_pitch5172_090.out:
Pitch = 0.5172", 100% IMD	0.9312	0.0006	0.9324	we17_pitch5172_100.out:

Table 6-20
Results of Optimum Pitch Studies
(Continued)

Description	K_{keno}	σ_{keno}	K_{eff}	Filename
CE 14x14, 4.9 wt. % U-235, 2300 ppm, 15 mg B-10/cm^2 (Type B Basket)				
Pitch = 0.4400", 70% IMD	0.6852	0.0007	0.6866	ce14_pitch_min_070.out:
Pitch = 0.4400", 80% IMD	0.6915	0.0008	0.6931	ce14_pitch_min_080.out:
Pitch = 0.4700", 70% IMD	0.7560	0.0008	0.7576	ce14_pitch_470_070.out:
Pitch = 0.4700", 80% IMD	0.7626	0.0009	0.7644	ce14_pitch_470_080.out:
Pitch = 0.5000", 70% IMD	0.8196	0.0008	0.8212	ce14_pitch_500_070.out:
Pitch = 0.5000", 80% IMD	0.8245	0.0008	0.8261	ce14_pitch_500_080.out:
Pitch = 0.5400", 70% IMD	0.8872	0.0008	0.8888	ce14_pitch_540_070.out:
Pitch = 0.5400", 80% IMD	0.8886	0.0009	0.8904	ce14_pitch_540_080.out:
Pitch = 0.5800", 70% IMD	0.9337	0.0007	0.9351	ce14_pitch_nom_070.out:
Pitch = 0.5800", 80% IMD	0.9336	0.0007	0.9350	ce14_pitch_nom_080.out:
Pitch = 0.6000", 70% IMD	0.9473	0.0007	0.9487	ce14_pitch_600_070.out:
Pitch = 0.6000", 80% IMD	0.9468	0.0007	0.9482	ce14_pitch_600_080.out:
Pitch = 0.6100", 60% IMD	0.9457	0.0008	0.9473	ce14_pitch_610_060.out:
Pitch = 0.6100", 70% IMD	0.9491	0.0008	0.9507	ce14_pitch_610_070.out:
Pitch = 0.6100", 80% IMD	0.9467	0.0007	0.9481	ce14_pitch_610_080.out:
Pitch = 0.6100", 90% IMD	0.9383	0.0008	0.9399	ce14_pitch_610_090.out:
Pitch = 0.6100", 100% IMD	0.9290	0.0007	0.9304	ce14_pitch_610_100.out:
Pitch = 0.6200", 60% IMD	0.9500	0.0007	0.9514	ce14_pitch_620_060.out:
Pitch = 0.6200", 70% IMD	**0.9512**	**0.0007**	**0.9526**	**ce14_pitch_620_070.out:**
Pitch = 0.6200", 80% IMD	0.9471	0.0007	0.9485	ce14_pitch_620_080.out:
Pitch = 0.6200", 90% IMD	0.9368	0.0008	0.9384	ce14_pitch_620_090.out:
Pitch = 0.6200", 100% IMD	0.9250	0.0007	0.9264	ce14_pitch_620_100.out:
Pitch = 0.6250", 60% IMD	0.9499	0.0007	0.9513	ce14_pitch_625_060.out:
Pitch = 0.6250", 70% IMD	0.9506	0.0007	0.9520	ce14_pitch_625_070.out:
Pitch = 0.6250", 80% IMD	0.9476	0.0008	0.9492	ce14_pitch_625_080.out:
Pitch = 0.6250", 90% IMD	0.9372	0.0007	0.9386	ce14_pitch_625_090.out:
Pitch = 0.6250", 100% IMD	0.9234	0.0008	0.9250	ce14_pitch_625_100.out:
Pitch = 0.6315", 60% IMD	0.9499	0.0007	0.9513	ce14_pitch_max_060.out:
Pitch = 0.6315", 70% IMD	0.9500	0.0008	0.9516	ce14_pitch_max_070.out:
Pitch = 0.6315", 80% IMD	0.9445	0.0007	0.9459	ce14_pitch_max_080.out:
Pitch = 0.6315", 90% IMD	0.9340	0.0008	0.9356	ce14_pitch_max_090.out:
Pitch = 0.6315", 100% IMD	0.9187	0.0007	0.9201	ce14_pitch_max_100.out:

Table 6-21
Results of the Single Ended Rod Shear Studies

Description	K_{keno}	σ_{keno}	K_{eff}	Filename
WE 15x15, 4.9 wt. % U-235, 2500 ppm, 32 mg B-10/cm^2 (Type D Basket)				
D=0.00 cm, 60% IMD	0.9224	0.0008	0.9240	we15_ss000_060.out:
D=0.00 cm, 70% IMD	0.9334	0.0007	0.9348	we15_ss000_070.out:
D=0.00 cm, 80% IMD	0.9381	0.0007	0.9395	we15_ss000_080.out:
D=0.00 cm, 90% IMD	0.9374	0.0007	0.9388	we15_ss000_090.out:
D=0.00 cm, 100% IMD	0.9326	0.0007	0.9340	we15_ss000_100.out:
D=0.15 cm, 60% IMD	0.9222	0.0008	0.9238	we15_ss015_060.out:
D=0.15 cm, 70% IMD	0.9344	0.0008	0.9360	we15_ss015_070.out:
D=0.15 cm, 80% IMD	0.9388	0.0007	0.9402	we15_ss015_080.out:
D=0.15 cm, 90% IMD	0.9378	0.0007	0.9392	we15_ss015_090.out:
D=0.15 cm, 100% IMD	0.9341	0.0007	0.9355	we15_ss015_100.out:
D=0.25 cm, 60% IMD	0.9212	0.0009	0.9230	we15_ss025_060.out:
D=0.25 cm, 70% IMD	0.9359	0.0007	0.9373	we15_ss025_070.out:
D=0.25 cm, 80% IMD	0.9394	0.0008	0.9410	we15_ss025_080.out:
D=0.25 cm, 90% IMD	0.9382	0.0007	0.9396	we15_ss025_090.out:
D=0.25 cm, 100% IMD	0.9352	0.0008	0.9368	we15_ss025_100.out:
D=0.35 cm, 60% IMD	0.9225	0.0008	0.9241	we15_ss035_060.out:
D=0.35 cm, 70% IMD	0.9355	0.0007	0.9369	we15_ss035_070.out:
D=0.35 cm, 80% IMD	**0.9403**	**0.0007**	**0.9417**	**we15_ss035_080.out:**
D=0.35 cm, 90% IMD	0.9391	0.0007	0.9405	we15_ss035_090.out:
D=0.35 cm, 100% IMD	0.9333	0.0007	0.9347	we15_ss035_100.out:
D=0.45 cm, 60% IMD	0.9238	0.0008	0.9254	we15_ss045_060.out:
D=0.45 cm, 70% IMD	0.9335	0.0008	0.9351	we15_ss045_070.out:
D=0.45 cm, 80% IMD	0.9378	0.0008	0.9394	we15_ss045_080.out:
D=0.45 cm, 90% IMD	0.9381	0.0008	0.9397	we15_ss045_090.out:
D=0.45 cm, 100% IMD	0.9330	0.0007	0.9344	we15_ss045_100.out:
D=0.52 cm (max), 60% IMD	0.9224	0.0007	0.9238	we15_ssmax_060.out:
D=0.52 cm (max), 70% IMD	0.9333	0.0008	0.9349	we15_ssmax_070.out:
D=0.52 cm (max), 80% IMD	0.9396	0.0008	0.9412	we15_ssmax_080.out:
D=0.52 cm (max), 90% IMD	0.9376	0.0007	0.9390	we15_ssmax_090.out:
D=0.52 cm (max), 100% IMD	0.9346	0.0007	0.9360	we15_ssmax_100.out:

Table 6-21
Results of the Single Ended Rod Shear Studies
(Continued)

Description	K_{keno}	σ_{keno}	K_{eff}	Filename
WE 17x17, 4.8 wt. % U-235, 2500 ppm, 32 mg B-10/cm^2 (Type D Basket)				
D=0.00 cm, 60% IMD	0.9155	0.0007	0.9169	we17_ss000_060.out:
D=0.00 cm, 70% IMD	0.9294	0.0008	0.9310	we17_ss000_070.out:
D=0.00 cm, 80% IMD	0.9366	0.0007	0.9380	we17_ss000_080.out:
D=0.00 cm, 90% IMD	0.9381	0.0007	0.9395	we17_ss000_090.out:
D=0.00 cm, 100% IMD	0.9327	0.0007	0.9341	we17_ss000_100.out:
D=0.15 cm, 60% IMD	0.9165	0.0007	0.9179	we17_ss015_060.out:
D=0.15 cm, 70% IMD	0.9300	0.0007	0.9314	we17_ss015_070.out:
D=0.15 cm, 80% IMD	0.9360	0.0007	0.9374	we17_ss015_080.out:
D=0.15 cm, 90% IMD	**0.9398**	**0.0008**	**0.9414**	**we17_ss015_090.out:**
D=0.15 cm, 100% IMD	0.9366	0.0007	0.9380	we17_ss015_100.out:
D=0.25 cm, 60% IMD	0.9168	0.0008	0.9184	we17_ss025_060.out:
D=0.25 cm, 70% IMD	0.9298	0.0009	0.9316	we17_ss025_070.out:
D=0.25 cm, 80% IMD	0.9381	0.0008	0.9397	we17_ss025_080.out:
D=0.25 cm, 90% IMD	0.9391	0.0008	0.9407	we17_ss025_090.out:
D=0.25 cm, 100% IMD	0.9370	0.0007	0.9384	we17_ss025_100.out:
D=0.35 cm, 60% IMD	0.9167	0.0007	0.9181	we17_ss035_060.out:
D=0.35 cm, 70% IMD	0.9318	0.0008	0.9334	we17_ss035_070.out:
D=0.35 cm, 80% IMD	0.9370	0.0007	0.9384	we17_ss035_080.out:
D=0.35 cm, 90% IMD	0.9389	0.0007	0.9403	we17_ss035_090.out:
D=0.35 cm, 100% IMD	0.9356	0.0007	0.9370	we17_ss035_100.out:
D=0.45 cm, 60% IMD	0.9160	0.0007	0.9174	we17_ss045_060.out:
D=0.45 cm, 70% IMD	0.9311	0.0008	0.9327	we17_ss045_070.out:
D=0.45 cm, 80% IMD	0.9378	0.0007	0.9392	we17_ss045_080.out:
D=0.45 cm, 90% IMD	0.9398	0.0007	0.9412	we17_ss045_090.out:
D=0.45 cm, 100% IMD	0.9363	0.0007	0.9377	we17_ss045_100.out:
D=0.55 cm (max), 60% IMD	0.9176	0.0008	0.9192	we17_ssmax_060.out:
D=0.55 cm (max), 70% IMD	0.9332	0.0007	0.9346	we17_ssmax_070.out:
D=0.55 cm (max), 80% IMD	0.9381	0.0006	0.9393	we17_ssmax_080.out:
D=0.55 cm (max), 90% IMD	0.9389	0.0007	0.9403	we17_ssmax_090.out:
D=0.55 cm (max), 100% IMD	0.9360	0.0007	0.9374	we17_ssmax_100.out:

Table 6-21
Results of the Single Ended Rod Shear Studies
(Continued)

Description	K_{keno}	σ_{keno}	K_{eff}	Filename
CE 14x14, 4.9 wt. % U-235, 2300 ppm, 15 mg B-10/cm^2 (Type B Basket)				
D=0.00 cm, 60% IMD	0.9309	0.0008	0.9325	ce14_ss000_060.out:
D=0.00 cm, 70% IMD	0.9348	0.0009	0.9366	ce14_ss000_070.out:
D=0.00 cm, 80% IMD	0.9343	0.0007	0.9357	ce14_ss000_080.out:
D=0.00 cm, 90% IMD	0.9289	0.0007	0.9303	ce14_ss000_090.out:
D=0.00 cm, 100% IMD	0.9214	0.0008	0.9230	ce14_ss000_100.out:
D=0.20 cm, 60% IMD	0.9303	0.0007	0.9317	ce14_ss020_060.out:
D=0.20 cm, 70% IMD	0.9383	0.0007	0.9397	ce14_ss020_070.out:
D=0.20 cm, 80% IMD	0.9357	0.0007	0.9371	ce14_ss020_080.out:
D=0.20 cm, 90% IMD	0.9311	0.0008	0.9327	ce14_ss020_090.out:
D=0.20 cm, 100% IMD	0.9230	0.0007	0.9244	ce14_ss020_100.out:
D=0.40 cm, 60% IMD	0.9336	0.0008	0.9352	ce14_ss040_060.out:
D=0.40 cm, 70% IMD	0.9391	0.0008	0.9407	ce14_ss040_070.out:
D=0.40 cm, 80% IMD	0.9400	0.0008	0.9416	ce14_ss040_080.out:
D=0.40 cm, 90% IMD	0.9335	0.0007	0.9349	ce14_ss040_090.out:
D=0.40 cm, 100% IMD	0.9254	0.0007	0.9268	ce14_ss040_100.out:
D=0.60 cm, 60% IMD	0.9335	0.0008	0.9351	ce14_ss060_060.out:
D=0.60 cm, 70% IMD	0.9407	0.0008	0.9423	ce14_ss060_070.out:
D=0.60 cm, 80% IMD	0.9402	0.0008	0.9418	ce14_ss060_080.out:
D=0.60 cm, 90% IMD	0.9345	0.0007	0.9359	ce14_ss060_090.out:
D=0.60 cm, 100% IMD	0.9248	0.0007	0.9262	ce14_ss060_100.out:
D=0.80 cm, 60% IMD	0.9340	0.0008	0.9356	ce14_ss080_060.out:
D=0.80 cm, 70% IMD	0.9403	0.0007	0.9417	ce14_ss080_070.out:
D=0.80 cm, 80% IMD	**0.9411**	**0.0008**	**0.9427**	**ce14_ss080_080.out:**
D=0.80 cm, 90% IMD	0.9342	0.0007	0.9356	ce14_ss080_090.out:
D=0.80 cm, 100% IMD	0.9252	0.0007	0.9266	ce14_ss080_100.out:
D=1.00 cm, 60% IMD	0.9351	0.0008	0.9367	ce14_ss100_060.out:
D=1.00 cm, 70% IMD	0.9410	0.0008	0.9426	ce14_ss100_070.out:
D=1.00 cm, 80% IMD	0.9401	0.0008	0.9417	ce14_ss100_080.out:
D=1.00 cm, 90% IMD	0.9336	0.0007	0.9350	ce14_ss100_090.out:
D=1.00 cm, 100% IMD	0.9233	0.0008	0.9249	ce14_ss100_100.out:

Table 6-21
Results of the Single Ended Rod Shear Studies
(Continued)

Description	K_{keno}	σ_{keno}	K_{eff}	Filename
CE 14x14, 4.9 wt. % U-235, 2300 ppm, 15 mg B-10/cm^2 (Type B Basket)				
D=1.20 cm, 60% IMD	0.9336	0.0007	0.9350	ce14_ss120_060.out:
D=1.20 cm, 70% IMD	0.9402	0.0008	0.9418	ce14_ss120_070.out:
D=1.20 cm, 80% IMD	0.9384	0.0007	0.9398	ce14_ss120_080.out:
D=1.20 cm, 90% IMD	0.9325	0.0007	0.9339	ce14_ss120_090.out:
D=1.20 cm, 100% IMD	0.9235	0.0007	0.9249	ce14_ss120_100.out:
D=1.35 cm, 60% IMD	0.9341	0.0007	0.9355	ce14_ssmax_060.out:
D=1.35 cm, 70% IMD	0.9386	0.0007	0.9400	ce14_ssmax_070.out:
D=1.35 cm, 80% IMD	0.9363	0.0008	0.9379	ce14_ssmax_080.out:
D=1.35 cm, 90% IMD	0.9291	0.0008	0.9307	ce14_ssmax_090.out:
D=1.35 cm, 100% IMD	0.9203	0.0007	0.9217	ce14_ssmax_100.out:

Table 6-22
Results of the Double Ended Rod Shear Studies

CE 14x14, 4.9 wt. % U-235, 2300 ppm, 15 mg B-10/cm^2 (Type B Basket)				
Description	**K_{keno}**	**σ_{keno}**	**K_{eff}**	**Filename**
No Shear				
Ratio=0, 60% IMD	0.9289	0.0008	0.9305	ce14_ds000_060.out:
Ratio=0, 70% IMD	0.9340	0.0008	0.9356	ce14_ds000_070.out:
Ratio=0, 80% IMD	0.9336	0.0007	0.9350	ce14_ds000_080.out:
Ratio=0, 90% IMD	0.9284	0.0008	0.9300	ce14_ds000_090.out:
Ratio=0, 100% IMD	0.9224	0.0007	0.9238	ce14_ds000_100.out:
Double Ended Shear with Minimum Distance Between the Sheared and Intact Rows				
Ratio=5/10, 60% IMD	0.9349	0.0007	0.9363	ce14_ds001_060.out:
Ratio=5/10, 70% IMD	0.9406	0.0009	0.9424	ce14_ds001_070.out:
Ratio=5/10, 80% IMD	0.9442	0.0007	0.9456	ce14_ds001_080.out:
Ratio=5/10, 90% IMD	0.9398	0.0008	0.9414	ce14_ds001_090.out:
Ratio=5/10, 100% IMD	0.9328	0.0008	0.9344	ce14_ds001_100.out:
Double Ended Shear with Maximum Distance Between the Sheared and Intact Rows				
Ratio=5/10, 60% IMD	0.9373	0.0007	0.9387	ce14_ds011_060.out:
Ratio=5/10, 70% IMD	0.9453	0.0008	0.9469	ce14_ds011_070.out:
Ratio=5/10, 80% IMD	**0.9492**	**0.0008**	**0.9508**	**ce14_ds011_080.out:**
Ratio=5/10, 90% IMD	0.9443	0.0007	0.9457	ce14_ds011_090.out:
Ratio=5/10, 100% IMD	0.9365	0.0007	0.9379	ce14_ds011_100.out:

Table 6-22
Results of the Double Ended Rod Shear Studies
(Continued)

Description	K_{keno}	σ_{keno}	K_{eff}	Filename
WE 15x15, 4.9 wt. % U-235, 2500 ppm, 32 mg B-10/cm^2 (Type D Basket)				
Ratio=0, 60% IMD	0.9209	0.0007	0.9223	we15_ds000_060.out:
Ratio=0, 70% IMD	0.9320	0.0008	0.9336	we15_ds000_070.out:
Ratio=0, 80% IMD	0.9382	0.0007	0.9396	we15_ds000_080.out:
Ratio=0, 90% IMD	0.9384	0.0007	0.9398	we15_ds000_090.out:
Ratio=0, 100% IMD	0.9335	0.0008	0.9351	we15_ds000_100.out:
Ratio=2/10, 60% IMD	0.9204	0.0007	0.9218	we15_ds210_060.out:
Ratio=2/10, 70% IMD	0.9321	0.0008	0.9337	we15_ds210_070.out:
Ratio=2/10, 80% IMD	0.9388	0.0008	0.9404	we15_ds210_080.out:
Ratio=2/10, 90% IMD	0.9381	0.0008	0.9397	we15_ds210_090.out:
Ratio=2/10, 100% IMD	0.9334	0.0007	0.9348	we15_ds210_100.out:
Ratio=3/10, 60% IMD	0.9214	0.0008	0.9230	we15_ds310_060.out:
Ratio=3/10, 70% IMD	0.9350	0.0008	0.9366	we15_ds310_070.out:
Ratio=3/10, 80% IMD	0.9408	0.0008	0.9424	we15_ds310_080.out:
Ratio=3/10, 90% IMD	0.9421	0.0008	0.9437	we15_ds310_090.out:
Ratio=3/10, 100% IMD	0.9367	0.0008	0.9383	we15_ds310_100.out:
Ratio=5/10, 60% IMD	0.9239	0.0008	0.9255	we15_ds510_060.out:
Ratio=5/10, 70% IMD	0.9371	0.0007	0.9385	we15_ds510_070.out:
Ratio=5/10, 80% IMD	**0.9438**	**0.0008**	**0.9454**	**we15_ds510_080.out:**
Ratio=5/10, 90% IMD	0.9425	0.0007	0.9439	we15_ds510_090.out:
Ratio=5/10, 100% IMD	0.9404	0.0009	0.9422	we15_ds510_100.out:

Table 6-22
Results of the Double Ended Rod Shear Studies
(Continued)

Description	K_{keno}	σ_{keno}	K_{eff}	Filename
WE 17x17, 4.8 wt. % U-235, 2500 ppm, 32 mg B-10/cm^2 (Type D Basket)				
Ratio=0, 60% IMD	0.9149	0.0007	0.9163	we17_ds000_060.out:
Ratio=0, 70% IMD	0.9304	0.0009	0.9322	we17_ds000_070.out:
Ratio=0, 80% IMD	0.9354	0.0007	0.9368	we17_ds000_080.out:
Ratio=0, 90% IMD	0.9369	0.0007	0.9383	we17_ds000_090.out:
Ratio=0, 100% IMD	0.9355	0.0008	0.9371	we17_ds000_100.out:
Ratio=2/10, 60% IMD	0.9159	0.0008	0.9175	we17_ds210_060.out:
Ratio=2/10, 70% IMD	0.9299	0.0007	0.9313	we17_ds210_070.out:
Ratio=2/10, 80% IMD	0.9371	0.0008	0.9387	we17_ds210_080.out:
Ratio=2/10, 90% IMD	0.9386	0.0008	0.9402	we17_ds210_090.out:
Ratio=2/10, 100% IMD	0.9372	0.0008	0.9388	we17_ds210_100.out:
Ratio=3/10, 60% IMD	0.9184	0.0008	0.9200	we17_ds310_060.out:
Ratio=3/10, 70% IMD	0.9319	0.0008	0.9335	we17_ds310_070.out:
Ratio=3/10, 80% IMD	0.9382	0.0007	0.9396	we17_ds310_080.out:
Ratio=3/10, 90% IMD	0.9415	0.0007	0.9429	we17_ds310_090.out:
Ratio=3/10, 100% IMD	0.9386	0.0008	0.9402	we17_ds310_100.out:
Ratio=5/10, 60% IMD	0.9179	0.0008	0.9195	we17_ds510_060.out:
Ratio=5/10, 70% IMD	0.9324	0.0008	0.9340	we17_ds510_070.out:
Ratio=5/10, 80% IMD	0.9404	0.0007	0.9418	we17_ds510_080.out:
Ratio=5/10, 90% IMD	**0.9444**	**0.0008**	**0.9460**	**we17_ds510_090.out:**
Ratio=5/10, 100% IMD	0.9403	0.0007	0.9417	we17_ds510_100.out:

Table 6-23
Evaluation of the Shifting of Fuel Rods Beyond the Poison

Description	K_{keno}	σ_{keno}	K_{eff}	Filename
CE 14x14, 4.9 wt. % U-235, 2300 ppm, 15 mg B-10/cm^2 (Type B Basket)				
Shift 4-inches, 60% IMD	0.9320	0.0008	0.9336	ce14_nopoison_04_060.out
Shift 4-inches, 70% IMD	0.9372	0.0008	0.9388	ce14_nopoison_04_070.out
Shift 4-inches, 80% IMD	**0.9371**	**0.0009**	**0.9389**	**ce14_nopoison_04_080.out**
Shift 4-inches, 90% IMD	0.9321	0.0008	0.9337	ce14_nopoison_04_090.out
Shift 4-inches, 100% IMD	0.9224	0.0008	0.9240	ce14_nopoison_04_100.out
Slide 6-inches, 60% IMD	0.9279	0.0008	0.9295	ce14_slide_06_060.out:
Slide 6-inches, 70% IMD	**0.9341**	**0.0007**	**0.9355**	**ce14_slide_06_070.out:**
Slide 6-inches, 80% IMD	0.9329	0.0008	0.9345	ce14_slide_06_080.out:
Slide 6-inches, 90% IMD	0.9276	0.0007	0.9290	ce14_slide_06_090.out:
Slide 6-inches, 100% IMD	0.9198	0.0007	0.9212	ce14_slide_06_100.out:
4" Shifting, WE 15x15, 4.9 wt. % U-235, 2500 ppm, 32 mg B-10/cm^2 (Type D Basket)				
Shift 4-inches, 60% IMD	0.9271	0.0009	0.9289	we15_np004_060.out:
Shift 4-inches, 70% IMD	0.9382	0.0008	0.9398	we15_np004_070.out:
Shift 4-inches, 80% IMD	**0.9424**	**0.0008**	**0.9440**	**we15_np004_080.out:**
Shift 4-inches, 90% IMD	0.9397	0.0008	0.9413	we15_np004_090.out:
Shift 4-inches, 100% IMD	0.9341	0.0007	0.9355	we15_np004_100.out:
6" Sliding, WE 15x15, 4.9 wt. % U-235, 2500 ppm, 32 mg B-10/cm^2 (Type D Basket)				
Slide 6-inches, 60% IMD	0.9190	0.0007	0.9204	we15_sl006_060.out:
Slide 6-inches, 70% IMD	0.9324	0.0008	0.9340	we15_sl006_070.out:
Slide 6-inches, 80% IMD	**0.9378**	**0.0008**	**0.9394**	**we15_sl006_080.out:**
Slide 6-inches, 90% IMD	0.9372	0.0008	0.9388	we15_sl006_090.out:
Slide 6-inches, 100% IMD	0.9319	0.0007	0.9333	we15_sl006_100.out:
WE 17x17, 4.8 wt. % U-235, 2500 ppm, 32 mg B-10/cm^2 (Type D Basket)				
Shift 4-inches, 60% IMD	0.9241	0.0009	0.9259	we17_np004_060.out:
Shift 4-inches, 70% IMD	0.9362	0.0007	0.9376	we17_np004_070.out:
Shift 4-inches, 80% IMD	0.9407	0.0007	0.9421	we17_np004_080.out:
Shift 4-inches, 90% IMD	**0.9411**	**0.0007**	**0.9425**	**we17_np004_090.out:**
Shift 4-inches, 100% IMD	0.9366	0.0008	0.9382	we17_np004_100.out:
6" Sliding, WE 17x17, 4.8 wt. % U-235, 2500 ppm, 32 mg B-10/cm^2 (Type D Basket)				
Slide 6-inches, 60% IMD	0.9153	0.0007	0.9167	we17_sl006_060.out:
Slide 6-inches, 70% IMD	0.9283	0.0007	0.9297	we17_sl006_070.out:
Slide 6-inches, 80% IMD	0.9344	0.0007	0.9358	we17_sl006_080.out:
Slide 6-inches, 90% IMD	**0.9364**	**0.0008**	**0.9380**	**we17_sl006_090.out:**
Slide 6-inches, 100% IMD	0.9346	0.0008	0.9362	we17_sl006_100.out:

Table 6-24
Most Reactive Damaged Assembly Configuration

Description	K_{keno}	σ_{keno}	K_{eff}	Filename
CE 14x14, 4.9 wt. % U-235, 2300 ppm, 15 mg B-10/cm^2 (Type B Basket)				
Optimum Pitch	**0.9512**	**0.0007**	**0.9526**	**ce14_pitch_620_070.out:**
Single Ended Shear	0.9411	0.0008	0.9427	ce14_ss080_080.out:
Double Ended Shear	0.9492	0.0008	0.9508	ce14_ds011_080.out:
Shift 4-inches	0.9371	0.0009	0.9389	ce14_nopoison_04_080.out
Slide 6-inches	0.9341	0.0007	0.9355	ce14_slide_06_070.out:
WE 15x15, 4.9 wt. % U-235, 2500 ppm, 32 mg B-10/cm^2 (Type D Basket), No BPRA				
Optimum Pitch	0.9417	0.0007	0.9431	we15_pitch5877_080.out:
Single Ended Shear	0.9403	0.0007	0.9417	we15_ss035_080.out:
Double Ended Shear	**0.9438**	**0.0008**	**0.9454**	**we15_ds510_080.out:**
Shift 4-inches	0.9424	0.0008	0.9440	we15_np004_080.out:
Slide 6-inches	0.9378	0.0008	0.9394	we15_sl006_080.out:
WE 17x17, 4.8 wt. % U-235, 2500 ppm, 32 mg B-10/cm^2 (Type D Basket), No BPRA				
Optimum Pitch	0.9405	0.0008	0.9421	we17_pitch5100_090.out:
Single Ended Shear	0.9398	0.0008	0.9414	we17_ss015_090.out:
Double Ended Shear	**0.9444**	**0.0008**	**0.9460**	**we17_ds510_090.out:**
Shift 4-inches	0.9411	0.0007	0.9425	we17_np004_090.out:
Slide 6-inches	0.9364	0.0008	0.9380	we17_sl006_090.out:

Table 6-25
Double Ended Rod Shear Study with BPRAs

Description	K_{keno}	σ_{keno}	K_{eff}	Filename
WE 15x15, 4.9 wt. % U-235, 2500 ppm, 32 mg B-10/cm^2 (Type D Basket), BPRA				
Ratio=5/10, 60% IMD	0.9132	0.0008	0.9148	we15bp_ds510_060.out:
Ratio=5/10, 70% IMD	0.9316	0.0008	0.9332	we15bp_ds510_070.out:
Ratio=5/10, 80% IMD	0.9410	0.0009	0.9428	we15bp_ds510_080.out:
Ratio=5/10, 90% IMD	0.9483	0.0008	0.9499	we15bp_ds510_090.out:
Ratio=5/10, 100% IMD	**0.9514**	**0.0007**	**0.9528**	**we15bp_ds510_100.out:**
WE 17x17, 4.8 wt. % U-235, 2500 ppm, 32 mg B-10/cm^2 (Type D Basket), BPRA				
Ratio=5/10, 60% IMD	0.9052	0.0008	0.9068	we17bp_ds510_060.out:
Ratio=5/10, 70% IMD	0.9257	0.0007	0.9271	we17bp_ds510_070.out:
Ratio=5/10, 80% IMD	0.9387	0.0007	0.9401	we17bp_ds510_080.out:
Ratio=5/10, 90% IMD	0.9462	0.0008	0.9478	we17bp_ds510_090.out:
Ratio=5/10, 100% IMD	**0.9478**	**0.0008**	**0.9494**	**we17bp_ds510_100.out:**

Table 6-26
WE 15x15 Class Damaged Assemblies With BPRAs - Final Results

Description	K_{keno}	σ_{keno}	K_{eff}	Filename
Type A Basket (7.0 mg B-10/cm^2), 2300 ppm Boron, 3.6 wt. % U-235				
60% IMD	0.9131	0.0007	0.9145	we15bpds_p07e36_060.out:
70% IMD	0.9249	0.0007	0.9263	we15bpds_p07e36_070.out:
80% IMD	0.9296	0.0007	0.9310	we15bpds_p07e36_080.out:
90% IMD	0.9267	0.0008	0.9283	we15bpds_p07e36_090.out:
100% IMD	0.9255	0.0007	0.9269	we15bpds_p07e36_100.out:
Type B Basket (15.0 mg B-10/cm^2), 2300 ppm Boron, 4.0 wt. % U-235				
60% IMD	0.9053	0.0007	0.9067	we15bpds_p15e40_060.out:
70% IMD	0.9223	0.0008	0.9239	we15bpds_p15e40_070.out:
80% IMD	0.9288	0.0008	0.9304	we15bpds_p15e40_080.out:
90% IMD	0.9314	0.0008	0.9330	we15bpds_p15e40_090.out:
100% IMD	0.9340	0.0007	0.9354	we15bpds_p15e40_100.out:
Type D Basket (32.0 mg B-10/cm^2), 2300 ppm Boron, 4.4 wt. % U-235				
60% IMD	0.8923	0.0008	0.8939	we15bpds_p32e44_060.out:
70% IMD	0.9121	0.0009	0.9139	we15bpds_p32e44_070.out:
80% IMD	0.9232	0.0007	0.9246	we15bpds_p32e44_080.out:
90% IMD	0.9324	0.0007	0.9338	we15bpds_p32e44_090.out:
100% IMD	0.9333	0.0008	0.9349	we15bpds_p32e44_100.out:
Type E Basket (50.0 mg B-10/cm^2), 2300 ppm Boron, 4.7 wt. % U-235				
60% IMD	0.8825	0.0008	0.8841	we15bpds_p50e47_060.out:
70% IMD	0.9068	0.0008	0.9084	we15bpds_p50e47_070.out:
80% IMD	0.9210	0.0008	0.9226	we15bpds_p50e47_080.out:
90% IMD	0.9316	0.0008	0.9332	we15bpds_p50e47_090.out:
100% IMD	0.9361	0.0007	0.9375	we15bpds_p50e47_100.out:
Type A Basket (7.0 mg B-10/cm^2), 2400 ppm Boron, 3.7 wt. % U-235				
60% IMD	0.9158	0.0008	0.9174	we15bpds_p07e37_060.out:
70% IMD	0.9264	0.0007	0.9278	we15bpds_p07e37_070.out:
80% IMD	0.9305	0.0007	0.9319	we15bpds_p07e37_080.out:
90% IMD	0.9288	0.0006	0.9300	we15bpds_p07e37_090.out:
100% IMD	0.9254	0.0008	0.9270	we15bpds_p07e37_100.out:
Type B Basket (15.0 mg B-10/cm^2), 2400 ppm Boron, 4.1 wt. % U-235				
60% IMD	0.9079	0.0007	0.9093	we15bpds_p15e41_060.out:
70% IMD	0.9230	0.0007	0.9244	we15bpds_p15e41_070.out:
80% IMD	0.9324	0.0009	0.9342	we15bpds_p15e41_080.out:
90% IMD	0.9332	0.0008	0.9348	we15bpds_p15e41_090.out:
100% IMD	0.9326	0.0007	0.9340	we15bpds_p15e41_100.out:

Table 6-26
WE 15x15 Class Damaged Assemblies With BPRAs - Final Results
(Continued)

Description	K_{keno}	σ_{keno}	K_{eff}	Filename
Type D Basket (32.0 mg B-10/cm^2), 2400 ppm Boron, 4.5 wt. % U-235				
60% IMD	0.8942	0.0007	0.8956	we15bpds_p32e45_060.out:
70% IMD	0.9139	0.0007	0.9153	we15bpds_p32e45_070.out:
80% IMD	0.9239	0.0007	0.9253	we15bpds_p32e45_080.out:
90% IMD	0.9309	0.0007	0.9323	we15bpds_p32e45_090.out:
100% IMD	0.9333	0.0007	0.9347	we15bpds_p32e45_100.out:
Type E Basket (50.0 mg B-10/cm^2), 2400 ppm Boron, 4.8 wt. % U-235				
60% IMD	0.8851	0.0009	0.8869	we15bpds_p50e48_060.out:
70% IMD	0.9078	0.0009	0.9096	we15bpds_p50e48_070.out:
80% IMD	0.9221	0.0008	0.9237	we15bpds_p50e48_080.out:
90% IMD	0.9318	0.0008	0.9334	we15bpds_p50e48_090.out:
100% IMD	0.9353	0.0007	0.9367	we15bpds_p50e48_100.out:
Type A Basket (7.0 mg B-10/cm^2), 2500 ppm Boron, 3.8 wt. % U-235				
60% IMD	0.9194	0.0007	0.9208	we15bpds_p07e38_060.out:
70% IMD	0.9286	0.0007	0.9300	we15bpds_p07e38_070.out:
80% IMD	0.9322	0.0008	0.9338	we15bpds_p07e38_080.out:
90% IMD	0.9327	0.0008	0.9343	we15bpds_p07e38_090.out:
100% IMD	0.9265	0.0007	0.9279	we15bpds_p07e38_100.out:
Type B Basket (15.0 mg B-10/cm^2), 2500 ppm Boron, 4.2 wt. % U-235				
60% IMD	0.9125	0.0007	0.9139	we15bpds_p15e42_060.out:
70% IMD	0.9240	0.0009	0.9258	we15bpds_p15e42_070.out:
80% IMD	0.9311	0.0007	0.9325	we15bpds_p15e42_080.out:
90% IMD	0.9349	0.0008	0.9365	we15bpds_p15e42_090.out:
100% IMD	0.9334	0.0007	0.9348	we15bpds_p15e42_100.out:
Type D Basket (32.0 mg B-10/cm^2), 2500 ppm Boron, 4.6 wt. % U-235				
60% IMD	0.8965	0.0008	0.8981	we15bpds_p32e46_060.out:
70% IMD	0.9144	0.0008	0.9160	we15bpds_p32e46_070.out:
80% IMD	0.9236	0.0007	0.9250	we15bpds_p32e46_080.out:
90% IMD	0.9315	0.0008	0.9331	we15bpds_p32e46_090.out:
100% IMD	0.9312	0.0009	0.9330	we15bpds_p32e46_100.out:
Type E Basket (50.0 mg B-10/cm^2), 2500 ppm Boron, 4.9 wt. % U-235				
60% IMD	0.8873	0.0007	0.8887	we15bpds_p50e49_060.out:
70% IMD	0.9084	0.0008	0.9100	we15bpds_p50e49_070.out:
80% IMD	0.9233	0.0009	0.9251	we15bpds_p50e49_080.out:
90% IMD	0.9295	0.0007	0.9309	we15bpds_p50e49_090.out:
100% IMD	0.9358	0.0008	0.9374	we15bpds_p50e49_100.out:

Table 6-26
WE 15x15 Class Damaged Assemblies With BPRAs - Final Results
(Continued)

Description	K_{keno}	σ_{keno}	K_{eff}	Filename
Type A Basket (7.0 mg B-10/cm^2), 2000 ppm Boron, 3.40 wt. % U-235				
60% IMD	0.9101	0.0008	0.9117	we15bpds_p07e34_060.out:
70% IMD	0.9249	0.0007	0.9263	we15bpds_p07e34_070.out:
80% IMD	0.9321	0.0008	0.9337	we15bpds_p07e34_080.out:
90% IMD	0.9324	0.0007	0.9338	we15bpds_p07e34_090.out:
100% IMD	0.9297	0.0008	0.9313	we15bpds_p07e34_100.out:
Type B Basket (15.0 mg B-10/cm^2), 2000 ppm Boron, 3.75 wt. % U-235				
60% IMD	0.9007	0.0007	0.9021	we15bpds_p15e38_060.out:
70% IMD	0.9205	0.0007	0.9219	we15bpds_p15e38_070.out:
80% IMD	0.9290	0.0007	0.9304	we15bpds_p15e38_080.out:
90% IMD	0.9352	0.0007	0.9366	we15bpds_p15e38_090.out:
100% IMD	**0.9372**	**0.0007**	**0.9386**	**we15bpds_p15e38_100.out:**
Type D Basket (32.0 mg B-10/cm^2), 2000 ppm Boron, 4.10 wt. % U-235				
60% IMD	0.8863	0.0008	0.8879	we15bpds_p32e41_060.out:
70% IMD	0.9088	0.0008	0.9104	we15bpds_p32e41_070.out:
80% IMD	0.9211	0.0008	0.9227	we15bpds_p32e41_080.out:
90% IMD	0.9307	0.0007	0.9321	we15bpds_p32e41_090.out:
100% IMD	0.9337	0.0008	0.9353	we15bpds_p32e41_100.out:
Type E Basket (50.0 mg B-10/cm^2), 2000 ppm Boron, 4.35 wt. % U-235				
60% IMD	0.8760	0.0007	0.8774	we15bpds_p50e44_060.out:
70% IMD	0.9020	0.0008	0.9036	we15bpds_p50e44_070.out:
80% IMD	0.9177	0.0008	0.9193	we15bpds_p50e44_080.out:
90% IMD	0.9274	0.0007	0.9288	we15bpds_p50e44_090.out:
100% IMD	0.9336	0.0008	0.9352	we15bpds_p50e44_100.out:

Table 6-27
WE 17x17 Class Damaged Assemblies With BPRAs - Final Results

Description	K_{keno}	σ_{keno}	K_{eff}	Filename
Type A Basket (7.0 mg B-10/cm^2), 2000 ppm Boron, 3.40 wt. % U-235				
60% IMD	0.9111	0.0008	0.9127	we17bpds_p07e34_060.out:
70% IMD	0.9238	0.0007	0.9252	we17bpds_p07e34_070.out:
80% IMD	0.9320	0.0007	0.9334	we17bpds_p07e34_080.out:
90% IMD	0.9340	0.0008	0.9356	we17bpds_p07e34_090.out:
100% IMD	0.9347	0.0006	0.9359	we17bpds_p07e34_100.out:
Type B Basket (15.0 mg B-10/cm^2), 2000 ppm Boron, 3.75 wt. % U-235				
60% IMD	0.8999	0.0007	0.9013	we17bpds_p15e38_060.out:
70% IMD	0.9188	0.0008	0.9204	we17bpds_p15e38_070.out:
80% IMD	0.9301	0.0007	0.9315	we17bpds_p15e38_080.out:
90% IMD	0.9357	0.0008	0.9373	we17bpds_p15e38_090.out:
100% IMD	0.9379	0.0006	0.9391	we17bpds_p15e38_100.out:
Type C Basket (20.0 mg B-10/cm^2), 2000 ppm Boron, 3.85 wt. % U-235				
60% IMD	0.8922	0.0008	0.8938	we17bpds_p20e39_060.out:
70% IMD	0.9125	0.0008	0.9141	we17bpds_p20e39_070.out:
80% IMD	0.9241	0.0008	0.9257	we17bpds_p20e39_080.out:
90% IMD	0.9321	0.0007	0.9335	we17bpds_p20e39_090.out:
100% IMD	0.9343	0.0007	0.9357	we17bpds_p20e39_100.out:
Type D Basket (32.0 mg B-10/cm^2), 2000 ppm Boron, 4.10 wt. % U-235				
60% IMD	0.8851	0.0007	0.8865	we17bpds_p32e41_060.out:
70% IMD	0.9075	0.0009	0.9093	we17bpds_p32e41_070.out:
80% IMD	0.9203	0.0008	0.9219	we17bpds_p32e41_080.out:
90% IMD	0.9327	0.0008	0.9343	we17bpds_p32e41_090.out:
100% IMD	0.9362	0.0007	0.9376	we17bpds_p32e41_100.out:
Type E Basket (50.0 mg B-10/cm^2), 2000 ppm Boron, 4.30 wt. % U-235				
60% IMD	0.8721	0.0008	0.8737	we17bpds_p50e44_060.out:
70% IMD	0.8977	0.0008	0.8993	we17bpds_p50e44_070.out:
80% IMD	0.9150	0.0007	0.9164	we17bpds_p50e44_080.out:
90% IMD	0.9270	0.0008	0.9286	we17bpds_p50e44_090.out:
100% IMD	0.9336	0.0008	0.9352	we17bpds_p50e44_100.out:
Type A Basket (7.0 mg B-10/cm^2), 2300 ppm Boron, 3.6 wt. % U-235				
60% IMD	0.9102	0.0007	0.9116	we17bpds_p07e36_060.out:
70% IMD	0.9227	0.0007	0.9241	we17bpds_p07e36_070.out:
80% IMD	0.9293	0.0008	0.9309	we17bpds_p07e36_080.out:
90% IMD	0.9303	0.0007	0.9317	we17bpds_p07e36_090.out:
100% IMD	0.9275	0.0008	0.9291	we17bpds_p07e36_100.out:

Table 6-27
WE 17x17 Class Damaged Assemblies With BPRAs - Final Results
(Continued)

Description	K_{keno}	σ_{keno}	K_{eff}	Filename
Type B Basket (15.0 mg B-10/cm^2), 2300 ppm Boron, 4.0 wt. % U-235				
60% IMD	0.9047	0.0007	0.9061	we17bpds_p15e40_060.out:
70% IMD	0.9211	0.0007	0.9225	we17bpds_p15e40_070.out:
80% IMD	0.9295	0.0008	0.9311	we17bpds_p15e40_080.out:
90% IMD	0.9349	0.0007	0.9363	we17bpds_p15e40_090.out:
100% IMD	0.9352	0.0008	0.9368	we17bpds_p15e40_100.out:
Type C Basket (20.0 mg B-10/cm^2), 2300 ppm Boron, 4.15 wt. % U-235				
60% IMD	0.8995	0.0008	0.9011	we17bpds_p20e42_060.out:
70% IMD	0.9191	0.0008	0.9207	we17bpds_p20e42_070.out:
80% IMD	0.9282	0.0008	0.9298	we17bpds_p20e42_080.out:
90% IMD	0.9349	0.0008	0.9365	we17bpds_p20e42_090.out:
100% IMD	0.9361	0.0008	0.9377	we17bpds_p20e42_100.out:
Type D Basket (32.0 mg B-10/cm^2), 2300 ppm Boron, 4.4 wt. % U-235				
60% IMD	0.8914	0.0008	0.8930	we17bpds_p32e44_060.out:
70% IMD	0.9107	0.0009	0.9125	we17bpds_p32e44_070.out:
80% IMD	0.9257	0.0007	0.9271	we17bpds_p32e44_080.out:
90% IMD	0.9333	0.0008	0.9349	we17bpds_p32e44_090.out:
100% IMD	0.9352	0.0007	0.9366	we17bpds_p32e44_100.out:
Type E Basket (50.0 mg B-10/cm^2), 2300 ppm Boron, 4.65 wt. % U-235				
60% IMD	0.8792	0.0008	0.8808	we17bpds_p50e47_060.out:
70% IMD	0.9040	0.0008	0.9056	we17bpds_p50e47_070.out:
80% IMD	0.9201	0.0008	0.9217	we17bpds_p50e47_080.out:
90% IMD	0.9290	0.0008	0.9306	we17bpds_p50e47_090.out:
100% IMD	0.9365	0.0008	0.9381	we17bpds_p50e47_100.out:
Type A Basket (7.0 mg B-10/cm^2), 2400 ppm Boron, 3.7 wt. % U-235				
60% IMD	0.9173	0.0007	0.9187	we17bpds_p07e37_060.out:
70% IMD	0.9271	0.0008	0.9287	we17bpds_p07e37_070.out:
80% IMD	0.9308	0.0007	0.9322	we17bpds_p07e37_080.out:
90% IMD	0.9335	0.0007	0.9349	we17bpds_p07e37_090.out:
100% IMD	0.9289	0.0008	0.9305	we17bpds_p07e37_100.out:
Type B Basket (15.0 mg B-10/cm^2), 2400 ppm Boron, 4.1 wt. % U-235				
60% IMD	0.9071	0.0007	0.9085	we17bpds_p15e41_060.out:
70% IMD	0.9216	0.0008	0.9232	we17bpds_p15e41_070.out:
80% IMD	0.9315	0.0009	0.9333	we17bpds_p15e41_080.out:
90% IMD	0.9363	0.0007	0.9377	we17bpds_p15e41_090.out:
100% IMD	0.9354	0.0008	0.9370	we17bpds_p15e41_100.out:

Table 6-27
WE 17x17 Class Damaged Assemblies With BPRAs - Final Results
(Continued)

Description	K_{keno}	σ_{keno}	K_{eff}	Filename
Type C Basket (20.0 mg B-10/cm^2), 2400 ppm Boron, 4.25 wt. % U-235				
60% IMD	0.9016	0.0009	0.9034	we17bpds_p20e43_060.out:
70% IMD	0.9184	0.0008	0.9200	we17bpds_p20e43_070.out:
80% IMD	0.9306	0.0008	0.9322	we17bpds_p20e43_080.out:
90% IMD	0.9351	0.0007	0.9365	we17bpds_p20e43_090.out:
100% IMD	0.9352	0.0008	0.9368	we17bpds_p20e43_100.out:
Type D Basket (32.0 mg B-10/cm^2), 2400 ppm Boron, 4.50 wt. % U-235				
60% IMD	0.8917	0.0008	0.8933	we17bpds_p32e45_060.out:
70% IMD	0.9133	0.0007	0.9147	we17bpds_p32e45_070.out:
80% IMD	0.9245	0.0008	0.9261	we17bpds_p32e45_080.out:
90% IMD	0.9350	0.0008	0.9366	we17bpds_p32e45_090.out:
100% IMD	0.9364	0.0008	0.9380	we17bpds_p32e45_100.out:
Type E Basket (50.0 mg B-10/cm^2), 2400 ppm Boron, 4.80 wt. % U-235				
60% IMD	0.8843	0.0008	0.8859	we17bpds_p50e48_060.out:
70% IMD	0.9074	0.0009	0.9092	we17bpds_p50e48_070.out:
80% IMD	0.9227	0.0008	0.9243	we17bpds_p50e48_080.out:
90% IMD	0.9325	0.0009	0.9343	we17bpds_p50e48_090.out:
100% IMD	**0.9388**	**0.0007**	**0.9402**	**we17bpds_p50e48_100.out:**
Type A Basket (7.0 mg B-10/cm^2), 2500 ppm Boron, 3.80 wt. % U-235				
60% IMD	0.9159	0.0008	0.9175	we17bpds_p07e38_060.out:
70% IMD	0.9302	0.0008	0.9318	we17bpds_p07e38_070.out:
80% IMD	0.9329	0.0007	0.9343	we17bpds_p07e38_080.out:
90% IMD	0.9334	0.0006	0.9346	we17bpds_p07e38_090.out:
100% IMD	0.9305	0.0006	0.9317	we17bpds_p07e38_100.out:
Type B Basket (15.0 mg B-10/cm^2), 2500 ppm Boron, 4.20 wt. % U-235				
60% IMD	0.9086	0.0009	0.9104	we17bpds_p15e42_060.out:
70% IMD	0.9228	0.0008	0.9244	we17bpds_p15e42_070.out:
80% IMD	0.9328	0.0008	0.9344	we17bpds_p15e42_080.out:
90% IMD	0.9364	0.0007	0.9378	we17bpds_p15e42_090.out:
100% IMD	0.9349	0.0007	0.9363	we17bpds_p15e42_100.out:
Type C Basket (20.0 mg B-10/cm^2), 2500 ppm Boron, 4.35 wt. % U-235				
60% IMD	0.9059	0.0008	0.9075	we17bpds_p20e44_060.out:
70% IMD	0.9210	0.0007	0.9224	we17bpds_p20e44_070.out:
80% IMD	0.9302	0.0007	0.9316	we17bpds_p20e44_080.out:
90% IMD	0.9353	0.0007	0.9367	we17bpds_p20e44_090.out:
100% IMD	0.9369	0.0006	0.9381	we17bpds_p20e44_100.out:

Table 6-27
WE 17x17 Class Damaged Assemblies With BPRAs - Final Results
(Continued)

Description	K_{keno}	σ_{keno}	K_{eff}	Filename
Type D Basket (32.0 mg B-10/cm^2), 2500 ppm Boron, 4.60 wt. % U-235				
60% IMD	60% IMD	60% IMD	60% IMD	60% IMD
70% IMD	70% IMD	70% IMD	70% IMD	70% IMD
80% IMD	80% IMD	80% IMD	80% IMD	80% IMD
90% IMD	90% IMD	90% IMD	90% IMD	90% IMD
100% IMD	100% IMD	100% IMD	100% IMD	100% IMD
Type E Basket (50.0 mg B-10/cm^2), 2500 ppm Boron, 4.9 wt. % U-235				
60% IMD	60% IMD	60% IMD	60% IMD	60% IMD
70% IMD	70% IMD	70% IMD	70% IMD	70% IMD
80% IMD	80% IMD	80% IMD	80% IMD	80% IMD
90% IMD	90% IMD	90% IMD	90% IMD	90% IMD
100% IMD	100% IMD	100% IMD	100% IMD	100% IMD

Table 6-28
Maximum k_{eff} for Intact Assemblies - Final Results

Description	K_{keno}	σ_{keno}	K_{eff}	Filename
CE 14x14, No BPRA, Type D Basket (7.0 mg B-10/cm^2), 2300 ppm Boron, 4.4 wt. % U-235				
70% IMD	0.9383	0.0007	0.9397	ce14b23_p07e44_070.out:
WE 15x15, No BPRA, Type D Basket (32.0 mg B-10/cm^2), 2500 ppm Boron, 4.9 wt. % U-235				
90% IMD	0.9383	0.0008	0.9399	we15b25_p32e49_090.out:
Dry	0.5340	0.0004	0.5348	we15b25_p32e49_000.out:
WE 15x15, BPRA, Type D Basket (32.0 mg B-10/cm^2), 2400 ppm Boron, 4.7 wt. % U-235				
100% IMD	0.9388	0.0007	0.9402	we15bp24_p32e47_100.out:
Dry	0.5408	0.0005	0.5418	we15bp24_p32e47_000.out:
WE 17x17, No BPRA, Type A Basket (7.0 mg B-10/cm^2), 2300 ppm Boron, 3.8 wt. % U-235				
70% IMD	0.9390	0.0007	0.9404	we17b23_p07e38_070.out:
Dry	0.5286	0.0004	0.5294	we17b23_p07e38_000.out:
WE 17x17, BPRA, Type A Basket (7.0 mg B-10/cm^2), 2500 ppm Boron, 3.9 wt. % U-235				
80% IMD	0.9381	0.0008	0.9397	we17bp25_p07e39_080.out:
Dry	0.5554	0.0004	0.5562	we17bp25_p07e39_000.out:
Regulatory Requirements				
Dry Storage : Bounded by Infinite array of Dry Casks	0.5554	0.0004	0.5562	we17bp25_p07e39_000.out:
Normal Conditions: Wet Loading	0.9388	0.0007	0.9402	we15bp24_p32e47_100.out:
Accident Conditions: Damaged Transfer Cask While Fuel Still Wet	0.9390	0.0007	0.9404	we17b23_p07e38_070.out:

Table 6-29
Maximum k_{eff} for Damaged Assemblies - Final Results

Description	K_{keno}	σ_{keno}	K_{eff}	Filename
CE 14x14, No BPRA, Type D Basket (15.0 mg B-10/cm^2), 2400 ppm Boron, 4.8 wt. % U-235				
70% IMD	0.9386	0.0007	0.9400	ce14d24_p15e48_070.out:
WE 15x15, BPRA, Type B Basket (15.0 mg B-10/cm^2), 2000 ppm Boron, 3.75 wt. % U-235				
100% IMD	0.9372	0.0007	0.9386	we15bpds_p15e38_100.out:
WE 17x17, BPRA, Type E Basket (50.0 mg B-10/cm^2), 2400 ppm Boron, 4.8 wt. % U-235				
100% IMD	0.9388	0.0007	0.9402	we17bpds_p50e48_100.out:
Dry	0.5264	0.0004	0.5272	we17bpds_p50e48_000.out:
Regulatory Requirements				
Dry Storage : Bounded by Infinite array of Dry Casks	0.5264	0.0004	0.5272	we17bpds_p50e48_000.out:
Normal Conditions: Wet Loading	0.9388	0.0007	0.9402	we17bpds_p50e48_100.out:
Accident Conditions: Damaged Transfer Cask While Fuel Still Wet	0.9364	0.0007	0.9378	we17bpds_p15e42_090.out:

Table 6-30
Benchmark Results

Run ID	U-235 Enrich. Wt. %	Pitch (cm)	H2O/Fuel volume	Assembly Separation (cm)	AEG	K_{eff}	1σ
B1645SO1	2.46	1.410	1.015	1.78	32.8118	0.9965	0.0008
B1645SO2	2.46	1.410	1.015	1.78	32.7528	1.0006	0.0008
BW1231B1	4.02	1.511	1.139		31.1429	0.9966	0.0009
BW1231B2	4.02	1.511	1.139		29.8872	0.9990	0.0007
BW1273M	2.46	1.511	1.376		32.2213	0.9961	0.0007
BW1484A1	2.46	1.636	1.841	1.64	34.5373	0.9975	0.0008
BW1484A2	2.46	1.636	1.841	4.92	35.1630	0.9934	0.0008
BW1484B1	2.46	1.636	1.841		33.9415	0.9984	0.0008
BW1484B2	2.46	1.636	1.841	1.64	34.5780	0.9961	0.0009
BW1484B3	2.46	1.636	1.841	4.92	35.2638	0.9978	0.0008
BW1484C1	2.46	1.636	1.841	1.64	34.6547	0.9936	0.0009
BW1484C2	2.46	1.636	1.841	1.64	35.2469	0.9944	0.0010
BW1484S1	2.46	1.636	1.841	1.64	34.5159	1.0002	0.0008
BW1484S2	2.46	1.636	1.841	1.64	34.5530	0.9990	0.0008
BW1484SL	2.46	1.636	1.841	6.54	35.4203	0.9944	0.0009
BW1645S1	2.46	1.209	0.383	1.78	30.1060	0.9987	0.0008
BW1645S2	2.46	1.209	0.383	1.78	29.9920	1.0049	0.0008
BW1810A	2.46	1.636	1.841		33.9524	0.9987	0.0006
BW1810B	2.46	1.636	1.841		33.9711	0.9995	0.0006
BW1810C	2.46	1.636	1.841		33.1503	0.9998	0.0008
BW1810D	2.46	1.636	1.841		33.0876	0.9981	0.0010
BW1810E	2.46	1.636	1.841		33.1520	0.9991	0.0007
BW1810F	2.46	1.636	1.841		33.9581	1.0029	0.0007
BW1810G	2.46	1.636	1.841		32.9414	0.9974	0.0008
BW1810H	2.46	1.636	1.841		32.9370	0.9981	0.0008
BW1810I	2.46	1.636	1.841		33.9613	1.0028	0.0007
BW1810J	2.46	1.636	1.841		33.1379	0.9995	0.0008
EPRU65	2.35	1.562	1.196		33.9138	0.9959	0.0008
EPRU65B	2.35	1.562	1.196		33.4073	1.0000	0.0009
EPRU75	2.35	1.905	2.408		35.8676	0.9968	0.0009
EPRU75B	2.35	1.905	2.408		35.3074	1.0002	0.0008
EPRU87	2.35	2.210	3.687		36.6120	1.0011	0.0009
EPRU87B	2.35	2.210	3.687		36.3460	1.0003	0.0008
NSE71SQ	4.74	1.260	1.823		33.7627	0.9978	0.0009
NSE71W1	4.74	1.260	1.823		34.0088	0.9981	0.0010
NSE71W2	4.74	1.260	1.823		34.3856	0.9995	0.0010
P2438BA	2.35	2.032	2.918	5.05	36.2244	0.9973	0.0009
P2438SLG	2.35	2.032	2.918	8.39	36.2906	0.9985	0.0009
P2438SS	2.35	2.032	2.918	6.88	36.2690	0.9979	0.0009
P2438ZR	2.35	2.032	2.918	8.79	36.2891	0.9976	0.0009
P2615BA	4.31	2.540	3.883	6.72	35.7276	1.0005	0.0011
P2615SS	4.31	2.540	3.883	8.58	35.7456	0.9959	0.0011
P2615ZR	4.31	2.540	3.883	10.92	35.7709	0.9980	0.0010
P2827L1	2.35	2.032	2.918	13.72	36.2491	1.0051	0.0008

Table 6-30
Benchmark Results
(Continued)

Run ID	U-235 Enrich. Wt. %	Pitch (cm)	H2O/Fuel volume	Assembly Separation (cm)	AEG	K_{eff}	1σ
P2827L2	2.35	2.032	2.918	11.25	36.2939	1.0005	0.0010
P2827L3	4.31	2.540	3.883	20.78	35.6740	1.0095	0.0009
P2827L4	4.31	2.540	3.883	19.04	35.7173	1.0066	0.0010
P2827SLG	2.35	2.032	2.918	8.31	36.3010	0.9957	0.0008
P3314BA	4.31	1.892	1.600	2.83	33.1874	1.0000	0.0009
P3314BC	4.31	1.892	1.600	2.83	33.2334	0.9992	0.0009
P3314BF1	4.31	1.892	1.600	2.83	33.2422	1.0024	0.0009
P3314BF2	4.31	1.892	1.600	2.83	33.2121	1.0001	0.0010
P3314BS1	2.35	1.684	1.600	3.86	34.8545	0.9957	0.0010
P3314BS2	2.35	1.684	1.600	3.46	34.8324	0.9940	0.0008
P3314BS3	4.31	1.892	1.600	7.23	33.4328	0.9996	0.0009
P3314BS4	4.31	1.892	1.600	6.63	33.4152	1.0000	0.0008
P3314SLG	4.31	1.892	1.600	2.83	34.0109	0.9971	0.0010
P3314SS1	4.31	1.892	1.600	2.83	33.9613	0.9984	0.0010
P3314SS2	4.31	1.892	1.600	2.83	33.7719	1.0014	0.0009
P3314SS3	4.31	1.892	1.600	2.83	33.8956	0.9995	0.0010
P3314SS4	4.31	1.892	1.600	2.83	33.7604	0.9962	0.0009
P3314SS5	2.35	1.684	1.600	7.80	34.9476	0.9947	0.0010
P3314SS6	4.31	1.892	1.600	10.52	33.5406	1.0010	0.0008
P3314W1	4.31	1.892	1.600		34.3962	1.0009	0.0010
P3314W2	2.35	1.684	1.600		35.2153	0.9972	0.0008
P3314ZR	4.31	1.892	1.600	2.83	33.9897	0.9977	0.0010
P3602BB	4.31	1.892	1.600	8.30	33.3198	1.0031	0.0010
P3602BS1	2.35	1.684	1.600	4.80	34.7746	1.0034	0.0009
P3602BS2	4.31	1.892	1.600	9.83	33.3649	1.0047	0.0010
P3602N11	2.35	1.684	1.600	8.98	34.7410	1.0025	0.0008
P3602N12	2.35	1.684	1.600	9.58	34.8378	1.0048	0.0009
P3602N13	2.35	1.684	1.600	9.66	34.9334	1.0006	0.0009
P3602N14	2.35	1.684	1.600	8.54	35.0287	0.9969	0.0010
P3602N21	2.35	2.032	2.918	10.36	36.2787	0.9999	0.0009
P3602N22	2.35	2.032	2.918	11.20	36.1963	1.0014	0.0008
P3602N31	4.31	1.892	1.600	14.87	33.2015	1.0063	0.0010
P3602N32	4.31	1.892	1.600	15.74	33.3085	1.0072	0.0010
P3602N33	4.31	1.892	1.600	15.87	33.4168	1.0084	0.0010
P3602N34	4.31	1.892	1.600	15.84	33.4653	1.0028	0.0010
P3602N35	4.31	1.892	1.600	15.45	33.5169	1.0030	0.0009
P3602N36	4.31	1.892	1.600	13.82	33.5832	1.0003	0.0010
P3602N41	4.31	2.540	3.883	12.89	35.5269	1.0127	0.0010
P3602N42	4.31	2.540	3.883	14.12	35.6711	1.0068	0.0009
P3602N43	4.31	2.540	3.883	12.44	35.7505	1.0049	0.0009
P3602SS1	2.35	1.684	1.600	8.28	34.8708	1.0007	0.0009
P3602SS2	4.31	1.892	1.600	13.75	33.4133	1.0026	0.0010
P3926L1	2.35	1.684	1.600	10.06	34.8569	1.0003	0.0009
P3926L2	2.35	1.684	1.600	10.11	34.9374	1.0020	0.0008

Table 6-30
Benchmark Results
(Concluded)

Run ID	U-235 Enrich. Wt. %	Pitch (cm)	H2O/Fuel volume	Assembly Separation (cm)	AEG	K_{eff}	1σ
P3926L3	2.35	1.684	1.600	8.50	35.0657	0.9967	0.0010
P3926L4	4.31	1.892	1.600	17.74	33.3262	1.0066	0.0009
P3926L5	4.31	1.892	1.600	18.18	33.4035	1.0054	0.0010
P3926L6	4.31	1.892	1.600	17.43	33.5141	1.0038	0.0009
P3926SL1	2.35	1.684	1.600	6.59	35.0674	0.9950	0.0009
P3926SL2	4.31	1.892	1.600	12.79	33.5810	0.9998	0.0009
P4267B1	4.31	1.890	1.590		31.7989	0.9992	0.0008
P4267B2	4.31	0.890	1.590		31.5288	1.0027	0.0007
P4267B3	4.31	1.715	1.090		30.9907	1.0057	0.0009
P4267B4	4.31	1.715	1.090		30.5098	0.9993	0.0008
P4267B5	4.31	1.715	1.090		30.1008	1.0009	0.0008
P4267SL1	4.31	1.890	1.590		33.4692	0.9987	0.0011
P4267SL2	4.31	1.715	1.090		31.9346	0.9995	0.0011
P62FT231	4.31	1.891	1.600	5.67	32.9228	1.0020	0.0009
P71F14F3	4.31	1.891	1.600	5.19	32.8227	1.0009	0.0010
P71F14V3	4.31	1.891	1.600	5.19	32.8587	0.9977	0.0010
P71F14V5	4.31	1.891	1.600	5.19	32.8662	0.9980	0.0010
P71F214R	4.31	1.891	1.600	5.19	32.8669	0.9976	0.0009
PAT80L1	4.74	1.600	3.807	2.00	35.0276	1.0014	0.0009
PAT80L2	4.74	1.600	3.807	2.00	35.1079	0.9986	0.0011
PAT80SS1	4.74	1.600	3.807	2.00	35.0125	0.9998	0.0009
PAT80SS2	4.74	1.600	3.807	2.00	35.1128	0.9967	0.0010
W3269A	5.70	1.422	1.930		33.1383	0.9976	0.0009
W3269B1	3.70	1.105	1.432		32.4010	0.9962	0.0008
W3269B2	3.70	1.105	1.432		32.3940	0.9965	0.0008
W3269B3	3.70	1.105	1.432		32.2464	0.9945	0.0008
W3269C	2.72	1.524	1.494		33.7731	0.9979	0.0009
W3269SL1	2.72	1.524	1.494		33.3854	0.9973	0.0010
W3269SL2	5.70	1.422	1.930		33.1006	1.0024	0.0010
W3269W1	2.72	1.524	1.494		33.5160	0.9972	0.0012
W3269W2	5.70	1.422	1.930		33.1786	1.0015	0.0010
W3385SL1	5.74	1.422	1.932		33.2320	1.0004	0.0009
W3385SL2	5.74	2.012	5.067		35.8876	1.0014	0.0010
Correlation	**0.321**	**0.379**	**0.187**	**0.656**	**0.036**	**N/A**	**N/A**

Table 6-31
USL-1 Results

Parameter	Range of Applicability	Formula to Determine USL
Pin Pitch (cm)	0.890 - 2.540	0.9366 + (4.2438E-03)*X (X < 1.796) 0.9442 (X ≥ 1.796)
Water to Fuel Volume Ratio	0.383 - 5.067	0.9421 + (7.6076E-04)*X (X < 2.146) 0.9438 (X ≥ 2.146)
Average Energy Group Causing Fission (AEG)	29.89 - 36.61	0.9466 - (8.5090E-05)*X (X < 32.548) 0.9438 (X ≥ 32.548)
Assembly Separation (cm)	1.640 - 20.78	0.9409 + (5.0514E-04)*X (X < 7.118) 0.9445 (X ≥ 7.118)
Boron Concentration (ppm)	15 - 3389	0.9435 + (5.3999E-07)*X (X < 2450) 0.9449 (X ≥ 2450)
Enrichment (wt. % U-235)	2.350 - 5.740	0.9403 + (1.0614E-03)*X (X < 3.597) 0.9442 (X ≥ 3.597)

Table 6-32
USL Determination for Criticality Analysis

Parameter	Value from Limiting WE 17x17 Analysis	Bounding USL-1
Pin Pitch (cm)	**1.25984**	**0.9419**
Water to Fuel Volume Ratio	1.6668	0.9433
Average Energy Group Causing Fission (AEG)	30.9147	0.9438
Assembly Separation (cm)	2.222	0.9420
Boron Concentration (ppm)	2300	0.9447
Enrichment (wt. % U-235)	3.700 (min)	0.9442
Parameter	**Value from Limiting WE 15x15 Analysis**	**Bounding USL**
Pin Pitch (cm)	1.43002	0.9426
Water to Fuel Volume Ratio	1.6751	0.9433
Average Energy Group Causing Fission (AEG)	31.3557	0.9438
Assembly Separation (cm)	2.222	0.9420
Boron Concentration (ppm)	2400	0.9448
Enrichment (wt. % U-235)	3.700 (min)	0.9442
Parameter	**Value from Limiting CE 14x14 Analysis**	**Bounding USL**
Pin Pitch (cm)	1.4732	0.9428
Water to Fuel Volume Ratio	1.6127	0.9433
Average Energy Group Causing Fission (AEG)	30.5980	0.9440
Assembly Separation (cm)	2.222	0.9420
Boron Concentration (ppm)	2400	0.9448
Enrichment (wt. % U-235)	3.700 (min)	0.9442

Table 6-33
CE 14x14 Class Intact Assemblies - Final Results

Description	K_{keno}	σ_{keno}	K_{eff}	Filename
Type A Basket (7.0 mg B-10/cm^2), 2000 ppm Boron, 4.05 wt. % U-235				
60% IMD	0.9290	0.0008	0.9306	ce14b20_p07e40_060.out:
70% IMD	0.9344	0.0009	0.9362	ce14b20_p07e40_070.out:
80% IMD	0.9338	0.0008	0.9354	ce14b20_p07e40_080.out:
90% IMD	0.9281	0.0007	0.9295	ce14b20_p07e40_090.out:
100% IMD	0.9192	0.0007	0.9206	ce14b20_p07e40_100.out:
Type B Basket (15.0 mg B-10/cm^2), 2000 ppm Boron, 4.55 wt. % U-235				
60% IMD	0.9239	0.0009	0.9257	ce14b20_p15e45_060.out:
70% IMD	0.9349	0.0008	0.9365	ce14b20_p15e45_070.out:
80% IMD	0.9364	0.0007	0.9378	ce14b20_p15e45_080.out:
90% IMD	0.9359	0.0008	0.9375	ce14b20_p15e45_090.out:
100% IMD	0.9299	0.0007	0.9313	ce14b20_p15e45_100.out:
Type C Basket (20.0 mg B-10/cm^2), 2000 ppm Boron, 4.70 wt. % U-235				
60% IMD	0.9183	0.0009	0.9201	ce14b20_p20e47_060.out:
70% IMD	0.9311	0.0007	0.9325	ce14b20_p20e47_070.out:
80% IMD	0.9357	0.0007	0.9371	ce14b20_p20e47_080.out:
90% IMD	0.9324	0.0007	0.9338	ce14b20_p20e47_090.out:
100% IMD	0.9294	0.0009	0.9312	ce14b20_p20e47_100.out:
Type D Basket (32.0 mg B-10/cm^2), 2000 ppm Boron, 5.00 wt. % U-235				
60% IMD	0.9091	0.0007	0.9105	ce14b20_p32e50_060.out:
70% IMD	0.9242	0.0009	0.9260	ce14b20_p32e50_070.out:
80% IMD	0.9320	0.0007	0.9334	ce14b20_p32e50_080.out:
90% IMD	0.9347	0.0008	0.9363	ce14b20_p32e50_090.out:
100% IMD	0.9317	0.0007	0.9331	ce14b20_p32e50_100.out:
Type A Basket (7.0 mg B-10/cm^2), 2300 ppm Boron, 4.40 wt. % U-235				
60% IMD	0.9356	0.0008	0.9372	ce14b23_p07e44_060.out:
70% IMD	**0.9383**	**0.0007**	**0.9397**	**ce14b23_p07e44_070.out:**
80% IMD	0.9338	0.0007	0.9352	ce14b23_p07e44_080.out:
90% IMD	0.9282	0.0008	0.9298	ce14b23_p07e44_090.out:
100% IMD	0.9159	0.0008	0.9175	ce14b23_p07e44_100.out:
Type B Basket (15.0 mg B-10/cm^2), 2300 ppm Boron, 4.90 wt. % U-235				
60% IMD	0.9286	0.0007	0.9300	ce14b23_p15e49_060.out:
70% IMD	0.9359	0.0009	0.9377	ce14b23_p15e49_070.out:
80% IMD	0.9377	0.0008	0.9393	ce14b23_p15e49_080.out:
90% IMD	0.9327	0.0007	0.9341	ce14b23_p15e49_090.out:
100% IMD	0.9256	0.0007	0.9270	ce14b23_p15e49_100.out:

Table 6-33
CE 14x14 Class Intact Assemblies – Final Results
(Continued)

Description	K_{keno}	σ_{keno}	K_{eff}	Filename
Type C Basket (20.0 mg B-10/cm^2), 2300 ppm Boron, 5.00 wt. % U-235				
60% IMD	0.9196	0.0007	0.9210	ce14b23_p20e50_060.out:
70% IMD	0.9295	0.0007	0.9309	ce14b23_p20e50_070.out:
80% IMD	0.9305	0.0008	0.9321	ce14b23_p20e50_080.out:
90% IMD	0.9285	0.0008	0.9301	ce14b23_p20e50_090.out:
100% IMD	0.9223	0.0007	0.9237	ce14b23_p20e50_100.out:
Type A Basket (07.0 mg B-10/cm^2), 2400 ppm Boron, 4.45 wt. % U-235				
60% IMD	0.9317	0.0007	0.9331	ce14b24_p07e44_060.out:
70% IMD	0.9347	0.0007	0.9361	ce14b24_p07e44_070.out:
80% IMD	0.9305	0.0008	0.9321	ce14b24_p07e44_080.out:
90% IMD	0.9221	0.0007	0.9235	ce14b24_p07e44_090.out:
100% IMD	0.9124	0.0008	0.9140	ce14b24_p07e44_100.out:
Type B Basket (15.0 mg B-10/cm^2), 2400 ppm Boron, 5.00 wt. % U-235				
60% IMD	0.9290	0.0007	0.9304	ce14b24_p15e50_060.out:
70% IMD	0.9358	0.0008	0.9374	ce14b24_p15e50_070.out:
80% IMD	0.9358	0.0007	0.9372	ce14b24_p15e50_080.out:
90% IMD	0.9306	0.0007	0.9320	ce14b24_p15e50_090.out:
100% IMD	0.9238	0.0007	0.9252	ce14b24_p15e50_100.out:
Type A Basket (07.0 mg B-10/cm^2), 2500 ppm Boron, 4.55 wt. % U-235				
60% IMD	0.9345	0.0007	0.9359	ce14b25_p07e45_060.out:
70% IMD	0.9370	0.0008	0.9386	ce14b25_p07e45_070.out:
80% IMD	0.9295	0.0008	0.9311	ce14b25_p07e45_080.out:
90% IMD	0.9237	0.0007	0.9251	ce14b25_p07e45_090.out:
100% IMD	0.9139	0.0007	0.9153	ce14b25_p07e45_100.out:

Table 6-34
CE 14x14 Class Damaged Assemblies - Final Results

Description	K_{keno}	σ_{keno}	K_{eff}	Filename
Type A Basket (7.0 mg B-10/cm^2), 2000 ppm Boron, 3.90 wt. % U-235				
60% IMD	0.9371	0.0007	0.9385	ce14d20_p07e39_060.out:
70% IMD	0.9375	0.0007	0.9389	ce14d20_p07e39_070.out:
80% IMD	0.9304	0.0007	0.9318	ce14d20_p07e39_080.out:
90% IMD	0.9181	0.0007	0.9195	ce14d20_p07e39_090.out:
100% IMD	0.9046	0.0008	0.9062	ce14d20_p07e39_100.out:
Type B Basket (15.0 mg B-10/cm^2), 2000 ppm Boron, 4.35 wt. % U-235				
60% IMD	0.9331	0.0008	0.9347	ce14d20_p15e43_060.out:
70% IMD	0.9381	0.0007	0.9395	ce14d20_p15e43_070.out:
80% IMD	0.9354	0.0008	0.9370	ce14d20_p15e43_080.out:
90% IMD	0.9282	0.0007	0.9296	ce14d20_p15e43_090.out:
100% IMD	0.9180	0.0007	0.9194	ce14d20_p15e43_100.out:
Type C Basket (20.0 mg B-10/cm^2), 2000 ppm Boron, 4.50 wt. % U-235				
60% IMD	0.9293	0.0007	0.9307	ce14d20_p20e45_060.out:
70% IMD	0.9348	0.0007	0.9362	ce14d20_p20e45_070.out:
80% IMD	0.9342	0.0007	0.9356	ce14d20_p20e45_080.out:
90% IMD	0.9273	0.0007	0.9287	ce14d20_p20e45_090.out:
100% IMD	0.9187	0.0007	0.9201	ce14d20_p20e45_100.out:
Type D Basket (32.0 mg B-10/cm^2), 2000 ppm Boron, 4.85 wt. % U-235				
60% IMD	0.9263	0.0007	0.9277	ce14d20_p32e48_060.out:
70% IMD	0.9370	0.0008	0.9386	ce14d20_p32e48_070.out:
80% IMD	0.9385	0.0006	0.9397	ce14d20_p32e48_080.out:
90% IMD	0.9338	0.0007	0.9352	ce14d20_p32e48_090.out:
100% IMD	0.9257	0.0008	0.9273	ce14d20_p32e48_100.out:
Type E Basket (50.0 mg B-10/cm^2), 2000 ppm Boron, 5.00 wt. % U-235				
60% IMD	0.9111	0.0007	0.9125	ce14d20_p50e50_060.out:
70% IMD	0.9240	0.0008	0.9256	ce14d20_p50e50_070.out:
80% IMD	0.9296	0.0008	0.9312	ce14d20_p50e50_080.out:
90% IMD	0.9253	0.0007	0.9267	ce14d20_p50e50_090.out:
100% IMD	0.9197	0.0008	0.9213	ce14d20_p50e50_100.out:
Type A Basket (7.0 mg B-10/cm^2), 2300 ppm Boron, 4.20 wt. % U-235				
60% IMD	0.9382	0.0007	0.9396	ce14d23_p07e42_060.out:
70% IMD	0.9363	0.0007	0.9377	ce14d23_p07e42_070.out:
80% IMD	0.9280	0.0008	0.9296	ce14d23_p07e42_080.out:
90% IMD	0.9161	0.0007	0.9175	ce14d23_p07e42_090.out:
100% IMD	0.8999	0.0007	0.9013	ce14d23_p07e42_100.out:

Table 6-34
CE 14x14 Damaged Assemblies – Final Results
(Continued)

Description	K_{keno}	σ_{keno}	K_{eff}	Filename
Type B Basket (15.0 mg B-10/cm^2), 2300 ppm Boron, 4.70 wt. % U-235				
60% IMD	0.9369	0.0009	0.9387	ce14d23_p15e47_060.out:
70% IMD	0.9380	0.0007	0.9394	ce14d23_p15e47_070.out:
80% IMD	0.9349	0.0007	0.9363	ce14d23_p15e47_080.out:
90% IMD	0.9242	0.0007	0.9256	ce14d23_p15e47_090.out:
100% IMD	0.9118	0.0008	0.9134	ce14d23_p15e47_100.out:
Type C Basket (20.0 mg B-10/cm^2), 2300 ppm Boron, 4.85 wt. % U-235				
60% IMD	0.9314	0.0008	0.9330	ce14d23_p20e48_060.out:
70% IMD	0.9357	0.0008	0.9373	ce14d23_p20e48_070.out:
80% IMD	0.9346	0.0008	0.9362	ce14d23_p20e48_080.out:
90% IMD	0.9260	0.0007	0.9274	ce14d23_p20e48_090.out:
100% IMD	0.9135	0.0007	0.9149	ce14d23_p20e48_100.out:
Type D Basket (32.0 mg B-10/cm^2), 2300 ppm Boron, 5.00 wt. % U-235				
60% IMD	0.9170	0.0007	0.9184	ce14d23_p32e50_060.out:
70% IMD	0.9231	0.0007	0.9245	ce14d23_p32e50_070.out:
80% IMD	0.9237	0.0007	0.9251	ce14d23_p32e50_080.out:
90% IMD	0.9173	0.0007	0.9187	ce14d23_p32e50_090.out:
100% IMD	0.9081	0.0007	0.9095	ce14d23_p32e50_100.out:
Type A Basket (07.0 mg B-10/cm^2), 2400 ppm Boron, 4.25 wt. % U-235				
60% IMD	0.9356	0.0007	0.9370	ce14d24_p07e42_060.out:
70% IMD	0.9322	0.0007	0.9336	ce14d24_p07e42_070.out:
80% IMD	0.9235	0.0007	0.9249	ce14d24_p07e42_080.out:
90% IMD	0.9113	0.0007	0.9127	ce14d24_p07e42_090.out:
100% IMD	0.8952	0.0006	0.8964	ce14d24_p07e42_100.out:
Type B Basket (15.0 mg B-10/cm^2), 2400 ppm Boron, 4.80 wt. % U-235				
60% IMD	0.9366	0.0007	0.9380	ce14d24_p15e48_060.out:
70% IMD	**0.9386**	**0.0007**	**0.9400**	**ce14d24_p15e48_070.out:**
80% IMD	0.9323	0.0007	0.9337	ce14d24_p15e48_080.out:
90% IMD	0.9242	0.0007	0.9256	ce14d24_p15e48_090.out:
100% IMD	0.9115	0.0007	0.9129	ce14d24_p15e48_100.out:
Type C Basket (20.0 mg B-10/cm^2), 2400 ppm Boron, 4.95 wt. % U-235				
60% IMD	0.9318	0.0008	0.9334	ce14d24_p20e49_060.out:
70% IMD	0.9354	0.0008	0.9370	ce14d24_p20e49_070.out:
80% IMD	0.9313	0.0008	0.9329	ce14d24_p20e49_080.out:
90% IMD	0.9247	0.0007	0.9261	ce14d24_p20e49_090.out:
100% IMD	0.9121	0.0007	0.9135	ce14d24_p20e49_100.out:

Table 6-34
CE 14x14 Class Damaged Assemblies – Final Results
(Continued)

Description	K_{keno}	σ_{keno}	K_{eff}	Filename
Type A Basket (07.0 mg B-10/cm^2), 2500 ppm Boron, 4.35 wt. % U-235				
60% IMD	0.9364	0.0007	0.9378	ce14d25_p07e43_060.out:
70% IMD	0.9323	0.0007	0.9337	ce14d25_p07e43_070.out:
80% IMD	0.9235	0.0006	0.9247	ce14d25_p07e43_080.out:
90% IMD	0.9087	0.0007	0.9101	ce14d25_p07e43_090.out:
100% IMD	0.8926	0.0007	0.8940	ce14d25_p07e43_100.out:
Type B Basket (15.0 mg B-10/cm^2), 2500 ppm Boron, 4.90 wt. % U-235				
60% IMD	0.9375	0.0009	0.9393	ce14d25_p15e49_060.out:
70% IMD	0.9380	0.0007	0.9394	ce14d25_p15e49_070.out:
80% IMD	0.9327	0.0008	0.9343	ce14d25_p15e49_080.out:
90% IMD	0.9220	0.0007	0.9234	ce14d25_p15e49_090.out:
100% IMD	0.9077	0.0008	0.9093	ce14d25_p15e49_100.out:
Type C Basket (20.0 mg B-10/cm^2), 2500 ppm Boron, 5.00 wt. % U-235				
60% IMD	0.9297	0.0007	0.9311	ce14d25_p20e50_060.out:
70% IMD	0.9326	0.0007	0.9340	ce14d25_p20e50_070.out:
80% IMD	0.9277	0.0007	0.9291	ce14d25_p20e50_080.out:
90% IMD	0.9178	0.0007	0.9192	ce14d25_p20e50_090.out:
100% IMD	0.9059	0.0007	0.9073	ce14d25_p20e50_100.out:

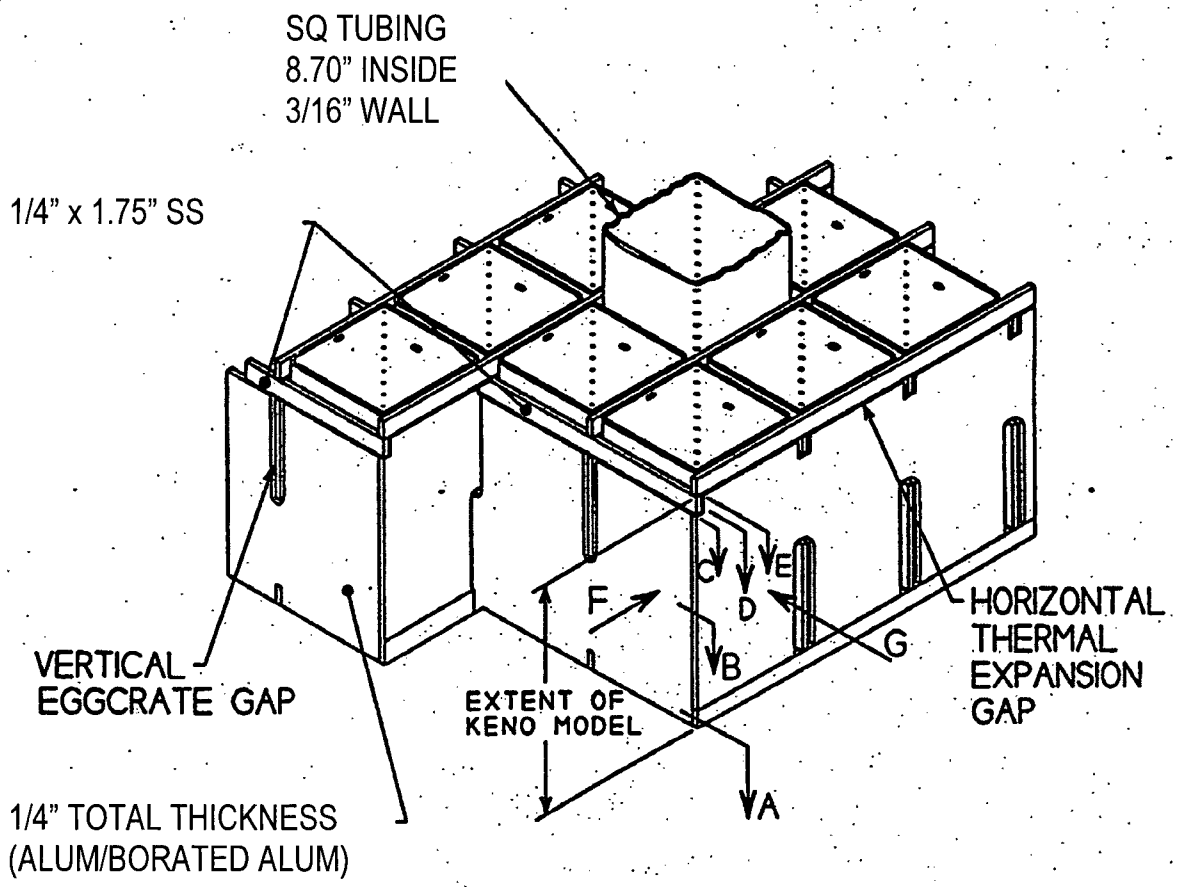

Figure 6-1
Basket Views and Dimensions

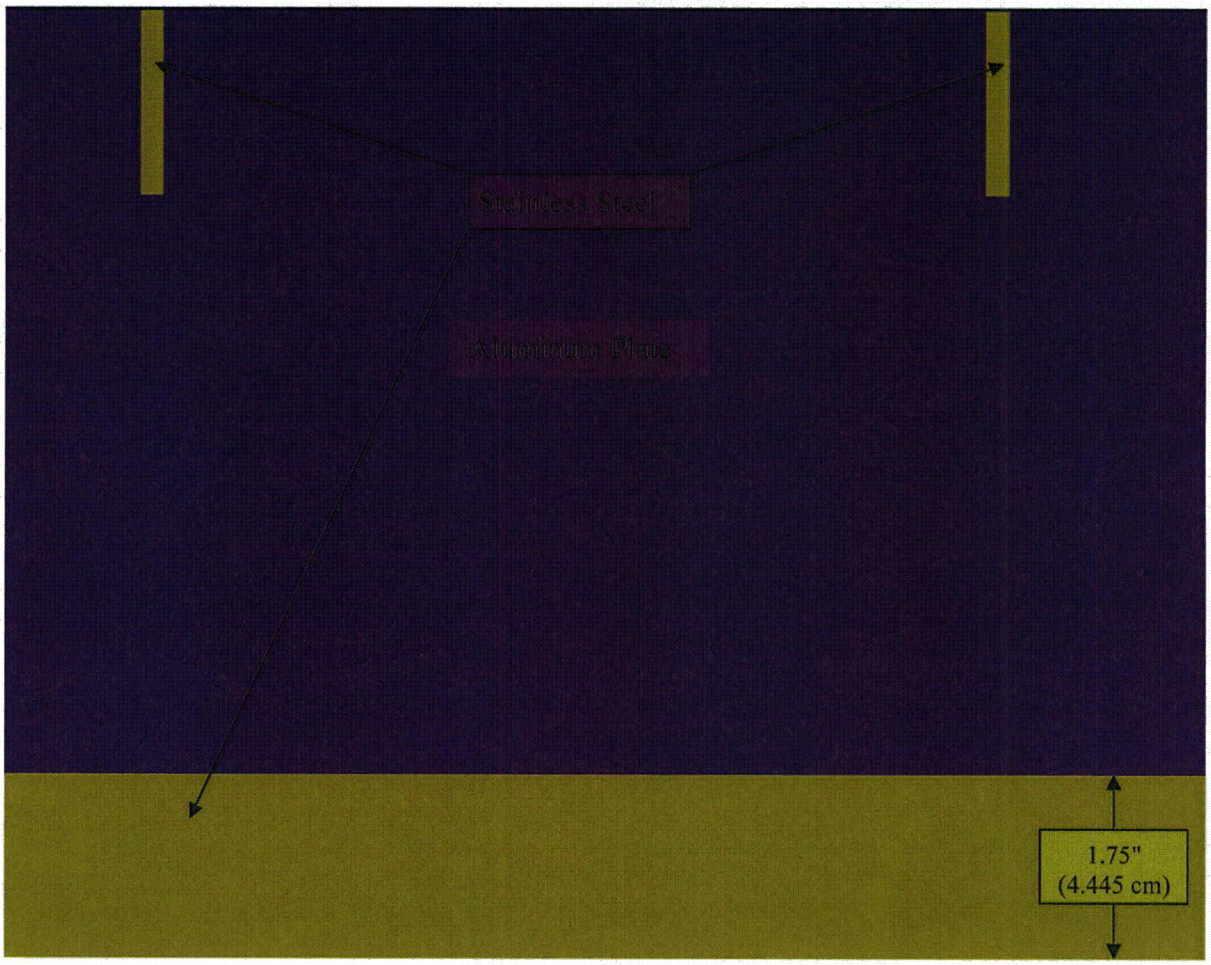

Periodic Boundary at the Bottom of Model

Figure 6-2
Basket Model Compartment Wall (View G)

Periodic Boundary at the Top of Model

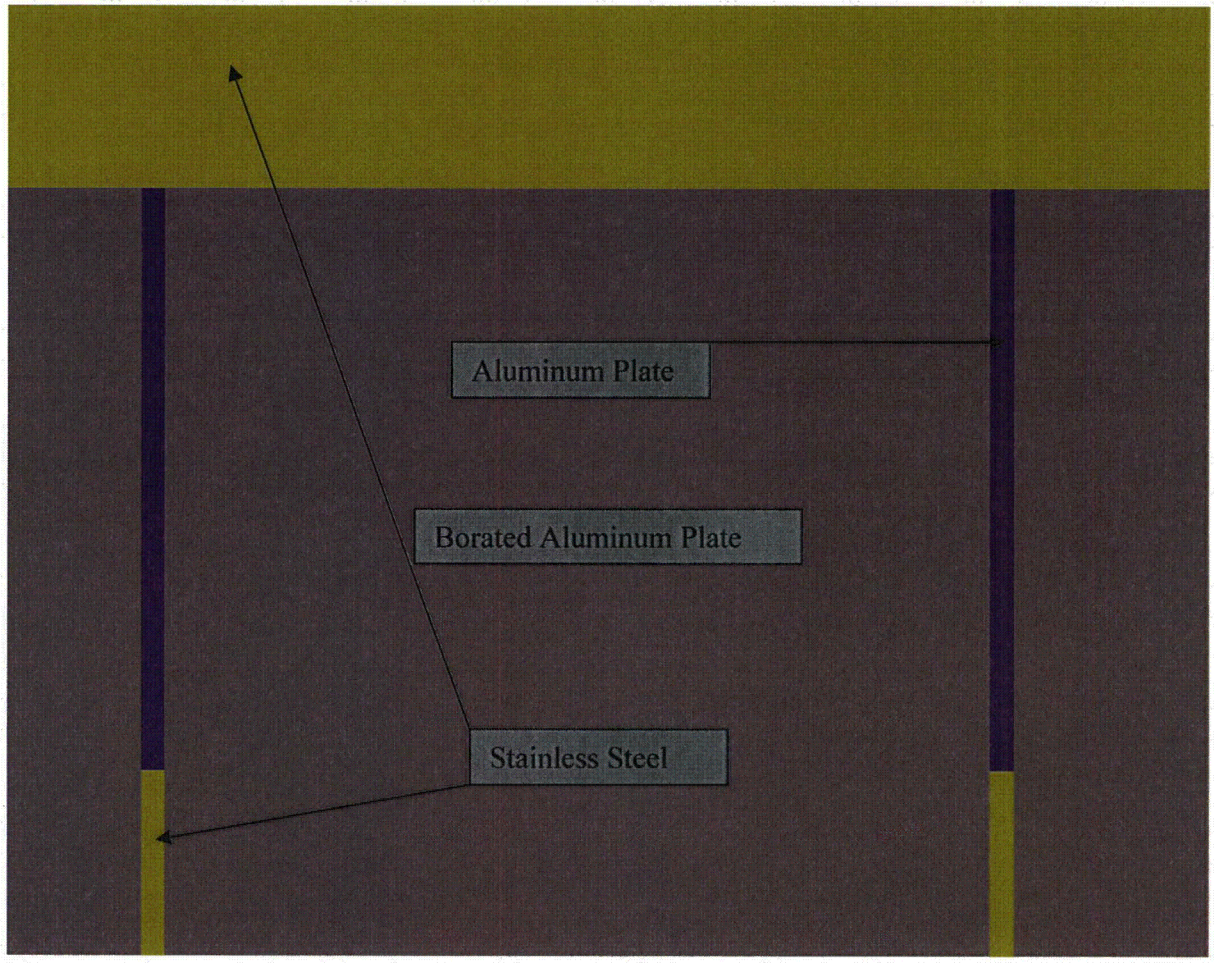

Figure 6-3
Basket Model Compartment Wall (View F)

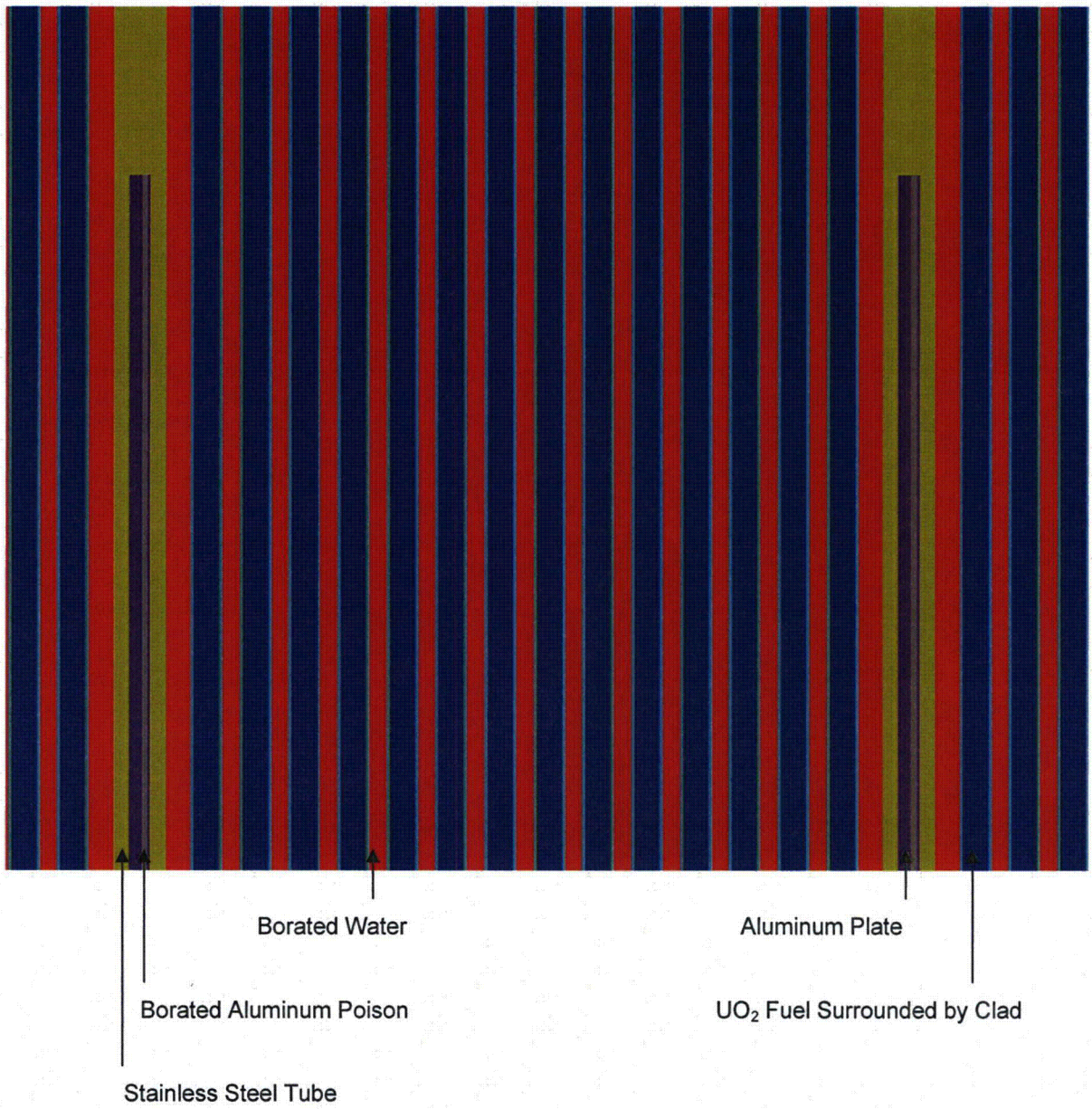

Figure 6-4
Basket Model Compartment Wall With Fuel Assembly (View G)

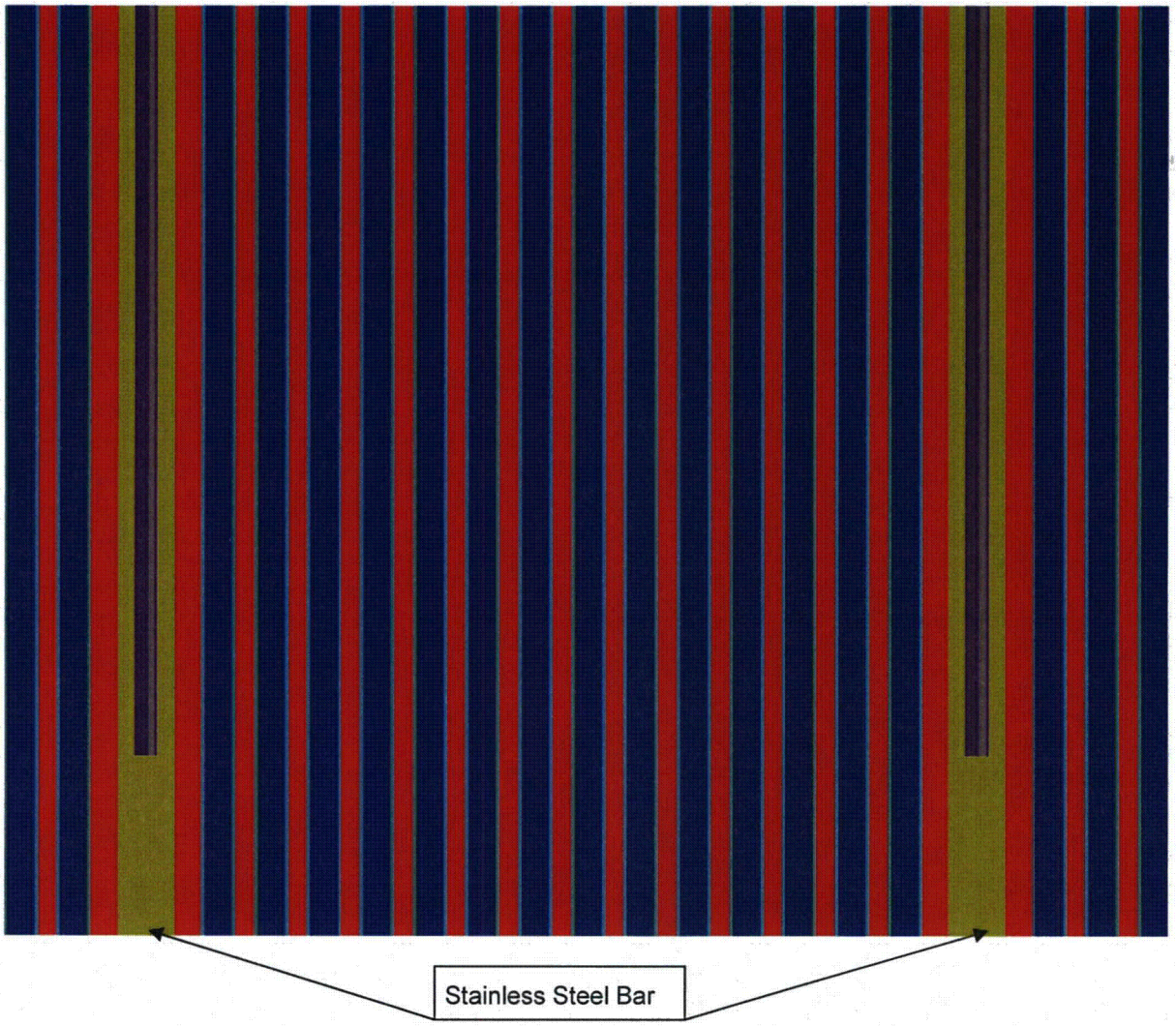

Figure 6-5
Basket Model Compartment Wall With Fuel Assembly (View F)

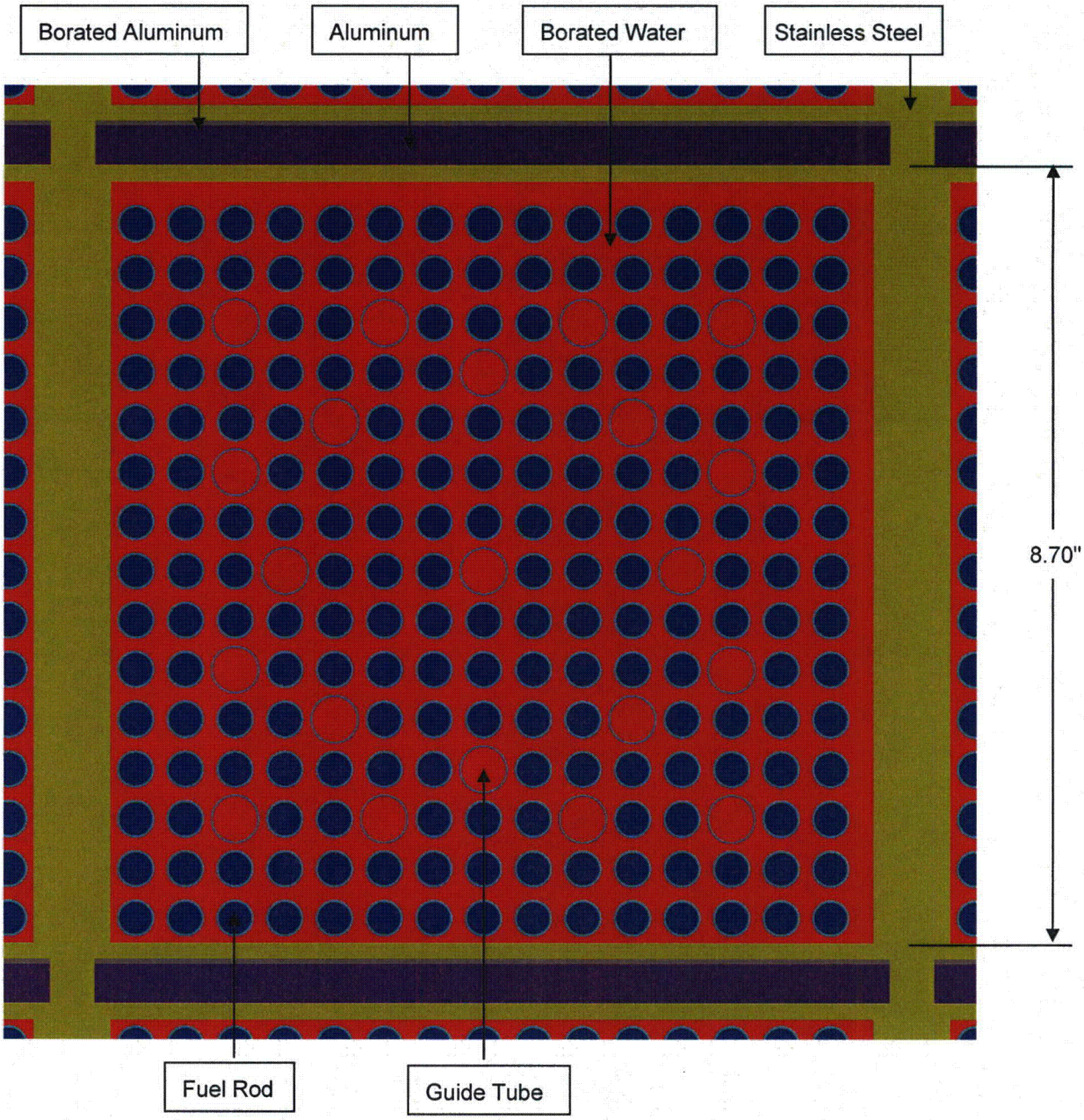

Figure 6-6
Basket Compartment With Fuel (Section A)

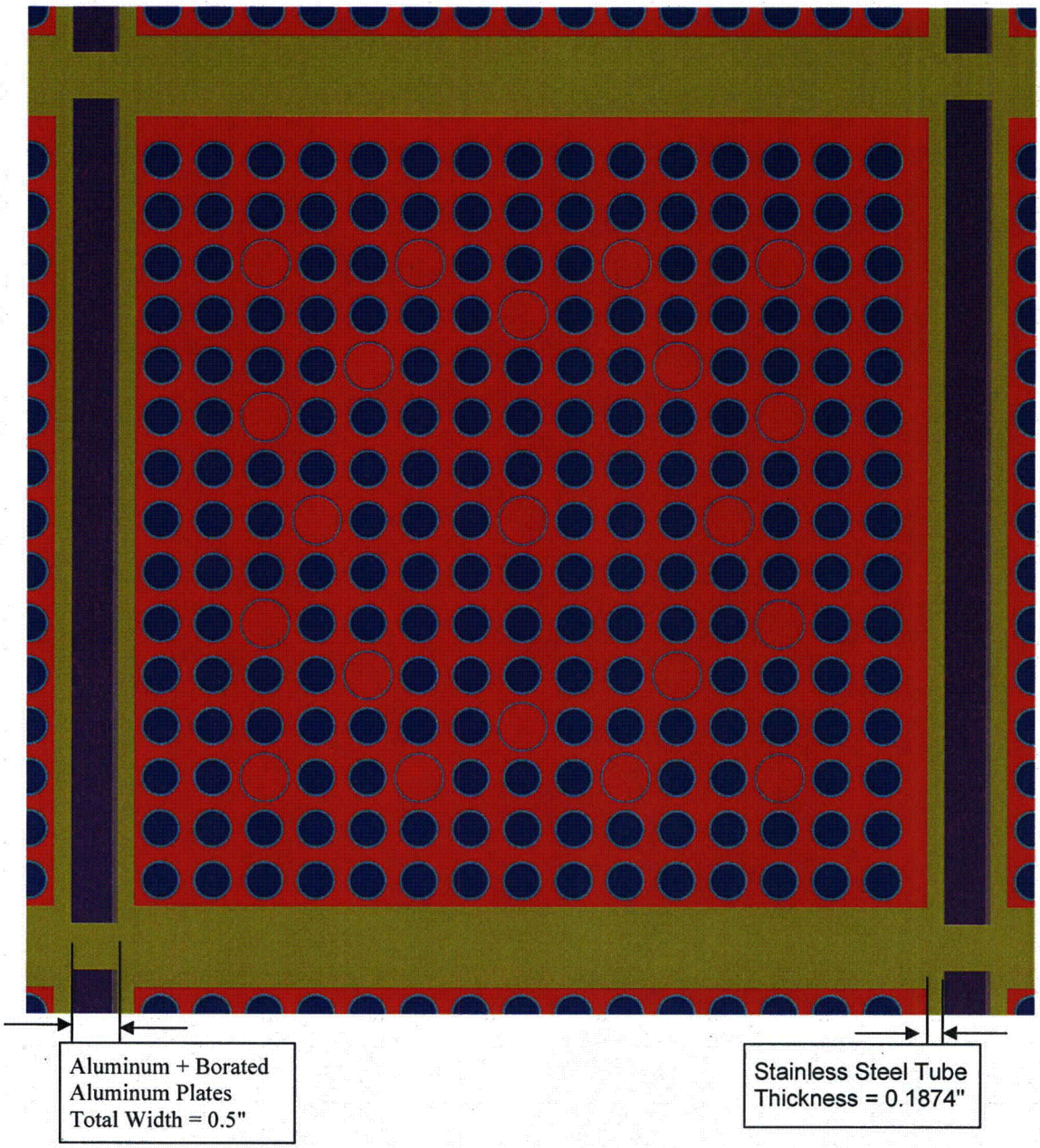

Figure 6-7
Basket Compartment With Fuel (Section B)

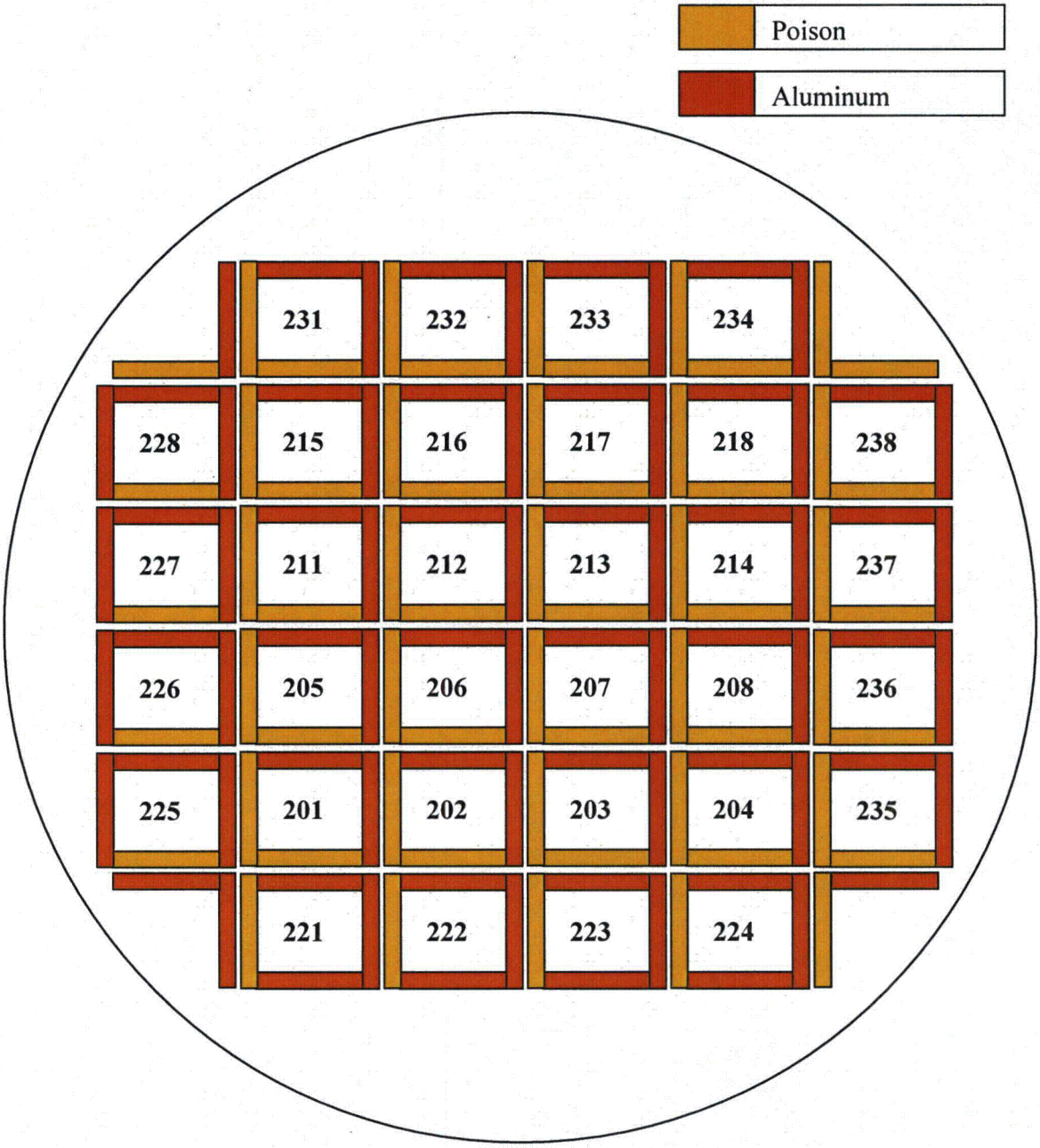

Figure 6-8
Fuel Assembly Positions and Poison Plate Locations in the Basket

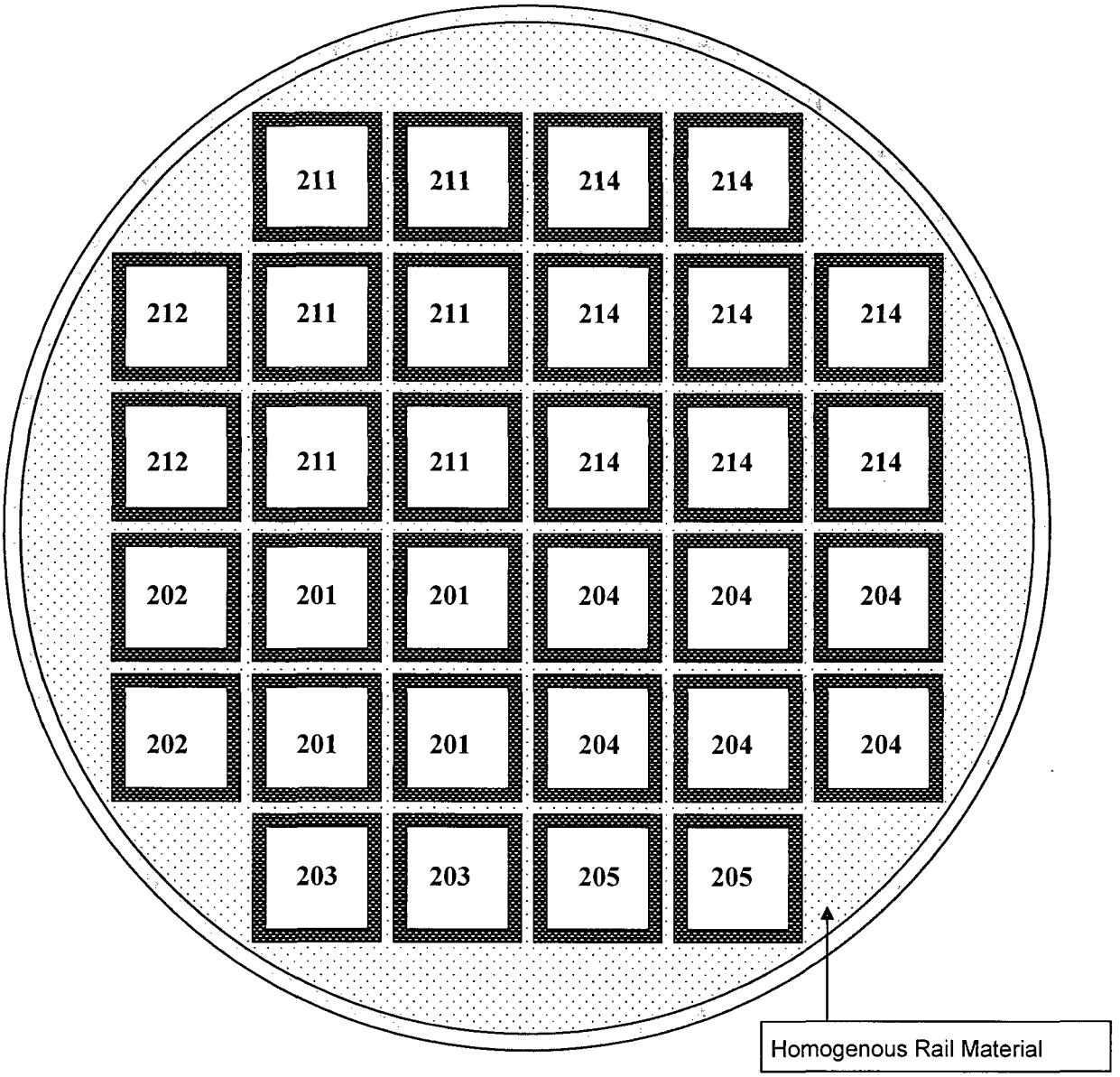

Figure 6-9
Fuel Assembly Positions by KENO Unit ID

Figure Withheld Under 10 CFR 2.390

Figure 6-10
Canister and Transfer Cask Description in the KENO Model

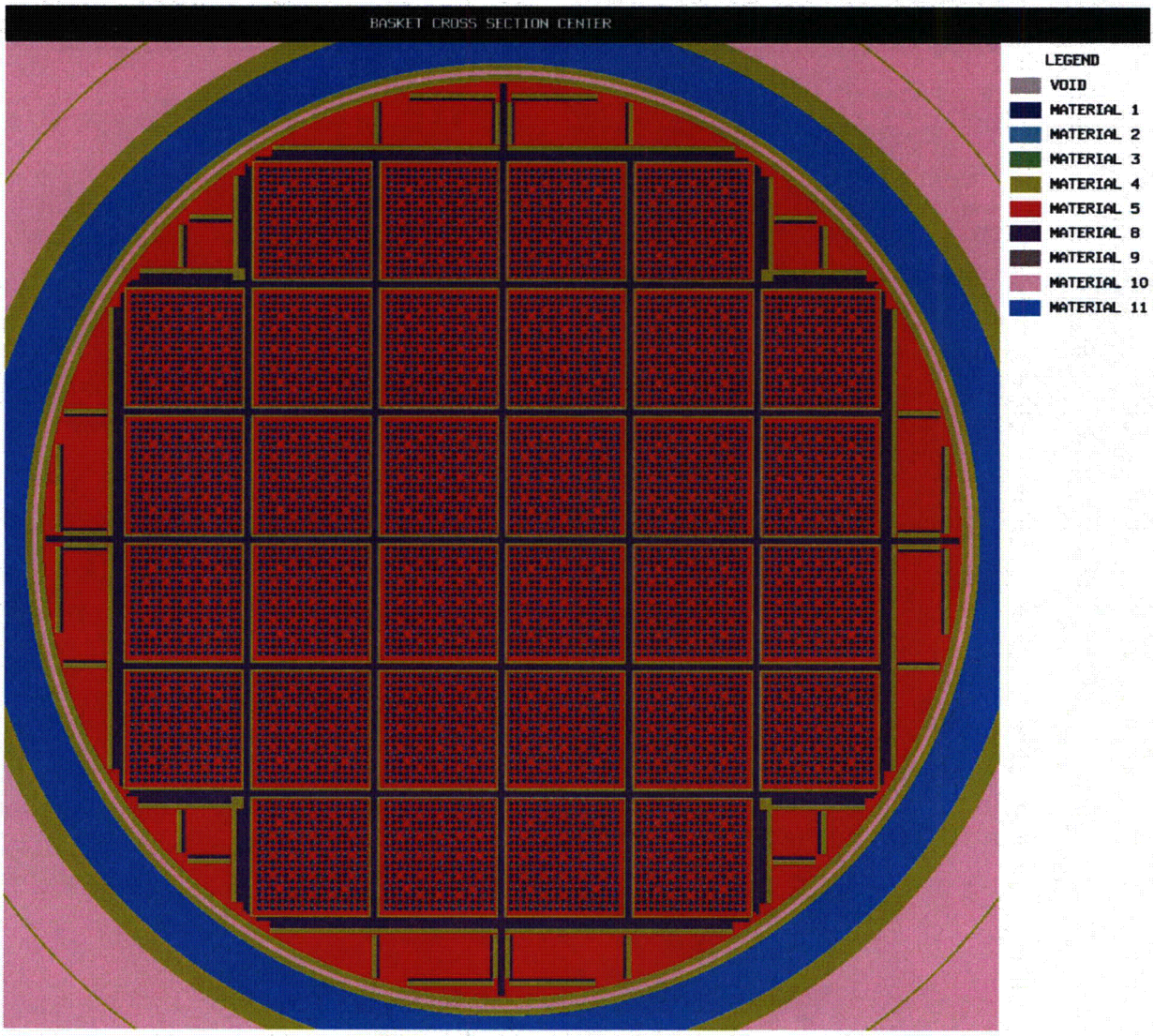

Figure 6-11
Radial Cross Section of the Detailed KENO Model

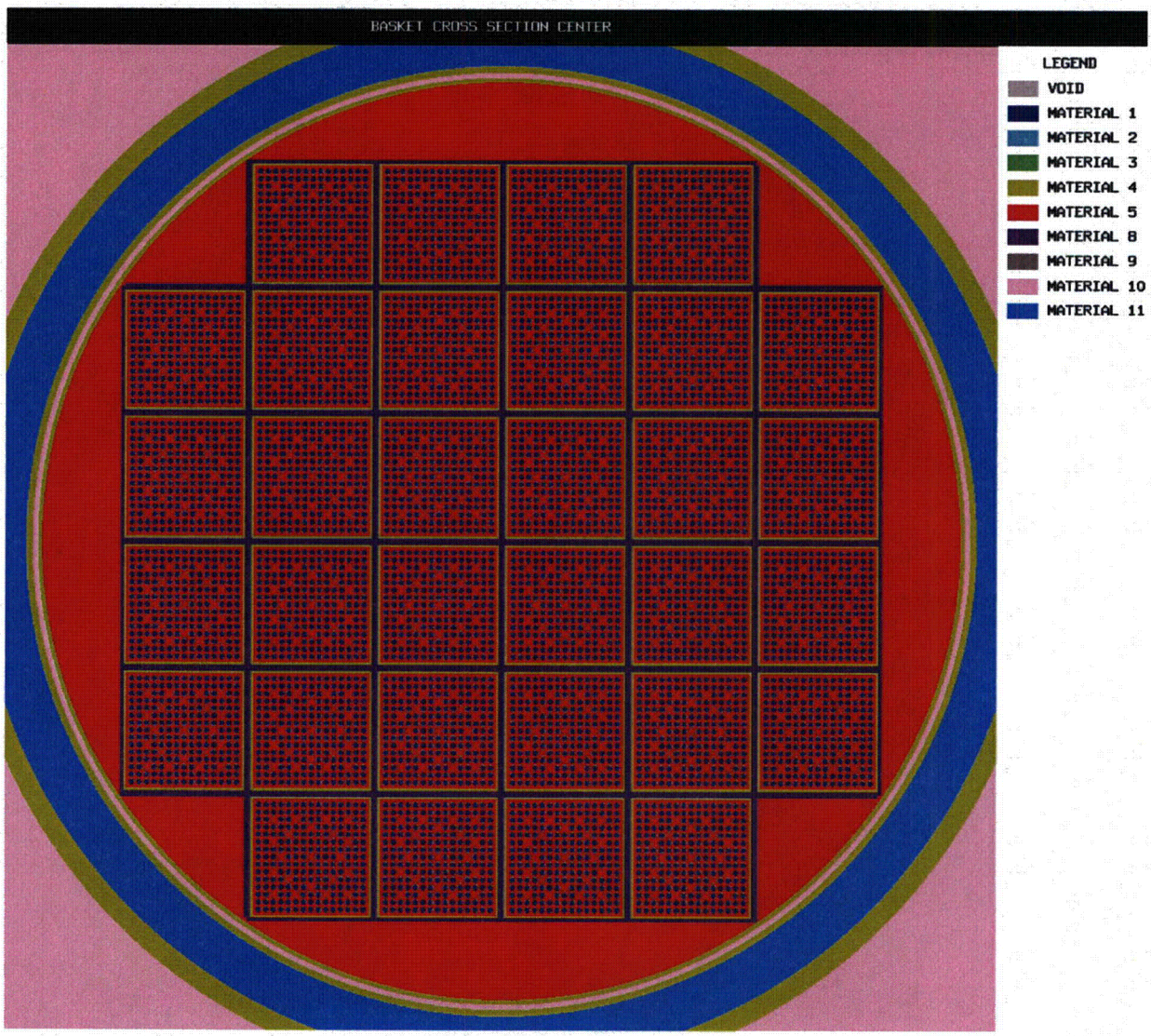

Figure 6-12
WE 15x15 Fuel Assemblies in the Centered Position

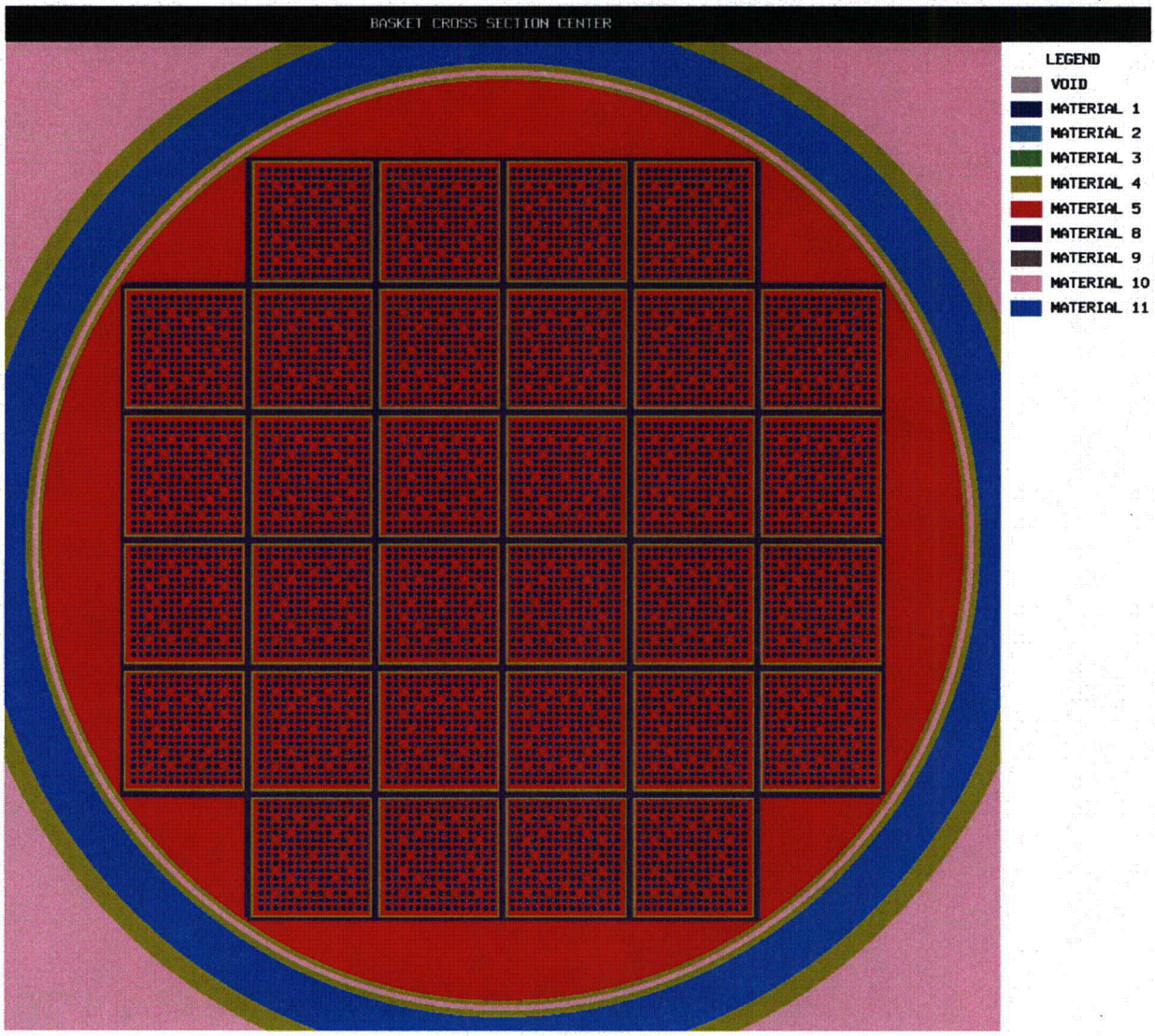

Figure 6-13
WE 15x15 Fuel Assemblies in the Inward Position

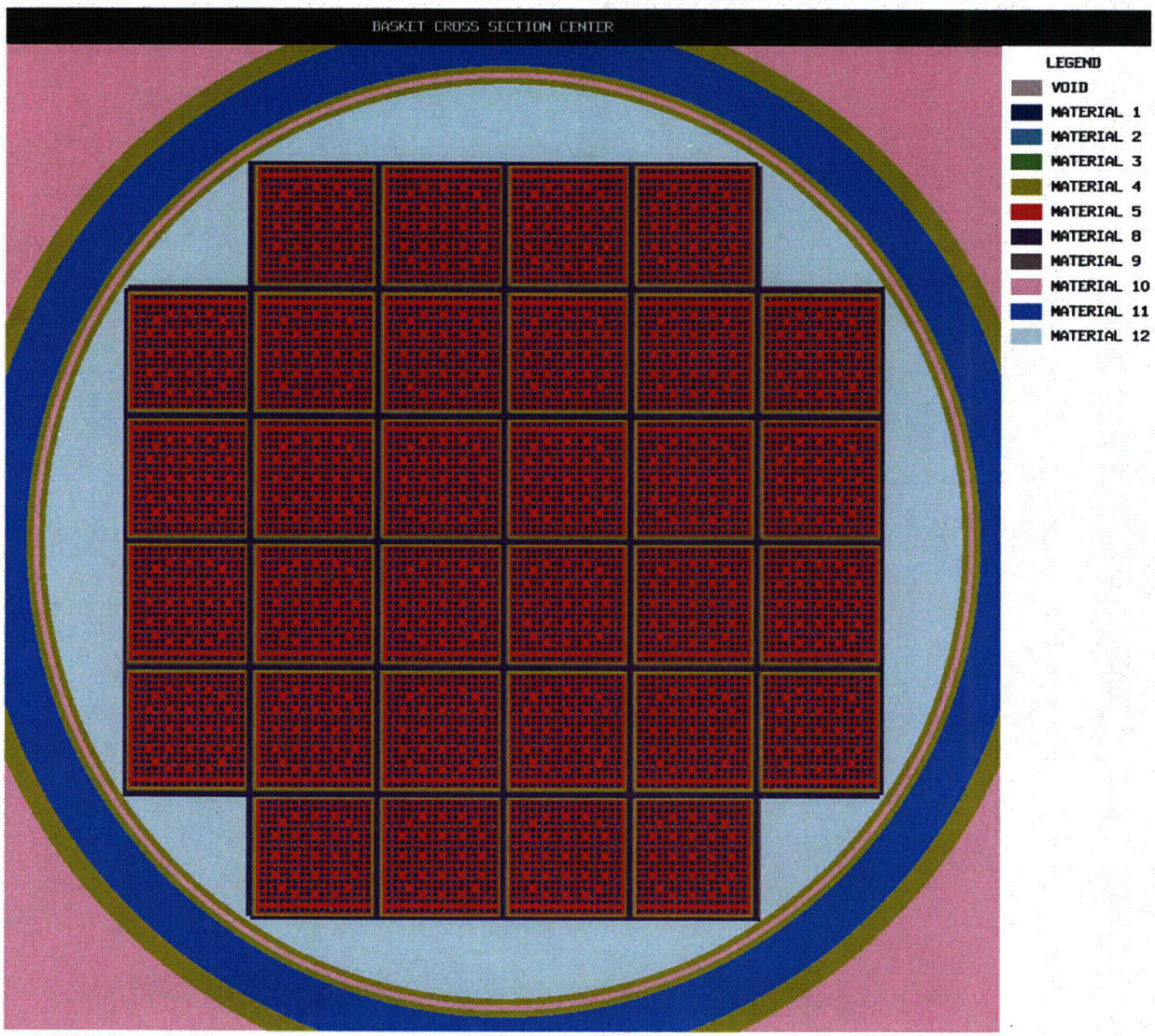

Figure 6-14
CE 14x14 Fuel Assembly : Optimum Pitch Study

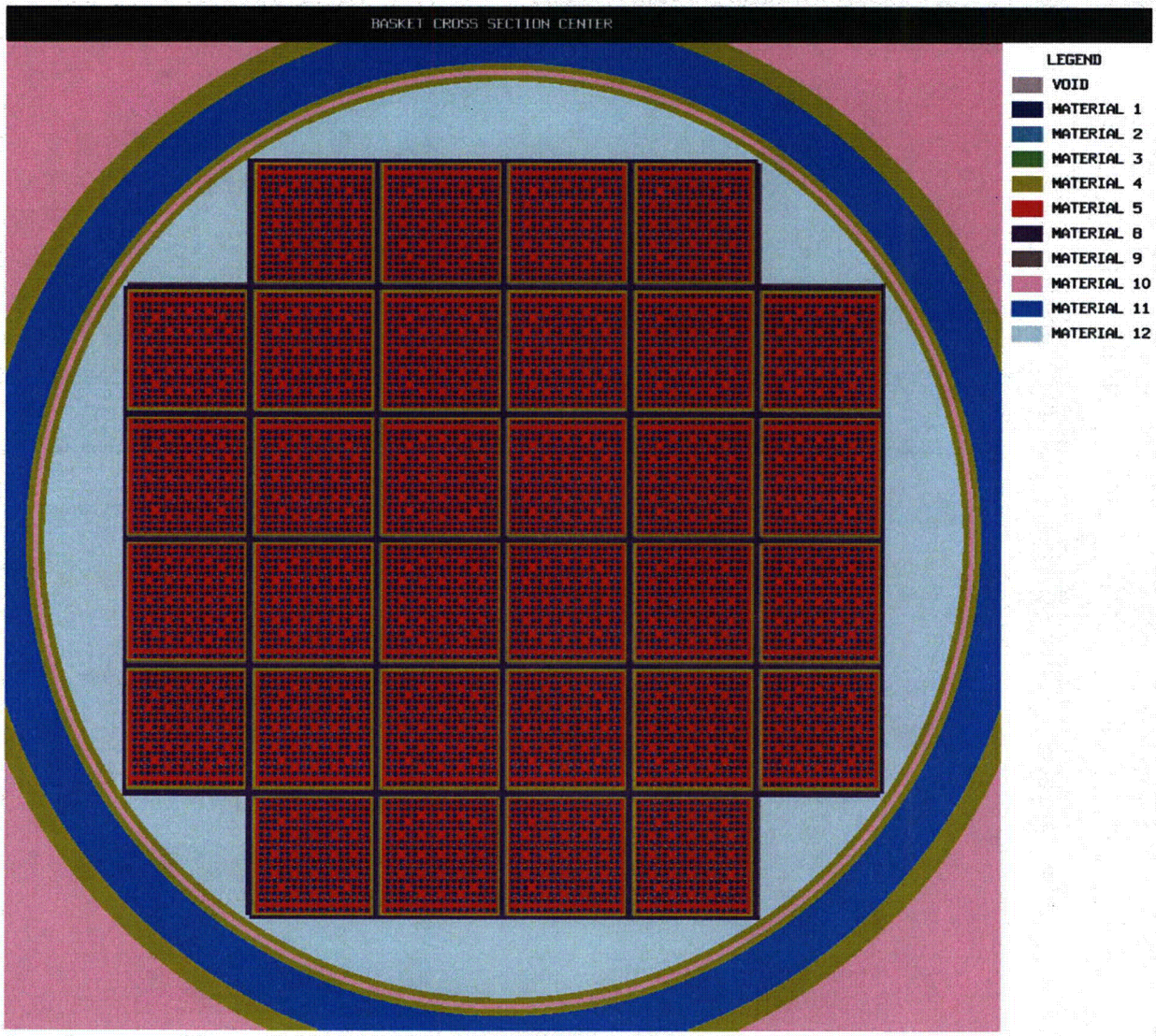

Figure 6-15
WE 17x17 Fuel Assembly : Single Ended Rod Shear Study

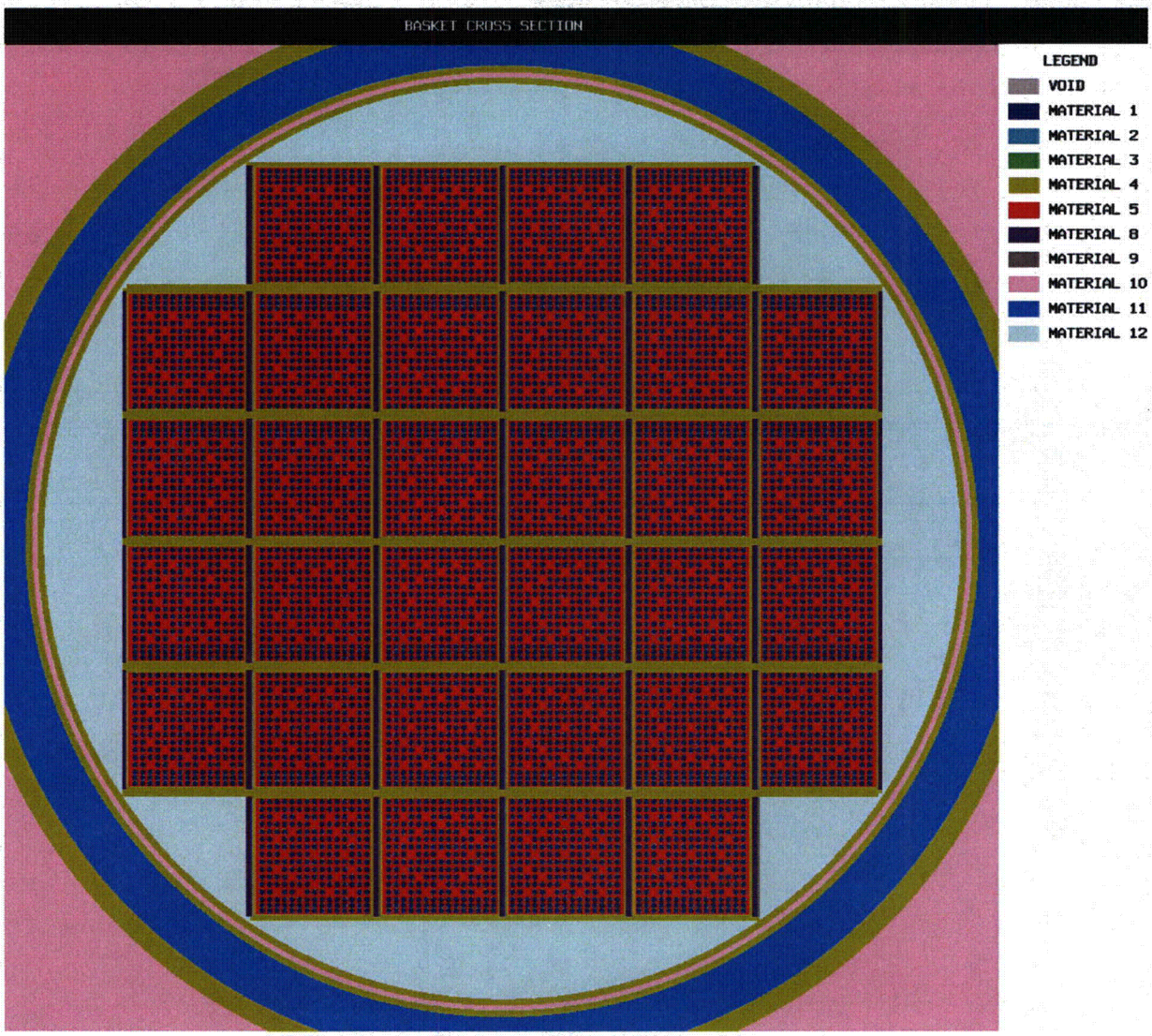

Figure 6-16
WE 15x15 Fuel Assembly : Double Ended Rod Shear Study

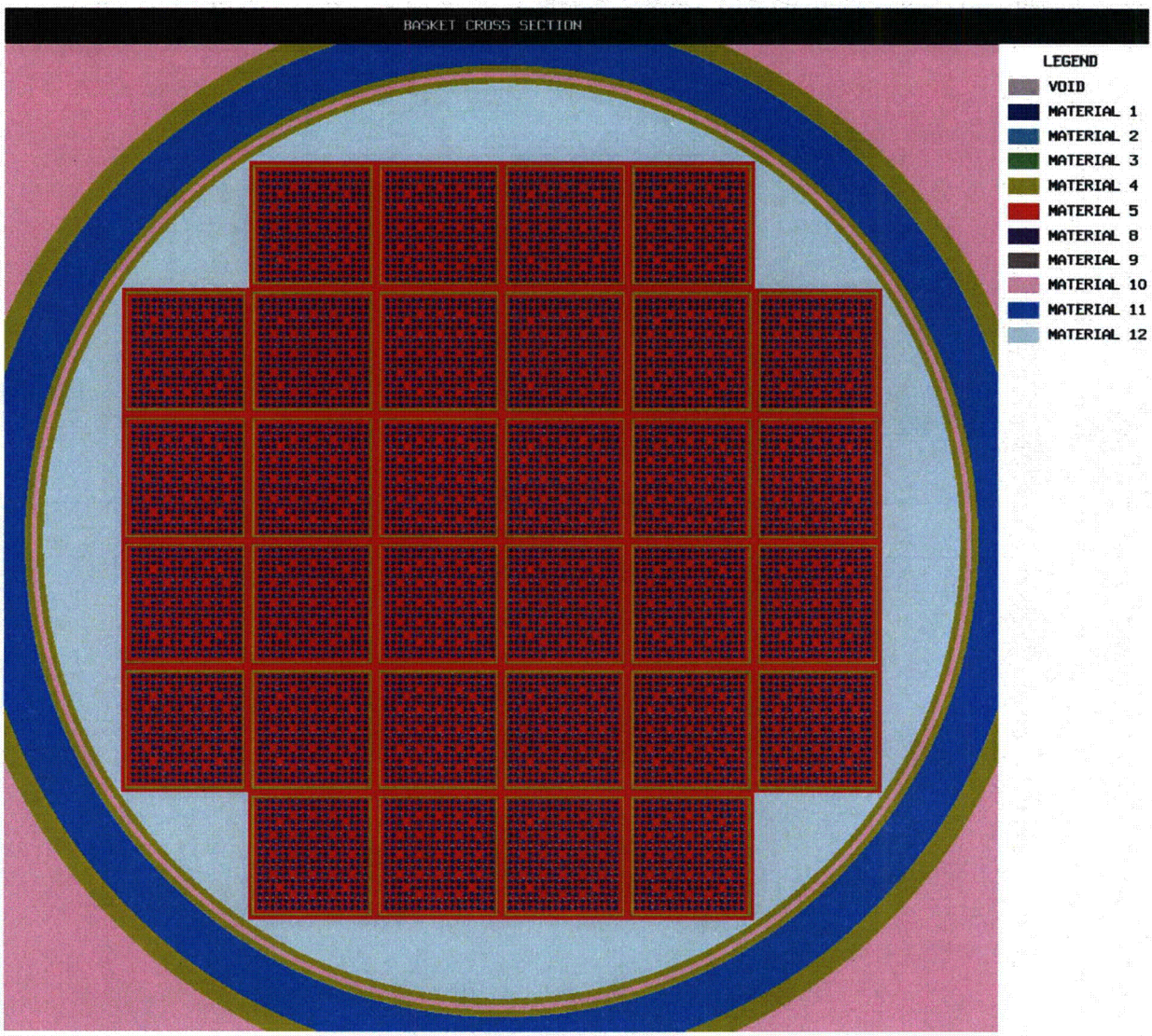

Figure 6-17
WE 17x17 Fuel Assembly : 4-inch Shift of Fuel Assembly

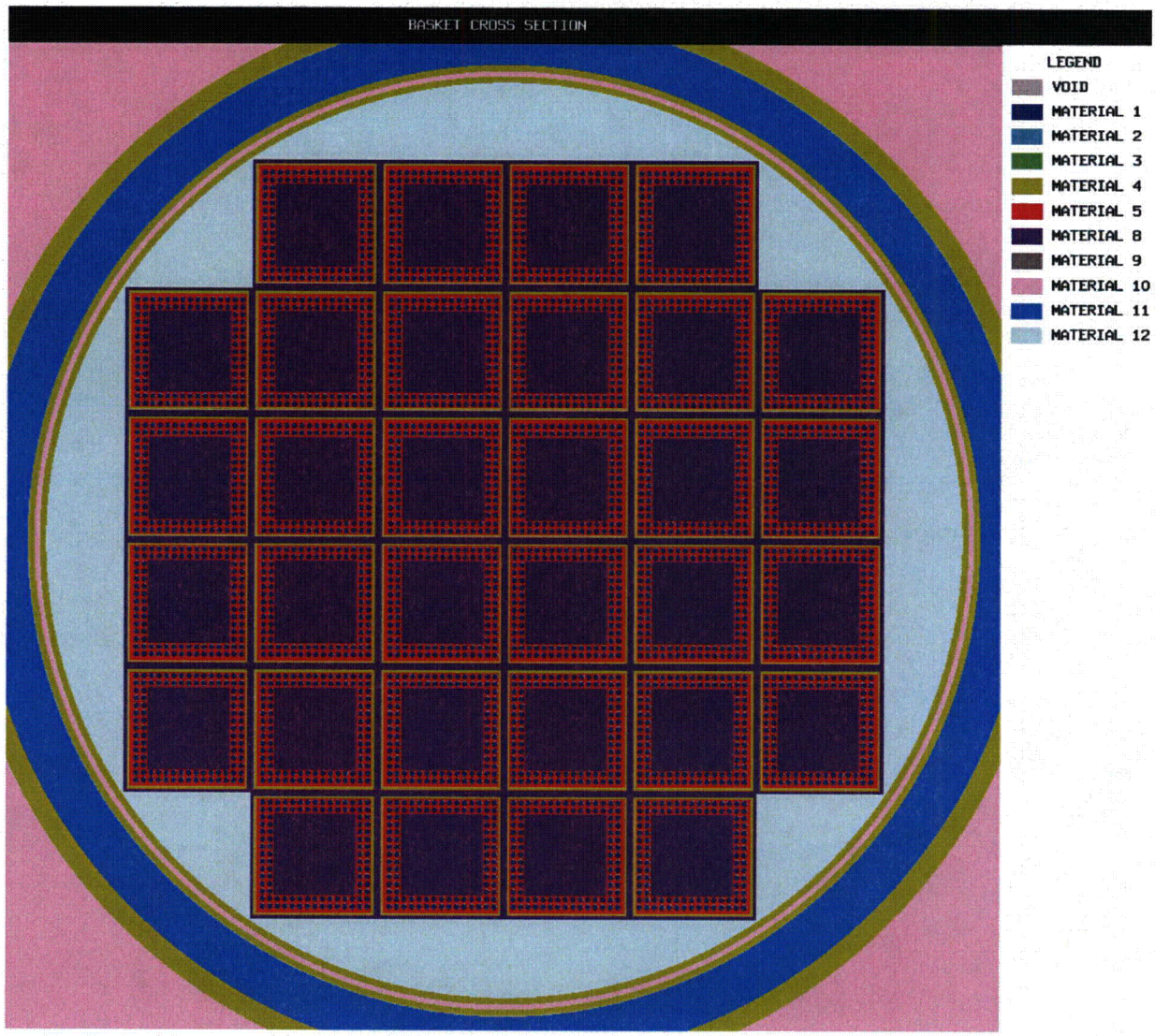

Figure 6-18
WE 15x15 Fuel Assembly : 6-inch Shift of Fuel Rods

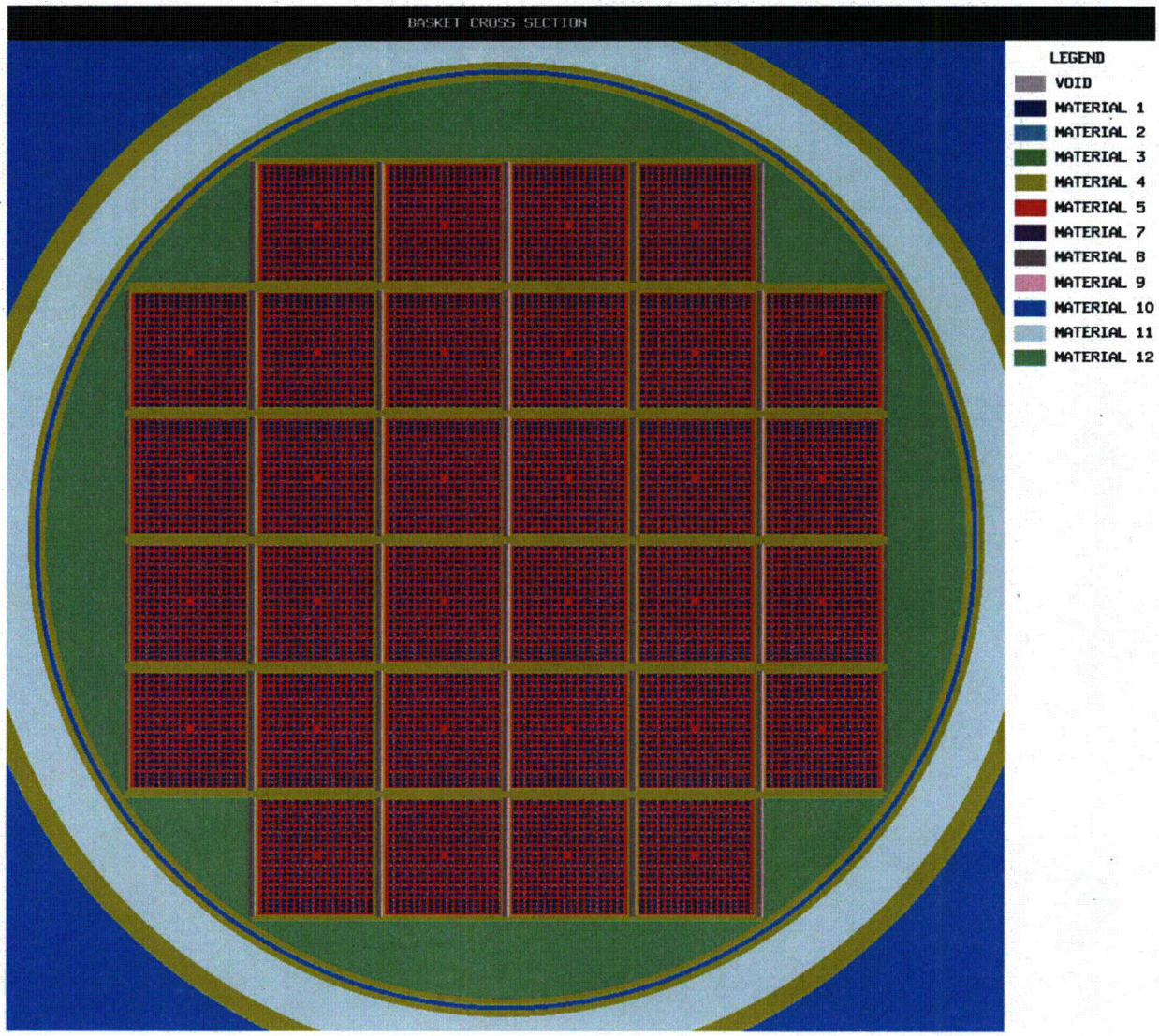

Figure 6-19
WE 15x15 Fuel Assembly : Double Ended Rod Shear with BPRAs

CHAPTER 7
CONFINEMENT

TABLE OF CONTENTS

7. CONFINEMENT 7-1

7.1 Confinement Boundary 7-1
7.1.1 Confinement Vessel 7-1
7.1.2 Confinement Penetrations 7-2
7.1.3 Seals and Welds 7-2
7.1.4 Closure 7-2

7.2 Requirements for Normal Conditions of Storage 7-3
7.2.1 Release of Radioactive Material 7-3
7.2.2 Pressurization of Confinement Vessel 7-3

7.3 Confinement Requirements for Hypothetical Accident Conditions 7-4
7.3.1 Fission Gas Products 7-4
7.3.2 Release of Contents 7-4

7.4 Supplemental Data 7-5
7.4.1 Confinement Monitoring Capability 7-5
7.4.2 References 7-5

LIST OF FIGURES

7-1 32PTH DSC Confinement Boundaries and Welds

7. CONFINEMENT

7.1 Confinement Boundary

The 32PTH DSC is a high integrity stainless steel welded vessel that provides confinement of radioactive materials encapsulates the fuel in a helium atmosphere and provides biological shielding during 32PTH DSC closure and transfer and storage operations. The 32PTH DSC is designed to maintain confinement of radioactive material within the limits of 10CFR 72.104(a), 10CFR 72.106(b) and 10CFR 20 under normal, off-normal, and credible accident conditions. Chapter 3 concludes that the design including the helium atmosphere within the 32PTH DSC will adequately protect the spent fuel cladding against degradation that might otherwise lead to gross ruptures during storage. The design ensures that fuel degradation during storage will not pose operational safety problems with respect to removal of the fuel from storage.

The DSC cylindrical shell, the inner top cover/shield plug[1], and shell bottom form the confinement boundary for the spent fuel. The vent and siphon covers and welds are also included in the confinement boundary. The outer top cover plate is a structural attachment to the confinement boundary. The dimensions and material descriptions for the confinement boundary assemblies and the redundantly welded barriers are discussed in Chapter 1. The components important to safety are identified in Chapter 2.

7.1.1 Confinement Vessel

The cylindrical shell and inner shell to bottom cover plate welds are made during fabrication of the 32PTH DSC and are fully compliant to ASME Section III, Subsection NB. The welds between the shell and inner top cover/shield plug[1] (including siphon and vent cover welds and option 2 or option 3 design welds shown in Figure 7-1) are made after fuel loading. These welds are designed, fabricated, inspected and tested using alternatives to the ASME code specified in SAR Section 3.10.

Stringent design and fabrication requirements ensure that the confinement function of the 32PTH DSC is maintained. The cylindrical shell and shell bottom are pressure tested in accordance with the ASME Code, Section III, Subarticle NB-6300. This pressure test is performed after installation of the shell bottom at the fabricator's facility and may be performed concurrently with the leak test, provided the requirements of NB-6300 are met.

Following the pressure test, a leak test of the shell assembly, including the shell bottom, is performed in accordance with ANSI N14.5 [2] and the ASME Code, Section V, Article 10. These tests are typically performed at the fabricator's facility. The acceptance criteria for the test are "leaktight" as defined in [2].

The process involved in leak testing the 32PTH DSC involves temporarily sealing the shell from the top end. The gas filled envelope and evacuated envelope testing methodologies have the

[1] For option 2 design (described in Chapter 1 drawings): Top casing plate, siphon/vent block, alignment pin block and lifting post are included in the confinement boundary
For option 3 design (described in Chapter 1 drawings): Top shield plug outer plate is included in the confinement boundary

required nominal test sensitivity for leaktight construction and are used for leak testing. A helium mass spectrometer is used to detect any leakage as defined in [2].

During final drying and sealing operations of the 32PTH DSC, the top closure confinement welds are applied to confine radioactive materials within the cavity.

The inner top cover/shield plug weld (including option 2 or option 3 inner top cover welds discussed in Figure 7-1) is welded to the DSC shell using automated welding equipment. Once the 32PTH DSC has been vacuum dried, a pressure test is performed by backfilling the DSC cavity with helium. Following a satisfactory completion of the pressure test, the siphon/vent covers are welded and a leak test is performed to verify that the weld between the DSC shell and the inner top cover/shield plug (including option 2 or option 3 design welds shown in Figure 7-1) and the siphon/vent cover welds meet the leak-tight criteria of [2]. The outer top cover plate is also welded in place using automated welding equipment. The outer top cover plate is a structural attachment to the confinement boundary.

7.1.2 Confinement Penetrations

All penetrations in the 32PTH DSC confinement boundary are welded closed. The 32PTH DSC is designed to have no credible leakage as described above.

7.1.3 Seals and Welds

The welds made during fabrication of the 32PTH DSC that affect the confinement boundary include the weld applied to the shell bottom and the circumferential and longitudinal seam welds applied to the cylindrical shell. These welds are inspected (radiographic or ultrasonic inspection, and liquid penetrant inspection) according to the requirements of Subsection NB of the ASME Code.

The welds applied to the vent and siphon port covers and the inner top cover/shield plug (including option 2 or option 3 inner cover) during closure operations, define the confinement boundary at the top end of the 32PTH DSC. These welds are applied using a multiple-layer technique with multi-level PT in accordance with alternatives to the ASME code as specified in SAR Section 3.10. This effectively eliminates any pinhole leak which might occur in a single-pass weld, since the chance of pinholes being in alignment on successive weld passes is negligibly small. Figure 7-1 provides a graphic representation of the confinement boundaries and welds.

7.1.4 Closure

The 32PTH DSC is closed entirely by welding and thus, no closure devices are utilized for confinement.

7.2 Requirements for Normal Conditions of Storage

The 32PTH DSC shell is designed to prevent the leakage of radioactive materials. No discernable undetected leakage is credible and the dose at the controlled area boundary from atmospheric release is negligible.

7.2.1 Release of Radioactive Material

Analyses for determining the annual dose equivalent to an individual located at the site boundary or outside the controlled area resulting from releases of radioactive material are not required in accordance with NRC Spent Fuel Project Office Interim Staff Guidance-5 (ISG-5) [3], since the 32PTH DSC is designed to have no credible leakage. Analyses required for determining the annual dose equivalent based on direct radiation for normal, off-normal, and accident conditions are discussed in Chapter 10.

7.2.2 Pressurization of Confinement Vessel

The design provides for drying and evacuation of the 32PTH DSC interior as part of the loading operations. The design is acceptable for the pressures that may be experienced during these operations as discussed in Chapter 4. On completion of fuel loading, the gas fill of the 32PTH DSC interior is at a pressure level that will maintain a non-reactive environment for at least the 40 year storage life of the 32PTH DSC interior under normal, off-normal, and accident conditions.

7.3 Confinement Requirements for Hypothetical Accident Conditions

7.3.1 Fission Gas Products

The 32PTH DSC confinement boundary is designed to prevent the leakage of radioactive materials. The analyses presented in Chapters 3 and 11 demonstrate that the confinement boundary is not compromised following hypothetical accident conditions. Therefore, estimating the maximum quantity of fission gas products is not necessary in accordance with ISG-5[3].

7.3.2 Release of Contents

The 32PTH DSC confinement boundary is designed to prevent the leakage of radioactive materials. The analyses presented in Chapters 3 and 11 demonstrate that the confinement boundary is not compromised following hypothetical accident conditions. End and corner drops are not considered credible events during storage and transfer. However, the DSC and transfer cask have been evaluated for these drops to support evaluations required for postulated events under 10CFR50 and 10CFR71. The cladding integrity must be demonstrated by the user for 10CFR50 postulated end drops and will be evaluated in the 10CFR71 transport safety analysis report for hypothetical accidents during transports. Therefore, confinement analyses for the release of radioactive materials are not necessary in accordance with ISG-5 [3].

7.4 Supplemental Data

7.4.1 Confinement Monitoring Capability

The NUHOMS® HD System is a self-contained passive system that does not produce routine, solid, liquid or gaseous effluents. Effluent processing systems, or monitoring for airborne or liquid radioactivity, are not required to protect personnel or the environment during storage conditions. Since the 32PTH DSC is closed entirely by welding, a closure monitoring system is not utilized in accordance with NRC ISG-5 [3].

7.4.2 References

1. American Society of Mechanical Engineers, Boiler & Pressure Vessel Code, Section III, 1998 Edition with Addenda through 2000.

2. American National Standards Institute, ANSI N14.5-1997, Leakage Tests on Packages for Shipment of Radioactive Materials.

3. NRC Spent Fuel Project Office, Interim Staff Guidance, ISG-5, Revision 1, Confinement Evaluation.

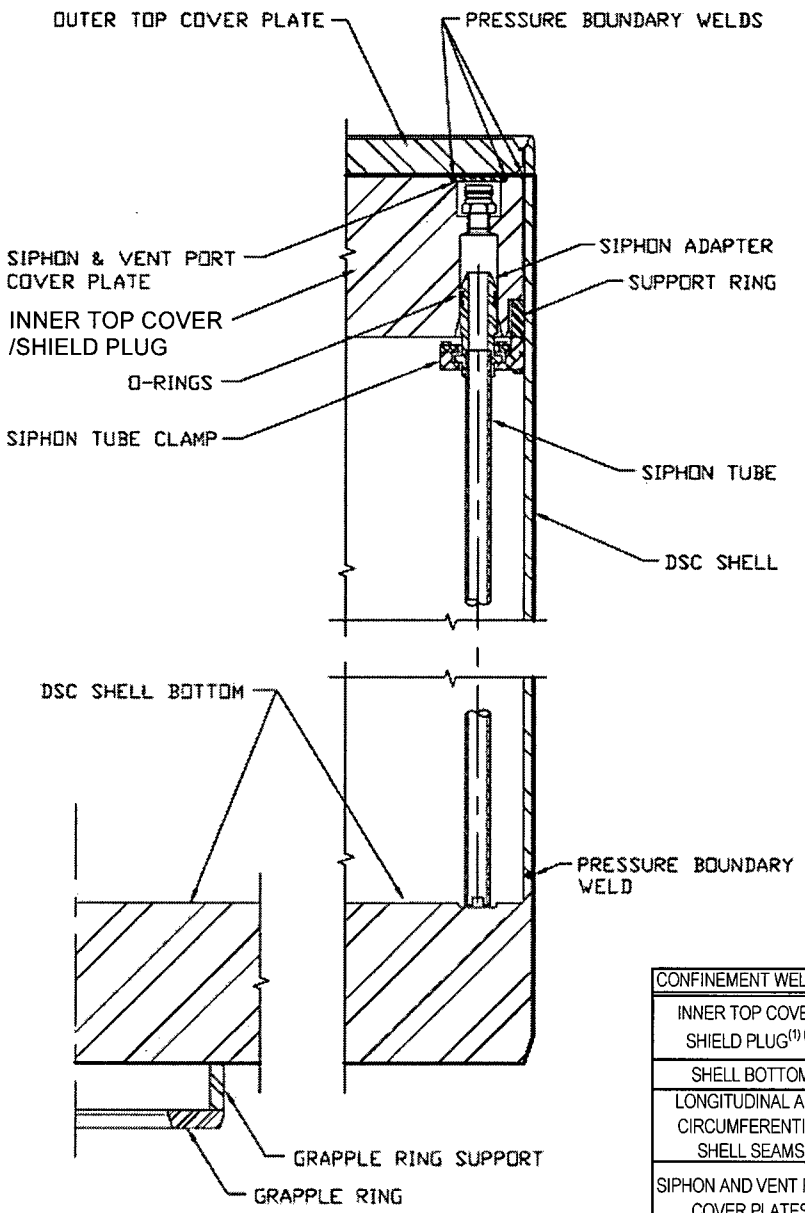

NDE REQUIREMENTS FOR CONFINEMENT BOUNDARY WELDS

CONFINEMENT WELD	NDE REQUIREMENTS	WELD TYPE
INNER TOP COVER/ SHIELD PLUG(1) (2)	MULTI-LEVEL PT	PARTIAL PENETRATION
SHELL BOTTOM	RT OR UT AND PT	FULL PENETRATION
LONGITUDINAL AND CIRCUMFERENTIAL SHELL SEAMS	RT AND PT	FULL PENETRATION
SIPHON AND VENT PORT COVER PLATES	MULTI-LEVEL PT	PARTIAL PENETRATION

(1) Includes shell to the top casing plate weld, shell to the siphon/vent block weld, and shell to the alignment pin block weld for option 2 design described in Chapter 1 drawings

(2) Includes shell to the top shield plug outer plate weld for option 3 design described in Chapter 1 drawings

Figure 7-1
32PTH DSC Confinement Boundaries and Welds

CHAPTER 8
OPERATION PROCEDURES

TABLE OF CONTENTS

8.0 OPERATING PROCEDURES 8-1

8.1 Procedures for Loading the DSC and Transfer to the HSM-H 8-1
8.1.1 Narrative Description 8-1

8.2 Procedures for Unloading the DSC 8-10
8.2.1 DSC Retrieval from the HSM-H 8-10
8.2.2 Removal of Fuel from the DSC 8-11

8.3 Supplemental Information 8-14
8.3.1 Other Operating Systems 8-14
8.3.2 Operation Support System 8-14
8.3.3 Surveillance and Maintenance 8-14

8.4 References 8-15

LIST OF TABLES

8-1 Major Equipment Used During NUHOMS® HD System Loading and Unloading Operations

LIST OF FIGURES

8-1 NUHOMS® HD System Loading Operations

8.0 OPERATING PROCEDURES

This chapter outlines a sequence of operations to be incorporated into procedures for preparation of the NUHOMS® HD System DSC, loading of fuel, closure of the DSC, transport to the ISFSI, transfer into the HSM-H, monitoring operations, and retrieval and unloading. Operations are presented in their anticipated approximate performance sequence. Alternate sequencing that achieves the same purpose is acceptable. Temporary shielding may be used throughout as appropriate to maintain doses as low as reasonably achievable (ALARA). Use nitrogen or helium to assist in removal of water. After water is drained from the DSC, (sections 8.1.1.2 & 8.1.1.3), the DSC shall be backfilled with nitrogen or helium.

8.1 Procedures for Loading the DSC and Transfer to the HSM-H

8.1.1 Narrative Description

The following steps describe the recommended generic operating procedures for the NUHOMS® System. A list of major equipment used during loading and unloading operations is provided in Table 8-1. A pictorial representation of key phases of this process is provided in Figure 8-1.

8.1.1.1 Transfer Cask and DSC Preparation

1. Verify by plant records or other means that candidate fuel assemblies meet the physical, thermal and radiological criteria specified in the Technical Specifications.
2. Clean or decontaminate the transfer cask as necessary to meet licensee pool and ALARA requirements, and to minimize transfer of contamination from the cask cavity to the DSC exterior.
3. Examine the transfer cask cavity for any physical damage.
4. Verify specified lubrication of the transfer cask rails.
5. Examine the DSC for any physical damage and for cleanliness. Verify that bottom fuel spacers or damaged fuel bottom end caps, if required, are present in all fuel compartments. Remove damaged fuel top end caps if they are in place. Record the DSC serial number which is located on the grappling ring. Verify the basket type by identifying the last character in the serial number.
6. Install lifting rods and eyes into the four threaded sockets in the bottom of the DSC cavity. Verify specified thread engagement.
7. Lift the DSC into the cask cavity and rotate the DSC to match the transfer cask alignment marks.
8. Remove the lifting rods and eyes.
9. Fill the transfer cask/DSC annulus with clean water.
10. Seal the top of the annulus, using for example an inflatable seal.
11. A tank filled with clean water, and kept above the pool surface may be connected to the top vent port of the transfer cask via a hose to provide a

positive pressure in the annulus. This is an optional arrangement, which provides additional assurance that contaminated water from the fuel pool will not enter the annulus. Do not pressurize this tank, nor raise it sufficiently high to float the DSC. For the 32PTH DSC with a 69.75 inch OD, and an empty weight of 49,000 lb, a differential pressure of 12.8 psi, equivalent to 29.6 ft of pure water, would be sufficient to lift the DSC.

12. If the DSC top covers were trial fitted, they must be removed prior to filling the DSC with water. The vent port quick connect fitting in the inner top cover may be removed to facilitate hydrogen monitoring later. The drain port fitting may be either left in place or removed – water may be pumped from the DSC either with or without the fitting.

13. Fill the DSC with water from the fuel pool or an equivalent source meeting the minimum boron concentration required by the Technical Specifications. Optionally, this may be done at the time of immersing the cask in the pool. If the pool water is allowed flow over the transfer cask lip and into the DSC, provision must be made to protect the annulus seal from being dislodged by the water running over it.

14a. Optionally, secure a sheet of suitable material to the bottom of the cask to minimize the potential for ground-in contamination. This step may be done at any convenient time prior to immersion.

14b. Drain or fill the transfer cask liquid neutron shield, as required by licensee ALARA requirements and crane weight limits. This step may be done at any convenient time prior to immersion.

15. Prior to the cask being lifted into the fuel pool, the water level in the pool should be adjusted as necessary to accommodate the transfer cask and DSC volume. If the water placed in the DSC cavity was obtained from the fuel pool, a level adjustment may not be necessary.

8.1.1.2 DSC Fuel Loading

1. Verify proper engagement of the lifting yoke with the transfer cask lifting trunnions.

2. Lift the transfer cask / DSC and position them over the cask loading area of the spent fuel pool.

3. Lower the cask into the fuel pool until the bottom of the cask is at the height of the fuel pool surface. As the cask is lowered into the pool, spray the exterior surface of the cask with clean water to minimize surface adhesion of contamination.

4. Place the cask in the location of the fuel pool designated as the cask loading area.

5. Disengage the lifting yoke from the transfer cask lifting trunnions and move the yoke clear of the cask. Spray the lifting yoke with clean water if it is raised out of the fuel pool.

6. Load pre-selected spent fuel assemblies into the DSC basket compartments. The licensee shall develop procedures to verify that the boron content of the water conforms to the Technical Specifications, and that fuel identifications are verified and documented. Damaged fuel must be loaded only in designated compartments fitted with a damaged fuel bottom end cap.

7. After all the fuel assemblies have been placed into the DSC and their identities verified, install damaged fuel top end caps into designated compartments containing damaged fuel.

8. Lower the inner top cover/shield plug[1] in the DSC, aligning it with the guide on the DSC wall, and engaging the drain tube, until it seats on its support ring.

9. Visually verify that the inner top cover/shield plug is properly seated in the DSC. Reseat if necessary.

10. Position the lifting yoke and verify that it is properly engaged with the transfer cask trunnions.

11. Lift the transfer cask to the pool surface and spray the exposed portion of the cask with clean water.

12. Drain any water from above the inner top cover/shield plug back to the spent fuel pool. Up to 1300 gallons of water may be removed from the DSC prior to lifting the transfer cask clear of the pool surface. Up to 15 psig of nitrogen or helium may be used to assist the removal of water. The DSC shall be backfilled with nitrogen or helium after drainage of bulk water.

13. Lift the cask from the fuel pool, continuing to spray the cask with clean water.

14. Move the cask with loaded DSC to the area designated for DSC draining and closure operations. The set-down area should be level or slightly sloped toward the DSC drain tube.

8.1.1.3 DSC Closing, Drying, and Backfilling

1. Fill the transfer cask liquid neutron shield if it was drained for weight reduction during preceding operations.

2. Decontaminate the transfer cask exterior.

3. Disengage the rigging from the inner top cover/shield plug, and remove the eyebolts. Disengage the lifting yoke from the trunnions.

[1] Including option 2 or option 3 inner top cover as described in Chapter 1 drawings.

4. Disconnect the annulus overpressure tank if one was used, decontaminate the exposed surfaces of the DSC shell perimeter, remove any remaining water from the top of the annulus seal, and remove the seal.

5. Open the cask cavity drain port and allow water from the annulus to drain out until the water level is approximately twelve inches below the top of the DSC shell. Take swipes around the outer surface of the DSC shell to verify conformance with Technical Specification limits.

6. Cover the transfer cask / DSC annulus to prevent debris and weld splatter from entering the annulus.

7. If water was not drained from the DSC earlier, connect a pump to the DSC drain port and remove up to 1300 gallons of water. Use nitrogen or helium to assist the removal of water. This lowers the water sufficiently to allow welding of the inner top cover/shield plug, while keeping about half of the water in the DSC to cool the spent fuel (Pay special attention to step 14 below). Up to 15 psig of nitrogen, or helium gas may be applied at the vent port to assist the water pump down.

   CAUTION: Radiation dose rates are expected to be high at the vent and siphon port locations. Use proper ALARA practices (e.g., use of temporary shielding, appropriate positioning of personnel, etc.) to minimize personnel exposure.

8. Install the automated welding machine onto the inner top cover/shield plug.

9. Continuous hydrogen monitoring during the welding of the inner top cover/shield plug is required [1]. Insert a hydrogen monitor intake line through the vent port such that it terminates just below the inner top cover/shield plug. Temperature monitoring of the TC cavity/annulus water is also required, see step 14.

10. Verify that the hydrogen concentration does not exceed 2.4% [1]. If this limit is exceeded, stop all welding operations and purge the DSC cavity with helium (or other inert gas) via the vent port to reduce hydrogen concentration safely below the 2.4% limit.

11. Complete the inner top cover/shield plug welding and perform the non-destructive examinations as required by the Technical Specifications. The weld must be made in at least two layers.

12. Remove the automated welding machine.

13. Pump remaining water from the DSC. Remove as much free standing water as possible to shorten vacuum drying time. Up to 15 psig of nitrogen, or helium gas may be applied at the vent port to assist the water pump down.

14. There are three methods described in Chapter 4 to assure that the fuel temperature limit is not exceeded during vacuum drying. Each method is associated with a time limit for vacuum drying, starting from the time that pumping of liquid water from the DSC is complete as required by the Technical Specifications for vacuum drying. As required by the technique chosen, either

    a) install annulus water circulation equipment, or

    b) drain annulus water if temperature exceeds 180°F

    c) for either a or b, the DSC may be evacuated to 100 mbar or lower, and backfilled with helium to atmospheric pressure prior to start of vacuum drying.

    All helium used in backfilling operations shall be at least 99.99% pure (this may be done as part of step 15).

    NOTE: Proceed cautiously when evacuating the dry shielded canister (DSC) to avoid freezing consequences.

15. Connect a vacuum pump / helium backfill manifold to the vent port or to both the vent and drain ports. The quick connect fittings may be removed and replaced with stainless steel pipe nipple / vacuum hose adapters to improve vacuum conductance. Make provision to prevent icing, for example by avoiding traps (low sections) in the vacuum line. Provide appropriate measures as required to control any airborne radionuclides in the vacuum pump exhaust. Purge air from the helium backfill manifold.

    Optionally, leak test the manifold and the connections to the DSC. The DSC may be pressurized to no more than 15 psig for leak testing.

    CAUTION: Radiation dose rates are expected to be high at the vent and siphon port locations. Use proper ALARA practices (e.g., use of temporary shielding, appropriate positioning of personnel, etc.) to minimize personnel exposure.

16. Evacuate the DSC to the pressure required by the Technical Specification for vacuum drying, and isolate the vacuum pump. The isolation valve should be as near to the DSC as possible, with a pressure gauge on the DSC side of the valve.

17. Maintain the water condition in the transfer cask / DSC annulus as required by the technique chosen (step 14).

18. If the Technical Specification is satisfied, i.e., if the pressure remains below the specified limit for the required duration with the pump isolated, continue to the next step. If not, repeat steps 16 and 17.

19a. Purge air from the backfill manifold, open the isolation valve, and backfill the DSC cavity with helium to 16.5 to 18 psig and hold for 10 minutes.

19b. Reduce the DSC cavity pressure to atmospheric pressure, or slightly over.

20. If the quick connect fittings were removed for vacuum drying, remove the vacuum line adapters from the ports, and re-install the quick connect fittings using suitable pipe thread sealant.

CAUTION: Radiation dose rates are expected to be high at the vent and siphon port locations. Use proper ALARA practices (e.g., use of temporary shielding, appropriate positioning of personnel, etc.) to minimize personnel exposure.

21. Evacuate the DSC through the vent port quick connect fitting to a pressure 100 mbar or less.

22. Backfill the DSC with helium to the pressure specified in the Technical Specifications, and disconnect the vacuum / backfill manifold from the DSC.

23. Repeat steps 21 and 22 if the DSC interior is exposed to nitrogen during any succeeding operations.

24a. Weld the covers over the vent and drain ports, performing non-destructive examination as required by the Technical Specifications. The welds shall have at least two layers.

24b. Install a temporary test head fixture (or any other alternative means). Perform a leak test of the inner top cover/shield plug to the DSC shell welds and siphon/vent cover welds in accordance with the Technical Specification limits. Verify that the personnel performing the leak test are qualified in accordance with SNT-TC-1A.

25. Install the automated welding machine onto the outer top cover plate and place the outer top cover plate with the welding system onto the DSC. Verify correct rotational alignment of the cover and the DSC shell.

26. Complete the outer top cover welding and perform the non-destructive examinations as required by the Technical Specifications. The weld must be made in at least two layers.

27. Remove everything except the DSC from the transfer cask cavity: welding machine, protective covering from the transfer cask / DSC annulus, annulus temperature monitoring or water circulation equipment, temporary shielding, etc.

28. Install the transfer cask lid and bolt it.

29. Evacuate the transfer cask cavity to below 100 mbar, and backfill the transfer cask annulus with helium in accordance with the Technical Specifications pressure tolerance and time limit.

8.1.1.4 Transfer Cask Downending and Transport to ISFSI

1. Drain or fill the transfer cask liquid neutron shield, as required by licensee ALARA requirements and crane weight limits.

2. The transfer trailer should be positioned so that the cask support skid is accessible to the crane with the trailer supported on its vertical jacks. If required due to space limitations, the crane may remain in a stationary position while the cask support skid and trailer translate underneath the cask as it is downended, (the trailer cannot be supported on the vertical jacks.)

3. Engage the lifting yoke and lift the transfer cask over the cask support skid onto the transfer trailer.

4. Position the cask lower trunnions onto the transfer trailer support skid pillow blocks.

5. Move the crane while simultaneously lowering the cask until the cask upper trunnions are just above the support skid upper trunnion pillow blocks. Alternatively, if the crane is to remain stationary as identified above, slowly move the trailer and support skid as the cask is lowered until the upper trunnions are just above the support skid upper trunnion pillow blocks.

6. Verify that the cask and trunnion pillow blocks are properly aligned.

7. Lower the cask onto the skid until the weight of the cask is distributed to the trunnion pillow blocks.

8. Verify the trunnions are properly seated onto the skid and install the trunnion tower closure plates. Refill the cask liquid neutron shield, if it was drained in step 1 above.

8.1.1.5 DSC Transfer to the HSM-H

1. The maximum lifting height and ambient temperature requirements of the Technical Specifications must be met during transfer from the fuel building to the HSM-H.

2. Prior to loading the DSC into the HSM-H, verify that there is no debris in the HSM-H, the air inlet and outlets are not blocked, the air inlet and outlet screens are not damaged, and the rails are lubricated as specified.

3. Tow the transfer trailer with the loaded cask to the ISFSI.

4. Position the transfer trailer to within a few feet of the HSM-H to maintain doses ALARA when the cask lid is removed.

5. Verify that the centerline of the HSM-H and cask approximately coincide. Reposition the trailer as necessary following appropriate ALARA practices.

6. Using a portable crane, unbolt and remove the cask lid.

7. Back the trailer to within a few inches of the HSM-H, set the trailer brakes and disengage the tractor. Drive the tractor clear of the trailer and extend the transfer trailer vertical jacks.

8. Remove the skid tie-down bracket fasteners and use the hydraulic skid positioning system to bring the cask into approximate vertical and horizontal alignment with the HSM-H. Using optical survey equipment and the alignment marks on the cask and the HSM-H, adjust the position of the cask until it is aligned with the HSM-H.

9. Using the skid positioning system, fully insert the cask into the HSM-H access opening docking collar.

10. Secure the cask to the front wall embedments of the HSM-H using the cask restraints.

11. Verify the alignment of the transfer cask is within specified tolerance using the optical survey equipment.

12. Remove the bottom ram access cover plate from the transfer cask. Extend the ram through the bottom cask opening into the DSC grapple ring.

13. Activate the hydraulic cylinder on the ram grapple and engage the grapple arms with the grapple ring.

14. Activate the hydraulic ram to initiate insertion of the DSC into the HSM-H. Stop the ram when the DSC reaches the support rail stops at the back of the module.

15. Disengage the ram grapple mechanism so that the grapple is retracted away from the grapple ring.

16. Retract and disengage the hydraulic ram system from the cask and move it clear of the cask. Remove the cask restraints from the HSM-H. Replace the bottom ram access cover plate.

17. Using the skid positioning system, disengage the cask from the HSM-H access opening.

18. Install the DSC seismic restraint.

19. Install the HSM-H door and secure it in place.

20. Replace the transfer cask lid. Secure the skid to the trailer, retract the vertical jacks.

21. Tow the trailer and cask from the ISFSI.

22. Adjust the seismic restraint on the DSC one week following initial placement.

8.1.1.6 Monitoring Operations

1. Perform routine security surveillance in accordance with the licensee's ISFSI security plan.

2. Perform a daily visual surveillance of the HSM-H air inlets and outlets (bird screens) to verify that no debris is obstructing the HSM-H vents in accordance with Technical Specification requirements.

3. Perform a temperature measurement for each HSM-H in accordance with Technical Specification requirements.

8.2 Procedures for Unloading the DSC

The following section outlines the procedures for retrieving the DSC from the HSM-H and for removing the fuel assemblies from the DSC.

8.2.1 DSC Retrieval from the HSM-H

1. The maximum lifting height and ambient temperature requirements of the Technical Specifications must be met during transfer from the HSM-H to the fuel building.

2. Ready the transfer cask, transfer trailer, and support skid for service and tow the trailer to the HSM-H. Fill the transfer cask liquid neutron shield and remove the bottom access plate from the transfer cask.

3. Remove HSM-H door and seismic restraint. Remove the transfer cask lid. Back the trailer to within a few inches of the HSM-H.

4. Using the skid positioning system align the transfer cask with the HSM-H and position the skid until the transfer cask is docked with the HSM-H access opening.

5. Using optical survey equipment verify alignment of the transfer cask with respect to the HSM-H within specified tolerance. Install the transfer cask restraints.

6. Install and align the hydraulic ram with the transfer cask.

7. Extend the ram through the transfer cask into the HSM-H until it is inserted in the DSC grapple ring.

8. Activate the arms on the ram grapple mechanism to engage the grapple ring.

9. Retract the ram and pull the DSC into the transfer cask.

10. Retract the ram grapple arms.

11. Disengage the ram from the transfer cask.

12. Replace the cask ram access cover plate and remove the transfer cask restraints.

13. Using the skid positioning system, disengage the transfer cask from the HSM-H.

14a. Install the transfer cask top cover plate and ready the trailer for transfer/transport.

14b. Evacuate the transfer cask cavity to below 100 mbar, and backfill with helium in accordance with the Technical Specifications pressure tolerance and time limit, if using a transfer cask. If using a transportation cask, follow applicable requirements for the transportation cask.

15. Replace the door and seismic restraint on the HSM-H.

8.2.2 Removal of Fuel from the DSC

If it is necessary to remove fuel from the DSC, it can be removed in dry transfer facility or the initial fuel loading sequence can be reversed and the plant's spent fuel pool utilized.

Procedures for wet unloading of the DSC are presented here. Dry unloading procedures are essentially identical up to the removal of the DSC vent and drain port covers.

1. Tow the trailer with the loaded cask to the cask handling area inside the plant's fuel handling building. Drain the transfer cask liquid neutron shield as required by licensee ALARA requirements and crane weight limits.

2. Position and ready the trailer for access by the crane.

3. Engage the lifting yoke with the trunnions of the transfer cask.

4. Verify that the yoke lifting hooks are properly aligned and engaged onto the transfer cask trunnions.

5. Lift the transfer cask approximately one inch off the trunnion supports. Verify that the yoke lifting hooks are properly positioned on the trunnions.

6. Move the crane in a horizontal motion while simultaneously raising the crane hook vertically and lift the transfer cask off the trailer. Move the transfer cask to the cask decontamination area.

7. Lower the transfer cask into the cask staging area in the vertical position.

8. Unbolt the transfer cask lid and remove it.

9. Install temporary shielding to reduce personnel exposure as required. Fill the transfer cask/DSC annulus with clean water and seal the top of the annulus, using, for example, an inflatable seal.

10. Locate the drain and vent port using the indications on the outer top cover plate. Place a portable drill press on the top of the DSC. Align the drill over the drain port.

11. Cut or drill a hole through the top cover plate to expose the drain port on the inner top cover. Remove the drain port cover plate with an annular hole cutter. Repeat for the vent port.

CAUTION: Radiation dose rates are expected to be high at the vent and siphon port locations. Use proper ALARA practices (e.g., use of temporary shielding, appropriate positioning of personnel, etc.) to minimize personnel exposure.

12. Obtain a sample of the DSC atmosphere. Confirm acceptable hydrogen concentration and check for presence of fission gas indicative of degraded fuel cladding.

13. If degraded fuel is suspected, additional measures appropriate for the specific conditions are to be planned, reviewed, and implemented to minimize exposures to workers and radiological releases to the environment.

14. Verify that the boron content of the fill water conforms to the Technical Specifications. Fill the DSC with water from the fuel pool or equivalent source through the drain port with the vent port open. The vented cavity gas may include steam, water, and radioactive material, and should be routed accordingly. Monitor the vent pressure and regulate the water fill rate to ensure that the pressure does not exceed 15 psig.

15. Provide for continuous hydrogen monitoring of the DSC cavity atmosphere during all subsequent cutting operations to ensure that hydrogen concentration does not exceed 2.4%. Purge with helium (or any other inert gas) as necessary to maintain the hydrogen concentration below this limit.

16. Provide suitable protection for the transfer cask during cutting operations. To prevent damage to the transfer cask during cutting, up to 8 inches at the top of the canister may be raised clear of the cask by removing the ram access port from the cask, and setting the cask down over a pedestal which fits inside the DSC grapple ring, lifting the DSC.

17. Using plasma arc-gouging, a mechanical cutting system, or other suitable means, remove the weld of the outer top cover plate to the DSC shell.

18. Remove the outer top cover plate.

19. Remove the weld of the inner top cover/shield plug to the shell in the same manner as the outer cover plate. Do not remove the inner top cover/shield plug at this time unless the removal is being done remotely in a dry transfer system.

20. Remove any remaining excess material on the inside shell surface by grinding.

21. Clean the transfer cask surface of dirt and any debris which may be on the transfer cask surface as a result of the weld removal operation.

22. Engage the yoke onto the trunnions, install eyebolts or other lifting attachment(s) into the inner top cover/shield plug, and connect the rigging cables to the eyebolts/lifting attachment(s).

23. Verify that the lifting hooks of the yoke are properly positioned on the trunnions.

24. Lift the transfer cask just far enough to allow the weight of the transfer cask to be distributed onto the yoke lifting hooks. Verify that the lifting hooks are properly positioned on the trunnions.

25. Optionally install suitable protective material onto the bottom of the transfer cask to minimize cask contamination. Move the transfer cask to the spent fuel pool.

26. Prior to lowering the transfer cask into the pool, adjust the pool water level, if necessary, to accommodate the volume of water which will be displaced by the transfer cask during the operation.

27. Position the transfer cask over the cask loading area in the spent fuel pool.

28. Lower the transfer cask into the pool. As the transfer cask is being lowered, the exterior surface of the transfer cask should be sprayed with clean water.

29. Disengage the lifting yoke from the transfer cask and lift the inner top cover/shield plug from the DSC.

30. Remove any failed fuel top end caps.

31. Remove the fuel from the DSC.

8.3 Supplemental Information

8.3.1 Other Operating Systems

The NUHOMS® System is a passive storage system and requires no operating systems other than those systems used in transferring the DSC to and from the HSM-H.

8.3.2 Operation Support System

The NUHOMS® System is a self contained passive system and requires no effluent processing systems during storage conditions.

8.3.3 Surveillance and Maintenance

Surveillance and maintenance requirements are discussed in Chapters 9 and 12. The only required surveillances during storage are monitoring of the HSM-H air exhaust temperature, and visual verification that the inlet and outlet vents are not blocked. There is no normally required maintenance of the HSM-H or DSC.

8.4 References

1. U.S. Nuclear Regulatory Commission, Office of the Nuclear Material Safety and Safeguards, "Safety Evaluation of VECTRA Technologies' Response to Nuclear Regulatory Commission Bulletin 96-04 for NUHOMS®-24P and NUHOMS®-7P Dry Spent Fuel Storage System," November 1997 (Dockets 72-1004, 72-3, 72-4, 72-8, and 72-14).

2. NUREG-0612 , "Control of Heavy Loads at Nuclear Power Plants," USNRC, July 1980.

Table 8-1
Major Equipment Used During NUHOMS® HD System Loading and Unloading Operations

NUHOMS® HD System	Function
Dry Shielded Canister (DSC)	Fuel confinement.
Horizontal Storage Module (HSM-H)	Shielding, physical protection
Transfer Cask	Handling and transport of loaded DSC
Transfer trailer with support frame, ram, alignment system, and hydraulic power pack, pressure gauges and pressure relief	Transport of loaded transfer cask, and transfer of DSC into or retrieval from HSM-H; monitor and limit force applied to DSC by ram

Other Equipment and Instruments	Function
Lift yoke	Lifting transfer cask empty or loaded, in conformance to NUREG-0612 [2]
Lifting eyes, slings, rigging, etc.	Lifting the empty DSC, DSC covers, and the transfer cask lid in conformance to NUREG-0612 [2]
Water pump, hoses, connectors, fittings	Draining the DSC
Transfer cask / DSC annulus seal	Contamination control of the DSC exterior by pool water
Small water tank and hose	Maintaining positive pressure in annulus
Vacuum pump / helium backfill manifold, valves, hoses, fittings, adapters, pressure and vacuum gauges, etc.	Pressure test, vacuum drying and backfill of DSC; helium backfill of transfer cask cavity
Helium leak test equipment, including test head	Leak test closure welds
Gas bottles (nitrogen and/or helium)	Pressurize canister cavity for blowdown pressure test, helium backfill, etc.
Tractor	Towing the transfer trailer
Mobile crane and rigging	Removal of HSM-H door and transfer cask lid at ISFSI
Scaffolding, manlifts, etc	As required for easy access during operations
Temporary shielding	As required to maintain doses ALARA
Automatic welder	Remote welding of inner and outer top covers
Manual or automatic welder	Welding of vent and drain cover plates
Radiation detectors	Surveys to maintain doses ALARA
Transit with platform	Align transfer cask and ram with HSM-H
Hydrogen detector	Monitoring DSC cavity hydrogen during welding (loading) or cutting (unloading) of inner top cover
Temperature sensor and/or water circulation system	Optional, monitoring or circulation of water in transfer cask / DSC annulus

DSC Opening Equipment and Instruments	Function
Plasma torch or other cutting machine	Removal of lids for unloading of fuel
Portable drill press and annular cutters	Removal of vent and siphon covers
Gas sampling cylinder with quick connect adapter	Sampling of cavity gas prior to opening of DSC
Pressure gauge and water flow control valve	Limiting DSC pressure during reflooding

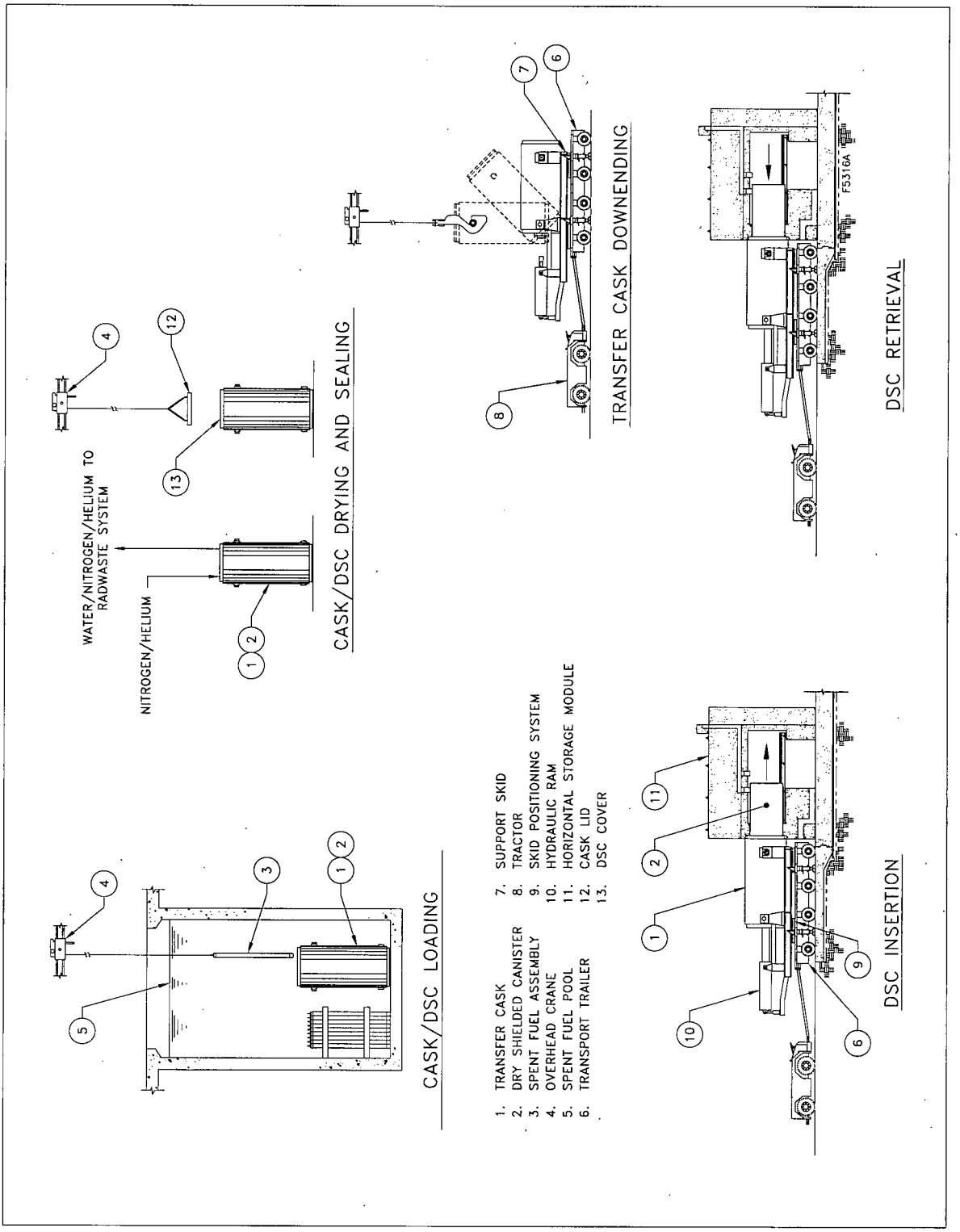

Figure 8-1
NUHOMS® HD System Loading Operations

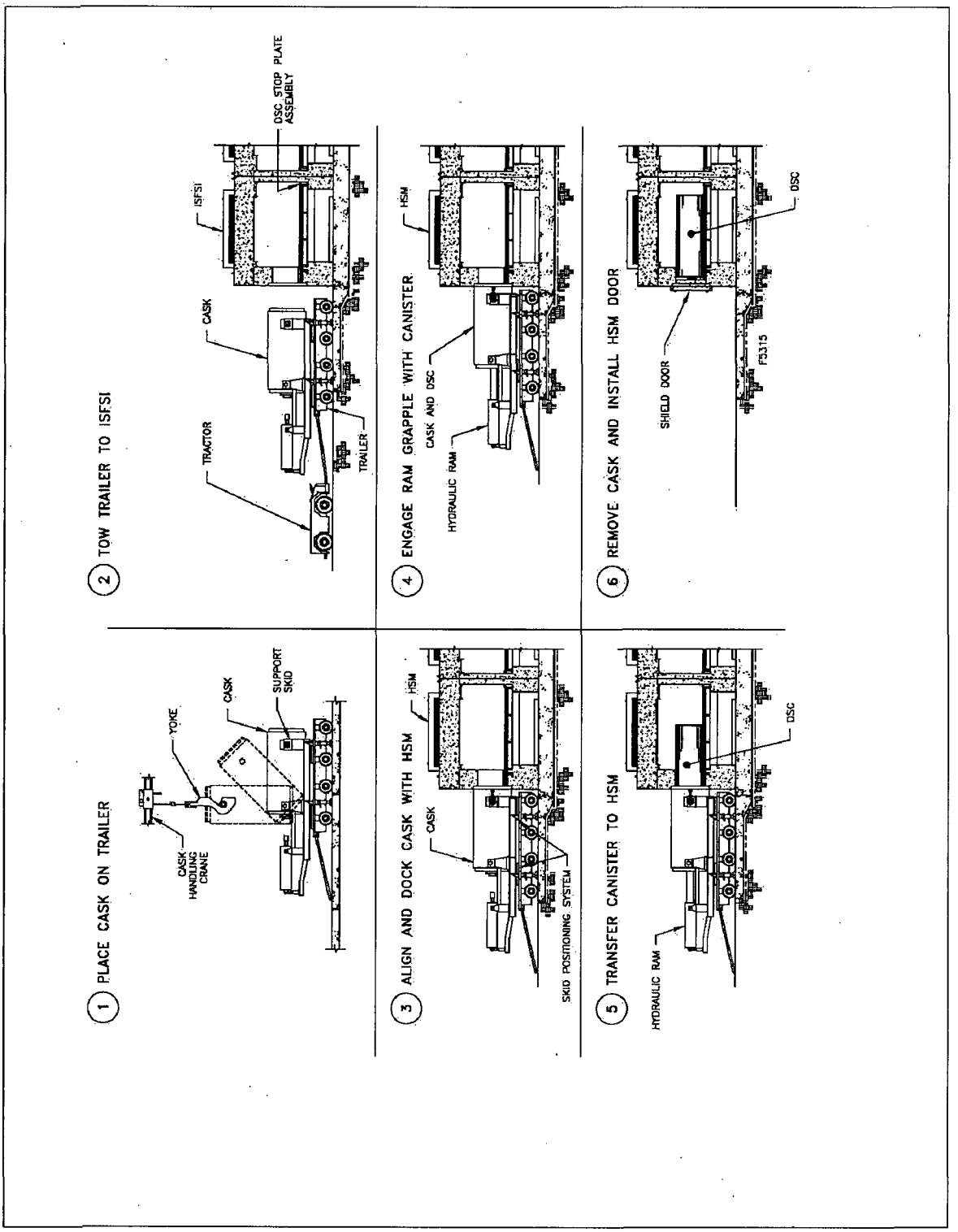

Figure 8-1
NUHOMS® HD System Loading Operations
(concluded)

CHAPTER 9
ACCEPTANCE TESTS AND MAINTENANCE PROGRAM

TABLE OF CONTENTS

9. ACCEPTANCE TESTS AND MAINTENANCE PROGRAM 9-1
9.1 Acceptance Criteria 9-1
9.1.1 Visual inspection and Non-Dectructive Examination (NDE) 9-1
9.1.2 Structural and Pressure tests 9-1
9.1.3 Leak Tests 9-1
9.1.4 Components 9-2
9.1.5 Shielding Integrity 9-2
9.1.6 Thermal Acceptance 9-2
9.1.7 Neutron Absorber Tests 9-3
9.2 Maintenance Program 9-5
9.2.1 Inspection 9-5
9.2.2 Tests 9-5
9.2.3 Repair, Replacement and Maintenance 9-6
9.3 Marking 9-6
9.4 Pre-Operational Testing and Training Exercise 9-6
9.5 Specification for Neutron Absorbers 9-7
9.5.1 Specification for Thermal Conductivity Testing of Neutron Absorbers . 9-7
9.5.2 Specification for Acceptance Testing of Neutron Absorbers by Neutron Transmission 9-8
9.5.3 Specification for Qualification testing of Metal Matrix Composites 9-9
9.5.4 Specification for Process Controls for Metal Matrix Composites 9-12
9.6 References 9-14

LIST OF TABLES

9-1 Boron Content of Neutron Absorbers

9-2 Thermal Conductivity as a Function of Temperature for Sample Neutron Absorbers

9-3 Sample Determination of Thermal Conductivity Acceptance Criteria

9. ACCEPTANCE TESTS AND MAINTENANCE PROGRAM

9.1 Acceptance Criteria

9.1.1 Visual Inspection and Non-Destructive Examination (NDE)

Visual inspections are performed at the fabricator's facility to ensure that the 32PTH DSC, the OS187H Transfer Cask and the HSM-H conform to the drawings and specifications. The visual inspections include weld, dimensional, surface finish, and cleanliness inspections. Visual inspections specified by codes applicable to a component are performed in accordance with the requirements and acceptance criteria of those codes.

All weld inspection is performed using qualified processes and qualified personnel according to the applicable code requirements, e.g., ASME or AWS. Non-destructive examination (NDE) requirements for welds are specified on the drawings provided in Chapter 1; acceptance criteria are as specified by the governing code. NDE personnel are qualified in accordance with SNT-TC-1A [2].

The confinement welds on the DSC are inspected in accordance with ASME B&PV Code Subsection NB [1] including alternatives to ASME Code specified in SAR Section 3.10.

DSC non-confinement welds are inspected to the NDE acceptance criteria of ASME B&PV Code Subsection NG or NF, based on the applicable code for the components welded.

The Transfer Cask welds are inspected in accordance with ASME B&PV Code Subsection NC for class 2 components, as modified by code alternates identified in Section 3.10 of Chapter 3.

9.1.2 Structural and Pressure Tests

The DSC confinement boundary except inner top cover/shield plug (including option 2 or option 3 inner top cover as described in the SAR) to the DSC shell weld is pressure tested at the fabricator's shop in accordance with ASME Article NB-6300. The test pressure is set between 16.5 to18 psig which bounds 1.1 x DSC design pressure of 15 psig.

The inner top cover/shield plug (including option 2 or option 3 inner top cover) to the DSC shell weld is also pressure tested between 16.5 to 18 psig at the field after the fuel assemblies are loaded in the canister. This test is in accordance with the alternatives to the ASME code specified in SAR Section 3.10.

HSM-H reinforcement and concrete are tested as described in Section 2.5.2 and footnotes to Tables 4.1-5 and 4.4-3.

The Transfer Cask lifting (top) trunnions will be load tested in accordance with ANSI N14.6 [3] for a single failure proof design, i.e., three times the design load. The design load is conservatively set at 250,000 lbs (Section 3.2.2); therefore, the test load is 750,000 lbs (375,000 lbs/trunnion).

9.1.3 Leak Tests

DSC confinement welds in the DSC shell and bottom are leak tested at the fabricator's shop to an acceptance criterion of 1×10^{-7} ref cm^3/s, i.e., "leaktight" as defined in ANSI N14.5 [4]. Personnel performing the leak test are qualified in accordance with SNT-TC-1A [2].

The weld between the DSC shell and inner top cover/shield plug (including option 2 or option 3 inner top cover) and siphon/vent cover welds are also leak tested to an acceptance criteria of 1 x 10^{-7} ref cm^3/s at the field after the fuel assemblies are loaded in the canister.

The Transfer Cask lid, ram access, vent, and drain cover o-rings, vent and drain quick connect fittings, neutron shield welds, and neutron shield fittings are leak tested prior to first use.

If bubble leak testing is used, no leak indication is allowed. If pressure drop or helium leak testing is used, the maximum allowable leak for each of the components listed is 10^{-3} ref cm^3/s.

9.1.4 Components

The NUHOMS® System does not include any components such as valves, rupture discs, pumps, or blowers. The gaskets in the Transfer Cask do not require acceptance testing other than the leak testing cited above. No other components of the NUHOMS® System require testing, except as discussed in this chapter.

9.1.5 Shielding Integrity

The Transfer Cask poured lead shielding integrity will be confirmed via gamma scanning prior to first use. The detector and examination grid will be matched to provide coverage of the entire lead-shielded surface area. For example, for a 6" × 6" grid, the detector will encompass a 6" × 6" square. The acceptance criterion is attenuation greater than or equal to that of a test block matching the cask through-wall configuration with lead and steel thicknesses equal to the design minima less 5%.

The radial neutron shielding is provided by filling the neutron shield shell with water during operations. No testing is necessary. The neutron shield material in the lid and bottom end is a proprietary polymer resin. The shielding performance of the resin will be assured by written procedures controlling temperature, measuring, and mixing of the components, degassing of the resin, and verification of the mass or volume of resin installed.

The gamma and neutron shielding materials of the storage system itself are limited to concrete HSM components and steel shield plugs in the DSC. The integrity of these shielding materials is ensured by the control of their fabrication in accordance with the appropriate ASME, ASTM or ACI criteria. No additional acceptance testing is required.

9.1.6 Thermal Acceptance

No thermal acceptance testing is required to verify the performance of each storage unit other than that specified in the Technical Specifications for initial loading of each HSM-H.

The heat transfer analysis for the basket includes credit for the thermal conductivity of neutron-absorbing materials, as specified in Section 4.3. Because these materials do not have publicly documented values for thermal conductivity, testing of such materials will be performed in accordance with Section 9.5.1.

9.1.7 Neutron Absorber Tests

CAUTION

Sections 9.1.7.1 through 9.1.7.3 below are incorporated by reference into the NUHOMS® CoC 1030 Technical Specifications (paragraph 4.3.1) and shall not be deleted or altered in any way without a CoC amendment approval from the NRC. The text of these sections is shown in bold type to distinguish it from other sections.

The neutron absorber used for criticality control in the DSC basket may consist any of the following types of material:

(a) Boron-aluminum alloy (borated aluminum)

(b) Boron carbide-aluminum metal matrix composite

(c) Boral®

The 32PTH DSC safety analyses do not rely upon the tensile strength of these materials. The radiation and temperature environment in the cask is not sufficiently severe to damage these metallic/ceramic materials. To assure performance of the neutron absorber's design function only the presence of B10 and the uniformity of its distribution need to be verified, with testing requirements specific to each material. The boron content of these materials is given in Table 9-1.

9.1.7.1 Boron Aluminum Alloy (Borated Aluminum)

See the Caution in Section 9.1.7 before deletion or modification to this section.

The material is produced by direct chill (DC) or permanent mold casting with boron precipitating as a uniform fine dispersion of discrete AlB_2 or TiB_2 particles in the matrix of aluminum or aluminum alloy. For extruded products, the TiB_2 form of the alloy shall be used. For rolled products, either the AlB_2, the TiB_2, or a hybrid may be used.

Boron is added to the aluminum in the quantity necessary to provide the specified minimum B10 areal density in the final product, with sufficient margin to minimize rejection, typically 10 % excess. The amount required to achieve the specified minimum B10 areal density will depend on whether boron with the natural isotopic distribution of the isotopes B10 and B11, or boron enriched in B10 is used. In no case shall the boron content in the aluminum or aluminum alloy exceed 5% by weight.

The criticality calculations take credit for 90% of the minimum specified B10 areal density of borated aluminum. The basis for this credit is the B10 areal density acceptance testing, which shall be as specified in Section 9.5.2. The specified acceptance testing assures that at any location in the material, the minimum specified areal density of B10 will be found with 95% probability and 95% confidence.

Visual inspections shall follow the recommendations in Aluminum Standards and Data, Chapter 4 "Quality Control, Visual Inspection of Aluminum Mill Products and Castings"[5]. Local or cosmetic conditions such as scratches, nicks, die lines, inclusions,

abrasion, isolated pores, or discoloration are acceptable. Widespread blisters, rough surface, or cracking shall be evaluated for acceptance in accordance with the Certificate Holder's QA procedures.

9.1.7.2 Boron Carbide / Aluminum Metal Matrix Composites (MMC)

See the Caution in Section 9.1.7 before deletion or modification to this section.

The material is a composite of fine boron carbide particles in an aluminum or aluminum alloy matrix. The material shall be produced by either direct chill casting, permanent mold casting, powder metallurgy, or thermal spray techniques. It is a low-porosity product, with a metallurgically bonded matrix. The boron carbide content shall not exceed 40% by volume.

Prior to use in the 32PTH DSC, MMCs shall pass the qualification testing specified in Section 9.5.3, and shall subsequently be subject to the process controls specified in Section 9.5.4.

The criticality calculations take credit for 90% of the minimum specified B10 areal density of MMCs. The basis for this credit is the B10 areal density acceptance testing, which is specified in Section 9.5.2. The specified acceptance testing assures that at any location in the final product, the minimum specified areal density of B10 will be found with 95% probability and 95% confidence.

Visual inspections shall follow the recommendations in Aluminum Standards and Data, Chapter 4 "Quality Control, Visual Inspection of Aluminum Mill Products and Castings" [5]. Local or cosmetic conditions such as scratches, nicks, die lines, inclusions, abrasion, isolated pores, or discoloration are acceptable. Widespread blisters, rough surfaces, or cracking shall be evaluated for acceptance in accordance with the Certificate Holder's QA procedures.

References to metal matrix composites throughout this chapter are not intended to refer to Boral®, which is described in the following section.

9.1.7.3 Boral®

See the Caution in Section 9.1.7 before deletion or modification to this section.

This material consists of a core of aluminum and boron carbide powders between two outer layers of aluminum, mechanically bonded by hot-rolling an "ingot" consisting of an aluminum box filled with blended boron carbide and aluminum powders. The core, which is exposed at the edges of the sheet, is slightly porous. The average size of the boron carbide particles in the finished product is approximately 50 microns after rolling. The nominal boron carbide content shall be limited to 65% (+ 2% tolerance limit) of the core by weight.

The criticality calculations take credit for 75% of the minimum specified B10 areal density of Boral®. B10 areal density will be verified by chemical analysis and by certification of the B10 isotopic fraction for the boron carbide powder, or by neutron transmission testing. Areal density testing is performed on an approximately 1 cm^2 area of a coupon taken near

one of the corners of the sheet produced from each ingot. If the measured areal density is below that specified, all the material produced from that ingot will be either rejected, or accepted only on the basis of alternate verification of B10 areal density for each of the final pieces produced from that ingot.

Visual inspections shall verify that the Boral® core is not exposed through the face of the sheet at any location.

9.2 Maintenance Program

The NUHOMS® HD System is designed to be totally passive with minimal maintenance requirements. The 32PTH DSC does not require any maintenance once it is loaded into the HSM-H. The HSM-H does not require any maintenance other than that indicated in off-normal operations, Chapter 11, such as clearing of blocked air inlets. Periodic inspection is therefore limited to the Transfer Cask.

9.2.1 Inspection

The following inspections of the transfer cask should be performed prior to each fuel loading or unloading campaign:

A. Visual inspection of the transfer cask trunnions for damaged bearing surfaces

B. Visual or functional inspection of all taps, threaded inserts, and bolts

C. Functional inspection of all quick-connect fittings

D. Visual inspection of the interior surface of the cask for any indications of excessive wear.

E. Visual inspection of the neutron shield jacket for indications of damage

F. Visual inspection of all Transfer Cask o-rings for indications of damage

Within the year prior to any loading or unloading campaign, the top trunnion bearing surfaces and accessible welds shall be examined by dye penetrant. No linear indications shall be acceptable other than surface scratches and wear.

9.2.2 Tests

The Transfer Cask lid, ram access, vent, and drain cover o-rings, vent and drain quick connect fittings, and neutron shield fittings shall be leak tested within the year before the start of any fuel loading or unloading campaign. If bubble leak testing is used, no leak indication is allowed. If pressure drop or helium leak testing is used, the maximum allowable leak for each of the components listed is 10^{-3} ref cm^3/s. If any of the listed components is replaced, that component shall be leak tested before use in fuel loading or unloading operations.

No periodic testing of the 32PTH DSC, HSM-H or routine support equipment is required.

Temperature and radiation monitoring is provided in accordance with the Technical Specifications. Periodic calibration of the monitoring equipment shall be as required by the licensee's quality program.

9.2.3 Repair, Replacement, and Maintenance

Any parts which fail inspections listed in 9.1.2 shall be repaired or replaced. Such parts may be also be accepted as-is if determined appropriate by engineering and licensing review.

9.3 Marking

The HSM-H and 32PTH DSC are marked with the model number, unique identification number, and empty weight in accordance with 10 CFR 72.236(k) as shown in drawing 10494-72-7.

9.4 Pre-Operational Testing and Training Exercise

A dry run training exercise of the loading, closure, handling, unloading, and transfer of the NUHOMS® HD System shall be performed by each licensee prior to their first use of the system to load spent fuel assemblies. The dry run shall be conducted with simulated fuel to match the weight of the actual fuel. The dry run need not be performed in the sequence of operations in Chapter 8. The dry run shall include:

(a) Loading of mock-up fuel

(b) DSC draining, vacuum drying, welding, and backfilling

(c) Loading of the Transfer Cask onto the Transfer Trailer, and transfer to the ISFSI

(d) DSC transfer to the HSM-H

(e) DSC retrieval from the HSM-H

(f) Re-flooding of a sealed 32PTH DSC

(g) Removal of the covers from a sealed 32PTH DSC

The dry run will simulate, as nearly as possible, the detailed written procedures developed by the licensee for NUHOMS® HD System operations. Guidelines for the dry run follow.

A. An actual or a mock-up 32PTH DSC loaded with mock-up fuel is typically utilized. The 32PTH DSC is loaded into the transfer cask; the transfer cask/DSC annulus seal is installed.

B. Functional testing is performed with the transfer cask and lifting equipment. These tests are to ensure that the transfer cask can be safely lifted from the plant's cask receiving area to the cask washdown area. The cask is partially lowered into the spent fuel pool and positioned in the cask loading area to verify clearances and travel path. The inner top cover is installed to verify handling and alignment operations.

C. The transfer cask is placed on the transfer trailer, which is moved to the ISFSI aligned with an HSM-H. Compatibility of the transfer trailer with the transfer cask, verification of the transfer route to the ISFSI, and maneuverability within the confines of the ISFSI are verified.

D. The transfer trailer is aligned and docked with the HSM-H. The hydraulic ram is used to insert the 32PTH DSC loaded with mock-up fuel assemblies into the HSM-H and then to retrieve it. Transfer of the 32PTH DSC to the HSM-H will verify that the support skid positioning system and the hydraulic ram system operate safely for both insertion and retrieval.

E. A weld mockup, typically a shortened 32PTH DSC mockup modeling the top end, covers, and drain tube, is used to demonstrate closure welding, draining, drying, backfill, re-flooding, and canister opening operations.

F. The dry run is deemed successful if the expected results are achieved safely and without damage to any of the components or associated equipment.

G. Should any equipment or components require modification in order to achieve the expected results, it will be retested, as necessary, to confirm that the modification is adequate. Should the dry run indicate that procedures require change in order to achieve the expected results, the changes will be incorporated into the appropriate operating procedures prior to use for fuel transfer.

9.5 Specification for Neutron Absorbers

9.5.1 Specification for Thermal Conductivity Testing of Neutron Absorbers

Testing shall conform to ASTM E1225[1], ASTM E1461[2], or equivalent method, performed at room temperature on coupons taken from the rolled or extruded production material. Previous testing of borated aluminum and metal matrix composite, Table 9-2, shows that thermal conductivity increases slightly with temperature. Initial sampling shall be one test per lot, defined by the heat or ingot, and may be reduced if the first five tests meet the specified minimum thermal conductivity.

If a thermal conductivity test result is below the specified minimum, additional tests may be performed on the material from that lot. If the mean value of those tests falls below the specified minimum, the associated lot shall be rejected.

After twenty five tests of a single type of material, with the same aluminum alloy matrix, the same boron content, and the boron appearing in the same phase, e.g., B_4C, TiB_2, or AlB_2, if the mean value of all the test results less two standard deviations meets the specified thermal conductivity, no further testing of that material is required. This exemption may also be applied to the same type of material if the matrix of the material changes to a more thermally conductive alloy (e.g., from 6000 to 1000 series aluminum), or if the boron content is reduced without changing the boron phase.

The thermal analysis in Chapter 4 assumes a 3/16 inch thick neutron absorber paired with a 5/16 inch aluminum 1100 plate. The specified thickness of the neutron absorber may vary, and the

[1] ASTM E1225, "Thermal Conductivity of Solids by Means of the Guarded-Comparative-Longitudinal Heat Flow Technique"
[2] ASTM E1461, "Thermal Diffusivity of Solids by the Flash Method"

thermal conductivity acceptance criterion for the neutron absorber will be based on the nominal thickness specified. The minimum thermal conductivity shall be such that the total thermal conductance (sum of conductivity * thickness) of the neutron absorber and the aluminum 1100 plate shall equal the conductance assumed in the analysis, as shown in Table 9-3, where the acceptance criterion is highlighted.

The aluminum 1100 plate does not need to be tested for thermal conductivity; the material may be credited with the values published in the ASME Code Section II part D. The neutron absorber material need not be tested for thermal conductivity if the nominal thickness of the aluminum 1100 plate is 0.425 inch or greater. This case is examined explicitly in chapter 4, where no credit is taken for the thermal conductivity of Boral®.

9.5.2 Specification for Acceptance Testing of Neutron Absorbers by Neutron Transmission

CAUTION

Section 9.5.2 is incorporated by reference into the NUHOMS® CoC 1030 Technical Specifications (paragraph 4.3.1) and shall not be deleted or altered in any way without a CoC amendment approval from the NRC. The text of this section is shown in bold type to distinguish it from other sections.

Neutron Transmission acceptance testing procedures shall be subject to approval by the Certificate Holder. Test coupons shall be removed from the rolled or extruded production material at locations that are systematically or probabilistically distributed throughout the lot. Test coupons shall not exhibit physical defects that would not be acceptable in the finished product, or that would preclude an accurate measurement of the coupon's physical thickness.

A lot is defined as all the pieces produced from a single ingot or heat. If this definition results in lot size too small to provide a meaningful statistical analysis of results, an alternate larger lot definition may be used, so long as it results in accumulating material that is uniform for sampling purposes.

The sampling rate for neutron transmission measurements shall be such that there is at least one neutron transmission measurement for each 2000 square inches of final product in each lot.

The B10 areal density is measured using a collimated thermal neutron beam of up to 1.2 centimeter diameter. A beam size greater than 1.2 centimeter diameter but no larger than 1.7 centimeter diameter may be used if computations are performed to demonstrate that the calculated $k_{effective}$ of the system is still below the calculated Upper Subcritical Limit (USL) of the system assuming defect areas the same area as the beam. Alternatively, the confidence and probability levels can be increased such that it will result in equivalent acceptance rates for the material as the 1.2 centimeter diameter beam size.

The neutron transmission through the test coupons is converted to B10 areal density by comparison with transmission through calibrated standards. These standards are

composed of a homogeneous boron compound without other significant neutron absorbers. For example, boron carbide, zirconium diboride or titanium diboride sheets are acceptable standards. These standards are paired with aluminum shims sized to match the effect of neutron scattering by aluminum in the test coupons. Uniform but non-homogeneous materials such as metal matrix composites may be used for standards, provided that testing shows them to provide neutron attenuation equivalent to a homogeneous standard.

Alternatively, digital image analysis may be used to compare neutron radioscopic images of the test coupon to images of the standards. The area of image analysis shall be up to 1.1 cm^2.

The minimum areal density specified shall be verified for each lot at the 95% probability, 95% confidence level or better. The following illustrates one acceptable method.

The acceptance criterion for individual plates is determined from a statistical analysis of the test results for their lot. The minimum B10 areal densities determined by neutron transmission are converted to volume density, i.e., the minimum B10 areal density is divided by the thickness at the location of the neutron transmission measurement or the maximum thickness of the coupon. The lower tolerance limit of B10 volume density is then determined, defined as the mean value of B10 volume density for the sample, less K times the standard deviation, where K is the one-sided tolerance limit factor for a normal distribution with 95% probability and 95% confidence [7].

Finally, the minimum specified value of B10 areal density is divided by the lower tolerance limit of B10 volume density to arrive at the minimum plate thickness which provides the specified B10 areal density.

Any plate which is thinner than this minimum or the minimum design thickness, whichever is greater, shall be treated as non-conforming, with the following exception. Local depressions are acceptable, so long as they total no more than 0.5% of the area on any given plate, and the thickness at their location is not less than 90% of the minimum design thickness.

Non-conforming material shall be evaluated for acceptance in accordance with the Certificate Holder's QA procedures.

9.5.3 Specification for Qualification Testing of Metal Matrix Composites

9.5.3.1 Applicability and Scope

Metal matrix composites (MMCs) shall consist of fine boron carbide particles in an aluminum or aluminum alloy matrix. The ingot shall be produced by either powder metallurgy (PM), thermal spray techniques, or by direct chill (DC) or permanent mold casting. In any case, the final MMC product shall have density greater than 98% of theoretical, a metallurgically bonded matrix, and boron carbide content no greater than 40% by volume. Boron carbide particles for the products considered here typically have an average size in the range 10-40 microns, although the actual specification may be by mesh size, rather than by average particle size. No more than 10% of the

particles shall be over 60 microns. The material shall have negligible interconnected porosity exposed at the surface or edges.

Prior to initial use in a spent fuel dry storage or transport system, such MMCs shall be subjected to qualification testing that will verify that the product satisfies the design function. Key process controls shall be identified per Section 9.5.4 so that the production material is equivalent to or better than the qualification test material. Changes to key processes shall be subject to qualification before use of such material in a spent fuel dry storage or transport system.

ASTM test methods and practices are referenced below for guidance. Alternative methods may be used with the approval of the certificate holder.

9.5.3.2 Design Requirements

In order to perform its design functions the product must have at a minimum sufficient strength and ductility for manufacturing and for the normal and accident conditions of the storage/ transport system. This is demonstrated by the tests in Section 9.5.3.4. It must have a uniform distribution of boron carbide. This is demonstrated by the tests in Section 9.5.3.5.

9.5.3.3 Durability

There is no need to include accelerated radiation damage testing in the qualification. Such testing has already been performed on MMCs, and the results confirm what would be expected of materials that fall within the limits of applicability cited above. Metals and ceramics do not experience measurable changes in mechanical properties due to fast neutron fluences typical over the lifetime of spent fuel storage, about 10^{15} neutrons/cm^2.

The need for thermal damage and corrosion (hydrogen generation) testing shall be evaluated case-by-case based on comparison of the material composition and environmental conditions with previous thermal or corrosion testing of MMCs.

Thermal damage testing is not required for MMCs consisting only of boron carbide in an aluminum 1100 matrix, because there is no reaction between aluminum and boron carbide below 842°F, well above the basket temperature under normal conditions of storage or transport[3].

Corrosion testing is not required for full density MMCs consisting only of boron carbide in an aluminum 1100 matrix, because testing on one such material has already been performed by Transnuclear[4].

9.5.3.4 Required Qualification Tests and Examinations to Demonstrate Mechanical Integrity

At least three samples, one each from the two ends and middle of the test material production run shall be subject to:

[3] Sung, C., "Microstructural Observation of Thermally Aged and Irradiated Aluminum/Boron Carbide (B_4C) Metal Matrix Composite by Transmission and Scanning Electron Microscope," 1998

[4] Boralyn testing submitted to the NRC under docket 71-1027, 1998

a) room temperature tensile testing (ASTM- B557[5]) demonstrating that the material has the following tensile properties:

- Minimum yield strength, 0.2% offset: 1.5 ksi
- Minimum ultimate strength: 5 ksi
- Minimum elongation in 2 inches: 0.5%
  (Alternatively show that the material fails in a ductile manner, e.g., by scanning electron microscopy of the fracture surface or by bend testing.)

and

b) testing (ASTM-B311[6]) to verify more than 98% of theoretical density. Testing or examination for exposed interconnected porosity shall be performed by a means to be approved by the Certificate Holder.

9.5.3.5 Required Tests and Examinations to Demonstrate B10 Uniformity

CAUTION

Section 9.5.3.5 is incorporated by reference into the NUHOMS® CoC 1030 Technical Specifications (paragraph 4.3.1) and shall not be deleted or altered in any way without a CoC amendment approval from the NRC. The text of this section is shown in bold type to distinguish it from other sections.

Uniformity of the boron distribution shall be verified either by:

(a) Neutron radioscopy or radiography (ASTM E94[7], E142[8], and E545[9]) of material from the ends and middle of the test material production run, verifying no more than 10% difference between the minimum and maximum B10 areal density, or

(b) Quantitative testing for the B10 areal density, B10 density, or the boron carbide weight fraction, on locations distributed over the test material production run, verifying that one standard deviation in the sample is less than 10% of the sample mean. Testing may be performed by a neutron transmission method similar to that specified in Section 9.5.2, or by chemical analysis for boron carbide content in the composite.

9.5.3.6 Approval of Procedures

Qualification procedures shall be subject to approval by the Certificate Holder.

---

[5] ASTM B557 Standard Test Methods of Tension Testing Wrought and Cast Aluminum and Magnesium-Alloy Products.

[6] ASTM B311, Test Method for Density Determination for Powder Metallurgy (P/M) Materials Containing Less Than Two Percent Porosity

[7] ASTM E94, Recommended Practice for Radiographic Testing

[8] ASTM E142, Controlling Quality of Radiographic Testing

[9] ASTM E545, Standard Method for Determining Image Quality in Thermal Neutron Radiographic Testing

9.5.3.7 Required Computations for Using Neutron Beam Size Greater than 1.2 cm. Diameter

As described in Section 9.5.2, a neutron beam greater than 1.2 cm diameter but no larger than 1.7 cm diameter may be used for acceptance testing if a criticality calculation shows that neutron absorber material with the following defects would still result in k_{eff} below the Upper Subcritical Limit as calculated in Chapter 6:

1. Defects of the same area as the proposed neutron beam or larger have an areal density significantly below the specified minimum areal density.

2. These defects are distributed randomly or systematically over the material, or in a manner that is conservative for the design analysis.

3. The total of such defective areas amounts to (100-x) percent of the neutron absorber material area, where x is the probability level used for determining the lower tolerance limit.

Alternately, apply more rigorous statistical criteria for lot acceptance, i.e., increase the factor K in the following expression:

Lower tolerance limit = average of sample – K * standard deviation of sample ≥ Technical Specification areal density acceptance criterion,

where, K is the one-sided tolerance limit factor for a normal distribution with a specified sample size, probability, and confidence.

The value of K should be increased to compensate for the decreased standard deviation that results from using a larger neutron beam to examine a material which has defect areas whose characteristic dimension is 1.2 cm.

9.5.4 Specification for Process Controls for Metal Matrix Composites

9.5.4.1 Applicability and Scope

The applicability of this section is the same as that of Section 9.5.3. It addresses the process controls to ensure that the material delivered for use is equivalent to the qualification test material.

Key processing changes shall be subject to qualification prior to use of the material produced by the revised process. The Certificate Holder shall determine whether a complete or partial re-qualification program per Section 9.5.4 is required, depending on the characteristics of the material that could be affected by the process change.

9.5.4.2 Definition of Key Process Changes

Key process changes are those which could adversely affect the uniform distribution of the boron carbide in the aluminum, reduce density, or reduce the mechanical strength or ductility of the MMC.

9.5.4.3 Identification and Control of Key Process Changes

CAUTION

Section 9.5.4.3 is incorporated by reference into the NUHOMS® CoC 1030 Technical Specifications (paragraph 4.3.1) and shall not be deleted or altered in any way without a CoC amendment approval from the NRC. The text of this section is shown in bold type to distinguish it from other sections.

The manufacturer shall provide the Certificate Holder with a description of materials and process controls used in producing the MMC. The Certificate Holder and manufacturer shall identify key process changes as defined in Section 9.5.4.2.

An increase in nominal boron carbide content over that previously qualified shall always be regarded as a key process change. The following are examples of other changes that may be established as key process changes, as determined by the Certificate Holder's review of the specific applications and production processes:

(a) Changes in the boron carbide particle size specification that increase the average particle size by more than 5 microns or that increase the amount of particles larger than 60 microns from the previously qualified material by more than 5% of the total distribution but less than the 10% limit,

(b) Change of the billet production process, e.g., from vacuum hot pressing to cold isostatic pressing followed by vacuum sintering,

(c) Change in the nominal matrix alloy,

(d) Changes in mechanical processing that could result in reduced density of the final product, e.g., for PM or thermal spray MMCs that were qualified with extruded material, a change to direct rolling from the billet,

(e) For MMCs using a 6000 series aluminum matrix, changes in the billet formation process that could increase the likelihood of magnesium reaction with the boron carbide, such as an increase in the maximum temperature or time at maximum temperature, and

(f) Changes in powder blending or melt stirring processes that could result in less uniform distribution of boron carbide, e.g., change in duration of powder blending.

In no case shall process changes be accepted if they result in a product outside the limits in Sections 9.5.3.1 and 9.5.3.4.

9.6 References

1. ASME Boiler and Pressure Vessel Code, Section III, 1998 Edition with 2000 Addenda.

2. SNT-TC-1A, "American Society for Nondestructive Testing, Personnel Qualification and Certification in Nondestructive Testing," 1992.

3. ANSI N14.6, "American National Standard for Special Lifting Devices for Shipping Containers Weighing 10,000 Pounds or More for Nuclear Materials," New York, 1996.

4. ANSI N14.5-1997, "American National Standard for Leakage Tests on Packages for Shipment of Radioactive Materials", February 1998.

5. "Aluminum Standards and Data, 2003" The Aluminum Association.

6. Topical report: Credit for 90% of the 10B in Boral®", AAR Report 1829, AAR Manufacturing, Oct 2004

7. Natrella, "Experimental Statistics," Dover, 2005

Table 9-1
Boron Content of Neutron Absorbers

Borated Aluminum and Metal Matrix Composites, 90% B10 credit

NUHOMS®-32PTH DSC Basket Type	B10 Areal Density, (g/cm^2)	Nom wt % boron in enriched borated aluminum 0.187" thk (notes 1, 2, 3)	Nom wt % boron in natural borated aluminum 0.187" thk (notes 2, 3)	Nominal vol % B_4C in MMC, 0.187" thick (notes 2, 3)
AI	0.007	0.6	3.1	4.1
BI	0.015	1.3	Note 4	8.9
CI	0.020	1.7		11.8
DI	0.032	2.7		18.9
EI	0.050	4.2		29.5

0.075 inch thick Boral®, 75% B10 credit

NUHOMS®-32PTH DSC Basket Type	B10 Areal Density, (g/cm^2)	Boral® nominal core thickness, inch
AII	0.009	0.0535 (note 5)
BII	0.019	
CII	0.025	
DII	N/A	Note 6
EII	N/A	

Notes:

1. Enriched boron is nominally 95 atom % B10
2. The neutron absorber manufacturer may increase this value to provide margin against rejection of the product
3. If a neutron absorber thinner than 0.187 inch is used, the boron content varies in inverse proportion to the thickness to maintain the same areal density
4. The necessary boron content in this range is too high (>5%) to use boron with its naturally-occurring isotopic distribution (nominal 20 atom % B10) in borated aluminum
5. Boral® sheet and core thickness remain the same; boron carbide / aluminum powder ratio is varied to achieve the required areal density
6. Boral® in this range requires a sheet thicker than 0.075 inches

Table 9-2
Thermal Conductivity as a Function of Temperature for Sample Neutron Absorbers

Material >	1	2	3	4
20	193	170	194	194
100	203	183	207	201
200	208	-	-	
250	-	201	218	206
300	211	204	220	203
314	-	-	-	202
342	-	-	-	202

Units: W/mK

Materials:

1) Boralyn® MMC, aluminum 1100 with 15% B_4C
2) Borated aluminum 1100, 2.5% boron as TiB_2
3) Borated aluminum 1100, 2.0% boron as TiB_2
4) Borated aluminum 1100, 4.3% boron as AlB_2

Sources:

Thermal Conductivity Measurements of Boron Carbide/Aluminum Specimens, Oct 1998, testing by Precision Measurements and Instruments Corp. for Transnuclear, Inc.

Qualification of Thermal Conductivity, Borated Aluminum 1100, Eagle Picher Report AAQR06, May 2001

Table 9-3
Sample Determination of Thermal Conductivity Acceptance Criterion

	Al 1100	n absorber	total	
thickness (inch)	0.3125	0.1875	0.5	as modeled
conductivity at 70 F (Btu/hr.in.F)	11.09	**6.98**	n/a	
conductance (Btu/hr.F)	3.466	1.309	4.774	
thickness (inch)	0.28	0.22	0.5	thicker neutron absorber
conductivity at 70 F (Btu/hr.in.F)	11.09	**7.59**	n/a	
conductance (Btu/hr.F)	3.105	1.670	4.775	
thickness (inch)	0.35	0.15	0.5	thinner neutron absorber
conductivity at 70 F (Btu/hr.in.F)	11.09	**5.95**	n/a	
conductance (Btu/hr.F)	3.882	0.893	4.774	

The acceptance criterion is identified by boldface type for each thickness.

CHAPTER 10
RADIATION PROTECTION

TABLE OF CONTENTS

10. RADIATION PROTECTION 10-1

10.1 Ensuring That Occupational Radiation Exposures Are As Low As Reasonably Achievable (ALARA) 10-1
10.1.1 Policy Considerations 10-1
10.1.2 Design Considerations 10-1
10.1.3 Operational Considerations 10-3

10.2 Radiation Protection Design Features 10-4
10.2.1 NUHOMS® HD System Design Features 10-4
10.2.2 Offsite Dose Calculations 10-4

10.3 Estimated Onsite Collective Dose Assessment 10-8
10.3.1 DSC Loading, Transfer and Storage Operations 10-8
10.3.2 DSC Retrieval Operations 10-8
Fuel Unloading Operations 10-9
10.3.4 Maintenance Operations 10-9
10.3.5 Doses During ISFSI Array Expansion 10-9

10.4 References 10-10

LIST OF TABLES

10-1 Occupational Exposure Summary, NUHOMS® HD System
10-2 Total Annual Exposure from 32PTH DSC in HSM-H
10-3 NUHOMS® HD System, 32PTH DSC/ HSM-H Spectra
10-4 Summary of ISFSI Surface Activities, 32PTH DSC in HSM-H
10-5 MCNP Front Detector Dose Rates for 2x10 Array, 32PTH DSC in HSM-H
10-6 MCNP Back Detector Dose Rates for the Two 1x10 Arrays, 32PTH DSC in HSM-H
10-7 MCNP Side Detector Dose Rates, 32PTH DSC in HSM-H

LIST OF FIGURES

10-1 Annual Exposure from the ISFSI as a Function of Distance, 32PTH DSC in HSM-H

10. RADIATION PROTECTION

10.1 Ensuring That Occupational Radiation Exposures Are As Low As Reasonably Achievable (ALARA)

10.1.1 Policy Considerations

The licensee's radiation safety and ALARA policies should be applied to the ISFSI. The ALARA program should follow the general guidelines of Regulatory Guides 1.8 4, 8.8 1, 8.10 3 and 10 CFR 20 6. ISFSI personnel should be trained in the proper operation, inspection, repair and maintenance of the NUHOMS® HD System and updated on ALARA practices and dose reduction techniques. Implementation of ISFSI procedures should be reviewed by the licensee to ensure ALARA exposure.

10.1.2 Design Considerations

The thick inner cover of the DSC is designed to minimize exposure during draining, drying, and closure operations. The vent and drain ports are designed for maximum water flow rate and vacuum conductance to minimize the time (and thereby the exposure) associated with draining and vacuum drying. The design of the cover welds minimizes exposure during closure operations. The welds are designed to be easily performed by remote welding equipment. Because the cover welds are not used to lift the canister, they are relatively small, reducing the time needed to complete them. Because they are austenitic welds, no pre-heating is required. These welds are tested to be leak-tight as described in Chapter 7. Therefore, exposure associated with a leaking DSC is eliminated.

Lead, steel, water, and borated plastic in the transfer cask provide required gamma and neutron shielding during transfer activities. The exterior of the transfer cask is decontaminated prior to transfer to the ISFSI, thereby minimizing exposure of personnel to surface contamination.

The NUHOMS® HSM-H storage modules include no active components which require periodic maintenance thereby minimizing potential personnel dose due to maintenance activities.

The shielding design features of the storage modules storage minimize occupational exposure for any activities on or near the ISFSI. These features are:

- The DSCs are loaded and sealed prior to transfer to the ISFSI. Seals are austenitic stainless welds with at least two layers.
- The fuel will not be unloaded nor will the DSCs be opened at the ISFSI unless the ISFSI is specifically licensed for these purposes.
- The fuel is stored in a dry inert environment inside the DSCs so that no radioactive liquid is available for leakage.

- The DSCs are sealed with a helium atmosphere to prevent oxidation of the fuel. The leaktight design features are described in Chapter 7.
- The DSCs are heavily shielded on both ends to reduce external dose rates. The shielding design features are discussed in Chapter 5.
- No radioactive material will be discharged during storage since the DSC is designed, fabricated, and tested to be leaktight.
- The DSC outside surface is contamination free due to the use of clean water sealed in the annulus between the cask and DSC during loading operations.
- HSM's provide thick concrete shielding, while placement of modules immediately adjacent to one another enhances the effectiveness of this shielding.

Regulatory Position 2 of Regulatory Guide 8.8 1, is incorporated into the design considerations, as described below:

- Regulatory Position 2a on access control is met by use of a fence with a locked gate that surrounds the ISFSI and prevents unauthorized access.
- Regulatory Position 2b on radiation shielding is met by the heavy shielding of the NUHOMS® System which minimizes personnel exposures.
- Regulatory Position 2c on process instrumentation and controls is met by designing the instrumentation for a long service life and locating readouts in a low dose rate location. The use of thermocouples for temperature measurements located in embedded thermowells provides reliable, easily maintainable instrumentation for this monitoring function.
- Regulatory Position 2d on control of airborne contaminants may be applicable for vacuum drying operations of DSCs containing damaged fuel. Diversion of the vacuum pump exhaust to an appropriate filtration system is recommended in the Chapter 8 operations. The regulatory position does not apply during transfer or storage because neither gaseous releases nor significant surface contamination are expected.
- Regulatory Position 2e on crud control is not applicable to the ISFSI because there are no systems at the ISFSI that could transport crud. The leaktight DSC design ensures that spent fuel crud will not be released or transferred from the DSC. Draining back to the spent fuel pool provides control over any crud that could be entrained in the outflow from the DSC draining operations.
- Regulatory Position 2f on decontamination is met because the transfer cask is decontaminated prior to transfer to the ISFSI. The transfer cask accessible surfaces are designed to facilitate decontamination.

Regulatory Position 2g on radiation monitoring does not apply. There is no need for airborne radioactivity monitoring because the DSCs are sealed by leaktight welds. Airborne radioactivity due to damaged fuel is discussed under Regulatory Position 2d

above. Area radiation monitors are not required because the ISFSI will not be occupied on a regular basis.

- Regulatory Position 2h on resin and sludge treatment systems is not applicable to the ISFSI because there are no radioactive systems containing resins or sludge associated with the ISFSI.
- Regulatory Position 2i concerning other miscellaneous ALARA items is not applicable because these items refer to radioactive systems not present at the ISFSI.

10.1.3 Operational Considerations

The operations description in Chapter 8 makes provision for measures which can minimize doses during operations including

- using temporary shielding,
- wetting equipment with clean water prior to pool immersion to improve ease of decontamination,
- preventing contamination of the DSC exterior by the use of clean water in a sealed transfer cask/DSC annulus,
- using remote equipment for welding, long-handled tools for decontamination, etc., and
- controlling gases and liquids removed from the DSC during DSC vacuum drying and during fuel unloading.

The areas of highest operational dose are the front of a loaded HSM-H at the air inlet vent, at the cask side or DSC top with a partially or completely drained DSC (cover welding, transfer operations) and at the cask/DSC annulus. Operating procedures, temporary shielding, and personnel training should minimize personnel exposure in these areas.

The DSCs contain no radioactive liquids and, for intact fuel assemblies, are not expected to contain any radioactive gases. The DSC is designed and welded to be leaktight.

The NUHOMS® HD System HSM-H and 32PTH DSC are designed to be essentially maintenance free. It is a passive system without any moving parts. The only anticipated maintenance procedures are the visual inspection of the bird screens on the HSM ventilation inlet and outlet openings, and periodic maintenance of the thermocouples. Maintenance operations on the transfer cask, transfer equipment and other auxiliary equipment are normally performed in a low dose environment during periods when fuel movement is not occurring.

The ISFSI contains no systems that process liquids or gases or contain, collect, store, or transport radioactive liquids or solids other than payloads identified in Chapter 2. Therefore, the ISFSI meets ALARA requirements since there are no systems to be maintained other than the transfer and auxiliary equipment.

10.2 Radiation Protection Design Features

10.2.1 NUHOMS® HD System Design Features

The NUHOMS® HD System has design features which ensure a high degree of integrity for the confinement of radioactive materials and reduction of direct radiation exposures during storage. Those features are described in Section 10.1.2.

10.2.2 Offsite Dose Calculations

Calculated dose rates in the immediate vicinity of the NUHOMS® HD System are presented in Chapter 5, which provides a detailed description of source term configuration, analysis models and bounding dose rates. Off-site dose rates and doses are presented in this section. This evaluation determines the neutron and gamma-ray off-site dose rates including skyshine in the vicinity of the two generic ISFSI layouts containing design-basis contents in the DSCs.

The first generic ISFSI evaluated is a 2x10 back-to-back array of HSM-Hs loaded with design-basis fuel and control components (NFAH) in NUHOMS® 32PTH DSCs. The second generic layout evaluated is two 1x10 front-to-front arrays. This evaluation provides results for distances ranging from 6.1 to 600 meters from each face of the two arrays.

The total annual exposure for each ISFSI layout as a function of distance from each face is given in Table 10- and plotted in Figure 10-1. The total annual exposure estimates assume 100% occupancy for 365 days.

The Monte Carlo computer code MCNP 2 calculates the dose rates at the specified locations around the arrays of HSMs. The results of this calculation provide an example of how to demonstrate compliance with the relevant radiological requirements of 10 CFR 20 6, 10 CFR 72 5, and 40 CFR 190 8 for a specific site. Each site must perform specific site calculations to account for the actual layout of the HSMs and fuel source.

The assumptions for the MCNP analyses are summarized below.

- The 20 HSMs in the 2x10 back-to-back array are modeled as a box enveloping the 2x10 array of HSMs including the 3-foot shield walls on the two ends of the array. MCNP starts the source particles on the surfaces of the box.

- The 20 HSMs in the two 1x10 front-to-front arrays are modeled as two boxes which envelope each 1x10 array of HSMs including the 3-foot shield walls on the two ends and back of each array. MCNP starts the source particles on the surfaces of one of the boxes.

- The ISFSI approach slab is modeled as concrete. Because the ground composition has, at best, only a secondary impact on the dose rates at the detectors, any differences between this

assumed layout and the actual layout would not have a significant affect on the site dose rates.

- For the 2x10 array, the interiors of the HSMs and shield walls are modeled as air. Most particles that enter the interiors of the HSMs and shield walls will therefore pass through unhindered.

- For the two 1x10 arrays, the interiors of one array of HSMs and shield walls are modeled as air Most particles that enter the interiors of these HSMs and shield walls will therefore pass through unhindered. The other 1x10 array is modeled as concrete to simulate the shielding provided by the second array of HSMs for the direct radiation from the front of the opposing 1x10 array.

- The "universe" is a sphere surrounding the ISFSI. To account for skyshine radius of this sphere (r=500,000 cm) is more than 10 mean free paths for neutrons and 50 mean free paths for gammas greater than that of the outermost surface, thus ensuring that the model is of a sufficient size to include all interactions, including skyshine, affecting the dose rate at the detectors.

- The HSM-H surface sources are bootstrapped (input to provide an equivalent boundary condition) using the surface average dose rates calculated in Section 5.4 and shown in Table 5-2.

- MCNP starts the source particles on the ISFSI array surface with initial directions following a cosine distribution. Radiation fluxes outside thick shields such as the HSM walls and roof tend to have forward peaked angular distributions; therefore, a cosine function is a reasonable approximation for the starting direction distribution. Vents through shielding regions such as the HSM vents tend to collimate particles such that a semi-isotropic assumption would not be appropriate.

- Point detectors determine the dose rates on the four sides of the ISFSI as a function of distance from the ISFSI. All detectors represent the dose rate at three feet above ground level.

- Source information required by MCNP includes gamma-ray and neutron spectra for the HSM array surfaces, total gamma-ray and neutron activities for each HSM-H array face and total gamma-ray and neutron activities for the entire ISFSI. The neutron and gamma-ray spectra are determined using the MCNP spectra determined in the HSM-H dose calculations (from Section 5.4) using the design-basis in-core neutron and gamma fuel sources. Use of the roof is conservative because it represents the thickest cross section of the HSM-H shield. The thicker shield increases the dose rate importance of the higher energy neutrons and gamma-rays from the fuel because the thicker shield filters out the lower energy particles. Therefore, use of the thickest part of the shield results in a harder spectrum for all of the other surfaces. The HSM-H spectra as determined from MCNP are normalized to a one mrem/hour source using the flux-to-dose-factors from ANSI/ANS 6.1.1-1977 9. These normalized spectra are then input in the MCNP ERG source variable.

- The probability of a particle being born on a given surface is proportional to the total activity of

that surface. The activity of each surface is determined by multiplying the sum of the normalized group fluxes, calculated above, by the average surface dose rate and by the area of the surface. This calculation is performed for the roof, sides, back and front of the HSM-H. The sum of the surface activities is then input as the tally multiplier for each of the MCNP tallies to convert the tally results to fluxes (particles per second per square centimeter).

- Neutron and gamma-ray spectra are shown in Table 10-. The group fluxes on the roof are taken from the MCNP run. The dose rate contribution from each group is the product of the flux and the flux-to-dose factor. The "Input Current" column in the tables is simply the roof flux in each group, divided by half the total dose rate and represents the roof current normalized to one mrem per hour.

10.2.2.1 Activity Calculations

The surface activities are summarized in Table 10-4.

10.2.2.2 Dose Rates

Dose rates are calculated for distances of 6.1 meters (20 feet) to 600 meters from the edges of the two ISFSI designs.

Neutron and gamma-ray sources are placed on each surface using the spectra and activities determined above. The angular distribution of source particles is modeled as a cosine distribution. The contribution of capture gamma-rays has been neglected, as has the contribution of bremsstrahlung electrons. The inclusion of coherent scattering greatly increases the variance in a problem with point detector tallies without improving the accuracy of the calculation. Thus, coherent scattering of photons is ignored.

For the 2x10 back-to-back array with end shield walls, the "box" dimensions are 1260 cm wide, 3129 cm long, and 564 cm high.

For the two 1x10 front-to-front arrays with end and back shield walls, the "box" dimensions for each array are 721 cm wide, 3129 cm long, and 564 cm high. The two 1x10 arrays are 1026 cm (34 feet) apart.

Point detectors are placed at the following locations as measured from each face of the "box": 6.095 m (20 feet), 10 m, 20 m, 30 m, 40 m, 50 m, 60 m, 70 m, 80 m, 90 m, 100 m, 200 m, 300 m, 400 m, 500 m, and 600 m. Each point detector is placed 91.4 cm (3 feet) above the ground.

The MCNP results for each detector from the front of 2x10 back-to-back array are summarized in Table 10-. The MCNP results as a function of distance from the back of the two 1x10 front-to-front arrays are summarized in Table 10-. The MCNP results as a function of distance from the side of the 2x10 back-to-back array and the two 1x10 front-to-front arrays are summarized in Table 10-7.

The preceding analyses and results are intended to provide high estimates of dose rates for generic ISFSI layouts. The written evaluations performed by a licensee for an actual ISFSI must consider

the type and number of storage units, layout, characteristics of the irradiated fuel to be stored, site characteristics (e.g., berms, distance to the controlled area boundary, etc.), and reactor operations at the site in order to demonstrate compliance with 10CFR72.104.

10.3 Estimated Onsite Collective Dose Assessment

This section provides estimates of occupational for typical ISFSI operations. Offsite dose rates for normal and anticipated conditions controlled by 10 CFR 72.104 are addressed in Section 10.2. Dose rates from accident conditions controlled by 10 CFR 72.106 are addressed in Chapters 5 and 11.

Assumed annual occupancy times, including the anticipated maximum total hours per year for any individual and total person-hours per year for all personnel for each radiation area during normal operation and anticipated operational occurrences will be evaluated by the licensee in a 10 CFR 72.212 evaluation to address the site specific ISFSI layout, inspection, and maintenance requirements. In addition, the estimated annual collective doses associated with loading operations will be addressed by the licensee in a 10 CFR 72.212 evaluation.

10.3.1 DSC Loading, Transfer and Storage Operations

The estimated occupational exposures to ISFSI personnel during loading, transfer, and storage of the DSC (time and manpower may vary depending on individual ISFSI practices) is shown in Table 10-1. The task times, number of personnel required and total doses are listed in this table. The total dose is estimated to be 2.2 rem per loaded canister. This is a bounding estimate; measured doses from Standardized NUHOMS® System loading campaigns have been 600 mrem or lower per canister for normal operations.

The average distance for a given operation takes into account that the operator may be in contact with the transfer cask, but this duration will be limited. For draining activities and vacuum drying the attachment of fittings will take place closer to the cask than the operation of the pumps. For decontamination activities, although operators could be near the cask for some activities, other parts of the operation could be performed from farther away. For this reason, 1 foot or 3 feet is an appropriate average distance for these operations.

The operator's hands may be in a high dose rate location momentarily, for example when connecting fittings at the ports. This does not translate into a whole-body dose, and therefore, these localized streaming effects are not considered here.

For operations near the top end of the 32PTH DSC, most of the work will take place around the perimeter and a smaller portion will take place directly over the shielded inner top cover.

Regulatory Guide 8.34 [7] is to be employed in defining the on-site occupational dose and monitoring requirements.

10.3.2 DSC Retrieval Operations

Occupational exposures to ISFSI personnel during 32PTH DSC retrieval are similar to those exposures calculated for 32PTH DSC insertion. Dose rates for retrieval operations will be lower than those for insertion operations due to radioactive decay of the spent fuel inside the HSM. Therefore, the dose rates for 32PTH DSC retrieval are bounded by the dose rates calculated for insertion.

10.3.3 Fuel Unloading Operations

The process of unloading the 32PTH DSC is similar to that used for loading the 32PTH DSC. The identical ALARA procedures utilized for loading should also be applied to unloading.

Occupational exposures to plant personnel are bounded by those exposures calculated for 32PTH DSC loading.

10.3.4 Maintenance Operations

The dose rate for surveillance activities is obtained from Table 10-5, Table 10-6, and Table 10-7 for doses rates 6.1 meters from the front of an HSM-H. The 6.1 meter dose rate is a conservative estimate for surveillance activities. The HSM-H surface dose rate provided in Chapter 5 is a conservative estimate for thermocouple maintenance activities including calibration and repair. The surface dose rate calculated in Chapter 5 also provides a conservative estimate of a dose rate at 3 feet from the HSM-H which may be encountered during operations associated with removal of debris from HSM-H vents.

The ISFSI license applicant will evaluate the additional dose to station personnel from ISFSI operations, based on the particular storage configuration and site personnel requirements.

10.3.5 Doses During ISFSI Array Expansion

ISFSI expansion should be planned to eliminate the need for entry into a module adjacent to a loaded module. Similarly, during array expansion, when the shield wall is removed, personnel access to the area should be controlled. For a module separated from a loaded HSM-H by an empty module, with temporary shielding at the vent ports of the empty module, the resulting dose will be less than that calculated in Chapter 5 for the side dose rate of an array with an installed shield wall.

10.4 References

1. U.S. Nuclear Regulatory Commission, Regulatory Guide 8.8, Information Relevant to Ensuring That Occupational Exposures at Nuclear Power Stations will be As Low As Is Reasonably Achievable, Revision 3, June 1978.

2. MCNP4C2, Monte Carlo N-Particle Transport Code System, Oak Ridge National Laboratory, CCC-701, RSICC Computer Code Collection, June 2001.

3. U.S. Nuclear Regulatory Commission, Regulatory Guide 8.10, Operating Philosophy for Maintaining Occupational Radiation Exposures as low as is reasonably Achievable, Revision 1-R, May 1977.

4. U.S. Nuclear Regulatory Commission, Regulatory Guide 1.8, Qualification and Training of Personnel for Nuclear Power Plants, Revision 2, April 1987.

5. Title 10 Code of Federal Regulations Part 72, Licensing Requirements for the Independent Storage of Spent Nuclear Fuel and High-Level Radioactive Waste.

6. Title 10 Code of Federal Regulations Part 20, Standards for Protection Against Radiation.

7. U.S. Nuclear Regulatory Commission, Regulatory Guide 8.34, Monitoring Criteria and Methods to Calculate Occupational Radiation Doses, July 1992.

8. Title 40 Code of Federal Regulations Part 190, Environmental Radiation Protection Standards for Nuclear Power Operations.

9. American National Standard Neutron and Gamma-Ray Fluence-to-Dose Factors, ANSI/ANS-6.1.1-1977, American Nuclear Society, LaGrange Park, Illinois, March 1977.

10. US Nuclear Regulatory Commission Interim Staff Guidance ISG-18, The Design/Qualification of Final Closure Welds on Austenitic Stainless. Steel Canisters as Confinement Boundary for Spent Fuel Storage and Containment Boundary for Spent Fuel Transportation.

Table 10-1
Occupational Exposure Summary, NUHOMS® HD System

Location	Task Description	Number of workers	Duration (hr)	Total exposure (person-mrem)	Fraction of the Total Time	Fraction of the Total Dose
Auxiliary Building and Fuel Pool	Place the DSC into the transfer cask	3	1	6	0.016	0.003
	Fill the cask/DSC annulus with clean water and Install the annulus seal	2	2	8	0.031	0.004
	Fill the DSC cavity with water	1	6	12	0.094	0.005
	Place the cask containing the DSC in the fuel pool	5	0.5	5	0.008	0.002
	Load the fuel assemblies into the DSC	3	5	39	0.102	0.018
	Place the inner top cover on the DSC	2	1	4	0.016	0.002
	Remove the cask/DSC from the fuel pool and place them in the decon area	5	0.5	5	0.008	0.002
		1	0.033	9(84)*	0.001	0.004
		1	1	119 (1140)*	0.016	0.053
Cask Decontamination Area	Decontaminate the outer surface of the transfer cask	1	1.75	208	0.028	0.093
		1	1	2	0.016	0.001
	Decontaminate the top region of the cask and DSC	2	0.5	457	0.008	0.205
		1	1	2	0.016	0.001
	Drain water from the DSC	1	0.083	21	0.001	0.009
	Remove cask/DSC annulus seal and set-up welding machine	1	0.25	51	0.004	0.023
		1	1.25	141	0.020	0.063
		1	1.5	3	0.024	0.001
	Weld the inner top cover to the DSC shell and Perform NDE (PT)	2	6	24	0.094	0.011
		1	0.5	57	0.008	0.026
	Drain the cask/DSC annulus and the DSC cavity	1	0.25	28	0.004	0.013
		1	0.017	3	0.000	0.001
		1	0.5	1	0.008	0.000
	Vacuum dry and backfill the DSC with helium	As above	0.78	33	0.012	0.015
	Weld vent and drain port covers and perform NDE (PT)	1	0.5	57	0.008	0.026
	Fit-up the DSC outer top cover plate	1	0.5	1	0.008	0.000
		1	0.5	57	0.008	0.026
	Weld the outer top cover plate to DSC shell and perform NDE (PT)	1	1.25	141	0.020	0.063
		1	1.5	3	0.024	0.001
		2	14	56	0.220	0.025
		1	0.5	57	0.008	0.026
	Install the transfer cask lid	2	1	18	0.016	0.008

continued

Table 10-1
Occupational Exposure Summary, NUHOMS® HD System
(concluded)

Location	Task Description	No. of workers	Duration (hr)	Total exposure (person-mrem)	Fraction of the Total Time	Fraction of the Total Dose
Reactor/Fuel Building Bay	Prepare the cask support skid and transport trailer	2	2	8	0.031	0.004
	Place the cask onto the skid and trailer	2	0.5	152 (1600)*	0.008	0.068
	Secure the cask to the skid	1	0.25	38 (400)*	0.004	0.017
ISFSI Site	Prepare the HSM-H and hydraulic ram	2	2	0	0.031	0.000
	Transport the Cask to ISFSI	6	1	0	0.016	0.000
	Position the Cask in Close Proximity with the HSM-H	3	1	0	0.016	0.000
	Remove the Cask Lid	2	1	68	0.016	0.031
	Align and Dock the Cask with the HSM-H	2	0.25	87	0.004	0.039
	Position and Align Ram with Cask	2	0.5	173	0.008	0.078
	Remove Ram Access Cover Plate	1	0.25	21	0.004	0.009
	Transfer the DSC from the Cask to the HSM-H	3	0.5	0	0.008	0.000
	Lift the Ram Back onto the Trailer and Un-Dock the Cask from the	2	0.083	29	0.001	0.013
	Install HSM-H Access Door	2	0.5	21	0.008	0.009
	Totals	N/A	63.5	2225	1	1

* - Exposure if the transfer cask liquid neutron shield is drained. For this condition, the duration and number of workers should be minimized, the working distance from the cask increased and temporary shielding utilized as required to meet ALARA.

Table 10-2
Total Annual Exposure from 32PTH DSC in HSM-H

Two 1x10 Front To Front Array

Distance (meters)	Back Total Dose (mrem)	1σ Uncertainty (mrem)	1σ Relative Uncertainty
6.1	5850	13	0.002
10	4720	13	0.003
20	2970	10	0.003
30	2070	10	0.005
40	1510	8	0.005
50	1140	7	0.006
60	876	6	0.006
70	691	5	0.007
80	553	4	0.007
90	440	3	0.007
100	362	4	0.010
200	63	2	0.027
300	13	0.5	0.035
400	3.8	0.3	0.069
500	0.9	0.03	0.040
600	0.3	0.02	0.066

Distance (meters)	Side Total Dose (mrem)	1σ Uncertainty (mrem)	1σ Relative Uncertainty
6.1	21100	34	0.002
10	11600	25	0.002
20	4460	15	0.003
30	2530	14	0.005
40	1680	10	0.006
50	1210	10	0.008
60	889	7	0.007
70	691	6	0.009
80	543	6	0.012
90	434	6	0.013
100	348	5	0.014
200	56	1	0.022
300	13	1	0.050
400	3.1	0.2	0.061
500	0.7	0.04	0.049
600	0.2	0.01	0.031

2x10 Back To Back Array

Distance (meters)	Front Total Dose (mrem)	1σ Uncertainty (mrem)	1σ Relative Uncertainty
6.1	57900	46	0.001
10	35500	35	0.001
20	13800	21	0.002
30	7030	14	0.002
40	4210	11	0.003
50	2760	9	0.003
60	1910	7	0.004
70	1400	7	0.005
80	1039	5	0.005
90	812	5	0.006
100	623	4	0.006
200	89	1	0.013
300	18	0.4	0.020
400	4.4	0.1	0.026
500	1.3	0.1	0.052
600	0.4	0.03	0.062

Distance (meters)	Side Total Dose (mrem)	1σ Uncertainty (mrem)	1σ Relative Uncertainty
6.1	6080	14	0.002
10	4530	14	0.003
20	2710	13	0.005
30	1840	11	0.006
40	1340	8	0.006
50	1000	6	0.006
60	769	6	0.007
70	615	6	0.009
80	493	5	0.011
90	395	5	0.012
100	319	4	0.012
200	57	2	0.038
300	12	1	0.068
400	2.6	0.1	0.034
500	0.7	0.03	0.036
600	0.2	0.02	0.104

Table 10-3
NUHOMS® HD System, 32PTH DSC / HSM-H Spectra

Neutron

Group Number	E_{upper} (MeV)	E_{mean} (MeV)	Flux-Dose (Ref. [10]) (mR/hr)/(n/cm^2-sec)	Roof Flux (n/cm^2-sec)	Dose Rate (mR/hr)	Input Current (n/cm^2-sec per mrem/hr)
1	1.00E-02	5.00E-03	3.575E-03	3.48E+02	1.24E+00	9.020E+01
2	1.00E-01	5.50E-02	3.675E-03	2.40E+01	8.83E-02	6.223E+00
3	2.50E-01	1.75E-01	3.598E-02	3.12E+00	1.12E-01	8.086E-01
4	5.00E-01	3.75E-01	7.146E-02	1.64E+00	1.17E-01	4.259E-01
5	1.00E+00	7.50E-01	1.137E-01	1.42E+00	1.61E-01	3.670E-01
6	1.50E+00	1.25E+00	1.299E-01	5.39E-01	7.00E-02	1.395E-01
7	2.00E+00	1.75E+00	1.275E-01	3.47E-01	4.42E-02	8.978E-02
8	4.00E+00	3.00E+00	1.326E-01	5.77E-01	7.64E-02	1.494E-01
9	6.00E+00	5.00E+00	1.562E-01	7.55E-02	1.18E-02	1.957E-02
10	1.00E+01	8.00E+00	1.471E-01	1.43E-02	2.10E-03	3.705E-03
11	1.50E+01	1.25E+01	1.853E-01	3.19E-03	5.92E-04	8.269E-04
12	2.00E+01	1.75E+01	2.200E-01	3.41E-03	7.51E-04	8.842E-04
			Totals	3.80E+02	1.93E+00	**98.4**

Gamma

Group Number	E_{upper} (MeV)	E_{mean} (MeV)	Flux-Dose (Ref. [10]) (mR/hr)/(γ/cm^2-sec)	Roof Flux (γ/cm^2-sec)	Dose Rate (mR/hr)	Input Current (γ/cm^2-sec per mrem/hr)
1	5.00E-02	2.50E-02	8.002E-04	3.60E+02	2.88E-01	1.292E+01
2	1.00E-01	7.50E-02	2.583E-04	1.73E+04	4.48E+00	6.230E+02
3	2.00E-01	1.50E-01	3.793E-04	1.16E+04	4.38E+00	4.150E+02
4	3.00E-01	2.50E-01	6.310E-04	3.21E+03	2.03E+00	1.153E+02
5	4.00E-01	3.50E-01	8.780E-04	1.28E+03	1.12E+00	4.583E+01
6	6.00E-01	5.00E-01	1.153E-03	7.21E+02	8.31E-01	2.590E+01
7	8.00E-01	7.00E-01	1.304E-03	2.33E+02	3.03E-01	8.355E+00
8	1.00E+00	9.00E-01	1.268E-03	1.46E+02	1.86E-01	5.260E+00
9	1.33E+00	1.17E+00	1.079E-03	1.75E+02	1.89E-01	6.297E+00
10	1.66E+00	1.50E+00	7.918E-04	1.20E+02	9.49E-02	4.304E+00
11	2.00E+00	1.83E+00	5.430E-04	2.05E+01	1.11E-02	7.358E-01
12	2.50E+00	2.25E+00	3.241E-04	2.77E+01	8.98E-03	9.946E-01
			Totals	3.52E+04	1.39E+01	**1263.9**

Table 10-4
Summary of ISFSI Surface Activities, 32PTH DSC in HSM-H

2x10 Back-To-Back Array

Source	Area (cm^2)	Neutron Activity (neutrons/sec)	Gamma-Ray Activity (γ/sec)
Roof	3.942E+06	7.490E+08	6.936E+10
Front 1	1.765E+06	8.598E+07	4.523E+10
Front 2	1.765E+06	8.598E+07	4.523E+10
Side 1	7.104E+05	1.294E+07	3.430E+08
Side 2	7.104E+05	1.294E+07	3.430E+08
Total	8.892E+06	9.468E+08	1.605E+11

Two 1x10 Front-to-Front Arrays

Source	Area (cm^2)	Neutron Activity (neutrons/sec)	Gamma-Ray Activity (γ/sec)
Roof	2.257E+06	4.288E+08	3.971E+10
Front 1	1.765E+06	8.598E+07	4.523E+10
Front 2	1.765E+06	4.104E+05	1.079E+09
Side 1	4.068E+05	7.407E+06	1.964E+08
Side 2	4.068E+05	7.407E+06	1.964E+08
Total	6.600E+06	5.300E+08	8.641E+10

Table 10-5
MCNP Front Detector Dose Rates for 2x10 Array, 32PTH DSC in HSM-H

Distance (meters)	Gamma Dose Rate (mrem/hr)	Gamma MCNP 1σ error(1)	Neutron Dose Rate (mrem/hr)	Neutron MCNP 1σ error(1)	Total Dose Rate (mrem/hr)(2)	Combined MCNP 1σ error(3)
6.10E+00	6.24E+00	8.00E-04	3.68E-01	4.10E-03	6.61E+00	0.0008
1.00E+01	3.79E+00	1.00E-03	2.57E-01	4.90E-03	4.05E+00	0.0010
2.00E+01	1.44E+00	1.50E-03	1.34E-01	7.30E-03	1.58E+00	0.0015
3.00E+01	7.17E-01	1.80E-03	8.53E-02	9.90E-03	8.02E-01	0.0019
4.00E+01	4.20E-01	2.20E-03	6.06E-02	1.41E-02	4.81E-01	0.0026
5.00E+01	2.71E-01	3.20E-03	4.32E-02	1.36E-02	3.15E-01	0.0033
6.00E+01	1.85E-01	3.10E-03	3.23E-02	1.59E-02	2.18E-01	0.0035
7.00E+01	1.35E-01	4.50E-03	2.53E-02	1.77E-02	1.60E-01	0.0047
8.00E+01	9.92E-02	4.10E-03	1.94E-02	1.83E-02	1.19E-01	0.0046
9.00E+01	7.63E-02	5.50E-03	1.64E-02	2.59E-02	9.27E-02	0.0064
1.00E+02	5.90E-02	5.90E-03	1.21E-02	2.16E-02	7.11E-02	0.0061
2.00E+02	8.25E-03	1.31E-02	1.86E-03	4.21E-02	1.01E-02	0.0132
3.00E+02	1.70E-03	2.21E-02	3.28E-04	4.42E-02	2.03E-03	0.0199
4.00E+02	4.18E-04	2.05E-02	8.92E-05	1.16E-01	5.07E-04	0.0265
5.00E+02	1.20E-04	5.38E-02	2.36E-05	1.61E-01	1.43E-04	0.0521
6.00E+02	3.88E-05	5.99E-02	9.45E-06	1.99E-01	4.83E-05	0.0620

(1) Fractional Error from MCNP
(2) Sum of columns 2 and 4
(3) Quadrature sum of columns 3 and 5 (weighted by means)

Table 10-6
MCNP Back Detector Dose Rates for the Two 1x10 Arrays, 32PTH DSC in HSM-H

Distance (meters)	Gamma Dose Rate (mrem/hr)	Gamma MCNP 1σ error(1)	Neutron Dose Rate (mrem/hr)	Neutron MCNP 1σ error(1)	Total Dose Rate (mrem/hr)(2)	Combined MCNP 1σ error(3)
6.10E+00	5.13E-01	0.0019	1.55E-01	0.0074	6.67E-01	0.0022
1.00E+01	4.07E-01	0.0025	1.33E-01	0.0085	5.39E-01	0.0028
2.00E+01	2.49E-01	0.0029	9.08E-02	0.0093	3.39E-01	0.0033
3.00E+01	1.72E-01	0.0047	6.48E-02	0.0113	2.37E-01	0.0046
4.00E+01	1.24E-01	0.0046	4.86E-02	0.0138	1.72E-01	0.0051
5.00E+01	9.29E-02	0.0061	3.67E-02	0.0167	1.30E-01	0.0064
6.00E+01	7.10E-02	0.0058	2.90E-02	0.0173	1.00E-01	0.0065
7.00E+01	5.64E-02	0.0055	2.25E-02	0.0199	7.88E-02	0.0069
8.00E+01	4.47E-02	0.0061	1.85E-02	0.0198	6.32E-02	0.0072
9.00E+01	3.58E-02	0.0057	1.44E-02	0.0206	5.02E-02	0.0072
1.00E+02	2.95E-02	0.0099	1.18E-02	0.0238	4.13E-02	0.0098
2.00E+02	4.99E-03	0.0239	2.18E-03	0.0691	7.17E-03	0.0268
3.00E+02	1.10E-03	0.0355	4.18E-04	0.0860	1.52E-03	0.0350
4.00E+02	3.01E-04	0.0705	1.33E-04	0.1589	4.33E-04	0.0690
5.00E+02	7.80E-05	0.0469	2.01E-05	0.0726	9.82E-05	0.0402
6.00E+02	2.31E-05	0.0833	6.89E-06	0.0674	3.00E-05	0.0660

(1) Fractional Error from MCNP
(2) Sum of columns 2 and 4
(3) Quadrature sum of columns 3 and 5 (weighted by means)

Table 10-7
MCNP Side Detector Dose Rates, 32PTH DSC in HSM-H

2x10 Back-to-Back Array

Distance (meters)	Gamma Dose Rate (mrem/hr)	Gamma MCNP 1σ error(1)	Neutron Dose Rate (mrem/hr)	Neutron MCNP 1σ error(1)	Total Dose Rate (mrem/hr)(2)	Combined MCNP 1σ error(3)
6.10E+00	4.96E-01	2.20E-03	1.97E-01	6.10E-03	6.94E-01	0.0023
1.00E+01	3.73E-01	3.20E-03	1.44E-01	7.50E-03	5.17E-01	0.0031
2.00E+01	2.21E-01	3.90E-03	8.80E-02	1.32E-02	3.09E-01	0.0047
3.00E+01	1.50E-01	5.50E-03	5.97E-02	1.49E-02	2.10E-01	0.0058
4.00E+01	1.09E-01	5.90E-03	4.37E-02	1.49E-02	1.53E-01	0.0060
5.00E+01	8.12E-02	6.30E-03	3.31E-02	1.62E-02	1.14E-01	0.0065
6.00E+01	6.31E-02	7.50E-03	2.47E-02	1.73E-02	8.77E-02	0.0073
7.00E+01	5.00E-02	8.50E-03	2.02E-02	2.53E-02	7.02E-02	0.0095
8.00E+01	4.01E-02	1.14E-02	1.62E-02	2.40E-02	5.63E-02	0.0107
9.00E+01	3.24E-02	1.30E-02	1.27E-02	2.52E-02	4.51E-02	0.0117
1.00E+02	2.59E-02	8.20E-03	1.05E-02	3.60E-02	3.64E-02	0.0119
2.00E+02	4.46E-03	2.24E-02	2.09E-03	1.08E-01	6.55E-03	0.0378
3.00E+02	9.34E-04	2.84E-02	4.03E-04	2.16E-01	1.34E-03	0.0680
4.00E+02	2.22E-04	4.09E-02	7.07E-05	6.02E-02	2.92E-04	0.0343
5.00E+02	5.89E-05	3.50E-02	2.03E-05	9.88E-02	7.92E-05	0.0363
6.00E+02	1.91E-05	1.34E-01	6.41E-06	1.07E-01	2.55E-05	0.1039

Two 1x10 Front-To-Front Arrays

Distance (meters)	Gamma Dose Rate (mrem/hr)	Gamma MCNP 1σ error(1)	Neutron Dose Rate (mrem/hr)	Neutron MCNP 1σ error(1)	Total Dose Rate (mrem/hr)(2)	Combined MCNP 1σ error(3)
6.10E+00	2.18E+00	1.60E-03	2.32E-01	6.80E-03	2.41E+00	0.0016
1.00E+01	1.16E+00	2.00E-03	1.70E-01	9.50E-03	1.33E+00	0.0021
2.00E+01	4.13E-01	3.30E-03	9.68E-02	1.11E-02	5.10E-01	0.0034
3.00E+01	2.24E-01	5.60E-03	6.51E-02	1.45E-02	2.89E-01	0.0054
4.00E+01	1.43E-01	5.00E-03	4.90E-02	1.92E-02	1.92E-01	0.0062
5.00E+01	1.01E-01	7.10E-03	3.68E-02	2.43E-02	1.38E-01	0.0083
6.00E+01	7.42E-02	7.30E-03	2.73E-02	1.88E-02	1.02E-01	0.0074
7.00E+01	5.68E-02	7.80E-03	2.21E-02	2.65E-02	7.89E-02	0.0093
8.00E+01	4.49E-02	1.21E-02	1.71E-02	2.89E-02	6.19E-02	0.0118
9.00E+01	3.55E-02	1.29E-02	1.40E-02	3.27E-02	4.96E-02	0.0131
1.00E+02	2.81E-02	9.10E-03	1.17E-02	4.22E-02	3.98E-02	0.0139
2.00E+02	4.36E-03	1.34E-02	2.04E-03	6.41E-02	6.40E-03	0.0224
3.00E+02	9.96E-04	3.71E-02	4.41E-04	1.41E-01	1.44E-03	0.0504
4.00E+02	2.69E-04	6.74E-02	8.04E-05	1.35E-01	3.50E-04	0.0605
5.00E+02	6.37E-05	6.20E-02	1.92E-05	5.53E-02	8.29E-05	0.0493
6.00E+02	1.71E-05	3.27E-02	6.16E-06	7.19E-02	2.32E-05	0.0307

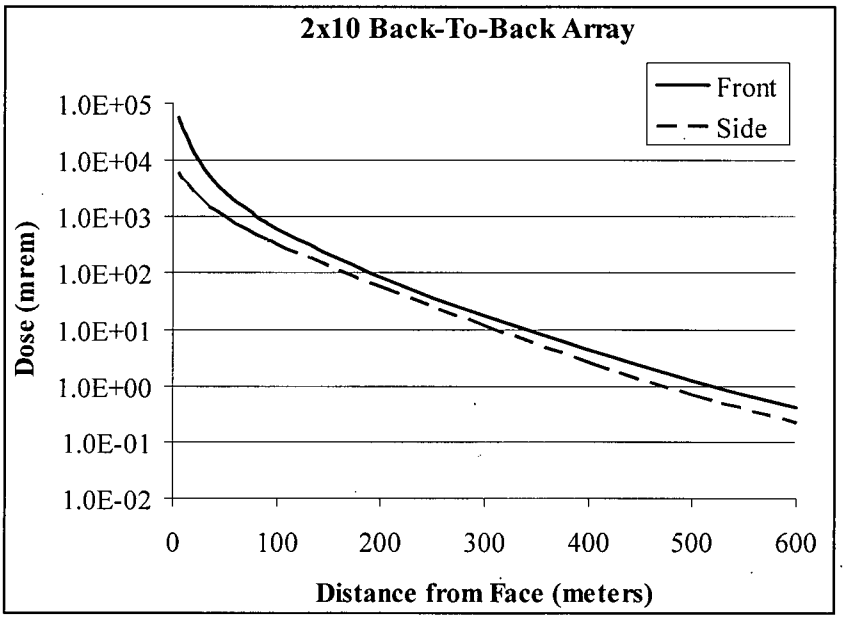

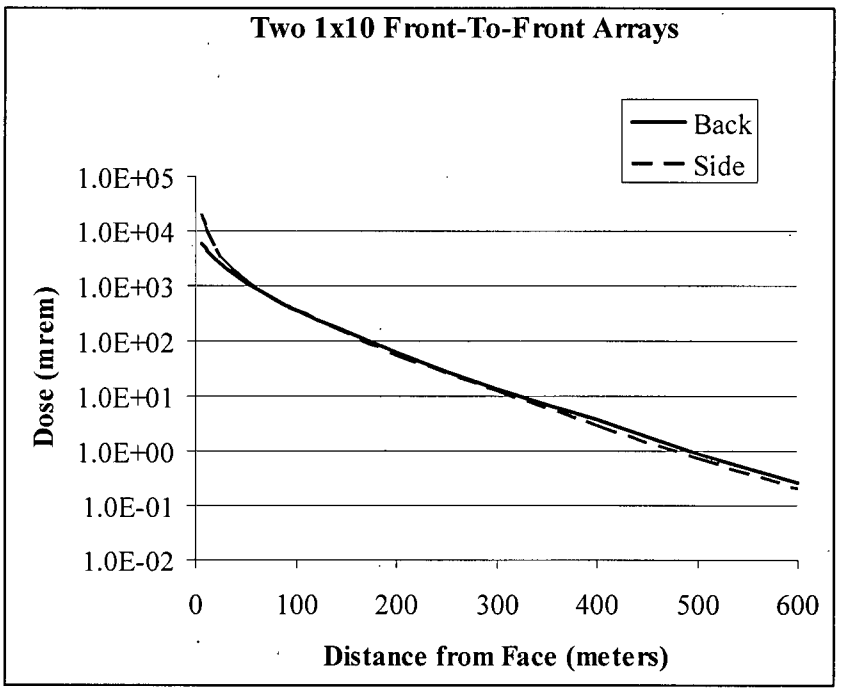

Figure 10-1
Annual Exposure from the ISFSI as a Function of Distance, 32PTH DSC in HSM-H

CHAPTER 11
ACCIDENT ANALYSIS

TABLE OF CONTENTS

11 Accident Analysis 11-1

11.1 Introduction 11-1

11.2 Off-Normal Operation 11-2
11.2.1 Off-Normal Transfer Load 11-3
11.2.2 Extreme Temperature 11-5
11.2.3 Radiological Impact from Off-Normal Operation 11-6

11.3 Postulated Accident 11-7
11.3.1 Cask Drop 11-8
11.3.2 Earthquake 11-10
11.3.3 Tornado Wind and Tornado Missiles Effect on HSM-H 11-11
11.3.4 Tornado Wind and Tornado Missiles Effect on Transfer Cask 11-18
11.3.5 Flood 11-25
11.3.6 Blockage of HSM-H Air Inlet and Outlet Opening 11-25
11.3.7 Lightning 11-26
11.3.8 Fire/Explosion 11-27

11.4 References 11-28

LIST OF FIGURES

11-1 HSM-H Dimensions for Missile Impact Stability Analysis

11 ACCIDENT ANALYSIS

11.1 Introduction

This Chapter describes the postulated off-normal and accident events that might occur during transfer/storage of the 32PTH DSC in an HSM-H at an ISFSI. In addition, this chapter also addresses the potential causes of these events, their detection and consequences, and the corrective course of action to be taken by ISFSI personnel. Accident analyses demonstrate that the functional integrity of the system is maintained by:

1. Maintaining sub-criticality within margins defined in Chapter 6.
2. Maintaining confinement boundary integrity
3. Ensuring fuel retrievability and
4. Maintaining doses within 10CFR 72.106 [1] limits (<5 rem).

The Accident Dose Calculations sections report the expected doses resulting from the postulated event in terms of whole body doses only. The leaktight canister design and the maintenance of confinement boundary integrity under all credible off-normal and accident scenarios ensures no radiation leakage from the 32PTH DSC, thereby limiting dose consequences to direct and scattered radiation doses without any associated inhalation or ingestion doses.

11.2 Off-Normal Operation

Off-normal operations are design events of the second type (Design Event II) as defined in ANSI/ANS 57.9 [2]. Design Event II conditions consist of that set of events that, although not occurring regularly, can be expected to occur with moderate frequency, or on the order of once during a calendar year of ISFSI operation.

For the NUHOMS® HD System, off-normal events could occur during fuel loading, trailer towing, 32PTH DSC transfer and other operational events. The two off-normal events, which bound the range of off-normal conditions, are:

1. A "jammed" 32PTH DSC during loading or unloading from the HSM-H
2. The extreme ambient temperatures of -20 °F (winter) and +115 °F (summer)**

These two events envelope the range of expected off-normal structural loads and temperatures acting on the NUHOMS® HD System.

** The HSM-H structural evaluation is conservative using an extreme ambient temperature of -40 °F (winter) and +117 °F (summer)

11.2.1 Off-Normal Transfer Load

Although unlikely, the postulated off-normal handling event assumes that the leading edge of the 32PTH DSC becomes jammed against some element of the support structure during transfer between the transfer cask and the HSM-H.

Cause of the Event

It is postulated that if the transfer cask is not accurately aligned with respect to the HSM-H, the 32PTH DSC could bind or jam during transfer operations.

The interiors of the transfer cask and the HSM-H are inspected prior to transfer operations to ensure there are no obstacles, and the 32PTH DSC has beveled lead-ins on each end, designed to avoid binding or sticking on small (less than 1/4 inch) obstacles. The transfer cask and the 32PTH DSC support rails inside the HSM-H are also designed with lead-ins to minimize binding or obstruction during 32PTH DSC transfer. The postulated off-normal handling load event assumes that the leading edge of the 32PTH DSC becomes jammed against some element of the support structure because of gross misalignment of the transfer cask.

The interfacing dimensions of the top end of the transfer cask and the HSM-H access opening sleeve are specified such that docking of the transfer cask with the HSM-H is not possible should gross misalignments between the transfer cask and HSM-H exist.

Detection of the Event

The normal load to push/pull the DSC in and out of the Transfer Cask/HSM-H is less than 32 kips (110 kips x 0.2/Cos 30). This movement is performed at a very low speed. System operating procedures and technical specification limits defining the safeguards to be provided ensure that the system design margins are not compromised. If the 32PTH DSC were to jam or bind during transfer, the hydraulic pressure in the ram would increase. The off-normal load set for the "jammed 32PTH DSC" for both push/pull is 80 kips. This load is administrative controlled to ensure that during the transfer operation this load will not be exceeded.

The maximum ram push/pull forces are limited by design features to a maximum load equal to 110 kips (accident condition). Override controls are available to the operator to increase the ram force up to its maximum design load, equal to 110 kips, or to interrupt the transfer operation at any time. During the transfer operation, the force exerted on the 32PTH DSC by the hydraulic ram is that required to first overcome the static frictional resisting force between the transfer cask rails and the 32PTH DSC. Once the 32PTH DSC begins to slide, the resisting force is a function of the sliding friction coefficient between the 32PTH DSC and the transfer cask rails and/or between the 32PTH-DSC and the HSM-H support rails. If motion is prevented, the hydraulic pressure increases, thereby increasing the force on the 32PTH DSC until the hydraulic ram system pressure limit is reached. This limit is controlled so that adequate force is available to overcome variations in surface finish, etc., but is sufficiently low to ensure that component damage does not occur.

Analysis of Effects and Consequences

The 32PTH DSC and the HSM-H are designed and analyzed for off-normal transfer loads of 80 kips and accident loads of 110 kips (maximum force that the ram is able to develop), during insertion (loading) and during retrieval (unloading) operations. These analyses are discussed in Chapter 3, Appendix 3.9.1, Load Cases 21 &22 for off-normal conditions (page 3.9.1-53) and Load Cases 23 & 24 for accident conditions (pages 53 & 54). For either loading or unloading of the 32PTH DSC under off-normal and accident conditions, the stresses on the shell assembly components are demonstrated to be within the ASME allowable stress limits. Therefore, permanent deformation of the 32PTH DSC shell components does not occur. The internal basket assembly components are unaffected by these loads based or clearances provided between support rods and 32PTH DSC internal envelope.

There is no breach of the confinement pressure boundary and, therefore, no potential for release of radioactive material exists.

Corrective Actions

The required corrective action is to reverse the direction of the force being applied to the 32PTH DSC by the ram, and return the 32PTH DSC to its previous position. Since no permanent deformation of the 32PTH DSC occurs, the sliding of the 32PTH DSC back to its previous position is unimpeded. The transfer cask alignment is then rechecked, and the transfer cask repositioned as necessary before attempts at transfer are renewed.

11.2.2 Extreme Temperature

The NUHOMS® HD System is designed for use at ambient temperatures of -20°F (winter) and 115°F (summer). The structural evaluation of the HSM-H concrete module is conservatively based on ambient temperatures of -40°F (winter) and 117°F (summer). Even though these extreme temperatures would likely occur for a short period of time, it is conservatively assumed that these temperatures occur for a sufficient duration to produce steady state temperature distributions in each of the affected NUHOMS® components. Each licensee should verify that this range of ambient temperatures envelopes the design basis ambient temperatures for the ISFSI site. The NUHOMS® HD system components affected by the postulated extreme ambient temperatures are the transfer cask and DSC during their transfer from the plant's fuel/reactor building to the ISFSI site, and the HSM-H during storage of a DSC.

Cause of the Event

Off-normal ambient temperatures are natural phenomena.

Detection of Event

Off-normal ambient temperature conditions will be confirmed by the licensee to be bounding for their site.

Analysis of Effects and Consequences

Thermal analysis of the Advanced NUHOMS® System for extreme ambient conditions is presented in Chapter 4. The effects of extreme ambient temperatures on the NUHOMS® HD System are analyzed as follows:

Components	SAR Sections
Basket	Appendix 3.9.1, Section 3.9.1.2.3 (page 3.9.1-12)
Canister	Appendix 3.9.1, Load Cases 4 & 5, (pages 3.9.1-58 & 59)
Transfer Cask	Appendix 3.9.2, Load Cases 4 & 5 (page 3.9.2-22)
HSM-H	Appendix 3.9.9, Section 3.9.9.9 (page 3.9.9-18)

Corrective Actions

None

11.2.3 Radiological Impact from Off-Normal Operations

For loading and unloading operations under off-normal conditions, the stresses on the 32PTH DSC shell assembly components are demonstrated to be within the ASME Code stress limits. Therefore, there is no permanent deformation of the shell. Since there is no potential for breach of the confinement pressure boundary, there is no potential for release of radioactive material.

The 32PTH DSC shell assembly stresses due to extreme ambient temperature conditions are also demonstrated to be less than the ASME Code stress limits as shown in Chapter 3, Appendix 3.9.1. The HSM-H stresses due to extreme ambient temperature conditions are within the provisions of the ACI Code (Appendix 3.9.9). Therefore, no damage will occur in the shell assembly or the HSM-H. There is no potential for breach of the confinement boundary and therefore, no potential for release of radioactive material.

11.3 Postulated Accident

The design basis accident events specified by ANSI/ANS 57.9-1984 [2] and other postulated accidents that may affect the normal safe operation of the NUHOMS® HD System are addressed in this section.

The following sections provide descriptions of the analyses performed for each accident condition. The analyses demonstrate that the requirements of 10CFR 72.122 are met and that adequate safety margins exist for the NUHOMS® HD System design. The resulting accident condition stresses in the NUHOMS® HD System components are evaluated and compared with the applicable code limits set forth in Chapter 2.

Radiological calculations are performed to confirm that on-site and off-site dose rates are within acceptable limits.

The postulated accident conditions addressed in this section include:

- Cask Drop
- Earthquake
- Tornado Wind Pressure and Tornado Generated Missiles
- Flood
- Blockage of HSM-H Air Inlet and Outlet Openings
- Lightning
- Fire/Explosion

11.3.1 Cask Drop

Cause of Accident

As described in Chapter 8, handling operations involving hoisting and movement of the on-site transfer cask and 32PTH DSC are typically performed inside the plant's fuel handling building. These include utilizing the crane for placement of the empty 32PTH DSC into the transfer cask cavity, lifting the transfer cask/32PTH DSC into and out of the plant's spent fuel pool, and placement of the transfer cask/32PTH DSC onto the transport skid/trailer. An analysis of the plant's lifting devices used for these operations, including the crane and lifting yoke, is needed to address a postulated drop accident for the transfer cask and its contents. The postulated drop accident scenarios addressed in the plant's 10CFR 50 licensing basis are plant specific and should be addressed by the licensee.

Once the transfer cask is loaded onto the transport skid/trailer and secured, it is pulled to the HSM-H site by a tractor vehicle. A predetermined route is chosen to minimize the potential hazards that could occur during transport. This movement is performed at very low speeds. System operating procedures and technical specification limits defining the safeguards to be provided ensure that the system design margins are not compromised. As a result, it is highly unlikely that any plausible incidents leading to a transfer cask drop accident could occur. Similarly, at the ISFSI site, the transport skid/trailer is backed-up to, and aligned with, the HSM-H using hydraulic positioning equipment. The transfer cask is then docked with, and secured to, the HSM-H access opening. The loaded 32PTH DSC is transferred to or from the HSM-H using a hydraulic ram system. The hold down mechanisms that secure the transfer cask to the transport skid/trailer remain in place at all times during the 32PTH DSC transport. As a result, there is no reasonable way during these operations for a cask drop accident to occur.

Lifts of the transfer cask loaded with the dry storage canister are made within the existing heavy loads requirements and procedures of the licensed nuclear power plant. The transfer cask design meets requirements of NUREG-0612 and ANSI N14.6.

The transfer cask is transported to the ISFAI in a horizontal configuration. Therefore, the only credible drop accident during storage or transfer operations is a side drop.

The transfer cask and dry storage canister are evaluated for a postulated end and corner drops to demonstrate structural integrity during transport and plant handling. However, the fuel cladding structural integrity has not been demonstrated for these scenarios. Therefore, the user is required to demonstrate fuel cladding structural integrity under 10CFR50 postulated drop accidents or demonstrate that the drop accidents are not credible.

Accident Analysis

The stress analyses are performed in Chapter 3, Appendix 3.9.1 for 32PTH DSC and Appendix 3.9.2 for the Transfer Cask.

Components	SAR Sections
Basket	Appendix 3.9.1, Section 3.9.1.2.3 (pages 3.9.1-15 to 19)
Canister	Appendix 3.9.1, Load Cases 6 through 17, (pages 3.9.1-46 to 50)
Transfer Cask	Appendix 3.9.2, Load Cases 7 through 9 (pages 3.9.2-24 to 25)
Fuel Cladding	Section 3.5.3, Appendix 3.9.8

Accident Dose Calculation

Based on analysis results presented in Appendix 3.9.1 and Appendix 3.9.2, the accidental transfer cask drop scenarios do not breach the transfer cask/32PTH DSC confinement boundaries. The function of transfer cask lead shielding is not compromised by these drops. The transfer cask neutron shield, however, may be damaged in an accidental drop.

The transfer cask surface dose rate, with the neutron shield intact for the 32PTH DSC in the transfer cask is calculated in Chapter 5 of this SAR as 384 mrem/hr gamma and 125 mrem/hr neutron.

The dose rate at the transfer cask surface due to the loss of the neutron shield is also calculated; at 1 meter from the cask, the peak dose is 186 mrem/hr gamma and 2200 mrem/hr neutron. The dose at the site boundary would be significantly below 2.4 rem/hr and thus meet the acceptance criteria of 5 rem.

Corrective Actions

The DSC will be inspected for damage, and the DSC opened and the fuel removed for inspection, as necessary. Removal of the transfer cask top cover plate may require cutting of the bolts in the event of a corner drop onto the top end. These operations will take place in the plant fuel building decontamination area and spent fuel pool after recovery of the transfer cask. Following recovery of the transfer cask and unloading of the DSC, the transfer cask will be inspected, repaired and tested as appropriate prior to reuse.

For recovery of the cask and contents, it may be necessary to develop a special sling/lifting apparatus to move the transfer cask from the drop site to the fuel pool. This may require several weeks of planning to ensure all steps are correctly organized. During this time, lead blankets may be added to the transfer cask to minimize on-site exposure to site operations personnel. The transfer cask would be roped off to ensure the safety of the site personnel.

11.3.2 Earthquake

Cause of Accident

The seismic design criteria for the NUHOMS® HD System is consistent with the criteria set forth in Chapter 2, Section 2.2.3, with the exception that the NRC Regulatory Guide 1.60 (R.G. 1.60) [3] response spectra is anchored to a maximum ground acceleration of 0.30g (instead of 0.25g) for the horizontal components and 0.20g (instead of 0.17g) for the vertical component. The results of the frequency analysis of the HSM-H structure (which includes a simplified model of the DSC) yield a lowest frequency of 23.2 Hz in the transverse direction and 28.4 Hz in the longitudinal direction. The lowest vertical frequency exceeds 33 Hz. Thus, based on the R.G. 1.60 response spectra amplifications, the corresponding seismic accelerations used for the design of the HSM-H are 0.37g and 0.33g in the transverse and longitudinal directions respectively and 0.20g in the vertical direction. The corresponding accelerations applicable to the DSC are 0.41g and 0.36g in the transverse and longitudinal directions, respectively, and 0.20g in the vertical direction.

Accident Analysis

The seismic analyses of the components which are important to safety are analyzed as follows:

Components	SAR Sections
Basket	Appendix 3.9.1, Section 3.9.1.2.3 (page 3.9.1-21)
Canister	Appendix 3.9.1, Section 3.9.1.3.2 (page 3.9.1-58)
Transfer Cask	Appendix 3.9.2, Load Case 6 (page 3.9.2-22)
HSM-H	Appendix 3.9.9, Section 3.9.9.2 (page 3.9.9-23)

The results of these analyses show that seismic stresses are well below ASME code allowables.

Accident Dose Calculations

All the components which are important to safety are designed and analyzed to withstand the design basis earthquake accident. Hence, no radiation is released and there is no associated dose increase due to this event.

Corrective Actions

After a seismic event, all components would be inspected for damage. Any debris would be removed. An evaluation would be performed to determine if the system components were still within the licensed design basis.

11.3.3 Tornado Wind and Tornado Missiles Effect on HSM-H

11.3.3.1 Cause of Accident

In accordance with ANSI-57.9 [2] and 10CFR 72.122 [1], the NUHOMS® HD System is designed for tornado effects including tornado wind loads. In addition, the NUHOMS® HD System is also designed for tornado missile effects. The NUHOMS® HD System is designed to be located anywhere within the United States; therefore, the most severe tornado wind and missile loadings specified by NUREG-0800 [4] and NRC Regulatory Guide 1.76 [5] are selected as a design basis for this postulated accident. The determination of the tornado wind pressures and tornado missile loads acting on the NUHOMS® HD System are detailed in Chapter 2, Section 2.2.1.

11.3.3.2 Stability and Stress Analysis

Stability and stress analyses are performed to determine the response of the HSM-H to tornado wind pressure loads. The stability analyses are performed using closed-form calculation methods to determine the sliding and overturning response of the HSM-H array. A single HSM-H with both the end and the rear shield walls is conservatively selected for the analyses. The stress analyses are performed using the ANSYS [6] finite element model of a single HSM-H to determine design forces and moments. These conservative generic analyses envelop the effects of wind pressures on the HSM-H array. These analyses are described in details in Appendix 3.9.9, Section 3.9.9.10.1. Thus, the requirements of 10CFR 72.122 are met.

In addition, the HSM-H is evaluated for tornado missiles. The adequacy of the HSM-H to resist tornado missile loads is addressed using empirical formulae [7]. These evaluations are described in the following sections.

11.3.3.3 Local Damage Evaluation

Local missile impact effects consist of (a) missile penetration into the target, (b) missile perforation through the target and (c) spalling and scabbing of the target. This also includes punching shear in the region of the target. As per the ACI code [8] if the concrete thickness is at least 20% greater than that required to prevent perforation, the punching shear requirement of the code need not be checked. Several empirical formulas are available and are used to predict local damage effects.

The following enveloping missiles (based on the mass of the missile) are considered for local damage:

- Utility pole
- Armor piercing artillery shell
- 12" diameter steel pipe missile

Large deformable missiles such as automobiles do not penetrate the structure. Therefore, the local effects from an automobile are evaluated using punching shear criteria of the ACI Code [8].

The following empirical formulas are used to determine the local damage effects:

Reinforced Concrete Target

(a) Modified National Defense Research Committee (NDRC) formulas for penetration depth [7]:

$$x = [4KNWd^{-0.8}(v_o/1000d)^{1.8}]^{0.5} \quad \text{for } x/d \leq 2.0$$
$$x = \{[KNW\,(v_o/1000d)^{1.8}] + d\} \quad \text{for } x/d > 2.0$$

where,
- x = Missile penetration depth, inches
- K = concrete penetrability factor = $180/\sqrt{fc'}$
- N = projectile shape factor
  - = 0.72 flat nosed
  - = 0.84 blunt nosed
  - = 1.0 bullet nosed (spherical end)
  - = 1.14 very sharp nose
- W = weight of missile, lbs
- v_o = striking velocity of missile, fps
- d = effective projectile diameter, inches.
  for a solid cylinder, d = diameter of projectile and
  for a non-solid cylinder, $d = (4A_c/\pi)^{1/2}$
- A_c = projectile impact area, in^2

(b) Modified NDRC formula for perforation thickness [7]:

$$(e/d) = 3.19(x/d) - 0.718(x/d)^2 \quad \text{for } x/d \leq 1.35$$
$$(e/d) = 1.32 + 1.24\,(x/d) \quad \text{for } 1.35 \leq x/d \leq 13.5$$

where e = perforation thickness, in.

In order to provide an adequate margin of safety, the design thickness $t_d = 1.2\,e$ [8]

(c) Modified NDRC formula for scabbing thickness [7]:

$$(s/d) = 7.91(x/d) - 5.06(x/d)^2 \quad \text{for } x/d \leq 0.65$$
$$(s/d) = 2.12 + 1.36\,(x/d) \quad \text{for } 0.65 \leq x/d \leq 11.75$$

where s = scabbing thickness, in.

In order to provide an adequate margin of safety, the design thickness $t_d = 1.2\,s$ [8]

The concrete targets of the HSM-H which may be subjected to local damage due to missile impact are:

- 44" thick roof
- 42" thick (minimum) front wall
- 36" thick end shield wall with 12" thick side wall (No gap between shield wall and side wall)
- 36" thick rear shield wall with 12" thick (minimum) rear wall
- 36" thick end shield wall at the side of the roof (with vent opening) and at the bottom with 6" gap between the shield wall and the side wall.
- 30.375" thick composite shielding door (7.875" steel in front, 22.5" concrete at rear)

Steel Targets

The steel barriers subjected to missile impact are designed to preclude perforation. The steel plate thickness for threshold of perforation is [9]:

$$T_p = (E_k)^{2/3} / 672D$$

Where: $E_k = M_m v_o^2/2$

T_p = steel plate thickness for threshold of perforation (in)

E_k = missile kinetic energy (ft-lbs)

M_m = mass of the missile (lb-sec^2 /ft)

v_o = missile striking velocity (fps)

D = missile diameter (in), for pipe missiles, D is the outside diameter of the pipe

The design thickness to prevent perforation is $t_p = 1.25\ T_p$ [9].

The steel target of the HSM-H which may be subjected to local damage due to missile impact is the composite steel door (7.875" steel in front).

(A) Local Missile Impact Effects of Utility Pole Missile

The wood missiles (utility pole missile) do not have sufficient strength to penetrate a concrete target and the scabbing thickness required for wood missiles is substantially less than that required for a steel missile with the same mass and velocity. Practical wooden pole missiles are not capable of causing local damage to walls 12 inches thick, or greater for the missile velocities considered. Because none of the concrete targets are less than 12 inch thick, the postulated wood missiles will not cause any local damage to the HSM-H concrete structure. Steel targets are also resistant to penetration which implies that only nondeformable missiles can perforate a steel target.

(B) Local Missile Impact Effects of Armor Piercing Artillery Shell

Concrete Wall Evaluation:

d	=	diameter of missile = 8"
W	=	280 lbs (conservatively assumed)
Vo	=	185 fps
fc'	=	5000 psi
K	=	180/√5000 = 2.55
N	=	0.84 blunt nosed

Penetration thickness	x	=	4.67 in for x/d = 0.584 ≤ 2
Perforation thickness	e	=	12.95"
Required Perforation thickness		=	1.2*12.95 = 15.5"
Scabbing thickness	s	=	23.1" inches
Required scabbing thickness		=	1.2*23.2 = 27.7"

Shielded Door Evaluation:

Required perforation thickness of steel is 0.66" which is less than 7.875". Therefore, the missile will not perforate the steel in the shielded door.

(C) Local Missile Impact Effects of 12 Inch Diameter Steel Pipe Missile

Concrete Wall Evaluation:

Diameter of missile = 12.75" (Outer diameter of 12" dia Sch 40 pipe)
Contact surface area = A_c = 15.7 in^2 (cross section metal area of 12" dia Sch 40 pipe)
Effective diameter = d = $(4*15.7/\pi)^{1/2}$ = 4.47 inches

W	=	1500 lbs
v_o	=	205 fps
f_c'	=	5000 psi
K	=	180/√5000 = 2.55
N	=	0.72 flat nosed

Perforation thickness x = 15.2 in for x/d > 2

Perforation thickness	e = 24.75 in
Required perforation thickness	1.2*24.75 = 29.7"
Scabbing thickness	s = 30.15 inches

Required scabbing thickness = 1.2*30.15 = 36.2 inches

The roof (44" thick), front wall (42" thick) and the shield walls (36" thick) will not be perforated. However, the missile may produce scabbing in the end shield wall above the side walls and lower 40" of the end shield wall. Assuming some scabbed concrete from the end shield will fall into the vent openings, it will not cause any problem in the safe retrieval of the DSC from the module.

Composite Shield Door Evaluation

M_m = 1500/32.2 = 46.6 lb-sec^2/ft

v_s = 205 fps

E_k = 46.6 * 205*205/2=979182

D = 12.75 in

Tp = $(979182)^{2/3}$ / (672*12.75) = 1.16 inches

The required thickness = 1.25 Tp = 1.25*1.16 = 1.45 inches

The composite shield door will not be perforated by this missile.

11.3.3.4 Missile Impact Analysis

The HSM-H stability and potential damage due to impact of the postulated DBT massive missile consisting of a 4000 lb. automobile, 20 sq. ft. frontal area traveling at 195 ft/sec., is evaluated. The massive missile is assumed to impact the shield wall of an end module in an array. Using the principles of conservation of momentum with a coefficient of restitution of zero, the analysis presented below demonstrates that the end module remains stable and the missile energy is dissipated by sliding or slight tipping of the module.

Using conservation of momentum, the missile impact force equals the change in linear (sliding) or angular (overturning) momentum of the HSM-H. The HSM-H velocities immediately after impact are:

Sliding: $V = (m*v_i) / (M+m)$ (Eq. 11.3-1)

Overturning: $\omega_b = (m*d_m*v_i) / (m*d_m^2 + I_B)$ (Eq. 11.3-2)

Where, V = initial linear velocity of module after impact

v_i = 195 ft/sec = initial velocity of missile (conservative)
ω_B = initial rotational velocity about bottom right corner of the module and end shield walls (Figure 11-1)
d_m = Vertical distance of the CG of the missile from B (Figure 11-1) = 198 inches
m = 4000/386.4 = 10.35 lb-sec²/in = mass of the missile
M = (290.0+110+2*172.0)*1000/386.4 = 1925.5 lb-sec² /in = Mass of loaded HSM-H + End Shield walls
d = = 118.77, Elevation of the CG of the loaded HSM-H
I_B = Mass moment of inertia of loaded HSM-H about point B (Figure 11-1) = 3.85 x 10^7 lb-sec²-in (conservatively used)

Sliding:

From Eq. 11.3-1: V = 12.51 in/sec = 1.043 ft/sec

For an impact at the bottom of the HSM-H wall, the kinetic energy imparted to the HSM-H is absorbed by sliding friction between the concrete of the HSM-H and the basemat. Coefficient of friction is 0.6 [8].

Assuming that the missile impact load results in sliding of the HSM-H and equating the kinetic energy generated by the moving module to the work done by sliding friction force gives:

$$\mu * g * (M+m) * \Delta = (M+m)*V^2/2$$
$$\Delta = 0.0281 \text{ ft} = 0.34 \text{ inch}$$

Therefore, a massive missile impact on a single HSM-H will slide the complete module approximately 0.34 inches sideways. The sliding distance will be significantly reduced due to presence of more than one module side by side.

Therefore, the sliding displacement of the modules due to a massive missile impact is insignificant and will not cause any structural damage.

Overturning:

When the massive missile impacts at the top of the HSM-H, the missile energy is absorbed by plastic deformation of the missile and in rotation of the HSM-H. Therefore, equating the loss of kinetic energy to increase in the potential energy:

$$I_B\, \omega_B^2 /2 = M *g*d\, [\cos(\beta+\alpha-90)-\cos\beta] \quad \text{(Figure 11-1)}$$

From Eq. 11.2-2: ω_B = 0.12372 rad/sec

β = $\tan^{-1}$ {(52)/ 118.77)= 24.65°

M = 1480 lb-sec²/in

cos(24.65+α-90) - cos (24.65) = 0.00433

$$\cos(24.65+\alpha-90) = 0.00433 + 0.907411 = 0.911741$$

$$90-\alpha = 24.85-24.25 = 0.60$$

Therefore, a loaded HSM-H rotates a maximum of 0.60° from vertical. The loaded HSM-H is stable against overturning as tip-over does not occur until the CG rotates past the edge point (point B, Figure 11-1) to an angle of more than 24.65° [= $\tan^{-1}(52.0/118.77)$].

11.3.3.5 Accident Dose Calculation

As shown in the above evaluation, the tornado wind and tornado missiles do not breach the confinement boundary. Localized scabbing of the end shield wall may be possible. Table 10-2 presents dose rates for an ISFSI array of HSM-Hs. Side and/or back dose rates at 100 meters are shown to be around 300 - 350 mrem. Localized scabbing of the end/back shield wall (one HSM-H unit), where a couple of inches of concrete may be removed, would have a negligible effect on the dose at 100 meters (site boundary) from the ISFSI. Even if one assumes that the calculated dose rate doubles, it remains well below the acceptance level of 5 rem.

11.3.3.6 Corrective Action

After excessive high winds or a tornado, the HSM-Hs would be inspected for damage. Any debris would be removed. Any damage resulting from impact with a missile would be evaluated to determine if the system was still within the licensed design basis.

11.3.4 Tornado Wind and Tornado Missiles Effect on Transfer Cask

The transfer cask is evaluated for the tornado wind speed and missile specified in Chapter 2, Section 2.2.1. The maximum DBT tornado wind speed of 360 mph produces a design pressure of 304 psf. The 4000 pound automobile and 276 pound eight inch diameter shell missiles were also considered. The other types of missiles are enveloped by the eight inch shell missile.

This analysis is performed for the cask secured in the horizontal position on the support skid. The following criteria are used to evaluate the adequacy of the transfer cask for the loads described above.

- Penetration Resistance
- Impact Stress Analysis

Stability analysis is not required since the cask is already evaluated for a design basis cask drop accident.

11.3.4.1 Penetration Resistance

There are two equations available from literatures for calculating the penetration, T, into the transfer cask outer structural shell and its end covers when the cask is impacted by the armor piercing artillery missile. The neutron shield shell outside the cask structural shell is conservatively ignored for absorbing any impact energy.

$$T_1 = [KE / (2.4S_u D^{1.6})]^{0.71} \quad [10]$$
$$T_2 = (KE^{2/3}) / (672D) \quad [11]$$

Where,

$KE = ½(mV^2)$
m = Mass of missile, lb_m
V = Velocity of missile, in/sec
D = Missile diameter, in
S_u = 94,200 psi (cask top cover, SA-240 Gr. XM-19)
= 66,200 psi (cask structural shell and bottom cover, SA-240 Gr.304)

The penetration and stress calculations for the cask under impact of missile 8" diameter, 276 lbs armor piercing artillery shell are as follows:

$m = 276\ lb_m$
$V = 185$ ft/sec
$D = 8$ in
$KE = ½ \times m \times V^2$
$= [½ \times 276\ lb_m \times (185 \times 12)^2\ in^2 / sec^2] \times [1\ lb_f / (386.4\ lb_m \times in / sec^2)]$
$= 1{,}760{,}143$ in-lb_f
$= 146{,}678$ ft-lb_f
$T_1 = [KE / (2.4S_u D^{1.6})]^{0.71}$

$= [1{,}760{,}143 / (2.4 \times 66{,}200 \times 8^{1.6})]^{0.71}$
$= 0.52" < 1.5"$

The thickness of the cask outer structural shell is 1.5 ", which is greater than the calculated missile penetration of 0.52". Therefore the missile will not penetrate through the cask structural outer shell. A second equation is also used for calculation of the missile penetration into the cask shell and provides a matching result as follows.

$T_2 = (KE^{2/3}) / (672D)$
$= (146{,}678^{2/3}) / (672 \times 8)$
$= 0.52" < 1.5"$

11.3.4.2 Impact Stress Analysis

Tornado Wind Load

Chapter 2, Section 2.2.1.1 specifies a maximum tornado wind speed at 360 mph. The corresponding velocity pressure, q_z , can be calculated by Eq. 6-1 of [12].

$$q_z = 0.00256 K_z K_{zt} V^2 I \ (lb/ft^2)$$

Where,

K_z = Velocity pressure exposure coefficient
= 1.03 (Height above ground < 15 ft in Exposure D, Table 6-3 of [12]
K_{zt} = Topographic factor
= 1
V = Basic wind speed
= 360 mph
I = Importance factor
= 1.15 (Category IV, Table 6-2 of [12])
$q_z = 0.00256 \times 1.03 \times 1 \times 1.15 = 393 \ lb/ft^2$

(a) Transverse wind pressure acting on cask shell surface

The projected area of the transfer cask normal to the wind is equal to the OD (92.2 inch) of the neutron shield multiplied to the length of the cask. The total wind force is then equal to the wind pressure multiplied to this projected area. This total wind force is equivalent to a line force, p, acting at the elevation of the cask centerline and along the entire cask length. This wind force will be assumed to be solely resisted only by the cask outer structural shell, which has a length of 193.2" with an OD of 82.7" and a thickness of 1.5".

$p = q_z \times$ (OD of neutron shield)
$= 393 \ lb/ft^2 \times (92.2 / 12) \ ft$

$= 3019.6$ lb/ft
$= 251.63$ lb/in

Case 9c in Table 31 of [13] provides stress formula for a thin-walled cylindrical vessel supported at both ends and subjected to a uniform load over the entire length of its top element as follows.

$B = [12(1-\upsilon^2)]^{1/8} = 1.348 \quad , \upsilon = 0.3$

Maximum hoop membrane stress,

$$\sigma_2 = -0.492\, B\, p\, R^{3/4} L^{-1/2} t^{-5/4}$$
$$= -0.492 \times (1.348) \times 251.63 \times (82.7/2)^{3/4} \times (193.32)^{-1/2} \times (1.5)^{-5/4}$$
$$= -117.9 \text{ psi}$$

Maximum hoop bending stress,

$$\sigma_2' = -1.217\, B^{-1}\, p\, R^{1/4} L^{1/2} t^{-7/4}$$
$$= -1.217 \times (1.348)^{-1} \times 251.63 \times (82.7/2)^{1/4} \times (193.32)^{1/2} \times (1.5)^{-7/4}$$
$$= -3939.7 \text{ psi}$$

Maximum hoop membrane plus bending stress,

$$(\sigma_2)_{Total} = \sigma_2 + \sigma_2' = -117.9 \text{ psi} - 3939.7 \text{ psi} = -4058 \text{ psi}$$

Maximum axial membrane stress,

$$\sigma_1 = \text{Axial membrane stress}$$
$$= -0.1188\, B^3\, p\, R^{1/4} L^{1/2} t^{-7/4}$$
$$= -0.1188 \times (1.348)^3 \times 251.63 \times (82.7/2)^{1/4} \times 193.32^{1/2} \times (1.5)^{-7/4}$$
$$= -1270 \text{ psi}$$

Maximum axial bending stress,

$$\sigma_1' \approx \upsilon \times \sigma_2' = 0.3 \times (-3939.7 \text{ psi}) = -1181.9 \text{ psi}$$

Maximum axial membrane plus bending stress,

$$(\sigma_1)_{Total} = \sigma_1 + \sigma_1' = -1270 \text{ psi} + (-1181.9 \text{ psi}) = -2451.7 \text{ psi}$$

Maximum membrane plus bending stress intensity $= 0 - (-4058) = 4058$ psi

The ASME code allowable stress for the general membrane stress intensity will be conservatively used for evaluation of the above calculated maximum membrane plus bending

stress intensity. The Service Level D allowable stress for the membrane stress intensity is the lesser of $2.4S_m$ and $0.7S_u$. For SA-240 Gr. 304 cask structural shell material, S_m = 20,000 psi at 300°F and S_u = 66,200 psi. Thus the allowable stress is $0.7S_u$ = 46,340 psi.

Therefore the maximum calculated membrane plus bending stress intensity, under tornado wind load, in the cask shell is acceptable.

(b) Axial wind pressure acting on the top end cover of the transfer cask

Case 10b in Table 24 of [13] provides formula for calculating the resultant moment on the 1.5" recessed flange thickness of the fixed cask top end plate under the wind pressure.

Maximum bending moment,

$$M_{ra} = -q_z a^2/8$$
$$= -393 \text{ lb/ft}^2 \times (1 \text{ ft}^2 / 144 \text{ in}^2) \times (82.7/2 \text{ in})^2 / 8$$
$$= -583.3 \text{ in-lb/in}$$

Maximum bending stress,

$$\sigma = 6M_{ra} / t^2$$
$$= 6 \times (583.3 \text{ in-lb/in}) / (1.5 \text{ in})^2$$
$$= 1555 \text{ psi} < 46{,}340 \text{ psi} \quad \text{OK}$$

(c) Axial wind pressure acting on the bottom end cover of the transfer cask

Case 2f in Table 24 of [13] provides formula for calculating the resultant moment on the 2" thick fixed bottom end plate of the cask under the wind pressure.

b = 14" = radius of the cask bottom ram penetration ring
a = 81.7" / 2 = 40.85" = Outer radius of bottom end plate
b/a = .3427 $\Rightarrow K_{Mra} = -0.0888$ (By interpolation)

Maximum bending moment,

$$M_{ra} = K_{Mra}\, q_z\, a^2 = -0.0888 \times 393/144 \times 40.85^2 = -404.4 \text{ in-lb/in}$$

Maximum bending stress,

$$\sigma = 6M_{ra} / t^2 = 6 \times (404.4 \text{ in-lb/in}) / (2 \text{ in})^2 = 607 \text{ psi} < 46{,}340 \text{ psi} \quad \text{OK}$$

Massive Automobile Missile

The impact forces applied to the cask as it is struck by the automobile missile is determined as follows:

The massive automobile missile is assumed to crush 3 feet under a constant force during the impact. The loss of kinetic energy is assumed to be dissipated by crushing of the missile. The frontal contact area of the automobile is specified to be 20 sq. ft.

$F_a \times 3ft = ½ [m_a v_o^2]$

$P_a = F_a / 20 ft^2$

where:

m_a = mass of missile = 4,000 lb
v_o = missile initial velocity = 195 ft/sec
F_a = Impact force on cask by missile automobile
p_a = Impact pressure on cask by missile automobile

$F_a = ½ \times \{4{,}000lbm \times [(195 \times 12) in/sec]^2\} / (3 \times 12) in$
$= 3.042 \times 10^8$ lbm- in/sec^2
$= 3.042 \times 10^8$ lb_m- in/sec^2 $\times$ [1 lb_f / (386.4 lb_m- in/sec^2)]
= 787,267 lb_f

P_a = 787,267 lb_f / [20×(12)^2 in^2]
= 273.4 psi

The automobile missile deforms and is crushed during the impact. The shear stress in the cask wall is conservatively calculated below. It is assumed that the impact force is concentrated on a small curved section of the cask wall having dimensions w x L It is also assumed that only two side edges of the impact section are tending to shear. Edges above and below the impact section are assumed to bend, not shear. It is also assumed that the concentrated impact section is 3 foot wide, half of the automotive width. The impact area is then 36" wide by 80" high (equals to 20 ft^2 area).

Shear Area = 2 × (20 ft^2 / 3ft) × the thickness of the cask outer structural shell

= 2 × 80" × 1.5" = 240 in^2

The shear stress, τ = Force/area = 787,267 lb / 240 in^2 = 3,280 psi.

The level D allowable shear stress for the cask shell is 0.42 S_u = 0.42 x 66,200 = 26,480 psi. The shear stress is well below the allowable shear stress.

Assuming that the impact on the side of the cask is reacted by a 36"×80" section of the cask shell, Case 1c from Table 26 of [13] is used to calculate the resulted stresses in the shell. This case represents a flat plate with simply supported edges under a uniform load over central rectangular area. It is conservative for this Case to represent the automotive crushing onto a curved section of the cask.

The transfer cask shell is made of a three-layer composite. It consists of a 1.5" outer structural shell, a 3.6" lead gamma shield, and a 0.5" inner liner (see sketch below). This sandwiched composite plate may be represented by an equivalent one-piece plate which has a thickness

producing the same moment of inertia as that of the composite. The thickness of its equivalent one-piece plate is calculated as follows.

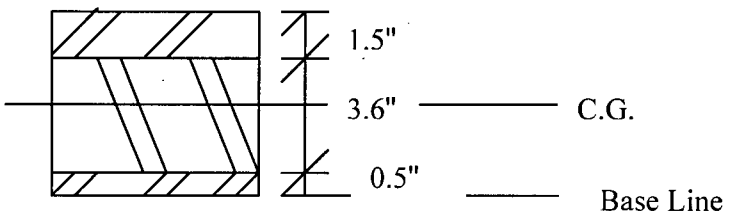

For unit length of the composite plate,
Neglecting the strength of the 3.6" thick lead,
The distance from Base Line to C.G.

$= [(1.5" \times 1") \times (1.5"/2 + 3.6" + 0.5") + (0.5"\times 1")\times(0.5"/2)] \div$
$[(1.5" \times 1") + (0.5"\times 1")]$
$= 7.4" \div 2$
$= 3.7"$

The combined moment of inertia of the composite structural plates, I_{comb}

$I_{comb} = (1\times 1.5^3/12) + (1.5\times 1)\times(1.5/2+3.6+0.5-3.7)^2 + (1\times 0.5^3/12) + (0.5\times 1) \times (3.7-0.5/2)^2$
$= 8.23 \text{ in}^4$

The thickness of the equivalent one-piece plate, t_{eq}

$I_{comb} = 8.23 \text{ in}^4 = (1\times t_{eq}^3)/12 \Rightarrow t_{eq} = 4.62"$

An automobile missile crushing into the horizontal cylindrical canister with an impact area of 36" wide by 80" high is conservatively analyzed by a case that the same impact is applied to a rectangular plate of dimensions at the cask length by the cask OD. All edges of the rectangular plate are assumed simply supported. Case 1c in Table 26 of [13] provides maximum stress calculation of this rectangular plate as follows.

$\text{Max } \sigma = (\beta W) / t^2$

$W = F_a = 787{,}267 \text{ lb}$
$t = t_{eq} = 4.62"$

$a_1 = 36"$, $b1 = 80"$
$a = 193.32"$ (cask length)
$b = 82.7"$ (cask OD)
$a_1 / b = 0.4353$
$b_1 / b = 0.967$
$a / b = 2.337$

Use $(b_1 / b) = 0.8$, and $(a_1 / b) = 0.4$ for the table given under the Case 1c in Table 26 of [13];

From this table,

$\beta = 0.68$ for $(a / b) = 1.4$, and $\beta = 0.76$ for $(a / b) = 2$

By extrapolation, $\beta = 0.81$ for $(a / b) = 2.337$

$\therefore$ Max $\sigma = (0.81 \times 787{,}267 \text{ lb}) / (4.62^2) = 29{,}876$ psi

The ASME code allowable stress for the general membrane stress intensity will be conservatively used for evaluation of the above calculated maximum membrane plus bending stress intensity. The Service Level D allowable stress for the membrane stress intensity is the lesser of $2.4S_m$ and $0.7S_u$. For SA-240 Gr. 304 cask structural shell material, $S_m = 20{,}000$ psi at 300°F and $S_u = 66{,}200$ psi. Thus the allowable stress is $0.7S_u = 46{,}340$ psi. Therefore the maximum membrane plus bending stress of 29,876 psi is acceptable.

11.3.4.3 Accident Dose Calculation

Based on the above analyses, the 32PTH DSC confinement boundary will not be breached as a result of the missile impacts. Accordingly, no 32PTH DSC damage or release of radioactivity is postulated.

The missile impact scenario may result in the loss of cask neutron shielding and local deformation/damage of the gamma shielding. The effect of loss of the neutron shielding due to a missile impact is bounded by that resulting from a cask drop scenario. The radiation dose due to local deformation/damage of the gamma shielding is negligible.

11.3.4.4 Corrective Action

The transfer cask will be inspected for damage. These operations will take place in the plant fuel building decontamination area and spent fuel pool after recovery of the transfer cask. Following recovery of the transfer cask and unloading of the DSC, the transfer cask will be inspected, repaired and tested as appropriate prior to reuse.

For recovery of the cask and contents, it may be necessary to develop a special sling/lifting apparatus to move the transfer cask from the site to the fuel pool. This may require several weeks of planning to ensure all steps are correctly organized. During this time, lead blankets may be added to the transfer cask to minimize on-site exposure to site operations personnel. The transfer cask would be roped off to ensure the safety of the site personnel.

11.3.5 Flood

Cause of Accident

Flooding conditions simulating a range of flood types, such as tsunami and seiches as specified in 10CFR72.122 (b) are considered. In addition, floods resulting from other sources, such as high water from a river or a broken dam, are postulated as the cause of the accident.

Accident Analysis

The HSM-H is evaluated for flooding in Appendix 3.9.9, Section 3.9.9.10.3. Based on the evaluation presented in that section, the HSM-H will withstand the design basis flood.

Accident Dose Calculation

The radiation dose due to flooding of the HSM-H is negligible. Flooding does not breach the confinement boundary. Therefore radioactive material inside the DSC will remain sealed in the DSC and, therefore, will not contaminate the encroaching flood water.

Corrective Actions

Because of the location and geometry of the HSM-H vents, it is unlikely that any significant amount of silt would enter an HSM-H should flooding occur. Any silt deposits would be removed using a pump suction hose or fire hose inserted through the inlet vent to suck the silt out, or produce a high velocity water flow to flush the silt through the HSM-H inlet vents.

11.3.6 Blockage of HSM-H Air Inlet and Outlet Openings

This accident conservatively postulates the complete blockage of the ventilation air inlet and outlet openings of the HSM-H.

Cause of Accident

Since the NUHOMS® HSM-Hs are located outdoors; there is a remote probability that the ventilation air inlet and outlet openings could become blocked by debris from such unlikely events as floods and tornados. The NUHOMS® design features such as the perimeter security fence and the redundant protected location of the air inlet and outlet openings reduce the probability of occurrence of such an accident. Nevertheless, for this conservative generic analysis, such an accident is postulated to occur and is analyzed.

Accident Analysis

The thermal evaluation of this event is presented in Chapter 4, Section 4 for 32PTH DSC (34.8 kw) and Amendment #8, Section P.4 for 24PTH DSC (40.8 kw). The analysis performed for HSM-H with 24PTH DSC bounding the values for HSM-H with 32PTH DSC. Therefore, the temperatures determined in Amendment #8, Section P.4 are used in the HSM-H structural

evaluation of this event, which is presented in Appendix 3.9.9, Section 3.9.9.10.4. The structural evaluation of the 32PTH DSC based on the thermal evaluation presented in Chapter 4 of this SAR is presented in Appendix 3.9.1, storage load case 6 (page 3.9.1-59).

Accident Dose Calculation

There are no off-site dose consequences as a result of this accident. The only significant dose increase is that related to the recovery operation where it is conservatively estimated that the on-site workers will receive an additional dose of no more than one man-rem during the eight hour period it is estimated may be required for removal of debris from the air inlet and outlet openings in the HSM-H.

Corrective Actions

Debris removal is all that is required to recover from a postulated blockage of the HSM ventilation air inlets and outlets. Cooling will begin immediately following removal of the debris from the inlets and outlets. The amount and nature of debris can vary, but even in the most extreme case, manual means or readily available equipment can be used to remove debris.

The debris is conservatively assumed to remain in place for 34 hours. The last seven hours of this period are assumed to be the time required to completely remove all the debris before the natural circulation air flow can be restored.

11.3.7 Lightning

Cause of Accident

The likelihood of lightning striking the HSM-H and causing an off-normal condition is not considered to be a credible event. Lightning protection system requirements are site specific and depend upon the frequency of occurrences of lightning storms in the proposed ISFSI location and the degree of protection offered by other grounded structures in the proximity of the HSM-Hs. The addition of simple lightning protection equipment, required by plant criteria, to HSM-H structures (i.e., grounded handrails, ladders, etc.) is considered a miscellaneous attachment.

Accident Analysis

Should lightning strike in the vicinity of the HSM-H the normal storage operations of the HSM-H will not be affected. The current discharged by the lightning will follow the low impedance path offered by the surrounding structures. Therefore, the HSM-H will not be damaged by the heat or mechanical forces generated by current passing through the higher impedance concrete. Since the HSM-H requires no equipment for its continued operation, the resulting current surge from the lightning will not affect the normal operation of the HSM-H.

Corrective Actions

Since no off-normal condition will develop as the result of lightning striking in the vicinity of the HSM-H, no corrective action would be necessary. Also, there would be no radiological consequences.

11.3.8 Fire/Explosion

Cause of Accident

Combustible materials will not normally be stored at an ISFSI. Therefore, a credible fire would be very small and of short duration such as that due to a fire or explosion from a vehicle or portable crane.

Direct engulfment of the HSM-H is highly unlikely. Any fire within the ISFSI boundary while the DSC is in the HSM would be bounded by the fire during transfer cask movement. The HSM-H concrete acts as a significant insulating fire wall to protect the DSC from the high temperatures of the fire.

Accident Analysis

The evaluation of the hypothetical fire event is presented in Chapter 4, Section 4. The fire thermal evaluation is performed primarily to demonstrate the confinement integrity and fuel retrievability of the 32PTH DSC. Peak temperatures for the NUHOMS®-32PTH System components are summarized in Table 4-5 of Chapter 4. Temperatures in this table are used for structural evaluations of the transfer Cask. The results of this analysis is presented in Appendix 3.9.2, Section 3.9.2.2.4, Load Case 10 (page 3.9.2-26).

Accident Dose Calculation

The 32PTH-DSC confinement boundary will not be breached as a result of the postulated fire/explosion scenario. Accordingly, no 32PTH-DSC damage or release of radioactivity is postulated. Because no radioactivity is released, no resultant dose increase is associated with this event.

The fire scenario may result in the loss of transfer cask neutron shielding should the fire occur while the 32PTH-DSC is in the cask. The effect of loss of the neutron shielding due to a fire is bounded by that resulting from a cask drop scenario. See Section 11.3.1 of this Chapter for evaluation of dose consequences of a cask drop.

Corrective Actions

Evaluation of transfer cask neutron shield damage as a result of a fire is to be performed to assess the need for temporary shielding (if fire occurs during transfer operations) and repairs to restore the transfer cask to pre-fire design conditions.

11.4 References

1. 10CFR Part 72, Licensing Requirement for Storage of Spent Fuel in an Independent Spent Fuel Storage Installation.
2. American Nuclear Society, ANSI/ANS-57.9-1984, Design Criteria for an Independent Spent Fuel Storage Installation (Dry Storage Type).
3. Regulatory Guide 1.60, "Design Response Spectra for Seismic Design of Nuclear Power Plants," U.S. Atomic Energy Commission, Revision 1, December 1973.
4. "Missiles Generated by Natural Phenomenon," Standard Review Plan, NUREG-0800, U.S. Nuclear Regulatory Commission
5. "Design Basis Tornado for Nuclear Power Plants," Regulatory Guide 1.76, U.S. Atomic Energy Commission, April 1974.
6. ANSYS Engineering Analysis System, Users Manual for ANSYS Rev. 5.6 and 6.0, Swanson Analysis Systems, Inc., Houston, PA.
7. "Structural Analysis and Design of Nuclear Plant Facilities," ASCE Publication No. 58.
8. "Code Requirements for Nuclear Safety Related Concrete Structures," ACI 349-97, American Concrete Institute, Detroit, MI.
9. "Design of Structures for Missile Impact", BC-TOP-9A, Revision 2, September 1974, Bechtel Power Corporation.
10. H.A. Nelms, "Structural Analysis of Shipping Casks, Effects of Jacket Physical Properties and Curvature and Puncture Resistance, "Vol. 3, ORNL TM-1312, Oak Ridge National Laboratory, Oak ridge Tennessee, June 1968.
11. Gwaltney, R. C., "Missile Generation and Protection in Light-Water Cooled Power Reactor Plants", ORNL NSIC-22, Oak Ridge National Laboratory, Oak Ridge, TN, for the USAEC, September 1968.
12. American Society of Civil Engineers, ASCE 7-95, Minimum Design Loads for Buildings and Other Structures, Approved June 6, 1996
13. "Formulas for Stress and Strain", 5th Edition, R. J. Roark and W. C. Young

Figure Withheld Under 10 CFR 2.390

Figure 11-1
HSM-H Dimensions for Missile Impact Stability Analysis

12 OPERATING CONTROLS AND LIMITS

The Technical Specifications for the NUHOMS® HD system are included in Attachment A to NUHOMS® HD CoC 1030 (Docket No. 72-1030) Amendment Number 0.

NUHOMS® HD SYSTEM TECHNICAL SPECIFICATION BASES

TABLE OF CONTENTS

B 12.2 FUNCTIONAL AND OPERATING LIMITS B12-1

B 12.3 LIMITING CONDITION FOR OPERATION (LCO) APPLICABILITY B12-2

B 12.3 SURVEILLANCE REQUIREMENT (SR) APPLICABILITY B12-5
B 12.3.1 32PTH DSC INTEGRITY B12-9

B 12.2 FUNCTIONAL AND OPERATING LIMITS

BASES

BACKGROUND

The 32PTH DSC design requires certain limits on spent fuel parameters, including fuel type, maximum allowable enrichment prior to irradiation, maximum burnup, minimum acceptable cooling time prior to storage in the 32PTH DSC, and physical condition of the spent fuel (i.e., intact or damaged fuel assemblies). Other important limitations are the radiological source terms from associated Burnable Poison Rod Assemblies (BPRAs), Vibration Suppressor Inserts (VSIs), and Thimble Plug Assemblies (TPAs). These limitations are included in the thermal, structural, radiological, and criticality evaluations performed for the canister.

APPLICABLE SAFETY ANALYSIS

Various analyses have been performed that use these fuel parameters as assumptions. These assumptions are included in the thermal, criticality, structural, shielding and confinement analyses.

Technical Specification Tables 12-1, 12-2, 12-3, 12-4, and 12-5 provide the key fuel parameters that require confirmation prior to 32PTH DSC loading.

FUNCTIONAL AND OPERATING LIMITS VIOLATIONS

If Functional and Operating Limits are violated, the limitations on the fuel assemblies in the canister have not been met. Actions must be taken to place the affected fuel assemblies in a safe condition. This safe condition may be established by returning the affected fuel assemblies to the spent fuel pool. However, it is acceptable for the affected fuel assemblies to remain in the canister if that is determined to be a safe condition.

Notification of the violation of a Functional and Operating Limit to the NRC is required within 24 hours. Written reporting of the violation must be accomplished within 30 days. This notification and written report are independent of any reports and notification that may be required by 10CFR 72.75.

REFERENCES

SAR Chapter 2

B 12.3 LIMITING CONDITION FOR OPERATION (LCO) APPLICABILITY

BASES

LCOs

LCO 12.3.0.1, 12.3.0.2, 12.3.0.4 and 12.3.0.5 establish the general requirements applicable to all Specifications and apply at all times, unless otherwise stated.

LCO 12.3.0.1

LCO 12.3.0.2 establishes the Applicability statement within each individual Specification as the requirement for when the LCO is required to be met (i.e., when the canister is in the specified conditions of the Applicability statement of each Specification).

LCO 12.3.0.2

LCO 12.3.0.2 establishes that upon discovery of a failure to meet an LCO, the associated ACTIONS shall be met. The Completion Time of each Required Action for an ACTIONS Condition is applicable from the point in time that an ACTIONS Condition is entered. The Required Actions establish those remedial measures that must be taken within specified Completion Times when the requirements of an LCO are not met. This Specification establishes that:

a. Completion of the Required Actions within the specified Completion Times constitutes compliance with a Specification; and

b. Completion of the Required Actions is not required when an LCO is met within the specified Completion Time, unless otherwise specified.

There are two basic types of Required Actions. The first type of Required Action specifies a time limit in which the LCO must be met. This time limit is the Completion Time to restore a system or component or to restore variables to within specified limits. If this type of Required Action is not completed within the specified Completion Time, the canister may have to be placed in the spent fuel pool and unloaded. (Whether stated as a Required Action or not, correction of the entered Condition is an action that may always be considered upon entering ACTIONS.) The second type of Required Action specifies the remedial measures that permit continued operation of the unit that is not further restricted by the Completion Time. In this case, compliance with the Required Actions provides an acceptable level of safety for continued operation.

Completing the Required Actions is not required when an LCO is met or is no longer applicable, unless otherwise stated in the individual Specifications.

The Completion Times of the Required Actions are also applicable when a system or component is removed from service intentionally. The reasons for intentionally relying on the ACTIONS include, but are not limited to, performance of Surveillances, preventive maintenance, corrective maintenance, or investigation of operational problems. Entering ACTIONS for these reasons must be done in a manner that does not compromise safety. Intentional entry into ACTIONS should not be made for operational convenience.

Individual Specifications may specify a time limit for performing an SR when equipment is removed from service or bypassed for testing. In this case, the Completion Times of the Required Actions are applicable when this time limit expires if the equipment remains removed from service or bypassed.

When a change in specified condition is required to comply with Required Actions, the equipment may enter a specified condition in which another Specification becomes applicable. In this case, the Completion Times of the associated Required Actions would apply from the point in time that the new Specification becomes applicable and the ACTIONS Condition(s) are entered.

LCO 12.2.0.3 This specification is not applicable to the NUHOMS® HD System. The placeholder is retained for consistency with the power reactor technical specifications.

LCO 12.3.0.4 LCO 12.2.0.4 establishes limitations on changes in specified conditions in the Applicability when an LCO is not met. It precludes placing the NUHOMS® HD System in a specified condition stated in that Applicability (e.g., Applicability desired to be entered) when the following exist:

a. Conditions are such that the requirements of the LCO would not be met in the Applicability desired to be entered; and

b. Continued noncompliance with the LCO requirements, if the Applicability were entered, would result in the equipment being required to exit the Applicability desired to be entered to comply with the Required Actions.

Compliance with Required Actions that permit continued operation of the equipment for an unlimited period of time in specified condition provides an acceptable level of safety for continued operation. Therefore, in such cases, entry into a specified condition in the Applicability may be made in accordance with the provisions of the Required Actions. The provisions of this Specification should not be interpreted as endorsing the failure to exercise the good practice of restoring systems or components before entering an associated specified condition in the Applicability.

The provisions of LCO 12.3.0.4 shall not prevent changes in specified conditions in the Applicability that are required to comply with ACTIONS. In addition, the provisions of LCO 12.3.0.4 shall not prevent changes in specified conditions in the Applicability that are related to the unloading of a canister.

Exceptions to LCO 12.3.0.4 are stated in the individual Specifications.

Exceptions may apply to all the ACTIONS or to a specific Required Action of a Specification.

Surveillances do not have to be performed on the associated equipment out of service (or on variables outside the specified limits), as permitted by SR 12.3.0.1. Therefore, changing specified conditions while in an ACTIONS Condition, either in compliance with LCO 12.3.0.4 or where an exception to LCO 12.3.0.4 is stated, is not a violation of SR 12.3.0.1 or SR 12.3.0.4 for those Surveillances that do not have to be performed due to the associated out of service equipment.

LCO 12.3.0.5

LCO 12.3.0.5 establishes the allowance for restoring equipment to service under administrative controls when it has been removed from service or not in service in compliance with ACTIONS. The sole purpose of this Specification is to provide an exception to LCO 12.3.0.2 (e.g., to not comply with the applicable Required Action(s)) to allow the performance of required testing to demonstrate:

a. The equipment being returned to service meets the LCO; or

b. Other equipment meets the applicable LCOs.

The administrative controls ensure the time the equipment is returned to service in conflict with the requirements of the ACTIONS is limited to the time absolutely necessary to perform the allowed required testing. This Specification does not provide time to perform any other preventive or corrective maintenance.

LCO 12.3.0.6

This specification is not applicable to the NUHOMS® HD System. The placeholder is retained for consistency with the power reactor technical specifications.

LCO 12.3.0.7

This specification is not applicable to the NUHOMS® HD System. The placeholder is retained for consistency with the power reactor technical specifications.

B 12.3 SURVEILLANCE REQUIREMENT (SR) APPLICABILITY

BASES

SRs

SR 12.3.0.1 through SR 12.3.0.4 establish the general requirements applicable to all Specifications in Sections 12.3.1,12.3.2 and 12.3.3 and apply at all times, unless otherwise stated.

SR 12.3.0.1

SR 12.3.0.1 establishes the requirement that SRs must be met during the specified conditions in the Applicability for which the requirements of the LCO apply, unless otherwise specified in the individual SRs. This Specification is to ensure that Surveillances are performed to verify systems and components, and that variables are within specified limits. Failure to meet a Surveillance within the specified Frequency, in accordance with SR 12.3.0.2, constitutes a failure to meet an LCO.

Systems and components are assumed to meet the LCO when the associated SRs have been met. Nothing in this Specification, however, is to be construed as implying that systems or components meet the associated LCO when:

a. The systems or components are known to not meet the LCO, although still meeting the SRs; or

b. The requirements of the Surveillance(s) are known to be not met between required Surveillance performances.

Surveillances do not have to be performed when the equipment is in a specified condition for which the requirements of the associated LCO are not applicable, unless otherwise specified.

Surveillances, including Surveillances invoked by Required Actions, do not have to be performed on equipment that has been determined to not meet the LCO because the ACTIONS define the remedial measures that apply. Surveillances have to be met and performed in accordance with SR 12.3.0.2, prior to returning equipment to service.

Upon completion of maintenance, appropriate post maintenance testing is required to declare equipment within its LCO. This includes ensuring applicable Surveillances are not failed and their most recent performance is in accordance with SR 12.3.0.2. Post maintenance testing may not be possible in the current specified conditions in the Applicability due to the necessary equipment parameters not having been established. In these situations, the equipment may be considered to meet the LCO provided testing has been satisfactorily completed to the extent possible and the equipment is not otherwise believed to be incapable of performing its function.

This will allow operation to proceed to a specified condition where other necessary post maintenance tests can be completed.

SR 12.3.0.2

SR 12.3.0.2 establishes the requirements for meeting the specified Frequency for Surveillances and any Required Action with a Completion Time that requires the periodic performance of the Required Action on a "once per..." interval.

SR 12.3.0.2 permits a 25% extension of the interval specified in the Frequency. This extension facilitates Surveillance scheduling and considers plant operating conditions that may not be suitable for conducting the Surveillance (e.g., transient conditions or other ongoing Surveillance or maintenance activities).

The 25% extension does not significantly degrade the reliability that results from performing the Surveillance at its specified Frequency. This is based on the recognition that the most probable result of any particular Surveillance being performed is the verification of conformance with the SRs. The exceptions to SR 12.3.0.2 are those Surveillances for which the 25% extension of the interval specified in the Frequency does not apply. These exceptions are stated in the individual Specifications. The requirements of regulations take precedence over the TS. Therefore, when a test interval is specified in the regulations, the test interval cannot be extended by the TS, and the SR includes a Note in the Frequency stating, "SR 12.3.0.2 is not applicable".

As stated in SR 12.3.0.2, the 25% extension also does not apply to the initial portion of a periodic Completion Time that requires performance on a "once per..." basis. The 25% extension applies to each performance after the initial performance. The initial performance of the Required Action, whether it is a particular Surveillance or some other remedial action, is considered a single action with a single Completion Time. One reason for not allowing the 25% extension to this Completion Time is that such an action usually verifies that no loss of function has occurred by checking the status of redundant or diverse components or accomplishes the function of the equipment in an alternative manner.

The provisions of SR 12.3.0.2 are not intended to be used repeatedly merely as an operational convenience to extend Surveillance intervals (other than those consistent with refueling intervals) or periodic Completion Time intervals beyond those specified.

SR 12.3.0.3

SR 12.3.0.3 establishes the flexibility to defer declaring affected equipment as not meeting the LCO or an affected variable outside the specified limits when a Surveillance has not been completed within the specified Frequency. A delay period of up to 24 hours or up to the limit of the specified Frequency,

whichever is less, applies from the point in time that it is discovered that the Surveillance has not been performed in accordance with SR 12.3.0.2, and not at the time that the specified Frequency was not met.

This delay period provides adequate time to complete Surveillances that have been missed. This delay period permits the completion of a surveillance before complying with Required Actions or other remedial measures that might preclude completion of the Surveillance. The basis for this delay period includes consideration of unit conditions, adequate planning, availability of personnel, the time required to perform the Surveillance, the safety significance of the delay in completing the required Surveillance, and the recognition that the most probable result of any particular Surveillance being performed is the verification of conformance with the requirements.

When a Surveillance with a Frequency based not on time intervals, but upon specified unit conditions or operational situations, is discovered not to have been performed when specified, SR 12.3.0.3 allows the full delay period of 24 hours to perform the Surveillance.

SR 12.3.0.3 also provides a time limit for completion of Surveillances that become applicable as a consequence of changes in the specified conditions in the Applicability imposed by Required Actions.

Failure to comply with specified Frequencies for SRs is expected to be an infrequent occurrence. Use of the delay period established by SR 12.3.0.3 is a flexibility which is not intended to be used as an operational convenience to extend Surveillance intervals.

If a Surveillance is not completed within the allowed delay period, then the equipment is considered not in service or the variable is considered outside the specified limits and the Completion Times of the Required Actions for the applicable LCO Conditions begin immediately upon expiration of the delay period. If a Surveillance is failed within the delay period, then the equipment is not in service, or the variable is outside the specified limits and the Completion Times of the Required Actions for the applicable LCO Conditions begin immediately upon the failure of the Surveillance. Completion of the Surveillance within the delay period allowed by this Specification, or within the Completion Time of the ACTIONS, restores compliance with SR 12.3.0.1.

SR 12.3.0.4 SR 12.3.0.4 establishes the requirement that all applicable SRs must be met before entry into a specified condition in the Applicability.

This Specification ensures that system and component requirements and variable limits are met before entry in the Applicability for which these systems and components ensure safe operation of the facility.

The provisions of this Specification should not be interpreted as endorsing the failure to exercise the good practice of restoring systems or components to an appropriate status before entering an associated specified condition in the Applicability. However, in certain circumstances, failing to meet an SR will not result in SR 12.3.0.4 restricting a change in specified condition. When a system, subsystem, division, component, device, or variable is outside its specified limits, the associated SR(s) are not required to be performed, per SR 12.3.0.1, which states that Surveillances do not have to be performed on such equipment. When equipment does not meet the LCO, SR 12.3.0.4 does not apply to the associated SR(s) since the requirement for the SR(s) to be performed is removed. Therefore, failing to perform the Surveillance(s) within the specified Frequency does not result in an SR 12.3.0.4 restriction to changing specified conditions of the Applicability. However, since the LCO is not met in this instance, LCO 12.3.0.4 will govern any restrictions that may (or may not) apply to specified condition changes.

The provisions of SR 12.3.0.4 shall not prevent changes in specified conditions in the Applicability that are required to comply with ACTIONS. In addition, the provisions of SR 12.3.0.4 shall not prevent changes in specified conditions in the Applicability that are related to the unloading of a HSM-H or 32PTH DSC.

The precise requirements for performance of SRs are specified such that exceptions to SR 12.3.0.4 are not necessary. The specific time frames and conditions necessary for meeting the SRs are specified in the Frequency, in the Surveillance, or both. This allows performance of Surveillances when the prerequisite condition(s) specified in a Surveillance procedure require entry into the specified condition in the Applicability of the associated LCO prior to the performance or completion of a Surveillance. A Surveillance that could not be performed until after entering the LCO Applicability would have its Frequency specified such that it is not "due" until the specific conditions needed are met. Alternatively, the Surveillance may be stated in the form of a Note as not required (to be met or performed) until a particular event, condition, or time has been reached. Further discussion of the specific formats of SR annotation is found in Section 12.1.4, operation to proceed to a specified condition where other necessary post maintenance tests can be completed.

B 12.3.1 32PTH DSC FUEL INTEGRITY

B 12.3.1.1 32PTH DSC Vacuum Drying Time (Duration) and Pressure

BASES

BACKGROUND

A 32PTH DSC is placed in the spent fuel pool and loaded with fuel assemblies meeting the requirements of the Functional and Operating Limits. A shield plug is then placed on the 32PTH DSC. Subsequent operations involve moving the 32PTH DSC to the decontamination area and removing water from the 32PTH DSC. After the 32PTH DSC shield plug is secured, vacuum drying of the 32PTH DSC is performed, and the 32PTH DSC is backfilled with helium. During normal storage conditions, the fuel assemblies are stored in the 32PTH DSC with an inert helium atmosphere, which is a better conductor than nitrogen or vacuum, which results in lower fuel clad temperatures and provides an inert atmosphere during storage conditions.

32PTH DSC vacuum drying is utilized to remove residual moisture from the cavity after the 32PTH DSC has been drained of water. Any water which was not drained from the 32PTH DSC evaporates from fuel or basket surfaces due to the vacuum. This vacuum drying operation is aided by the temperature increase due to the heat generation of the fuel.

APPLICABLE SAFETY ANALYSIS

The confinement of radioactivity during the storage of spent fuel in a 32PTH DSC is ensured by the use of multiple confinement barriers and systems. The barriers relied upon are the fuel pellet matrix, the fuel cladding tubes in which the fuel pellets are contained, and the 32PTH DSC in which the fuel assemblies are stored. Long-term integrity of the fuel cladding depends on storage in an inert atmosphere. This protective environment is accomplished by removing water from the 32PTH DSC and backfilling the 32PTH DSC with an inert gas. The removal of water is necessary to prevent phase change–related pressure increase upon heatup. Time limits on vacuum drying >23.2 kW per Procedure A, >16 kW per Procedure B, and > 22.4 kW heat loads are required for keeping the fuel cladding under the maximum temperature limits. This SAR evaluates and documents that the 32PTH DSC confinement boundary is not compromised due to any normal, off-normal or accident condition postulated (SAR Chapter 3 and 11 structural analyses) and the fuel clad temperature remains below allowable values (SAR Chapter 4).

LCO

A stable vacuum pressure of < 3 torr further ensures that all liquid water has evaporated in the 32PTH DSC cavity, and that the resulting inventory of oxidizing gases in the 32PTH DSC is below 0.25 volume %.

APPLICABILITY

This is applicable to all 32PTH DSCs.

ACTIONS

The actions specified require establishment of a helium pressure of at least 0.5 atmosphere within the time limits specified in the LCO. The timeframe specified applies to the vacuum drying operations and the helium backfill operations. If the required vacuum can not be established within the timeframe specified in the Condition column of the Actions table, a helium atmosphere (with a pressure of at least 0.5 atmosphere) is to be established within 6 hours or perform an assessment and implementation of corrective actions to return the 32PTH DSC to an analyzed condition or reflood the DSC submerging all fuel assemblies. The 15 psig limit in the action section is conservatively below the maximum analyzed blowdown pressure.

SURVEILLANCE REQUIREMENTS

Ensure a minimum oxidizing gas content.

REFERENCES

SAR Chapter 3 and 4

B12.3.1 32PTH DSC FUEL INTEGRITY

B 12.3.1.2 32PTH DSC Helium Backfill Pressure

BASES

BACKGROUND

A 32PTH DSC is placed in the spent fuel pool and loaded with fuel assemblies meeting the requirements of the Functional and Operating Limits. An inner top cover/shield plug is then placed on the 32PTH DSC. Subsequent operations involve moving the 32PTH DSC to the decontamination area and removing water from the 32PTH DSC. After the 32PTH DSC inner top cover/shield plug is welded, vacuum drying of the 32PTH DSC is performed, and the 32PTH DSC is backfilled with helium. During normal storage conditions, the 32PTH DSC is backfilled with helium, which is a better conductor than nitrogen or vacuum, which results in lower fuel clad temperatures. The inert helium environment protects the fuel from potential oxidizing environments.

APPLICABLE SAFETY ANALYSIS

Long-term integrity of the fuel cladding depends on storage in an inert atmosphere. SAR section 3.5 evaluates the effect of long term storage and short term temperature transients on fuel cladding integrity. Credit for the helium backfill pressure is taken to limit the potential for corrosion of the fuel cladding. SAR Chapter 4 evaluates the 32PTH DSC maximum pressure under normal, off-normal, and accident conditions.

LCO

32PTH DSC backpressure is maintained within a range of pressure that will ensure maintenance of the helium backfill pressure over time and will not result in excessive 32PTH DSC pressure in normal, off-normal and accident conditions.

APPLICABILITY

This specification is applicable to all 32PTH DSCs.

ACTIONS

The actions required and associated completion times are associated with the time limits established in specification 12.3.1.2. The total time for vacuum drying and helium backfill is specified in specification 12.3.1.2 as a function of 32PTH DSC heat load and operational procedure. These time limits are imposed to ensure that the 32PTH DSC fuel cladding will not exceed maximum allowable temperatures.

SURVEILLANCE REQUIREMENTS

To ensure that: (1) the atmosphere surrounding the irradiated fuel is a non-oxidizing inert gas; (2) the atmosphere is favorable for the transfer of decay heat.

REFERENCES

SAR Chapters 3 and 4

B12.3.1 32PTH DSC FUEL INTEGRITY

B 12.3.1.3 Transfer Cask Cavity Helium Backfill Pressure

BASES

BACKGROUND

A 32PTH DSC is placed in the spent fuel pool and loaded with fuel assemblies meeting the requirements of the Functional and Operating Limits. An inner top cover/shield plug is then placed on the 32PTH DSC. Subsequent operations involve moving the 32PTH DSC to the decontamination area and removing water from the 32PTH DSC. After the 32PTH DSC inner top cover/shield plug is welded, vacuum drying of the 32PTH DSC is performed, and the 32PTH DSC is backfilled with helium. The 32PTH DSC outer top cover plate is welded, and, if not previously done, the water drained from the transfer cask (TC) annulus. After installation of the TC lid, the TC cavity is backfilled with helium to assure adequate heat transfer which maintains the fuel cladding temperatures below the maximum allowable temperature.

APPLICABLE SAFETY ANALYSIS

Long-term integrity of the fuel cladding depends on storage in an inert atmosphere and maintaining fuel cladding temperature below an acceptable limit. SAR Chapter 4 evaluates the 32PTH DSC temperatures under normal, off-normal, and accident conditions.

LCO

The OS187H cavity is maintained within a range of pressure that will ensure maintenance of the helium backfill pressure over the transfer time and will not result in excessive pressure in normal, off-normal and accident conditions. The cavity helium backfill must commence within 12 hours after completion of DSC vacuum drying.

APPLICABILITY

This specification is applicable to OS187H transfer cask with loaded 32PTH DSC in transfer condition.

ACTIONS

Should the helium pressure not meet the requirements of this specification, the TC/32PTH DSC must be returned to an analyzed condition or unloaded.

SURVEILLANCE REQUIREMENTS

To ensure the transfer cask cavity is in a helium environment prior to transfer operations in the TC.

REFERENCES

SAR Chapter 4

CHAPTER 13
QUALITY ASSURANCE

TABLE OF CONTENTS

13. QUALITY ASSURANCE 13-1

13.1 Introduction 13-2

13.2 "Important-to-Safety & "Safety Related" NUHOMS® HD System Components 13-3

13.3 Description of TN 10CFR 72, Subpart G QA Program 13-5
13.3.1 Project Organization 13-5
13.3.2 QA Program 13-5
13.3.3 Design Control 13-5
13.3.4 Procurement Document Control 13-6
13.3.5 Procedures, Instructions, and Drawings 13-6
13.3.6 Document Control 13-6
13.3.7 Control of Purchased Items and Services 13-6
13.3.8 Identification and Control of Materials, Parts, and Components 13-7
13.3.9 Control of Special Processes 13-7
13.3.10 Inspection 13-7
13.3.11 Test Control 13-7
13.3.12 Control of Measuring and Test Equipment 13-7
13.3.13 Handling, Storage and Shipping 13-7
13.3.14 Inspection and Test Status 13-8
13.3.15 Control of Nonconforming Items 13-8
13.3.16 Corrective Action 13-8
13.3.17 Records 13-8
13.3.18 Audits and Surveillances 13-8

13.4 Conditions of Approval Records 13-9

13.5 Supplemental Information 13-10
13.5.1 References 13-10

LIST OF TABLES

13-1 TN QA Program Description Manual and Implementing Procedures Manual

LIST OF FIGURES

13-1 Project organization Chart

13. QUALITY ASSURANCE

TN's Quality Assurance (QA) program has been established in accordance with the requirements of 10CFR 72, Subpart G [1]. The QA program applies to the design, purchase, fabrication, handling, shipping, storing, cleaning, assembly, inspection, testing, operation, maintenance, repair, and modification of the NUHOMS® HD System and components identified as "important to safety" and "safety related." These components and systems are defined in Chapter 2 of the SAR.

13.1 Introduction

The complete description and specific commitments of the TN QA program are contained in the TN QA Program Description Manual [2]. This manual has been approved by the Nuclear Regulatory Commission (NRC) for performing 10CFR 72 related activities. Changes to the TN QA program shall be submitted to the NRC for approval within thirty (30) days of implementation. Changes to the TN QA program which decrease or delete previously approved QA commitments shall be submitted to the NRC for approval prior to implementation.

The matrix in Table 13-1 shows the 10CFR 72, Subpart G criteria and the respective sections of the TN QA Program Description Manual and TN Implementing Procedures Manual [3] that address the criteria.

Figure 13-1 shows the organization structure for the NUHOMS® HD System project.

13.2 "Important-to-Safety & "Safety Related" NUHOMS® HD System Components

TN will apply its QA program to the NUHOMS® HD System components within its scope of responsibility which are defined as "important to safety" and " safety related" as delineated in Section 2.5. QA procedures are used to establish the quality category of components, subassemblies, and piece parts according to each item's importance to safety.

In Section 2.5, each component is identified as "important to safety," "not important to safety," or "safety related". During the design process, items that are considered "important to safety" are further categorized using a graded quality approach. When the graded quality approach is used, a list shall be developed for each "important to safety" item which includes an assigned quality category consistent with the item's importance to safety. Quality categories are determined based on the following and the guidance provided in NUREG/CR-6407 [4]:

Category A items are critical to safe operation. These items include structures, components and systems whose failure or malfunction could directly result in a condition adversely affecting public health and safety. This would include conditions such as loss of primary containment with subsequent release of radioactive material, loss of shielding or an unsafe geometry compromising criticality control.

Category B items have a major impact on safety. These items include structures, components, and systems whose failure or malfunction could indirectly result in a condition adversely affecting public health and safety. An unsafe operation could result only if a primary event occurs in conjunction with a secondary event or other failure or environmental occurrence.

Category C items have a minor impact on safety. These items include structures, components, and systems whose failure or malfunction would not significantly reduce the packaging effectiveness and would be unlikely to create a condition adversely affecting public health and safety.

For "safety related" items the Quality Assurance program is applied as described for Category A items. The Quality Assurance program as described in Section 13.3 is applied to each "important to safety" graded category and is limited as follows.

Category A

A. The design is based on the most stringent industrial codes or standards. Design verification shall be accomplished by prototype testing or formal design review.

B. Vendors for items and services for this category may only be selected from the Approved Suppliers List.

C. TN suppliers and sub-tier suppliers must have a QA program based on applicable criteria in Subpart G to 10CFR 72, or equivalent.

D. Complete traceability of raw materials and the use of certified welders and processes is required.

E. All personnel performing Quality Assurance related inspections, tests, and examinations shall be qualified and certified in accordance with the requirements of the QA program.

F. Only qualified and certified auditors and lead auditors shall perform audits.

G. TN QA personnel shall be required to inspect and/or approve supplier fabricated components prior to authorizing shipment release.

H. Welding consumables shall be procured as a Category A item if the intended use is unknown. If purchased for a specific Category B or C application, the material must be identified and its use restricted to fabrication of the same level.

Category B

A. The design is based on the most stringent industrial codes and standards. But design verification may be accomplished by use of alternate calculations or computer codes.

B. The procurement of items may be from suppliers on the Approved Suppliers List or QA program requirements for the supplier may be based upon the inspection and test requirements of the procured item.

C. Traceability of materials is not required; however, specified welds require completion by qualified, certified welders.

D. Quality Assurance verification activities shall be performed by personnel qualified and certified in accordance with the requirements of the QA program.

E. Only lead auditor personnel require certification in accordance with the QA program.

Category C

A. Items may be purchased from a catalog or "off-the-shelf."

B. When received, the item shall be identified and checked for compliance with the purchase order and for damage.

Items not considered important-to-safety will be controlled in accordance with good industrial practices.

If a utility elects to perform construction, and has an NRC approved QA program (10CFR 50) [5]that is equivalent to or exceeds TN's program, then the utility QA program is considered an acceptable substitute for their scope of responsibility.

13.3 Description of TN 10CFR 72, Subpart G QA Program

13.3.1 Project Organization

The NUHOMS® HD System has been designed by a dedicated TN project organization.

QA duties are performed by the TN project organization, the QA Manager, and QA Specialists.

The organization structure for the NUHOMS® HD System project is presented in Table 13-1. A description of TN's organizational structure, functional responsibilities, levels of authority, and lines of internal and external (client and supplier) communication may be found in the TN QA Program Description Manual.

Project QA controls are determined by the Project Manager and approved by QA. All Project Plans, regardless of the indicated applicability of QA requirements, are reviewed by QA to assure that QA controls are commensurate with the specific activity, item complexity, importance to safety and client-imposed contractual requirements.

Project personnel are indoctrinated, trained, and qualified in accordance with the TN QA program.

13.3.2 QA Program

TN will apply the QA program to components defined in Section 2.5 as "important to safety" and "safety related" in accordance with the TN QA Program Description Manual.

TN has established and implemented a QA program for the control of quality in the design, purchase, fabrication, handling, shipping, storing, cleaning, assembly, inspection, testing, operation, maintenance, repair, and modification of storage containers for nuclear products. Training and/or evaluation of personnel qualifications in accordance with written procedures are required for personnel performing activities affecting quality. The QA program assures that all quality requirements, engineering specifications and specific provisions of any package design approval are met. Those characteristics critical to safety are emphasized.

The TN QA Manager regularly evaluates the TN QA program for adherence to the 18 point criteria in scope, implementation and effectiveness. Further, the TN President requires that the QA program, including the QA Program Description Manual and Implementing Procedures Manual, be implemented and enforced on all applicable projects at TN.

13.3.3 Design Control

"Important to safety" and "safety related" NUHOMS® HD System design activities shall be implemented in accordance with the TN QA Manual. Design verification will be performed by a competent individual with the appropriate skill level. However, this individual's skill level may not be the same as the originator but must be equivalent.

Errors and deficiencies in the design, including the design process, are documented in the form of Corrective Action Reports.

Industry standards and specifications are used for the selection of suitable materials, parts, equipment and processes for "important to safety" and "safety related" structures, systems, or components as defined in the various chapters and sections of this SAR.

13.3.4 Procurement Document Control

Procurement documents are prepared in accordance with the TN QA program which delineates the actions to be accomplished in the preparation, review, approval, and control of procurement documents. Review and approval of procurement documents by QA are documented on the procurement documents prior to release to assure the adequacy of quality requirements stated therein. This review determines that quality requirements are correctly stated, inspectable, and controllable; that there are adequate acceptance and rejection criteria; and that the procurement document has been prepared, reviewed, and approved in accordance with QA program requirements. Refer to Section 13.2 for supplier selection requirements.

The procurement documents shall identify the documentation required to be submitted for information, review, or approval by TN or TN's client. The time of submittal shall also be established. When TN requires the supplier to maintain specific QA records, the retention times and disposition requirements shall be prescribed.

13.3.5 Procedures, Instructions, and Drawings

As required by the TN QA program, activities affecting quality are prescribed in approved, written procedures, instructions, or drawings and these procedures, instructions, and drawings shall be followed.

13.3.6 Document Control

The issuance, distribution, and receipt of documents which prescribe activities affecting quality are controlled in accordance with the TN QA program. Controlled documents include, but are not limited to, the TN design specifications and criteria documents, drawings, instructions, and test procedures.

The individuals or groups responsible for reviewing, approving, and issuing documents and revisions thereto are identified in the "Responsibilities" sections of the TN QA implementing procedures.

13.3.7 Control of Purchased Items and Services

The control of purchased items and services shall be implemented in accordance with the TN QA program.

Surveillance of subcontracted activities is planned and performed in accordance with written procedures to assure conformance to the purchase order. These procedures provide for instructions that specify the characteristics to be witnessed, inspected or verified, and accepted;

the method of surveillance and the extent of documentation required; and those responsible for implementing these instructions.

TN suppliers shall furnish documentation that identifies any procurement requirements which have not been met, together with a description of those nonconformances dispositioned as "use-as-is" or "repair."

Documentation from TN suppliers which demonstrates compliance with procurement requirements (such as material test reports, NDE results, performance test results, etc.) is periodically evaluated by audits, independent inspections, or tests as necessary to assure its validity.

13.3.8 Identification and Control of Materials, Parts, and Components

Materials, parts, and components shall be identified and controlled in accordance with the TN QA program. Hardware identification requirements are determined during generation of design drawings and specifications such that the location and method of identification do not affect the form, fit, function, or quality of the item being identified.

13.3.9 Control of Special Processes

The control of special processes, such as nondestructive examination, chemical cleaning, welding, and heat treating shall be performed in accordance with the TN QA program.

13.3.10 Inspection

Receipt inspections, and in-process and final inspections of TN-fabricated, constructed, or erected items, systems, components, or structures shall be performed in accordance with the TN QA program.

13.3.11 Test Control

Test control shall be accomplished in accordance with the TN QA program.

13.3.12 Control of Measuring and Test Equipment

The TN QA program defines the requirements for calibration of measuring and test equipment. Calibration is against certified measurement standards which have known relationships to national standards, where such standards exist. Where such standards do not exist, the basis for calibration shall be documented.

13.3.13 Handling, Storage and Shipping

Handling, storage, and shipping shall be conducted in accordance with the TN QA program. Special handling, preservation, storage, cleaning, packaging, and shipping requirements are established and accomplished by qualified individuals in accordance with predetermined work and inspection instructions.

13.3.14 Inspection and Test Status

The use of inspection and test status tags shall be implemented in accordance with the TN QA program.

13.3.15 Control of Nonconforming Items

The TN QA program defines the requirements and assigns the responsibilities for the control, identification, segregation, documentation, and close-out of nonconforming items to prevent their inadvertent installation or use in fabrication, construction, or erection.

Nonconformance reports identify the item description and quantity, the disposition of the nonconformance, the inspection requirements, and signature approval of the disposition. They are periodically analyzed to show quality trends and help identify root causes of nonconformances. Significant results are reported to responsible management for review and assessment.

Nonconforming items are segregated from acceptable items and tagged to prevent inadvertent use until properly dispositioned and closed out.

13.3.16 Corrective Action

Corrective action for conditions adverse to quality shall be taken in accordance with the TN QA program. For significant conditions adverse to quality the cause is determined and action to preclude recurrence is taken and reported to the appropriate levels of management.

13.3.17 Records

The TN QA program defines the scope of the records program such that sufficient records are maintained to provide documentary evidence of the quality of items and activities affecting quality.

13.3.18 Audits and Surveillances

A comprehensive system of planned and documented audits, including audits of suppliers and site construction activities, verifies compliance with all aspects of the TN QA program and determines the effectiveness of the program.

Audits are performed by certified lead auditors and are planned, performed, and documented in accordance with the TN QA program.

Unannounced QA surveillances may be performed on activities affecting quality by the TN QA Manager, or his designee, on an as-needed basis to further assure compliance with QA requirements.

13.4 Conditions of Approval Records

As required by 10CFR 72, Subpart L, TN will establish and maintain records for each storage component fabricated under a certificate of compliance as required by §72.234(d). The records will be available for inspection as required by §72.234(e). Written procedures and appropriate tests will be established prior to use of the storage components which will be provided to each NUHOMS® HD System user as required by §72.234(f).

13.5 Supplemental Information

13.5.1 References

1. CFR Title 10, Part 72, Licensing Requirements for the Independent Storage of Spent Nuclear Fuel and High-Level Radioactive Waste.

2. "Transnuclear Quality Assurance Program Description Manual," current revision.

3. "Transnuclear Quality Implementing Procedures Manual," current revision.

4. NUREG/CR-6407, "Classification of Transportation Packaging and Dry Spent Fuel Storage System Components According to Importance to Safety," February 1996.

5. CFR Title 10, Part 50, Domestic Licensing of Production and Utilization Facilities.

Table 13-1
TN QA Program Description Manual and Implementing Procedures Manual

10CFR 72, Subpart G	QA Program	
.142	1.0	Organization
.144	2.0	QA Program
.146	3.0	Design Control
.148	4.0	Procurement Document Control
.150	5.0	Procedures, Instructions, and Drawings
.152	6.0	Document Control
.154	7.0	Control of Purchased Items and Services
.156	8.0	Identification and Control of Materials, Parts, and Components
.158	9.0	Control of Special Processes
.160	10.0	Inspection
.162	11.0	Test Control
.164	12.0	Control of Measuring and Test Equipment
.166	13.0	Handling, Storage, and Shipping
.168	14.0	Inspection and Test Status
.170	15.0	Control of Nonconforming Items
.172	16.0	Corrective Action
.174	17.0	Records
.176	18.0	Audits

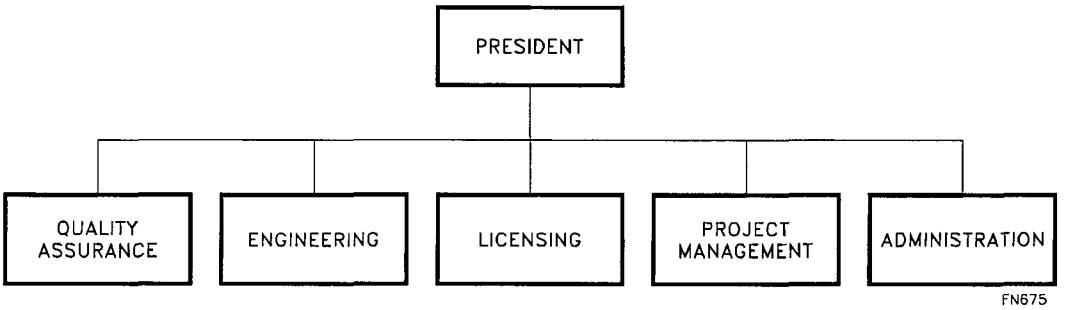

Notes: 1. Licensing may report to Engineering.
2. Administration activities may report to the various other organizations.

Figure 13-1
Project Organization Chart

CHAPTER 14
DECOMMISSIONING

TABLE OF CONTENTS

14. DECOMMISSIONING 14-1

14.1 Decommissioning Considerations 14-1

14.2 Supplemental Information 14-4
14.2.1 References 14-4

14. DECOMMISSIONING

14.1 Decommissioning Considerations

The NUHOMS® HD System design features inherent ease and simplicity for decommissioning by providing easily decontaminable surfaces and isolating the external surfaces of the 32PH1-DSC from contact with the fuel pool. At the end of its service life, the 32PTH DSC decommissioning could be performed by one of the options listed below:

- Option 1, the 32PTH DSC, including stored spent fuel, could be shipped to either a monitored retrievable storage system (MRS) or a geological repository for final disposal, or

- Option 2, the spent fuel could be removed from the 32PTH DSC (either at the ISFSI site or at another off site location) and shipped in an NRC approved transportation cask.

The first option requires that the 32PTH DSC be licensed to current Part 71 regulations. The design and licensing of a transport packaging for the 32PTH is planned.

The first option does not require any decommissioning of the 32PTH DSC. No residual contamination is expected to be left behind on the concrete HSM-H. The HSM-H, fence, and peripheral utility structures will require no decontamination or special handling after the last 32PTH DSC is removed. The HSM-H, fence, and peripheral utility structures could be demolished and recycled with normal construction techniques.

The second option would require decontamination of the 32PTH DSC and transfer cask (if applicable). The sources of contamination in the interior of the 32PTH DSC or transfer cask would be the primary contamination left from the spent fuel pool water; or crud, hot particles and fines from the spent fuel pins. This contamination could be removed with a high pressure water spray. If further surface decontamination of the 32PH1-DSC or transfer cask is necessary, electropolishing or chemical etching can be used to clean the contaminated surface. After decontamination, the 32PTH DSC and/or transfer cask could be cut up for scrap, partially scrapped, or refurbished for reuse. Any activated metal would be shipped as low level radioactive waste to a near surface disposal facility.

A review of cask activation analyses previously performed for similar systems (TN-32 cask 3 and NUHOMS® site license storage system) indicates that the levels of activation of the 32PTH DSC, HSM-H and transfer cask would be orders of magnitude below the specific activity of the isotopes listed in Tables 1 and 2 of 10CFR 61.55 2. A comparison of the source terms for this application to those referenced above including the activation analysis summary for the above applications is provided below. Although the 32PTH radiation sources are larger than the other systems, a detailed analysis is not considered necessary based on the significant margins determined from these analyses.

Comparison of Source Terms for Activation Analyses

Source Term (including Control Components)	32PTH DSC	TN-32 (Metal Cask)	NUHOMS® Site License HSM
γ (γ/sec/assy)	6.9×10^{15}	5.3×10^{15}	1.53×10^{15}
n (n/sec/assy)	1.1×10^{9}	3.3×10^{8}	2.23×10^{8}

TN 32 and NUHOMS® Site License HSM Activation Analysis Results

Nuclide	Activity Ci/m³			
	HSM Concrete	HSM Steel	TN-32	10CFR 61.55 Limit
H-3			8.3×10^{-11}	40
C-14			2.3×10^{-10}	8
Co-60	4.4×10^{-5}	8.1×10^{-2}	7.7×10^{-6}	700
Ni-59	1.4×10^{-10}	3.1×10^{-6}	2.5×10^{-6}	220
Ni-63	8.3×10^{-8}	3.2×10^{-4}	3.4×10^{-4}	3.5
Nb-94		3.9×10^{-8}		.2
<5 year half life	4.6×10^{-3}	2.0×10^{-1}	2.3×10^{-2}	700

Following surface decontamination, the radiation levels in the 32PTH DSC or transfer cask due to activation will be below the acceptable limits of Regulatory Guide 1.86 1. The activation levels of the 32PTH DSC or transfer cask materials will be far below the specific activity limits for both short and long lived nuclides for Class A waste. A detailed evaluation will be performed at the time of decommissioning to determine the appropriate mode of disposal, should refurbishment not be elected.

The procedure for decommissioning a 32PTH DSC or transfer cask not being returned to service is summarized below:

- Remove fuel in accordance with the unloading procedures of Chapter 8.

- Survey interior of 32PTH DSC or transfer cask. Wash down the inside of the 32PTH DSC or transfer cask. Pump out and filter contaminated water and cleaning agent. Survey interior of 32PTH DSC or transfer cask again, decontaminate as required. It is expected that surface decontamination will be minimal. If so, dispose of the 32PTH DSC or transfer cask body as scrap metal. If unable to decontaminate to acceptable levels, the 32PTH DSC and/or transfer cask body can be disposed of as low level radioactive waste.

- Decontaminate the top inner and outer cover plates until able to dispose of as scrap metal. If unable to achieve acceptable levels, dispose of them as low level radioactive waste.

The fuel unloading and decontamination steps for 32PTH DSC, HSM-H, or cask refurbishment are as outlined for the scrap choices, discussed above. However, the only pieces discarded are components damaged by unloading or that are considered to be difficult to decontaminate. Following a comprehensive survey to confirm continued 32PTH DSC, HSM-H or transfer cask

functionality within design basis, the components will be eligible for returning to spent fuel storage service.

The volume of waste material produced incidental to ISFSI decommissioning is expected to be limited to that necessary to accomplish surface decontamination of the 32PTH DSCs, if the spent fuel elements are removed. No chemical or mixed waste is anticipated. The licensee is responsible for the disposal of any waste generated by decontamination. Furthermore, it is estimated that the 32PTH DSC materials will be slightly activated as a result of their long term exposure to the relatively small neutron flux emanating from the spent fuel, and that the resultant activation level will be well below the allowable limits for general release as noncontrolled material. Therefore, it is anticipated that the 32PTH DSCs may be decommissioned from nuclear service by surface decontamination alone. This activity could be performed at the utility, or other suitable facility.

A detailed decommissioning plan will be submitted prior to the commencement of decommissioning activities. The costs of decommissioning the ISFSI are expected to represent a small and negligible fraction of the cost of decommissioning a nuclear power station.

14.2 Supplemental Information

14.2.1 References

1. Regulatory Guide 1.86, "Termination of Operating Licenses for Nuclear Reactors."

2. U.S. Nuclear Regulatory Commission, Title 10 Code of Federal Regulations, Part 61, "Licensing Requirements for Land Disposal or Radioactive Waste".

3. Safety Analysis Report for the TN-32 Cask, Docket 72-1021, Revision 0, January 2000.